



Sacramento River Ecological Flows Study: Off-Channel Habitat Study Final Report

Prepared for



Sacramento River Project
500 Main St.
Chico, CA 95928

Prepared by

G. Mathias Kondolf
2241 Ward Ave
Berkeley, CA 94705

And

Stillwater Sciences
2855 Telegraph Ave, Suite 400
Berkeley, CA, 94705

Funded by

CALFED Ecosystem Restoration Program
and the Resources Legacy Fund Foundation

December 2007



Suggested citation:

Kondolf, G. M. and Stillwater Sciences. 2007. Sacramento River Ecological Flows Study: Off-Channel Habitat Study Results. Technical Report prepared for The Nature Conservancy, Chico, California by G. Mathias Kondolf and Stillwater Sciences, Berkeley, California

Table of Contents

1 INTRODUCTION 1

2 STUDY OBJECTIVES AND SITES 3

 2.1 Study Objectives 3

 2.2 Study Sites 4

 2.2.1 Off-channel water bodies 4

 2.2.2 Scour channels on point bars 7

3 METHODS 9

 3.1 Analysis of Aerial Photographs and Historical Flow Data 9

 3.2 Survey of Sediment and Water Depths 9

 3.3 Radiometric Dating 10

 3.4 Water Surface Elevations and Flow Velocities 10

 3.5 Cross-Section Surveys 10

 3.6 Water Quality Sampling 10

 3.7 Macrophyte Mapping 10

 3.8 Thermograph Deployment in Scour Channels on Point Bars 11

 3.8.1 Thermograph set-up and calibration 11

 3.8.2 Field study implementation 11

 3.8.3 Data QA/QC and analysis 12

4 RESULTS 17

 4.1 Analysis of Aerial Photographs and Historical Flow Data 17

 4.2 Survey of Sediment and Water Depths 18

 4.3 Radiometric Dating of Former Channel Sediments 19

 4.4 Water Surface Elevations and Velocities 19

 4.4.1 Water surface elevations 19

 4.4.2 Surface velocities 20

 4.5 Cross Section Surveys 20

 4.6 Water Quality and Aquatic Macrophyte Survey 21

 4.7 Scour Channels on Point Bars 24

 4.7.1 River Mile 189.5L 29

 4.7.2 River Mile 203R 30

 4.7.3 River Mile 209L 31

 4.7.4 River Mile 239.5R 31

5 DISCUSSION AND SYNTHESIS 33

 5.1 Sedimentation Rates 33

 5.1.1 Patterns of sedimentation observed in oxbow lakes of the Sacramento River 33

 5.2 Water Quality 34

 5.3 Inundation of Scour Channels on Point Bars 35

 5.3.1 Inundated area 35

 5.3.2 Inlet connection flows 36

 5.3.3 Stage-discharge relationships in scour channels on point bars 38

 5.3.4 Data uncertainty 39

6 MANAGEMENT IMPLICATIONS/CONCLUSIONS 41

6.1	Off-Channel Water Bodies	41
6.2	Scour Channels on Point Bars.....	41
6.3	Future Research Needs	42

7 REFERENCES..... 43

List of Tables

Table 1.	Ownership and parameters measured at off-channel water body study sites.*.....	5
Table 2.	Summary of 17 seasonally inundated, shallow-water study sites selected for sampling in the Sacramento River between RM 243 and 184.....	8
Table 3.	CDWR flow gauges on the Sacramento River used for thermograph analysis from 2/15/2007 to 4/26/2007.....	14
Table 4.	Study site locations and flows during thermograph installation and removal.	15
Table 5.	Estimated age of off-channel water bodies in the Middle Sacramento River.....	17
Table 6.	Sedimentologic characteristics of OCWB study sites in the Middle Sacramento River.	18
Table 7.	Occurrence of vascular plant species during surveys of off-channel water bodies. ..	21
Table 8.	Average water quality measurements for OCWB sites.	23
Table 9.	Summary of habitat data from 15 scour channels on point bar study sites on the Sacramento River.....	25
Table 10.	Thermograph installation and monitoring summary.....	26
Table 11.	Summary of flows and estimated inundated areas.....	28

List of Figures.....46

Figure 1.	(A) Aerial photo of floodplain near river mile 167 taken in 2004. Based on radiocarbon data, Old Packer Lake is estimated to have formed over 800 years ago (Sullivan 1982). Historical maps of the vicinity show the formation of Packer Lake in 1874. (B) Aerial photo of floodplain near river mile 175 taken in 1997. Historical aerial photos show that Hartley Island formed in the late 1950's.
Figure 2.	Example of a scour channel that forms on the downstream end of a point bar, providing seasonally inundated, shallow-water habitat that can support rearing of salmonid fry. (Photo Source: CDWR 1999)
Figure 3.	Examples of off-channel water bodies studied for inundation flows on the Sacramento River: (A) Type 1- probe channel eroding behind an active point bar, (B) Type 2- an abandoned channel on the inside of a meander bend as the mainstem continues to erode outward, and (C) Type 3- a former main channel position on the outside of a bend that is abandoned as the main channel cuts behind a point bar.
Figure 4.	Conceptual cross-sections of inlets to (A) type 1 channels (probe channels eroding behind point bars) and (B) type 3 channels on the outside of meander bends that are potentially former mainstem channel locations.
Figure 5.	Miniature water temperature recorders can be used to identify periods of inundation and desiccation. Diurnal temperature fluctuations are generally muted during periods of inundation, and more pronounced when they are exposed to the open air (gray box).

- Figure 6. CA DWR flow gauges and flow diversions on the Sacramento River used to analyze OCWB study sites from 2/15/2007 to 4/30/2007.
- Figure 7. Results of principal component analysis on attributes of Sacramento River former channels as mapped from historical, sequential aerial photographs.
- Figure 8. Sediment thicknesses and water depths measured in OCWBs of the Sacramento River, presented as box-and-whisker plots (Tukey 1977), in which the spread of the middle 50% of the data is shown by the box, and upper and lower outliers indicated by points connected to the box by lines (whiskers). (Note: the y-axis is labeled using French terminology: epaisseur de sediments is thickness of sediments, profondeur d'eau is water depth.)
- Figure 9. Sedimentation rates measured in OCWBs plotted against age of the channel being cut off from the mainstem Sacramento River.
- Figure 10. Activity of ²¹⁰Pb in units of decays per minute per gram, through the depth of a sediment core from Packer Lake. The core was taken near the apex of the lake.
- Figure 11. Stage-discharge relations during recession limb of the March 2006 for the mainstem at Woodson Bridge and Hamilton City, and for five OCWBs. For each site shown, the point along the zero line at the top of the figure represents the highest reading (at the beginning of our period of measurement during the flood's recession limb). The later observations are along the line descending to the left. The mainstem lines show linear declines. The OCWBs with straight lines reflect good connection between side channel and mainstem, while the non-linear traces reflect poor connection to the main channel.
- Figure 12a. Surface velocity measurements during the recession limb of the March 2006 flood for Beehive Bend, Boggs Bend, Capay, Duck Lake, Indian Fisheries, Jacinto, Jenny Lind Bend, Kopta Main, Kopta Backwater, Kopta North, and La Barranca OCWBs. The x-axis is labeled with the name of the OCWB for each velocity measurement. If the velocity was zero, no bar is visible. If velocity was negative (i.e., in the upstream direction), the bar extends downward from the zero line. If velocity was positive (i.e., downstream), the bar extends upward.
- Figure 12b. Surface velocity measurements during the recession limb of the March 2006 flood for Lagoon, Merrills Landing, Old Razor Slough, Packer Lake, Phelan Island, R174, R178, R189, R192, R194, Wilson Landing, and Young Razor Slough. The x-axis is labeled with the name of the OCWB for each velocity measurement. If the velocity was zero, no bar is visible. If velocity was negative (i.e., in the upstream direction), the bar extends downward from the zero line. If velocity was positive (i.e., downstream), the bar extends upward.
- Figure 13. Cross section of Phelan Island OCWB. X-axis = distance from the right bank (m.)
- Figure 14. Cross section of Capay OCWB.
- Figure 15. Cross section of Jacinto OCWB.
- Figure 16. Cross section of Old Razor OCWB
- Figure 17. Cross section of Kopta main OCWB.
- Figure 18. Cross section of Jenny Lind Bend OCWB.
- Figure 19. Cross section of Young Razor slough OCWB.

- Figure 20. Conductivity measurements for selected OCWB sites taken during a range of Sacramento River discharge rates.
- Figure 21a. Inundated areas at site 13 (RM 187R) with flows of 7,600 cfs, areas observed and drawn during field mapping.
- Figure 21b. Inundated areas at site 13 (RM 187R) with flows of 8,600 cfs, areas observed and drawn during field mapping.
- Figure 22a. Inundated areas at site 14 (RM 189R) with flows of 10,500 cfs, areas observed and drawn during field mapping.
- Figure 22b. Inundated areas at site 14 (RM 189R) with flows of 13,400 cfs, areas based on thermograph temperature records and field surveys.
- Figure 23. Thermograph data for site 14 (RM 189R) and discharge at Ord Ferry between 2/22/07 and 3/3/07. Critical flow points depict thermograph changes between dry and wet status.
- Figure 24a. Inundated areas of site 15 (RM 189.5L) at flows of 7,600 cfs, areas observed and drawn during field mapping.
- Figure 24b. Inundated areas of site 15 (RM 189.5L) at flows of 8,600 cfs, areas observed and drawn during field mapping.
- Figure 24c. Inundated areas of site 15 (RM 189.5L) at flows of 10,600 cfs , areas based on thermograph temperature records and field surveys.
- Figure 24d. Inundated areas of site 15 (RM 189.5L) at flows of 12,200 cfs , areas based on thermograph temperature records and field surveys.
- Figure 25a. Thermograph data for site 15 (RM 189.5L) and discharge at Ord Ferry between 2/22/07 and 3/6/07. Critical flow points depict thermograph changes between dry and wet status.
- Figure 25b. Thermograph data for site 15 (RM 189.5L) and discharge at Ord Ferry between 2/22/07 and 3/6/07. Critical flow points depict thermograph changes between dry and wet status.
- Figure 26a. Inundated areas of site 16 (RM 191L) at flows of 7,600 cfs, areas observed and drawn during field mapping.
- Figure 26b. Inundated areas of site 16 (RM 191L) at flows of 8,500 cfs, areas observed and drawn during field mapping.
- Figure 26c. Inundated areas of site 16 (RM 191L) at flows of 12,000 cfs , areas based on thermograph temperature records and field surveys.
- Figure 27. Thermograph data for site 16 (RM 191L) and discharge at Ord Ferry between 2/22/07 and 3/4/07. Critical flow points depict thermograph changes between dry and wet status.
- Figure 28a. Inundated areas of site 17 (RM 191.7R) at flows of 7,600 cfs, areas observed and drawn during field mapping.
- Figure 28b. Inundated areas of site 17 (RM 191.7R) at flows of 8,500 cfs, areas observed and drawn during field mapping.
- Figure 28c. Inundated areas of site 17 (RM 191.7R) at flows of 14,400 cfs , areas based on thermograph temperature records and field surveys.

- Figure 29. Thermograph data for site 17 (RM 191.7R) and discharge at Ord Ferry between 2/22/07 and 3/2/07. Critical flow points depict thermograph changes between dry and wet status.
- Figure 30a. Inundated areas of site 22 (RM 203R) at flows of 7,600 cfs, areas observed and drawn during field mapping.
- Figure 30b. Inundated areas of site 22 (RM 203R) at flows of 10,200 cfs , areas based on thermograph temperature records and field surveys.
- Figure 30c. Inundated areas of site 22 (RM 203R) at flows of 12,300 cfs , areas based on thermograph temperature records and field surveys.
- Figure 31. Thermograph data for site 22 (RM 203R) and discharge at Hamilton City between 2/22/07 and 3/2/07. Critical flow points depict thermograph changes between dry and wet status.
- Figure 32a. Inundated areas of site 23 (RM 203L) at flows of 7,100 cfs, areas observed and drawn during field mapping.
- Figure 32b. Inundated areas of site 23 (RM 203L) at flows of 7,600 cfs, areas observed and drawn during field mapping.
- Figure 32c. Inundated areas of site 23 (RM 203L) at flows of 10,900 cfs , areas based on thermograph temperature records and field surveys.
- Figure 33. Thermograph data for site 23 (RM 203L) and discharge at Hamilton City between 2/21/07 and 3/3/07. Critical flow points depict thermograph changes between dry and wet status.
- Figure 34a. Inundated areas of site 25 (RM 209L) at flows of 7,900 cfs, areas observed and drawn during field mapping.
- Figure 34b. Inundated areas of site 25 (RM 209L) at flows of 8,700 cfs, areas observed and drawn during field mapping.
- Figure 34c. Inundated areas of site 25 (RM 209L) at flows of 12,000 cfs , areas based on thermograph temperature records and field surveys.
- Figure 34d. Inundated areas of site 25 (RM 209L) at flows of 14,800 cfs , areas based on thermograph temperature records and field surveys.
- Figure 35. Study site 25, (A) cross section plot with known water surface elevations, and (B) plot of stage – discharge relationships at cross section.
- Figure 36. Thermograph data for site 25 (RM 209L) and discharge at Vina Woodson Bridge between 2/21/07 and 3/3/07. Critical flow points depict thermograph changes between dry and wet status.
- Figure 37a. Inundated areas of site 27 (RM 211L) at flows of 7,900 cfs , areas observed and drawn during field mapping.
- Figure 37b. Inundated areas of site 27 (RM 211L) at flows of 12,400 cfs , areas based on thermograph temperature records and field surveys.
- Figure 38. Thermograph data for site 27 (RM 211L) and discharge at Vina Woodson Bridge between 2/22/07 and 3/3/07. Critical flow points depict thermograph changes between dry and wet status.

- Figure 39a. Inundated areas of site 33 (RM 221.6R) at flows of 7,300 cfs , areas based on thermograph temperature records and field surveys.
- Figure 39b. Inundated areas of site 33 (RM 221.6R) at flows of 8,100 cfs , areas observed and drawn during field mapping.
- Figure 39c. Inundated areas of site 33 (RM 221.6R) at flows of 12,000 cfs , areas based on thermograph temperature records and field surveys.
- Figure 39d. Inundated areas of site 33 (RM 221.6R) at flows of 14,700 cfs , areas based on thermograph temperature records and field surveys.
- Figure 40. Study site 33 (RM 221.6R) , (A) cross section plot with known water surface elevations, and (B) plot of stage – discharge relationships at cross section.
- Figure 41. Thermograph data for site 33 (RM 221.6R) and discharge at Vina Woodson Bridge between 2/21/07 and 3/2/07. Critical flow points depict thermograph changes between dry and wet status.
- Figure 42a. Inundated areas of site 35 (RM 226.5L) at flows of 7,100 cfs , areas based on thermograph temperature records and field surveys.
- Figure 42b. Inundated areas of site 35 (RM 226.5L) at flows of 8,900 cfs , areas observed and drawn during field mapping.
- Figure 42c. Inundated areas of site 35 (RM 226.5L) at flows of 14,900 cfs , areas based on thermograph temperature records and field surveys.
- Figure 43. Study site 35 (RM 226.5L), (A) cross section plot with known water surface elevations, and (B) plot of stage – discharge relationships at cross section.
- Figure 44. Thermograph data for site 35 (RM 226.5L) and discharge at Vina Woodson Bridge between 2/20/07 and 3/3/07. Critical flow points depict thermograph changes between dry and wet status.
- Figure 45a. Inundated areas of site 39 (RM 232.8L) at flows of 7,800 cfs , areas based on thermograph temperature records and field surveys.
- Figure 45b. Inundated areas of site 39 (RM 232.8L) at flows of 8,900 cfs , areas observed and drawn during field mapping.
- Figure 46. Thermograph data for site 39 (RM 232.8L) and discharge at Vina Woodson Bridge between 3/21/07 and 3/28/07. Critical flow points depict thermograph changes between dry and wet status.
- Figure 47a. Inundated areas of site 40 (RM 233.5R) at flows of 8,900 cfs , areas observed and drawn during field mapping.
- Figure 47b. Inundated areas of site 40 (RM 233.5R) at flows of 13,500 cfs , areas based on thermograph temperature records and field surveys.
- Figure 48. Thermograph data for site 40 (RM 233.5R) and discharge at Vina Woodson Bridge between 2/21/07 and 3/3/07. Critical flow points depict thermograph changes between dry and wet status.
- Figure 49a. Inundated areas of site 41 (RM 235.3R) at flows of 8,100 cfs , areas based on thermograph temperature records and field surveys.
- Figure 49b. Inundated areas of site 41 (RM 235.3R) at flows of 9,300 cfs, areas observed and drawn during field mapping.

- Figure 49c. Inundated areas of site 41 (RM 235.3R) at flows of 13,300 cfs , areas based on thermograph temperature records and field surveys.
- Figure 50. Study site 41 (RM 235.3R) , (A) cross section plot with known water surface elevations, and (B) plot of stage – discharge relationships at cross section.
- Figure 51. Thermograph data for site 41 (RM 235.3R) and discharge at Vina Woodson Bridge between 2/22/07 and 2/27/07. Critical flow points depict thermograph changes between dry and wet status.
- Figure 52a. Inundated areas of site 44 (RM 239.5R) at flows of 7,700 cfs , areas based on thermograph temperature records and field surveys.
- Figure 52b. Inundated areas of site 44 (RM 239.5R) at flows of 9,500 cfs , areas observed and drawn during field mapping.
- Figure 52c. Inundated areas of site 44 (RM 239.5R) at flows of 11,300 cfs , areas based on thermograph temperature records and field surveys.
- Figure 53. Thermograph data for site 44 (RM 239.5R) and discharge at Vina Woodson Bridge between 2/21/07 and 3/3/07. Critical flow points depict thermograph changes between dry and wet status.
- Figure 54. (A) Aerial photo of Duck Lake near river mile 181 taken in 2004. The diversion angle and core locations are shown within the photo. (B) Granulometric profile for core DLCOR1.
- Figure 55. (A) Aerial photo of Jenny Lind Bend near river mile 195 taken in 2004. The diversion angle and core locations are shown within the photo. (B) Granulometric profile for core JLBCOR4.
- Figure 56. (A) Aerial photo of Rio Vista near river mile 214 taken in 2004. The diversion angle and core locations are shown within the photo. (B) Granulometric profile for core RV2COR6.
- Figure 57. (A) Aerial photo of La Barranca near river mile 237 taken in 2004. The diversion angle and the core location are shown within the photo. (B) Granulometric profile for core LBCOR1.
- Figure 58. The average bankfull depth of meanders comprising the 1997 Sacramento River versus the average radius of curvature of each meander. Error bars represent one standard deviation.
- Figure 59. The average gravel thickness estimated for 14 oxbows within the study reach versus their diversion angles as measured using 2004 aerial photos
- Figure 60. The percentage that an oxbow has been filled, measured as the total thickness of sedimentary fill divided by its average original depth, versus average gravel thickness.
- Figure 61. The percentage that an oxbow has been filled, measured as the total thickness of sedimentary fill divided by its average original depth, versus average gravel thickness.
- Figure 62. Sedimentation rates grouped by geometric former channel type as distinguished from features measured on aerial photographs.

- Figure 63. OCWB sedimentation rate plotted against age of OCWB, with geometric channel type (from aerial photo analysis) identified. (Same as Figure 9 but with channel types identified.)
- Figure 64. Log-log scale regression model relating sedimentation rate to the age of the OCWB unit. The regression equation is $\text{Log } y = 1.82 - 0.7 \log x$, with $r^2 = 0.37$.
- Figure 65. (A) Cumulative connected, disconnected, and total inundated area at 5 study sites related to the Ord Ferry gauge on the Sacramento River. (B) Normalized connected, disconnected, and total inundated area at study sites related to Ord Ferry gauge on the Sacramento River. Each site is normalized by its maximum potential inundated area that could be characterized by the thermograph deployment, such that each site has equal weight in determining the % inundated area.
- Figure 66. (A) Cumulative connected, disconnected, and total inundated area at 2 study sites related to the Hamilton City gauge on the Sacramento River. (B) Normalized connected, disconnected, and total inundated area at study sites related to Hamilton City gauge on the Sacramento River. Each site is normalized by its maximum potential inundated area that could be characterized by the thermograph deployment, such that each site has equal weight in determining the % inundated area.
- Figure 67. (A) Cumulative connected, disconnected, and total inundated area at 8 study sites related to the Vina Woodson Bridge gauge on the Sacramento River. (B) Normalized connected, disconnected, and total inundated area at study sites related to Vina Woodson Bridge gauge on the Sacramento River. Each site is normalized by its maximum potential inundated area that could be characterized by the thermograph deployment, such that each site has equal weight in determining the % inundated area.
- Figure 68. (A) Cumulative connected, disconnected, and total inundated area at all study sites (15) at varying flows on the Sacramento River. (B) Normalized connected, disconnected, and total inundated area at all study sites at varying flows on the Sacramento River. Each site is normalized by its maximum potential inundated area that could be characterized by the thermograph deployment, such that each site has equal weight in determining the % inundated area.
- Figure 69. Average maximum daily water temperatures for submerged thermographs with inlets connected and disconnected to the mainstem. The maximum daily air temperature from Chico, CA (site maintained by CDF) is also displayed.
- Figure 70. Rates of stage change (ft) within OCWB study sites per 1,000 cfs changes in mainstem Sacramento River discharge for type 1, 2, and 3 OCWB channels.

List of Photographs

- Photo 1. Photo of study site 17 on 4/26/2007 depicting a site that has significant *Ludwigia* growing within its wetted areas.
- Photo 2. Photo of study site 13 on: (A) 2/21/2007 (8,600 cfs) during tidbit deployment when primary pool was connected to mainstem, and (B) on 4/26/2007 (7,600 cfs) when primary pool was disconnected from mainstem. Photo (A) depicts thermograph 13-1 which was installed to monitor connection of the main pool with the outlet and mainstem.

- Photo 3. Photo of study site 15 on: (A) 2/21/2007 during tidbit deployment (8,600 cfs) when outlet channel contained flow but was still disconnected at downstream end from mainstem, and (B) on 4/26/2007 during tidbit retrieval (7,600 cfs) when outlet channel was dry. See Figures GIS3a and 3b for planform map.
- Photo 4. Photo of study site 16 on 4/26/2007 2:00 PM at a discharge of 7,600 cfs at Ord Ferry gauge. Photo illustrates a contracting pool following recent inlet disconnection on 4/24/2007 9:00 PM.
- Photo 5. Photo of study site 44 on 2/15/2007 at a discharge of 9,500 cfs. Primary pool in picture was marginally connected to the mainstem at the outlet and juvenile Chinook salmon and Sacramento sucker were observed in this pool.

List of Appendices

- Appendix A. Detailed Description of Sites and Results for Scour Channels on Point Bars.
Appendix B. List of Researchers and Institutional Affiliations.
Appendix C. Lessons from Chute-Cutoff Modeling Exercises
Appendix D. Off-Channel Habitat Study Plan

1 INTRODUCTION

Geomorphic processes such as channel migration, chute-cutoff, and avulsion are crucial to the formation of oxbow lakes, sloughs, and side channels and other off-channel habitats on actively meandering rivers. In this report, we refer to off-channel habitats collectively as off-channel water bodies (OCWBs). OCWBs evolve over time as a function of sediment deposition and scour, vegetation colonization and succession, and the buildup of organic detritus from aquatic vegetation. A variety of riverine species depend on OCWBs for habitat. For example, in the Sacramento River corridor, OCWBs provide critical habitat for Western Pond Turtle (*Clemmys marmorata*), Sacramento sucker (*Catostomus occidentalis*), Sacramento pikeminnow (*Ptychochelilus grandis*), California roach (*Hesperoleucus symmetricus*) and Chinook salmon (*Oncorhynchus tshawytscha*). They also harbor several non-native species, such as largemouth bass (*Micropterus salmoides*), bullfrogs (*Rana catesbeiana*), and red-eared sliders (*Trachemys scripta*).

Geomorphic processes also help maintain channel complexity, which often includes shallow-water, seasonally inundated habitats on channel margins. These habitats are generated as a function of overbank flows (e.g., floodplains), point bar dynamics (e.g., scour channels on point bars and edge habitat), and inundation of former main channel positions. Shallow-water areas provide important rearing habitat for juvenile salmon (Lister and Genoe 1970, Bjornn and Reiser 1991), including the runs of Chinook salmon that occur in the Sacramento River basin (Sommer et al. 2001).

As with most aquatic riverine habitats, the formation and maintenance of secondary channels is a function of flow and sediment dynamics, both of which have been altered dramatically in the Sacramento River by the construction and operation of water storage and delivery systems and the installation of rock revetment along the river's banks. Flow regulation often reduces the frequency and magnitude of high flow events that drive the fundamental processes of bank erosion and meander migration, which are essential for creating OCWBs. Bank armoring activities are designed specifically to halt bank erosion and meander migration, thus preventing the creation of new OCWBs. However, other human activities may promote meander migration and concomitant channel cutoff, such as clearing of riparian vegetation within the river corridor.

Similarly, human activities influence the seasonal inundation of shallow-water habitat in the Sacramento River basin. For example, flow regulation has reduced the magnitude and frequency of high flow events, and levees have isolated the channel from its floodplains, thereby reducing the frequency, extent, and duration of floodplain inundation.

Understanding the processes controlling the evolution of off-channel water bodies (OCWBs) and seasonally inundated habitats within the bankfull channel is prerequisite to developing effective conservation and restoration strategies for these important habitat types in the Sacramento River. For example, the rate at which a former channel evolves from fully aquatic to terrestrial determines its persistence as aquatic habitat and its value to different species. Within the Sacramento River corridor, some oxbow lakes, such as Packer Lake and Old Packer Lake (Figure 1a), remain as open-water habitat for at least a century. Other oxbow lakes, such as Hartley Island (Figure 1b), are completely filled in within decades of their formation. Determining the factors that influence the evolution of OCWBs helps to inform the definition of management interventions to maintain existing units or to create new ones.

In the same way, it is important to understand what flow magnitudes are required to inundate shallow-water habitats that occur within the bankfull channel and thus provide habitat that supports multiple life history stages of different fish species. This study focuses on one type of shallow-water habitat—scour channels that form on point bars—to estimate the discharge magnitudes that inundate these features.

This technical report presents the results of a multi-disciplinary, multi-institutional, multi-year study that has combined funding from several different sources to optimize the amount and quality of data collected and analyzed. Funding sources include a CALFED grant administered by The Nature Conservancy (TNC), the Fulbright Alumni Incentives Award program administered by the Council for International Exchange of Scholars, and the French National Center for Scientific Research (CNRS). Appendix A displays investigators and their institutional affiliations.

2 STUDY OBJECTIVES AND SITES

2.1 Study Objectives

This study was guided by three objectives:

1. **Estimate the lifespan of existing OCWBs by estimating their rates of terrestrialization.**

It is unclear how human changes have influenced the lifespan of OCWBs in the Sacramento River. Flow regulation has generally reduced the frequency and magnitude of flood events that connect OCWBs with the mainstem channel, which in turn has reduced the frequency of events that either deposit or scour sediment in OCWBs. Also, changes in land use within the Sacramento River corridor have displaced riparian vegetation, substituting land uses such as agriculture, which contribute to higher rates of soil erosion (e.g., agriculture). As a result, fine sediment loading may be higher than occurred historically, thus increasing potential filling rates of OCWBs even if inundation occurs less frequently. By estimating the lifespan of existing OCWBs, we provide an indicator of how important it is to create new OCWBs (e.g., removal of bank armor coupled with high flow events) or preserve existing OCWBs (e.g., dredging OCWBs to increase their lifespan).

2. **Assess habitat conditions in OCWBs by monitoring water quality and mapping aquatic macrophytes.**

OCWBs vary in the type of species that they support, generally as a function of habitat characteristics that are influenced by the process of terrestrialization. For example, deeper OCWBs with open water habitat appear to provide better habitat for juvenile salmonids. In contrast, shallower OCWBs often support dense areas of aquatic vegetation (e.g., *Ludwigia*), which is more advantageous to a species like largemouth bass that can tolerate lower rates of dissolved oxygen and, as an ambush predator, can use the vegetation for concealment from prey. Habitat quality in OCWBs is also influenced by human activities such as agricultural runoff that can affect water quality. By monitoring water quality and mapping aquatic vegetation in existing OCWBs, we can make a coarse assessment of habitat conditions in them.

3. **Estimate the discharge magnitudes required to inundate scour channels on point bars to create seasonal, shallow-water habitat.**

The Sacramento River used to flood the Sacramento Valley extensively and frequently (Kelley 1989), creating an “inland sea” of shallow-water habitat that benefited multiple fish and avian species. However, flow regulation and levee construction have generally reduced the extent and frequency of floodplain inundation. Periodic flooding in the Yolo and Sutter bypasses provides vast increases in shallow-water habitat; however, these bypasses are located in the lower Sacramento River valley. In contrast, the middle Sacramento River, between Red Bluff (RM 243) and Colusa (RM 143), generally does not provide the same type of periodic expansion of shallow-water habitat. The middle Sacramento River is an important migratory corridor for juvenile salmonids, and shallow-water habitat provides important growth opportunities for salmonid fry. Faster growth can promote higher rates of survival for juvenile salmonids. As a result, it is important to identify ways to increase shallow-water habitat in the middle Sacramento River. This is especially true for the endangered winter-run Chinook salmon, because the seasonality of

inundation in the Yolo and Sutter bypasses generally does coincide with the fry dispersal period between August and December. There are several forms of shallow-water habitat that occur within the Sacramento River, often in association with point bars. Scour channels that form on point bars provides one type of seasonally inundated, shallow-water habitat within the bankfull channel (Figure 2). These shallow-water areas appear to provide rearing habitat for salmonid fry when they are inundated, but they can pose a stranding risk when they become disconnected from the channel (M. Limm, personal communication, May 1, 2005). Estimating the discharges that inundate these habitats and connect them with the mainstem channel can inform the definition of flow pulses to expand shallow-water habitat while simultaneously reducing stranding risk.

By pursuing these objectives, this study aims to inform the definition of management measures (e.g., flow releases, dredging) that create and maintain OCWBs and seasonally inundated, shallow-water habitat on point bars.

2.2 Study Sites

We sampled two different types of habitats: OCWBs and scour channels on point bars. As a result, the process used to select study sites differed for the two different habitat types.

2.2.1 Off-channel water bodies

An analysis of aerial photographs reveals that there are more than 70 OCWBs in the Sacramento River between Red Bluff (RM 243) and Colusa (RM 143). By necessity, the initial selection criterion was site access. OCWBs are not part of the navigable waterway, so access requires permission from landowners. We focused on OCWBs for which permission was likely to be granted, either because of public ownership or existing relationships with private landowners. Many of the selected study sites are within the Sacramento River National Wildlife Refuge, administered by the U.S. Fish and Wildlife Service and the Sacramento River Wildlife Area, administered by the California Department of Fish and Game. We conducted a reconnaissance-level field examination of candidate study sites. The selected study sites represent a wide range of OCWBs in terms of side-channel connectivity, age, and degree of terrestrialization. Our sample of 30 OCWBs between RM 236.8 and RM 161.2 represented the full range of OCWB types except for the very old, fully terrestrialized end member, and the very young cutoff channel that has not developed an alluvial plug at either end (Table 1).

Table 1. Ownership and parameters measured at off-channel water body study sites.*

Name	RM	Ownership	Sediment Depth (including date if sampled)		Sediment Sample	Macrophyte Survey	WSE	Water Quality (including date if sampled)		Water level changes during the receding of the March 06 flood + Sediment sampling	Cross-section survey
			X	Date				X	Date		
La Barranca	R 236.8	USFWS	X	08/13/05	X	X	X	X	11/05/05	X	
Ohm Right	R 234.8	USFWS	X	08/14/05				DRY		X	
Ohm Left	L 234	USFWS	X	10/16/05	X	X		DRY			
Kopta Slough North	R 221.7	TNC	X	09/02/05			X	X	11/10/05	X	
Kopta Slough Backwater	R 221.6	None	X	09/15/05	X	X		X	11/10/05	X	
Kopta Slough Main	R 218.4	State Parks	X	09/27/05	X	X		X	11/05/05	X	X
N/A	R 212	None	X	09/15/05	X	X		X	10/23/05		
Merrills Landing	L 212.7	DFG	X	08/15/05	X	X	X	X	11/11/05	X	
N/A	L 211	None	X	09/15/05	X	X		X	10/23/05		
Wilson Landing	L 203 205	DFG	X	09/24/05		X	X	X	11/05/05	X	
N/A	L 203	None	X	09/15/05	X	X		X	10/23/05		
Pine Creek Backwater	L 196	DFG	X	09/18/04							
Indian Fisheries	L 195	State Parks	X	08/16/05	X	X	X	X	11/05/05	X	
Jenny Lind Bend	R 195	DFG	X	09/19/04			X	DRY		X	X
N/A	R 194.3	TNC	X	09/13/05	X	X		X	11/07/05	X	
Capay	R 193.5	USFWS	X	08/31/05	X	X		X	11/08/05	X	X
N/A	R 192	USFWS	X	09/19/04				DRY		X	
Sam's Slough	R 190	USFWS	X					X	11/08/05	Phelan	Phelan
N/A	R 189	Private	X	09/13/05	X	X		X	11/05/05	X	
Lagoon	L 182.5	Llano Seco	X	10/19/05				DRY		X	
Duck Lake	L 180.8	Llano Seco	X	08/17/05				DRY		X	

Name	RM	Ownership	Sediment Depth (including date if sampled)		Sediment Sample	Macrophyte Survey	WSE	Water Quality (including date if sampled)		Water level changes during the receding of the March 06 flood + Sediment sampling	Cross-section survey
			X	08/22/05				X	10/08/05		
Jacinto	R 179.2	Llano Seco	X	08/22/05	X	X	X	X	10/08/05	X	X
N/A	R 178	None	X	10/18/05	X	X		X	11/08/05	X	
N/A	R 174	Private	X	09/24/05	X	X		X	11/08/05	X	
Beehive Bend	R 170	DFG	X	11/14/05	X	X	X	X	11/06/05	X	
Razor Slough	R 168.9	USFWS	X	11/17/05		X		DRY		X	X
Young Razor Slough	R 168.8	USFWS	X	09/25/05	X	X		DRY		X	X
Old Packer Lake	R 168.4	USFWS	X	09/25/05	X	X	X	X	11/06/05		
Packer Lake	R 167.2	USFWS	X	11/12/05		X	X	X	11/06/05	X	
Boggs Bend	L 161.2	DFG	X						11/06/05	X	

*Designation of "X" indicates that sampling of the indicated parameter(s) was conducted at the site.

2.2.2 Scour channels on point bars

We identified 44 candidate scour channel study sites using air-photo images from 1999, 2004, and 2005 to determine how channel planform location (i.e., curvature and wetted width), point bar dimensions, and vegetation patterns changed in recent time and at varying flow levels. Our air-photo analysis suggested that the processes and geomorphic conditions of the candidate study sites can be grouped into three general categories (Figure 3):

- **Type 1:** Channels that have been scoured behind active point bars, typically along the bank (i.e., within the bankfull channel at the edge of Sacramento River floodplain), with longitudinal axes oriented parallel to the mainstem. Some are supplemented laterally at high flow via point-bar spanning channels with planform morphology similar to what is seen on braided bars. The scour channels are generally perched above the main channel so that they are disconnected at both the inlet and outlet at low flows (Figure 4a). Scour holes within the scour channel often maintain residual pools after cessation of direct mainstem flow input, either from groundwater flow or simply via retention of water after connectivity with the mainstem is lost. In some sites, inlets are no longer distinct because of vegetation establishment and/or sediment deposition and shifts in the mainstem channel position that reduce the frequency of high flows breaching the point bar at the inlet.
- **Type 2:** Abandoned mainstem channels (or flow scars) on the insides of meander bends. Abandonment results from shifts in planform location, as a meander bend erodes its outer bank. These channels may alternatively be remnant channels from previous episodes of meander migration. Inlets are generally disconnected from the mainstem due to blockage by sediment deposits. In contrast, outlets are typically better connected with the mainstem because they are nearly at-grade with the channel bed. These Type 2 units differ from Type 1 scour channels with blocked inlets because they are not always within the bankfull channel, they have larger channel dimensions, and they have outlets that are not typically perched above the main channel. Mainstem inundation occurs via groundwater flow along the longitudinal axis and backwater flow from the outlet. Type 2 units are similar to sloughs, but they are generally smaller and they occur within the bankfull channel rather than the floodplain.
- **Type 3:** Former mainstem channels on the outsides of meander bends that have become ephemerally connected to the mainstem and are separated by small islands or perennially vegetated bars. Island formation differs from a full-blown meander bend cutoff event in that the mainstem cuts behind an active point bar, rather than across the river's floodplain. Inlets tend to be nearly at-grade with the mainstem channel bed, making them better connected than inlets of Type 1 and Type 2 units (Figure 4b). Outlets also tend to be nearly at-grade with the mainstem channel bed, such that outlet connectivity is similar to that of Type 2 units and greater than that of Type 1 units. Type 3 units resemble oxbow lakes, though they are smaller and they occur within the bankfull channel, rather than across the floodplain.

During a five-day field reconnaissance, we visited 32 of the 44 potential study sites. A subset of 17 sites was selected for monitoring of inundation and inlet and outlet connectivity (Table 2). The 17 sites were selected to span the range of morphologic types, while optimizing accessibility and estimated likelihood of capturing a range of inundation conditions for mainstem flows that were expected to occur during the study period (i.e., from 6,000 to 20,000 cfs).

Table 2. Summary of 17 seasonally inundated, shallow-water study sites selected for sampling in the Sacramento River between RM 243 and 184.

Site Number	RM	Bank	Number of Thermographs Installed	Number of Thermographs Recovered	Morphologic Type ¹
13	187	West	2	0	2
14	189	West	1	1	2
15	189.5	East	8	8	1
16	191	East	2	2	3
17	191.7	West	4	3	1 & 2 ²
22	203	West	7	7	1
23	203	East	2	2	3
25	208.9	East	8	8	1
27	211	East	2	2	3
30	219.9	East	3	0	1
31	220.4	East	4	1	1
33	221.6	West	5	5	1 & 2 ²
35	226.5	East	5	4	1
39	232.8	East	2	2	1
40	233.3	West	4	4	1
41	235.3	West	4	4	3
44	239.5	West	4	4	1

¹ See Figure 3 for illustration of morphologic types.

² In some cases, type 1 and type 2 channels coexist at a bend, joining together at the downstream end of the point bar, where the outlet of the abandoned channel intersects with the probe channel. At those sites, we focused our sampling along the probe channels and studied the connection between the abandoned channels and the probe channels.

3 METHODS

3.1 Analysis of Aerial Photographs and Historical Flow Data

We examined historical aerial photographs and historical flow data to estimate the age of OCWB study sites. We scanned, rectified, and analyzed aerial photographs of the middle Sacramento River (RM 243–143) dating from 1942, 1962, 1985, and 1999. We selected these photosets because they were flown during similar seasons and at similar discharges, which facilitates a time-series analysis of their evolution. Each photo was scanned at a resolution of 600-800 dpi. By analyzing a time series of aerial photographs, we were able to bracket the timeframe when a channel was cutoff from the mainstem channel. We then analyzed historical discharge records from intervening years between the aerial photo series to identify the high flow events that likely caused the channel to cutoff and an OCWB to form. In this manner, we were able to estimate the year in which an OCWB study site was formed for 12 of the 14 sampled sites.

We also used the aerial photographs to map the distribution and extent of OCWBs between RM 243 to RM 143, delineating the extent of open water, emergent aquatic vegetation, and riparian vegetation in each photo. We measured and tabulated basic descriptive data such as length, width, water surface area, vegetated surface, etc. We conducted a principal component analysis on the geometric characteristics of the OCWBs we measured from the 1999 aerial photos: surface area of the water body, sinuosity of the channel, length of the wetted former channels, length of the upstream plug, length of the downstream plug, and distance from the channel.

3.2 Survey of Sediment and Water Depths

We collected water and sediment depths in OCWB study sites. The depth of fine sediment in each study site, coupled with the estimated age of each site yielded by the analysis of aerial photos, allowed us to make an estimate of the sedimentation rate at each site.

We determined fine sediment depths by collecting sediment cores using a hand auger with a screw bit that penetrated fine-grained sediment quickly, but encountered resistance when it hit gravel. We assumed that the gravel surface defined the former channel bed at the time of cutoff. However, OCWBs with acute angles to the mainstem may have filled partially with gravel after the site was cut off from the mainstem channel, especially near their upstream ends. We considered this caveat when interpreting our results.

At the selected sampling sites, we collected at least three sediment cores—at an upstream, midpoint, and downstream location along the axis of each secondary channel. OCWBs that were inundated during the time of sampling were cored from a boat when flow magnitudes were sufficient to facilitate navigation. Access to OCWBs that were dry was by foot. All coring depths were ≤ 20 feet due to equipment limitations.

For inundated study sites, we measured water depth using a stadia rod.

3.3 Radiometric Dating

In collaboration with Dr. Rolf Aalto of the University of Washington, we conducted a ^{210}Pb analysis of an 80-cm long sediment core taken from the Packer Lake OCWB (RM 167.2). The radioisotope ^{210}Pb has been used with great success to measure rates of sedimentation in alluvial environments (Stokes and Walling 2003).

3.4 Water Surface Elevations and Flow Velocities

A flood event in March, 2006 inundated many of the study sites. We surveyed water-surface elevations (WSE) in study sites during the recession limb over the course of a week, recording WSEs for a wide range of discharge. At each sampled site, we established benchmarks to which WSEs could be related, and the California Department of Water Resources surveyed the benchmarks using a survey-grade GPS in a subsequent field effort. We also estimated flow velocities and direction in inundated OCWB study sites by tracking the movement of objects (e.g., oranges) placed in the water.

3.5 Cross-Section Surveys

We surveyed channel cross sections of seven OCWB study sites, as shown in Appendix A. We conducted the surveys using inflatable boats. Water depths were collected using a stadia rod. Where possible, we extended tapes across the channel for the survey, but in wider units we used stadia intercepts. We used the water surface only as a datum from which to develop channel bathymetry, but the water surface elevation itself was of no importance as the flows at which we surveyed different channels differed and were arbitrary.

3.6 Water Quality Sampling

We used a Hydrolab Minisonde (Hach, Loveland, Colorado) to monitor pH, water temperature, electrical conductivity, salinity, total dissolved solids (TDS) and dissolved oxygen in the OCWB study sites. To the extent possible, we sampled water quality in those OCWBs in which sediment coring and macrophyte mapping was conducted (Table 1). However, not all OCWB study sites were inundated during each sampling period, which prevented the collection of water quality data at some sites. To the extent possible, we also selected study sites to match those that were surveyed by a previous investigation conducted by Bornette and Morken in 2002. Water quality data included for analysis in this study were collected on the following occasions: June 2002, September 2004, October-November 2005, March 2006, November 2006, and April 2007.

3.7 Macrophyte Mapping

We mapped aquatic macrophytes in 21 OCWBs to better understand the composition and density of aquatic vegetation in these habitats (Table 1). The surveys identified the spatially dominant species of aquatic vegetation and estimated the percentage cover for each species. To the extent possible, we sampled aquatic macrophytes at sites surveyed during a prior investigation conducted in 2002 by Bornette and Morken.

3.8 Thermograph Deployment in Scour Channels on Point Bars

To identify periods of inundation in scour channels that form on point bars, we deployed data-logger thermographs (Stowaway Thermograph, Onset Computer Corporation, Bourne, MA) to continuously record temperatures at 15-minute intervals (Table 2). Previous research (Stillwater Sciences and Dietrich 2002) indicated that when the temperature recorders are exposed to the open air, diurnal fluctuations are more pronounced than when the recorders are inundated (Figure 5).

3.8.1 Thermograph set-up and calibration

Following the manufacturer's specifications, temperature was recorded in 0.16°C increments. Prior to installation, we calibrated the thermographs in tap-water and ice-water baths, to confirm the manufacturer-specified accuracy ($\pm 0.2^\circ\text{C}$), using United States National Institute of Standards and Technology (NIST) certified thermographs. Only thermographs passing an initial calibration check were deployed.

3.8.2 Field study implementation

Thermographs were deployed between 2/15/2007 and 2/21/2007. A total of 67 thermographs (47 dry and 20 wet) were placed at 17 point bar study sites; the number of thermographs deployed at each study site varied, ranging from 1 to 8 (Table 2). Thermographs were placed at a variety of morphologically significant points across the study sites, including: (i) points that would identify the initiation of water-surface connection between the mainstem and the study site inlets and outlets; (ii) points that would indicate longitudinal connectivity along the scour channel on the point bar (i.e., when isolated pools become connected with other portions of the study site and subsequently the mainstem); and (iii) points that would aid in quantifying lateral connectivity, and thus identify changes in wetted width and water depth within the study site. At some study sites, multiple thermographs were placed in a line oriented perpendicular to flow (i.e., in a cross-sectional array). Although the basic rationale for thermograph placement was consistent from site to site, there were places where deployment was precluded due to site-specific conditions. For example, at some sites the outlet was at or below grade with the mainstem channel bed, so that it was unlikely to disconnect during any of the flow magnitudes expected during the study period. Professional judgment was required to optimize the deployed array of thermographs according to the level of effort required, the number of thermographs available, and the data needs of the study.

At each temperature monitoring point, a steel stake was pounded into the channel or bank, and a thermograph was secured to the stake about 2 cm above the substrate with plastic cable ties. Each thermograph was given a unique numeric ID that matched the study site. UTM coordinates of thermographs were established using differential GPS (DGPS). At 10 of the sites, elevation control was also obtained, with 2-cm precision, by establishing benchmarks with the DGPS on dual-frequency carrier phase lock for a minimum of 60 minutes. Thermograph elevations were tied to the benchmark elevations using an auto-level. For cross-sectional arrays of thermographs, topographic cross-sections were also surveyed with the auto-level. At the seven sites that lacked monumented benchmarks, only 1 to 2 thermographs were installed. Relative elevations of those thermographs and water surface elevations were established using a hand-level in concert with the DGPS. The relative elevations are sufficient to establish the change in water surface stage required for local inundation or aerial exposure (depending on whether the thermograph was dry or wet at the time of deployment).

Several additional physical and biological parameters were inventoried at each study site during thermograph installation. The wetted area of each study site was mapped onto 2005 NAIP aerial photographs (which are 1-m orthophotos) printed at a scale of 1:3,000. Lengths and widths of both wetted and dry (i.e., that could potentially become wet) areas were measured using an Impulse Laser Range Finder (with 0.01-m manufacture-specified resolution). Water depths were measured in several locations with a stadia rod to determine the maximum and average depths at the time of thermograph deployment. At each site, we also estimated the percent coverage of the surface by the five major sediment grain size classes (i.e., silt/clay, sand, gravel, cobble, and boulder). Vegetation species growing in the wetted areas of the study sites were identified where possible, and visual estimates of the percent of the study site covered in submerged, floating, and emergent vegetation were also made. Fish observations were conducted from the banks or wetted edges of the inundated portion of study sites, and for deeper sites with good water clarity, a mask and snorkel were used. Observations of fish included the species, frequency, and size class where possible. Turbidity was qualitatively assessed based on a visual scale of 0–4 (i.e., 0 = clear, 4 = no visibility).

Thermographs were removed on 4/25/2007 and 4/26/2007 following 65 to 70 days of deployment. We recovered 57 of the 67 installed thermographs (Table 2). All of the missing thermographs are assumed stolen because: 1) the precision of the DGPS supported a high recovery rate of most thermographs, allowing us to reoccupy installation locations within 0.5 m, including one thermograph that was buried in sediment; 2) the majority were lost at three sites where the missing rate was 100%, suggesting systematic removal of the thermographs; and 3) thermographs disappeared from relatively high elevation points which had relatively low risk of scour and/or deposition and higher risk of being found by human traffic. During thermograph removal, wetted areas were mapped for a second time on 1-m 2005 NAIP imagery. For study sites where the mainstem was at a similar discharge during removal and installation, mapping during removal amounted to a ground truthing of the original mapping.

3.8.3 Data QA/QC and analysis

3.8.3.1 Post-recovery thermograph calibration

Prior to downloading data, all recovered thermographs were subjected to a post-recovery calibration check following methods described above. Following the post-recovery calibration check against NIST certified thermographs, 51 of the 57 recovered thermographs were found within the manufacturer's specified accuracy; 5 of the 6 thermographs that did not pass were just outside the specified accuracy range and had to be adjusted 0.1 to 0.3°C following the methods described by Wagner et al. (2000). One thermograph (thermograph ID #15-6) was further out of range and had to be adjusted 1.3°C. Although the precision of thermograph #15-6 would be too low for some applications, its temperature trends coincide with the temperature trends of the other 7 thermographs deployed at study site 15. This implies that it reliably depicts the timing of inundation and aerial exposure, making it sufficient for the purposes of this study.

3.8.3.2 Determination of inundation vs. aerial exposure

The calibrated temperature record for each thermograph was converted into a time series of alternating inundated and sub-aerial exposure records. Dry thermographs exhibit larger magnitude diurnal temperature variations and correspondingly faster rates of temperature change relative to wet thermographs, due to the higher heat capacity of water relative to air (Figure 5). Additional evidence was used to help delineate wet and dry conditions including:

- Air and water temperature records from Red Bluff Diversion Dam and air temperature and precipitation records from Chico were used to characterize the general temperature and storm patterns for the region during the study period.
- Direct observations of the status (i.e., wet vs. dry) of each thermograph at two discharges, during installation and removal. We were able to couple these observations with surveyed elevation differences among thermographs at some sites, to establish whether the inundation (or sub-aerial exposure) of one thermograph implies inundation (or sub-aerial exposure) of others.
- Comparative analyses using thermographs with known, constant status. Based on site layout, thermograph elevations, thermograph records, and the flows that occurred during the study period, we determined that some thermographs never became wet or dry within the study period. Temperatures recorded on these thermographs were used to determine when other thermographs were wet or dry. For example, inundation would be clearly indicated if a thermograph's temperature pattern first matched the pattern of a known dry thermograph and then rapidly deviated from it.
- Observations of lagged temperature responses for shallowly submerged sites (usually disconnected from the mainstem at the inlet), where the magnitude of diurnal temperature fluctuations can be similar to those observed in dry thermographs, due to the lack of incoming water and disconnection from the mainstem. Our observations indicate that the temperature response in shallow water lags 3 to 4 hours behind what we observe at sub-aerially exposed sites, particularly during the evening when temperature cooling in shallow pools occurs later and at a slower rate than dry sites, but may nevertheless approach or equal dry site temperatures by early morning.
- Correlation with other inundated and sub-aerially exposed events. The majority of thermographs were installed dry. If they became inundated, it typically occurred three times during short duration peak flows, separated by 2.5 days in the first half of the monitoring period. This helped establish a consistent relationship between discharge and inundation, which could be used to help identify the threshold discharge if the temperature signal was not definitive for one of the three peak flow events, as was the case with the second peak flow which deviated from the typical diurnal temperature pattern due to a concurrent storm event.

3.8.3.3 Flow data

Data from 4 CDWR flow gauges were analyzed for comparison with the thermograph temperature data (Table 3). Peak flow for the study period ranged from 14,724 to 17,040 cfs across the gauges, whereas minimum flow ranged from 6,150 to 7,123 cfs. In comparison, bankfull discharge on the mainstem Sacramento River is estimated at 88,300 cfs post Shasta Dam construction (Thomas 2000).

Table 3. CDWR flow gauges on the Sacramento River used for thermograph analysis from 2/15/2007 to 4/26/2007.

Gauge	RM	Max flow (cfs)	Min flow (cfs)
Bend Bridge	261.4	15,100	6,150
Vina Woodson Bridge	218.2	17,040	6,918
Hamilton City	199.3	14,724	6,202
Ord Ferry	184	15,577	7,123

The three highest flows at the gauges occurred between 2/22/07 and 3/1/07 and were characterized as three distinct peaks separated by about 2.5 days that had relatively quick rising and recessional limbs (Figure 6). A lower magnitude peak flow occurred near the end of the monitoring period, on 4/22/2007, following a brief spring storm. Flows were relatively low between mid-March and the late April storm, with the extreme lows for the study period occurring from 3/24 to 3/26/2007.

Because some deployed thermographs were located as far as 20 miles from the nearest flow gauge, it was necessary to adjust the time stamp of the flow data for comparison with the temperature data. To estimate a reasonable time-stamp adjustment for the comparative analysis, we calculated lag times for the arrival of flow peaks at the gauges for each of the three peak flows during the 2/22/07 to 3/1/07 interval. When coupled with the distance between the gauges, the lag times can be used to estimate the speed of flow peaks, which in this case averaged 4.5 mi/hr (± 0.5 mi/hr, $n = 15$). We used this speed to adjust the time stamps of the flow data of the relevant gauge to each site. For example study site 14 is located at RM 189, which is about 5 miles upstream of the Ord Ferry Gauge. For site 14, 1 hour was subtracted from flow data time stamps at Ord Ferry, so that a flow occurring at 8:00 AM at Ord Ferry was considered to be the local flow condition at 7:00 AM at site 14.

This adjustment should be reasonable, given that the majority of inundation and subsequent dry cycles at our study sites occurred during the three late February peak flows and 4.5 mi/hr rate is calculated specifically from these events. Once time stamps were adjusted, we were able to estimate local flow conditions during thermograph installation and removal and also at the time of inundation and subsequent sub-aerial exposure, based on temperature data from the thermographs (Table 4). Flow at the threshold of inundation was consistent for most thermographs, suggesting that the method of adjusting flow time stamps worked well. Nevertheless, some error is expected in matching gauge discharge with thermograph records due to separation distance. The amount of error associated with adjusting the time stamp of flow gauges is unknown, but the relatively consistent agreement between threshold flows for inundation during three peaks storms (with different sloped hydrographs during both rising and recessional limbs) suggests the method of time adjustment was reasonable. Discharges reported in this study are rounded to the nearest 100 cfs, in part, to reflect this uncertainty.

Table 4. Study site locations and flows during thermograph installation and removal.

Study site	River mile	Corresponding flow gauge	Flow ¹ during (cfs):	
			installation	removal
13	187	Ord Ferry	8,600	7,600
14	189	Ord Ferry	8,600	7,600
15	189.5	Ord Ferry	8,600	7,600
16	191	Ord Ferry	8,500	7,600
17	191.7	Ord Ferry	8,500	7,600
22	203	Hamilton City	7,600	6,700
23	203	Hamilton City	7,600	6,700
25	208.9	Vina Woodson	7,900	8,800
27	211	Vina Woodson	7,900	8,800
33	221.5	Vina Woodson Bridge	8,100	8,900
35	226.5	Vina Woodson Bridge	8,900	8,900
39	232.8	Vina Woodson Bridge	8,900	9,000
40	233.3	Vina Woodson Bridge	8,900	8,900
41	235.3	Vina Woodson Bridge	9,300	8,900
44	239.5	Bend Bridge	9,500	8,900

¹ All flows are based on data from nearest gauge after adjusting for time lag of 4.5 mi/hr (see Section 3.8.3.3).

The assumed 4.5 mi/hr travel time for flow is not expected to be representative of all peak flow events, because storm patterns, tributary and reservoir discharges, and ground saturation levels are likely to vary and affect the travel time. 4.5 mi/hr is also likely not representative of travel times for the low flow period of the study. However, given that stage tends to change slowly during non-storm periods, with discharges often remaining stable for several hours during low flow periods, using the 4.5 mi/hr time adjustment is assumed to be reasonable for our study purposes.

3.8.3.4 GIS analysis

Wetted areas were mapped by hand onto aerial photographs during thermograph deployment and retrieval and were digitized and projected into UTM NAD 1983, Zone 10N using ArcMap 9.2 software. These wetted area polygons were calibrated in the office by comparing the dimension of the digitized polygons with length and width measurements taken with the Laser Range Finder. Areas (m²) were calculated for each wetted polygon and divided into wetted polygons that are either connected to (by inlet and/or outlet) or disconnected from the mainstem.

After determining the discharges required to inundate (or expose to air) the thermographs, we identified the likely boundaries of inundated areas at different discharges, based on observed hydraulics, connectivity, survey data, and field sketches of features and slope breaks at elevations similar to those of the thermographs. For example, at one site, a thermograph was installed dry on an elevated bench (i.e., a terrace within the active channel) outside the wetted channel. We mapped the back edge of the bench onto air photos as the assumed boundary of inundation, should the thermograph installed on bench ever become inundated. When it eventually became

inundated, we assumed that the entire trace of the bench was wet when digitizing new polygons for the elevated flow levels. Key assumptions of this approach include: (i) surveyed cross-sections are often assumed to be representative of the adjoining channel up to several hundred meters, (ii) effects of channel slope within a study site are often disregarded (i.e., slope is assumed to be zero), and (iii) field judgment used to place thermographs at hydraulic control points is assumed to be accurate. These assumptions introduce significant, but difficult-to-quantify, uncertainties in our calculations of inundation areas.

4 RESULTS

4.1 Analysis of Aerial Photographs and Historical Flow Data

By examining a time series of aerial photographs, coupled with discharge data, we were able to estimate the age of several OCWBs in the Middle Sacramento River corridor (Table 5)

Table 5. Estimated age of off-channel water bodies in the Middle Sacramento River.

Name	River Mile	Date of cutoff		Age as of 2007
		beginning	end	
La Barranca	R 236.8	1991	1997	11
Ohm right side	R 234.8	1964	1969	38.5
Ohm left side	L 234	1991	1997	11
Kopta Slough North	R 221.7	1964	1969	38.5
Kopta Slough Backwater	R 221.6	1964	1969	38.5
Kopta Slough Main	R 218.4	1937	1946	63.5
Merrills Landing	L 212.7	1991	1997	11
N/A	R 212	1991	1997	11
N/A	L 211	1991	1997	11
Wilson's Landing	L 203-205	1976	1981	26.5
N/A	L 203	1976	1981	26.5
Pine Creek Backwater	L 196	1976	1981	26.5
Indian Fisheries	L 195	1937	1946	63.5
Jenny Lind Bend	R 195	1937	1946	63.5
N/A	R 194.3	1964	1969	38.5
Capay	R 193.5	1964	1969	38.5
N/A	R 192	1976	1969	32.5
Sam's Slough	R 190	1870	1870	135
N/A	R 189	1964	1969	38.5
Lagoon	L 182.5	1896	1908	103
Duck Lake	L 180.8	1870	1870	135
Jacinto	R 179.2	1960	1964	43
N/A	R 178	1991	1997	11
N/A	R 174	1991	1997	11
Beehive Bend	R 170	1923	1935	76
Rasor Slough	R 168.9	1870	1870	135
Young Rasor Slough	R 168.8	1960	1964	43
Old Packer Lake	R 168.4	1870	1870	135
Packer Lake	R 167.2	1870	1870	135
Boggs Bend	L 161.2	1937	1946	63.5

Based on cluster (ordination) analyses performed on principal components derived from a principal component analysis of the geometric characteristics of the former channels visible on 1999 air photos (Figure 7), we distinguish four distinct geometric types as a function of their straightness and proximity/hydrologic connection to the main channel:

- S1 = straight former channels close to the main channel
- S2 = straight former channels with a strong downstream connection
- M1 = meander former channels (long, sinuous and with a high surface area) far from the main channel
- M2 = meander former channels (long, sinuous and with a high surface area) close to the channel on its downstream entrance

4.2 Survey of Sediment and Water Depths

Our preliminary data show a range of sedimentation rates, ranging from 0 m to more than 5 m. The most commonly encountered sediment thickness is about 2 m (Figure 8). When we look at sedimentation rates as a function of age of the cut-off channel, we find a greater spread in rates among the recently cut-off channels (ranging from zero to 18 cm/year for cutoffs approximately a decade old) than in older cutoffs (ranging from 1 to 5 cm/y for 130-y-old cutoffs) (Table 6), Figure 9). Older OCWBs may have more consistent sedimentation rates because of the tendency for year-to-year variations in sedimentation rates to even out over time. OCWBs that initially fill rapidly will more quickly reach higher elevations, which require larger (and thus less frequent floods) to be inundated. Thus, their sedimentation rates will decrease over time. Channels that begin with slower sedimentation rates will remain at a lower elevation and thus continue to receive sediment over a longer time period than channels that fill rapidly and thus achieve elevations above the elevation of frequent inundation.

Table 6. Sedimentologic characteristics of OCWB study sites in the Middle Sacramento River.

Name	River Mile	Ownership	Age of cut-off (years)	Number of cores	Average sedimentation depth (cm)	Average sedimentation rate (cm/year)
La Barranca	R 236.8	USFWS	11	9	81.9	7.4
Ohm left side	L 234	USFWS	38.5	1	155.0	4.0
Ohm right side	R 234.8	USFWS	11	5	199.6	18.1
Kopta Slough North	R 221.7	TNC	38.5	8	201.4	5.2
Kopta Slough Backwater	R 221.6	None	38.5	5	76.2	2.0
Kopta Slough Main	R 218.4	State Parks	63.5	5	22.8	0.4
Merrills Landing	L 212.7	DFG	11	7	173.8	15.8
N/A	R 212	None	11	2	41.0	3.7
N/A	L 211	None	11	5	73.7	6.7
Wilson Landing	L 203-205	DFG	26.5	4	171.0	6.5
N/A	L 203	None	26.5	4	107.5	4.1
Pine Creek Back Water	L 196	DFG	26.5	5	274.6	10.4
Indian Fisheries	L 195	State Parks	63.5	4	339.7	5.3
Jenny Lind Bend	R 195	DFG	63.5	8	250.2	3.9
N/A	R 194.3	TNC	38.5	9	25.4	0.7
Capay	R 193.5	USFWS	38.5	5	151.6	3.9
N/A	R 192	USFWS	32.5	5	383.8	11.8
Sam's Slough	R 190	USFWS	135	2	268.5	2.0
N/A	R 189	Private	38.5	9	29.6	0.8

Name	River Mile	Ownership	Age of cut-off (years)	Number of cores	Average sedimentation depth (cm)	Average sedimentation rate (cm/year)
Lagoon	L 182.5	Llano Seco	103	1	296.0	2.9
Duke Lake	L 180.8	Llano Seco	135	2	453.0	3.4
Jacinto	R 179.2	Llano Seco	43	10	166.5	3.9
N/A	R 178	None	11	5	200.2	18.2
N/A	R 174	Private	11	7	0.0	0.0
Beehive Bend	R 170	DFG	76	6	232.8	3.1
Rasor Slough	R 168.9	USFWS	135	1	545.0	4.0
Young Rasor Slough	R 168.8	USFWS	43	5	149.8	3.5
Old Packer Lake	R 168.4	USFWS	135	1	467.0	3.5
Packer Lake	R 167.2	USFWS	135	4	249.5	1.8
Boggs Bend	L 161.2	DFG	63.5	3	175.0	2.8

Water depths (measured at various times during the year) varied among former channels. Some had consistently shallow depths of less than 1 m (e.g., 221.7 RM), while others had depths exceeding 3 to 4 m (Figure 8).

4.3 Radiometric Dating of Former Channel Sediments

Figure 10 illustrates the preliminary results from the ²¹⁰Pb analysis of the sediment core collected from Packer Lake (RM 167.2). The upper fill of the lake consists entirely of fines, signifying that the sediment core contains only material delivered by suspended load. The lack of significant peaks in the activity of ²¹⁰Pb implies that rates of sedimentation have been uniform through the recent past at Packer Lake. Converting the decay units of the ²¹⁰Pb data into units of sedimentation indicates an average overbank sedimentation rate in Packer Lake of 0.42 cm/yr.

4.4 Water Surface Elevations and Velocities

4.4.1 Water surface elevations

Analysis of stage data show some interesting differences among study sites, reflecting differences in hydrologic connectivity. For example, some sites remained well-connected to the mainstem, and experienced fluctuations that mimicked mainstem stage changes, while in others the fluctuations were muted, though in the same sense as the mainstem stage changes, reflecting the influence of floodplain water table changes, rather than a direct surface-water connection to the main channel. Stage-discharge relations during recession limb of the March 2006, with 0 stage set at the highest flow we measured at each site, are shown for the mainstem at Woodson Bridge and Hamilton City, and for five OCWBs, in Figure 11. For each site shown, the point along the zero line at the top of the figure represents the highest reading (at the beginning of our period of measurement during the flood's recession limb). The later observations are along the line descending to the left. The mainstem lines show linear declines. The OCWBs with straight lines reflect good connection between side channel and mainstem, while the non-linear traces reflect poor connection to the main channel.

4.4.2 Surface velocities

Surface velocity measurements during the recession limb of the March 2006 flood for each OCWB are presented in Figures 12a and 12b. The x-axis is labeled with the name of the OCWB for each velocity measurement. If the velocity was zero, no bar is visible. If velocity was negative (i.e., water flow in the upstream direction), the bar extends downward from the zero line. If velocity was positive (i.e., downstream), the bar extends upward. So that the figures are readable, we present the data for the complete set in two figures: Figure 12a presents data for Beehive Bend, Boggs Bend, Capay, Duck Lake, Indisan Fisheries, Jacinto, Jenny Lind Bend, Kopta Main, Kopta Backwater, Kopta North, and La Barranca. Figure 12b presents data for Lagoon, Merrills Landing, Old Razor Slough, Packer Lake, Phelan Island, R174, R178, R189, R192, R194, Wilson Landing, and Young Razor Slough.

From the plots in Figures 12a and 12b, we can identify some distinctive groups of OCWBs:

1. Those with active velocity whatever the discharge (e.g., R194, R174)
2. Those with active velocity but strong decrease in velocity with increasing discharge (e.g., R189, Phelan)
3. Those whose velocity decreased slowly with increasing discharge (e.g., Capay, Jacinto, Merril Landing, Lagoon, Wilson Landing, Indian Fisheries),
4. Those with no velocity whatever the discharge (e.g., Beehive, Duke, Jenny, Kopta main, Kopta North, Kopta Backwater, La Barranca, Ohm Right, Young Razor, Old Razor, Packer Lake), and
5. One with negative velocity with increasing discharge (R178).

These velocity observations provide clear evidence of the differing degrees of hydrologic connectivity with the mainstem Sacramento River among the OCWBs studied. For example, R178, R189, and R194 are all S2-type OCWBs and function as connected secondary channels, with relatively high velocities in the downstream direction. Some others were connected only at their maximum stage (roughly a Q5), such as the S-1 type OCWBs Jacinto, Kopta North, Lagoon, and Phelan, the M-1-type OCWB Merrills Landing, and the M-2 type OCWBs Wilson Landing and Indian Fisheries. Capay was unique as an S-2 connected with positive velocities for our first two observations at the beginning of the flood, but whose connection was severed as the stage declined. Finally, we measured no velocity in some OCWBs, such as the M-1 type OCWBs Beehive Bend, Boggs Bend, and Packer Lake, the M-2 type OCWBs Duck Lake, Old Razor, and Jenny Lind Bend, the S-1 type OCWBs Kopta Main and Ohm Right, and—surprisingly given their plan geometry—the S-2 type OCWBs Kopta Backwater and Young Razor Slough.

4.5 Cross Section Surveys

Figures 13-19 show cross sections of OCWB study sites in the Sacramento River surveyed in March 2006 (with follow-up surveys at lower flows as needed). The x-axis is horizontal distance (m) across the channel (left bank to right bank unless otherwise noted) and the y-axis is elevation (m) above an arbitrary datum. Note that some of the legends use French terms: *terrain* is ground surface, *eau* is water surface elevation, *niveau fin* is the base of the fine-grained sediment accumulated over the former channel gravel, and *arbustes immerges* is bushes submerged by water. These cross sections demonstrate the narrowing that has occurred post-cutoff. The main channel width is roughly 100 m, but the abandoned channels have narrowed, most to around 60 m (Capay to about 30 m). The depth of fine sediment shown for Phelan (Figure 13) is consistently about 3 m across this channel.

4.6 Water Quality and Aquatic Macrophyte Survey

Preliminary results of vegetative transect surveys to date are presented in Table 7. We seek to better understand the distribution of *Ludwigia* as a function of hydrologic connectivity, water quality (as influenced by surrounding land uses, groundwater exchange, etc.), and other factors.

Table 7. Occurrence of vascular plant species during surveys of off-channel water bodies.

Species	Location (RM)																													
		G4	G5	G7	G6	G8	174 R	D12 bis	D13	D12	G10	178 R	G11	G11	G13 bis	194 R	D26	G15 bis	D29	203 L	211 L	212 R	D33	G26	222 R	G34	G33v	G33	G33m	247 meander
<i>Azolla mexicana</i>		0	0	0	0	0	1	0	0	0	0	0	0	1	0	0	0	0	0	0	0	0	0	0	0	1	0	1	0	0
<i>Ceratophyllum demersum</i>		1	0	1	0	0	1	0	1	1	1	0	1	1	1	0	1	1	1	1	1	1	0	0	1	1	1	1	1	1
<i>Echinochloa muricata</i>		0	0	0	0	0	0	0	0	0	1	0	0	0	0	0	0	0	0	0	0	0	0	0	0	0	0	0	0	0
<i>Egeria densa</i>		0	0	0	0	0	0	0	0	0	0	0	0	0	1	0	0	1	0	1	0	0	0	0	1	1	0	0	0	0
<i>Elodea canadensis</i>		0	0	0	0	0	0	0	0	0	0	0	0	0	0	0	0	1	0	1	1	0	0	0	1	0	0	1	0	
<i>Elodea nuttallii</i>		0	0	0	0	0	0	0	0	0	0	0	0	0	0	0	0	1	0	0	1	0	0	0	1	1	0	1	1	
<i>Hibiscus californicus</i>		0	0	0	0	0	0	0	0	0	1	0	0	0	0	0	0	0	0	0	0	0	0	0	0	0	0	0	0	0
<i>Juncus effusus</i>		0	0	0	0	0	0	0	0	0	1	0	0	0	0	0	0	0	0	0	0	0	0	0	0	0	0	0	0	0
<i>Leersia oryzoides</i>		0	0	0	0	0	0	0	0	0	1	0	0	0	0	0	0	0	0	0	0	0	0	0	0	0	0	0	0	0
<i>Lemna minor</i>		0	0	0	0	0	0	0	0	0	0	0	1	1	1	0	0	0	0	0	0	0	0	0	0	1	1	1	0	0
<i>Lemna minuscula</i>		0	0	0	0	0	0	0	0	0	0	0	0	1	0	0	0	0	0	0	0	0	0	0	0	0	0	0	0	0
<i>Lemna minuta</i>		0	0	0	0	0	0	0	0	0	0	0	0	0	0	1	0	0	0	0	0	0	0	0	0	0	0	0	0	0
<i>Limnobium spongia</i>		0	0	0	0	0	0	0	0	0	0	0	0	1	0	0	0	0	0	0	0	0	0	0	0	0	0	0	0	0
<i>Ludwigia peploides</i> ssp. <i>montevidensis</i>		1	0	1	0	1	1	1	1	1	1	1	1	1	0	0	1	0	1	0	1	1	1	1	1	1	1	1	1	1
<i>Myriophyllum aquaticum</i>		0	0	0	0	0	0	0	0	0	0	0	0	0	0	0	0	0	0	0	1	0	1	0	0	1	0	1	1	
<i>Myriophyllum spicatum</i>		0	0	0	0	0	0	0	0	0	0	0	0	0	1	0	0	1	0	1	1	0	0	0	1	0	0	1	1	
<i>Nymphaea odorata</i>		0	0	0	0	0	0	1	1	1	0	0	0	0	0	0	0	0	0	0	0	0	0	0	0	0	0	0	0	0
<i>Phalaris</i> sp.		0	0	1	0	0	0	0	0	0	0	0	0	0	0	0	0	0	0	0	0	0	0	0	0	0	0	0	0	0
<i>Polygonum hydropiperoides</i>		0	0	0	0	0	0	0	0	0	1	0	0	0	0	0	0	0	0	0	0	0	0	0	0	0	0	0	0	1
<i>Polygonum punctatum</i>		0	0	0	0	0	0	0	0	0	1	0	0	0	0	0	0	0	0	0	0	0	0	0	0	0	0	0	0	1
<i>Potamogeton crispus</i>		0	0	0	0	0	0	0	0	0	1	0	0	0	0	0	1	0	0	0	0	0	0	0	0	0	0	1	1	

Table 8. Average water quality measurements for OCWB sites.

Site Name	RM	Number of Samples (n)	Temp. (°C)	Dissolved Oxygen (%)	Conductivity (µS/cm)	Salinity (g/L)	TDS (g/L)	pH
Bogg's Bend	161.5L	1	11.09	93.50	109.50	0.04	0.07	8.02
Packer Lake	167.2R	5	17.21	50.20	167.18	0.08	0.11	7.79
Old Packer Lake	168.4R	3	23.93	96.23	266.47	0.13	0.17	8.14
Young Razor	168.6R	4	22.69	112.30	249.31	0.12	0.16	8.39
Old Razor Slough	168.8R	4	24.79	71.88	319.33	0.16	0.21	7.95
Beehive Bend	170R	5	18.04	48.82	349.10	0.17	0.22	7.70
N/A	174R	2	11.04	107.15	132.50	0.06	0.08	8.35
N/A	178R	4	17.72	58.38	190.98	0.09	0.12	7.88
Jacinto	179.2R	5	16.40	65.78	301.26	0.15	0.19	8.14
Duck Lake	180.8L	1	13.32	53.20	146.80	0.06	0.09	7.65
Lagoon	182.5L	1	11.09	108.90	126.40	0.05	0.08	7.97
N/A	189R	2	13.39	156.25	522.20	0.27	0.33	8.17
Sam's Slough / Phelan Island	190R	3	19.69	64.00	1211.93	0.64	0.78	8.01
N/A	192R	2	18.41	22.48	426.25	0.22	0.27	7.98
Capay	193.5R	2	16.58	41.95	590.20	0.31	0.38	7.92
Jenny Lind Bend	194.5R	1	31.92	99.13	168.60	0.07	0.11	8.19
N/A	194.3R	3	16.36	89.67	129.44	0.05	0.08	8.27
Indian Fisheries	195L	5	20.65	87.85	563.37	0.29	0.42	8.54
N/A	203L	1	19.75	153.30	241.80	0.11	0.15	7.73
Wilson's Landing	203-204L	4	20.63	127.12	647.45	0.33	0.41	7.71
N/A	211L	1	17.04	54.60	130.30	0.05	0.08	7.64
N/A	212L	1	18.22	24.00	152.10	0.07	0.10	7.58
Merrills Landing	213-214L	4	17.98	25.77	324.35	0.18	0.21	7.57
Kopta Main	218.4R	4	17.47	91.29	172.92	0.08	0.11	7.58
Kopta Slough Backwater	221.6R	1	15.62	49.40	219.50	0.10	0.14	7.80
Kopta North	221.7R	1	15.44	69.40	252.50	0.12	0.16	7.49
Ohm	234.8R	2	28.66	107.62	369.78	0.18	0.24	7.76
La Barranta	236.8R	4	17.53	40.40	231.79	0.15	0.15	7.87
Sacramento River	Hamilton City Bridge	2	16.37	75.95	115.25	0.05	0.07	8.08

Average percent dissolved oxygen saturation rates at the sites ranged from 22.48% to 156.25%. The average percent dissolved oxygen was over 90% for approximately 40% (11) of the sites. Average conductivity measurements ranged from 109.50 to 1211.93 $\mu\text{S}/\text{cm}$, average salinity rates ranged from 0.04 to 0.64 g/L, and average TDS rates ranged from 0.07 to 0.78 g/L. Since conductivity, salinity, and TDS measurements all relate to the concentration of particles in the water, the low measurements for these parameters all occurred at the same site (Bogg's Bend) and the high measurements also all occurred at the same site (Sam's Slough/Phelan Island). Average pH measurements ranged from 7.49 to 8.54.

In Figure 20, conductivity measurements are shown for seven different OCWB sites taken at three different discharge rates of the Sacramento River. For all of the sites but one (Giesbrecht North), conductivity decreased as river discharge increased. In comparing conductivity measurements taken at various river discharges, preliminary results suggest that the greater the river discharge and thus the greater the hydrological connection to the main channel, the lower the conductivity measurements of the OCWB.

4.7 Scour Channels on Point Bars

Results from the habitat surveys are summarized for the 15 sites where thermographs were recovered. A majority of study sites (11 out of 15) were dominated by substrates finer than 2 mm (i.e., clay, silt, and sand) (Table 9). A majority of sites (13 out of 15) also have *Ludwigia* growing within their wetted areas (Table 9; Photo 1). *Ludwigia* is an invasive plant often found in OCWBs and other slack-water areas. The maximum water depth was 1.8 m whereas average water depth ranged from 0.2 to 0.7 m across the sites. Fish were observed at 6 of the 15 sites. With the exception of the adult green sunfish (*Lepomis cyanellus*) observed at site 13, all fish were of juvenile age class. Juvenile Chinook salmon (*Oncorhynchus tshawytscha*) were observed at four of the sites, with estimated number observed ranging from 50 to 320. Juvenile Sacramento Sucker (*Catostomus occidentalis*) and Sacramento pike minnow (*Ptychocheilus grandis*) were also observed.

Table 9. Summary of habitat data from 15 scour channels on point bar study sites on the Sacramento River.

Study Site	RM	Avg. Water Depth (m)	Max. Water Depth (m)	Dominant Substrate	Vegetation Surveys				Fish Species Observed		
					<i>Ludwigia</i> present	% emergent	% submerged	% floating	Species ¹	Count	Length Class (mm)
13	187		0.05	Gravel	No	5	0	0	LECY	50-100	150-220
14	189	0.46	0.58	Silt/ Sand/ Clay	Yes	5	1	0	None		
15	189.5	0.57	1.31	Silt/ Sand/ Clay	Yes	30	15	30	ONTS CAOC PTGR	100 75 465	40-80 40-80 40-80
16	191	N/A	N/A	Silt/ Sand/ Clay	Yes	5	5	5	None		
17	191.7	0.55	1.10	Silt/ Sand/ Clay	Yes	30	10	20	None		
22	203	0.4	1.37	Gravel	Yes	NA	NA	NA	ONTS RUTI	50 10	40-60 60-80
23	203	0.18	0.37	Gravel	No	0	0	0	None		
25	209	0.39	1.10	Silt/ Sand/ Clay	Yes	0	5	5	ONTS	130	40-60
27	211	0.69	1.28	Silt/ Sand/ Clay	Yes	0	2	0	None		
33	221.6	0.52	0.64	Silt/ Sand/ Clay	Yes	10	20	25	None		
35	226.5	0.7	0.73	Silt/ Sand/ Clay	Yes	1	15	0	None		
39	232.8	0.3	1.83	Silt/ Sand/ Clay	Yes	0	10	0	PTGR	50	20-60
40	233.3	0.4	0.98	Silt/ Sand/ Clay	Yes	1	40	2.5	None		
41	235.3	0.5	1.34	Silt/ Sand/ Clay	Yes	1	1	1	None		
44	239.5	0.69	0.99	Gravel	Yes	1	1	1	ONTS CAOC	320 5	20-80 40-60

¹ ONTS- Chinook salmon, CAOC- Sacramento sucker, PTGR Sacramento pike minnow, LECY-Green sunfish

Results from our analysis of threshold flows, maximum water temperatures, and inundation area at different discharges are summarized in Tables 10 and 11 along with references to relevant figures for each thermograph and study site. We present detailed results from four study sites: 15 (RM 189.5), 22 (RM 203), 25 (RM 209), and 44 (RM 239.5) in the sub-sections below. These sites were some of the more complex sites we monitored with a wide array of thermographs, and were also the four sites where juvenile Chinook salmon (*Oncorhynchus tshawytscha*) were observed. Detailed descriptions of the results for the remaining sites can be found in Appendix A.

Table 10. Thermograph installation and monitoring summary.

Thermograph ID	Wet vs. dry @ install	Inferred threshold flow¹ (cfs)	Number of inundation cycles during study period	Max temp when wet (°C)	Relevant Figure #'s
13-1	Wet	NA	not recovered	NA	21
13-2	Dry	NA	not recovered	NA	21
14-1	Dry	13,400	3	14.0	22-23
15-1	Dry	12,200	3	11.8	24-25
15-2	Dry	9,800	1	13.0	24-25
15-3	Dry	12,200	3	13.8	24-25
15-4	Dry	14,700	1	15.5	24-25
15-5	Dry	12,000	3	14.6	24-25
15-6	Dry	12,200	3	12.7	24-25
15-7	Dry	NA	always dry	NA	24-25
15-8	Wet	NA	always wet	28.8	24-25
16-1	Wet	8,000	4	18.1	26-27
16-2	Dry	12,000	2	10.7	26-27
17-1	Dry	NA	always dry	NA	28-29
17-2	Dry	14,400	2	15.2	28-29
17-3	Dry	NA	not recovered	NA	28-29
17-4	Dry	13,800	2	16.6	28-29
22-1	Dry	12,300	3	19.2	30-31
22-2	Dry	NA	always dry	NA	30-31
22-3	Dry	NA	always dry	NA	30-31
22-4	Dry	12,300	3	19.8	30-31
22-5	Dry	10,200	3	16.0	30-31
22-6	Wet	NA	always wet	23.2	30-31
22-7	Wet	NA	always wet	21.6	30-31
23-1	Wet	7,100	4	27.4	32-33
23-2	Dry	10,900	3	14.6	32-33
25-1	Wet	NA	always wet	18.7	34-36
25-2	Dry	10,100	2	15.9	34-36
25-3	Dry	14,800	2	16.1	34-36
25-4	Wet	NA	buried in sediment		34-36
25-5	Wet	NA	always wet	18.4	34-36
25-6	Dry	8,700	7	20.1	34-36
25-7	Dry	12,000	3	13.3	34-36
25-8	Dry	NA	always dry	NA	34-36
27-1	Wet	NA	always wet	16.2	37-38
27-2	Dry	12,400	3	12.3	37-38
33-1	Dry	14,700	2	15.0	39-41
33-2	Dry	NA	always dry	NA	39-41
33-3	Wet	7,300	1	24.9	39-41
33-4	Dry	NA	always dry	NA	39-41
33-5	Dry	12,000	3	15.8	39-41
35-1	Wet	NA	always wet	21.3	42-44
35-2	Wet	7,100	1	20.4	42-44

Thermograph ID	Wet vs. dry @ install	Inferred threshold flow¹ (cfs)	Number of inundation cycles during study period	Max temp when wet (°C)	Relevant Figure #'s
35-3	Wet	NA	always wet	20.8	42-44
35-4	Dry	14,900	2	18.0	42-44
35-5	Dry	NA	not recovered	NA	42-44
39-1	Wet	7,800	1	30.1	45-46
39-2	Dry	NA	always dry	NA	45-46
40-1	Dry	13,500	2	14.3	47-48
40-2	Wet	NA	always wet	26.2	47-48
40-3	Dry	NA	always dry	NA	47-48
40-4	Dry	NA	always dry	NA	47-48
41-1	Wet	8,100	3	26.3	49-51
41-2	Dry	13,300	4	30.3	49-51
41-3	Dry		always dry	NA	49-51
41-4	Wet	8,100	1	18.3	49-51
44-1	Wet		always wet	22.5	52-53
44-2	Wet		always wet	20.0	52-53
44-3	Wet	7,700	1	29.4	52-53
44-4	Dry	11,300	5	25.0	52-53

¹ All flows are based on data from nearest gauge after adjusting for time lag of 4.5 mi/hr (see text).

Table 11. Summary of flows and estimated inundated areas.

Site	RM	Type of measurement	Discharge ¹ (cfs)	Connected inundated area (m ²)	Disconnected inundated area (m ²)	Total inundated area (m ²)	Relevant Figure #’s
13	187	direct observation	7,600	4,770	14,950	19,720	21a
		direct observation	8,600	23,660		23,660	21b
14	189	direct observation	10,500	2,770	6,410	9,180	22a
		thermograph	13,400	9,300		9,300	22b
15	189.5	direct observation	7,600		1,270	1,270	24a
		direct observation	8,600		3,890	3,890	24b
		thermograph	10,600		9,230	9,230	24c
		thermograph	12,200	14,370		14,370	24d
16	191	direct observation	7,600	6,190		6,190	26a
		direct observation	8,500	10,830		10,830	26b
		thermograph	12,000	28,950		28,950	26c
17	191.7	direct observation	7,600	910		910	28a
		direct observation	8,500	3,040	1,890	4,930	28b
		thermograph	14,400	6,010	2,830	8,840	28c
22	203	direct observation	7,600	34,160	990	35,150	30a
		thermograph	10,200	36,330	1,320	37,650	30b
		thermograph	12,300	54,030		54,030	30c
23	203	direct observation	7,100	36,290	620	36,910	32a
		direct observation	7,600	38,100		38,100	32b
		thermograph	10,900	55,610		55,610	32c
25	209	direct observation	7,900	4,970	2,340	7,310	34a
		direct observation	8,700	5,570	2,170	7,740	34b
		thermograph	12,000	6,806	1,630	8,436	34c
		thermograph	14,800	11,400	1,630	13,030	34d
27	211	direct observation	7,900	21,710		21,710	37a
		thermograph	12,400	31,820		31,820	37b
33	221.6	thermograph	7,300	1,800	6,890	8,690	39a
		direct observation	8,100	3,480	6,890	10,370	39b
		thermograph	12,000	10,530		10,530	39c
		thermograph	14,700	13,600		13,600	39d

Site	RM	Type of measurement	Discharge ¹ (cfs)	Connected inundated area (m ²)	Disconnected inundated area (m ²)	Total inundated area (m ²)	Relevant Figure # ² s
35	226.5	thermograph	7,100	9,940		9,940	42a
		direct observation	8,900	15,000		15,000	42b
		thermograph	14,900	20,040		20,040	42c
39	232.8	thermograph	7,800	970		970	45a
		direct observation	8,900	3,690		3,690	45b
40	233.3	direct observation	8,900	460	1,770	2,230	47a
		thermograph	13,500	7,770		7,770	47b
41	235.3	thermograph	8,100	3,730		4,346	49a
		direct observation	9,300	11,900		11,900	49b
		thermograph	13,300	18,270		16,676	49c
44	239.5	thermograph	7,700	5,260		5,260	52a
		direct observation	9,500	5,770	350	6,120	52b
		thermograph	11,300	8,090		8,090	52c

¹ All flows are based on data from nearest gauge after adjusting for time lag of 4.5 mi/hr (see text).

4.7.1 River Mile 189.5L

Study site 15 is located on the east bank at RM 189.5L. Site 15 is a probe channel eroding behind an active point bar (Figure 24a). Under the classification scheme outlined in Section 2.2.2, site 15 is a type 1 unit, which we expect should generally exhibit poor hydraulic connectivity at both the inlet and outlet. Thermographs were installed on 2/21/2007, when flow was 8,600 cfs. Both the inlet and outlet were disconnected from the mainstem (Figure 24b). An array of eight thermographs was installed to investigate (i) the timing of connection to the mainstem, (ii) longitudinal connectivity within the site, and (iii) the timing of connection between Murphy Slough and the study site. Eight thermographs were recovered on 4/26/2007 when flow was 7,600 cfs.

During thermograph installation, Chinook salmon (*Oncorhynchus tshawytscha*), Sacramento Sucker (*Catostomus occidentalis*), and Sacramento pike minnow (*Ptychocheilus grandis*) were observed in isolated shallow pools near the disconnected inlet of the OCWB. Little vegetative canopy cover was located near the pools, and the substrate consisted largely of sand (75%) and gravel (25%). At 8,600 cfs, during installation of the thermographs, 6 disconnected pools were observed (Figure 24b). The pool located near thermograph 15-8 was deepest, with a maximum depth of 1.3 m. On average, pool depth was 0.4 m across the site.

Thermograph data indicates that the threshold flow for mainstem connection of all the pools along site 15's longitudinal axis is about 12,200 cfs (Figure 24d). However, the discharge for inlet connection varied from 11,900 to 12,800 (median of 12,200 cfs) during the three storm peaks (Figure 25); this variability may be attributed to local stage effects associated with Stony Creek which enters the Sacramento on the opposite bank just upstream from Site 15's inlet. These local stage effects may not be consistently reflected at the same flow level at the Ord Ferry

gauge. With the exception of thermograph 15-7, all of the thermographs became inundated during the three peaks of the 2/22/07–3/1/07 storm event (Figures 25a and 25b). Thermograph 15-2 became inundated at 9,800 cfs, prior to connection with the inlet, implying that pools within the study site received groundwater in response to a water table rise in the mainstem. Data from thermographs 15-3 (Figure 25a) and 15-6 (Figure 25b) suggest there was a 6 to 8 hour time lag for inundation following inlet connectivity after the arrival of the first peak at the site. Yet they became inundated rapidly following inlet inundation in the subsequent storm events, probably due to antecedent ground saturation and elevated water levels in previously isolated pools. The inlet and outlet appear to become inundated at roughly the same time, with a few exceptions; in some instances the outlet became inundated just prior to inundation of the inlet, suggesting the outlet connects to the mainstem from backwater in the eddy near the outlet prior to inlet connection at a flow of about 12,000 cfs. The peak flow during the study period (15,600 cfs) was insufficient to expand the wetted width out of the low flow channel to a higher elevation bench (about 0.5 m above the thalweg at thermograph 15-7) in the largest pool within the study site. During thermograph removal, at 7,600 cfs, the pool near the outlet was dry and several of the other pools had contracted in size relative to what was observed at 8,600 cfs (Figure 24a and Photo 3). We speculate that the remaining pools would eventually become dry if flow remained at or below 7,600 cfs.

Murphy Slough (RM 190) is located just upstream of site 15, and was nearly connected to site 15 during thermograph installation. The downstream end of Murphy Slough first connected to site 15 at a flow of about 14,700 cfs. Yet Murphy Slough remained connected to site 15 throughout the receding limbs of the triple-peaked storm in late February, until flows in the mainstem dropped to 9,100, 5 days after the last storm peak. We suspect that there may be a time lag between changing flows in the mainstem and water levels in Murphy Slough due to time delays associated with water table rises. This would imply that Murphy Slough connects to site 15 at a discharge lower than Ord Ferry gauge value that matched with the time of inundation for thermograph 15-4 and 14,700 cfs should be viewed as the maximum estimated discharge for connection to site 15.

4.7.2 River Mile 203R

Study site 22 is located on the west bank at RM 203R of the Sacramento River. Site 22 is type 1 unit as described in Section 2.2.2, which we expect should generally exhibit poor hydraulic connectivity at both the inlet and outlet (Figure 30a). Thermographs were installed on 2/20/2007 at a flow of 7,600 cfs (Figure 30a) at which time the inlet was disconnected and the outlet pool was connected to the mainstem. A few small isolated pools were present during the installation. Seven thermographs were installed in an array to investigate the timing at which the inlet became connected to the mainstem and the longitudinal and lateral connectivity within the site. Seven thermographs were recovered on 4/26/2007 at a flow of 6,700 cfs.

Chinook salmon and California Roach (*Lavinia symmetricus*) were observed in the isolated pools at this site. Small gravel and sand compose the majority of the substrate at site 22. *Ludwigia* is abundant in the small pools and throughout the site.

At a flow of about 12,300 cfs the inlet to site 22 becomes connected (Figure 30c), and within 2 hours the downstream thermographs became inundated (although the corresponding discharge with the time of inundation for further downstream thermographs is higher, it is assumed that the inlet connection provides the requisite flow and there is a time lag) (Figure 31). Following inlet disconnection, pools on along the longitudinal axis begin to isolate from the outlet at about

10,200 cfs (Figure 30b). A narrow channel (3 m wide) along the outer edge of the study site and an isolated pool remained submerged throughout the study period; water temperatures in these two areas reached maximums of 21 and 23°C, respectively.

4.7.3 River Mile 209L

Study site 25 is located on the east bank at RM 209L of the Sacramento River. Site 25 is a probe channel located at the downstream end of an active point bar complex that is currently being eroded away due to a shift in the upstream meander bend position. Thermographs were installed on 2/20/2007 at a flow of 7,900 cfs at which time the inlet was disconnected and the outlet connected to the mainstem (Figure 34a). Eight thermographs were installed in an array to investigate (i) inlet connectivity, (ii) lateral channel width expansion, and (iii) longitudinal connection of pools in a split high flow channel that extends upstream of the inlet and does not have a defined surface flow inlet connection with the mainstem. Eight thermographs were recovered on 4/26/2007 at a flow of 8,800 cfs and the inlet was connected (Figure 34b).

Two isolated pools located at site 25 provided habitat for a total of 130 juvenile Chinook salmon. Little cover was available in the small, shallow pools and the dominant substrate consisted of sand (75%) and gravel (20%). Fish observations were hampered throughout the rest of the site due to high turbidities. *Ludwigia* was sparsely distributed throughout the site.

The inlet to site 25 becomes connected at approximately 8,700 cfs (Figure 34b). The most downstream pool of the bifurcated high flow channel becomes connected to the study site and the mainstem at about 12,000 cfs (Figure 34c); however, a thermograph between pools further upstream in the bifurcated channel did not become inundated which suggests the lower pool was connected through backwater in the study site. By 14,800 cfs, flow depth within the site exceeded 1.3 m (4.1 ft), thermographs at the outer edge of site 15 became inundated and nearly the entire study site was submerged while likely receiving mainstem flow from multiple connection points (Figures 34d and 35). The stage discharge relationship recorded at a cross-section with the study site indicated that the rate of stage change relative to mainstem discharge was 0.1 m (0.34 ft) per 1,000 cfs change in discharge (Figure 35).

4.7.4 River Mile 239.5R

Study site 44 is a type 1 channel located on the west side of the Sacramento River at river mile 239.5R. Four thermographs were installed on 2/15/2007 at a flow of 9,500 cfs. At 9,500 cfs the inlet was disconnected and the outlet was connected (Figure 52b). The thermographs were installed in an array to investigate when the inlet and outlet were connected and the longitudinal connectivity within the site. All four thermographs were recovered on 4/25/2007 at a flow of 8,900 cfs.

The dominant substrate in the site is gravel that is intermixed with sand and cobble. *Ludwigia* was sparsely located throughout the site, with its most abundant location at the outlet. A relatively large number of juvenile Chinook salmon as well as five Sacramento sucker were observed in multiple pools that were marginally connected to the mainstem (Photo 5); Chinook and Sacramento sucker were also observed during thermograph retrieval in late April. Beaver activity was noted in site 44 in two locations, with one beaver dam influencing the channel hydraulics.

The inlet to study site 44 connected and disconnected 5 times during the study period, at approximately 11,300 cfs (Figures 52c and 53). Thermographs at the outlet and at a shallow riffle that represented a connection point between pools along the longitudinal axis did not go dry during the study period although they exhibited high water temperatures (maximum temperatures of 20 and 22.5°C) when the inlet was disconnected. Pools near the inlet that were disconnected from both the inlet and outlet during installation did go dry around 7,700 cfs (Figure 52a).

5 DISCUSSION AND SYNTHESIS

5.1 Sedimentation Rates

Our results show that sedimentation rates tend to even out over time, with slower-filling OCWBs (which are less connected hydrologically to the main channel) tending to catch up to faster-filling OCWBs over a period of decades (though with different granulometry, based on our data). Sedimentation rates did not appear to be related to geometric form of the former channel, but we found a strong relation between diversion angle and the evolutionary path (i.e., infill history) of oxbows in the Sacramento River. The diversion angle determines the extent to which gravel makes up the sedimentary fill of oxbows and the rate that oxbows are converted into terrestrial habitat. Oxbows with diversion angles $\leq 50^\circ$ fill in at least 5 times faster than those with diversion angles $> 70^\circ$. Lakes with high diversion angles function as long-term sinks for fine-grained sediment in the floodplain and may serve as storage sites for pollutants in the fluvial system.

5.1.1 Patterns of sedimentation observed in oxbow lakes of the Sacramento River

Our analyses of sediment collected at off-channel water bodies provide information on the precise nature of the fill and fine-scale temporal variability in sedimentation rates. Using standard granulometric methods, we analyzed sediment from seven off-channel water bodies. We hypothesized that the diversion angle is the primary control on the evolutionary pattern of the Sacramento River's oxbow lakes. Engineers have recognized that the diversion angle, or the angle between the main channel and the entrance to a diversion channel, is an important control on the division of the flow's momentum, and thus also on the ability of flow in the diversion to transport bed material (e.g., Law and Reynolds, 1966; Hager, 1984). Results from flume experiments revealed that discharge in the diversion is progressively reduced with increases in the diversion angle above 50° (Vanoni, 1975).

Sediment cores taken from four oxbow lakes with varying diversion angles reveal distinct granulometric profiles with depth. The profiles of cores from Duck Lake and Jenny Lind Bend (Figures 54 and 55), both with diversion angles greater than 75° , are dominated almost entirely by silt and clay above gravel bases. The profiles of cores from Rio Vista and La Barranca (Figures 56 and 57), both with diversion angles of about 50° , fine upwards from a gravel base, grading from mostly sand to mostly silt and clay near the surface.

Our interpretation of the granulometric data was that the profiles reflect the rate at which sediment plugs develop. Flow in an oxbow with a low diversion angle ($\leq 50^\circ$) is more able to transmit bed material, and thus the aggradation of bed material at the entrance is slowed or prevented. Such an oxbow remains hydraulically connected to the main channel at low flow-stages and receives bed material from the main channel over a greater duration of its history. Flow in an oxbow with a high diversion angle is less able to transmit bed material, which thus promotes the development of a sediment plug at the oxbow's entrance. This kind of oxbow is disconnected from the main channel soon after its formation and experiences sedimentation only during overbank-flow conditions.

Given that oxbows with low diversion angles progressively fill with gravel for some time after their formation, we devised a method of estimating their original depths because we were unable to core through coarse material. Using 1997 bathymetric data from the U.S. Army Corps of Engineers and similarly dated aerial photos of the study reach, we described a statistically significant linear regression between the average bankfull depth of a meander and its average radius of curvature (Figure 58). We used the equation that described the regression to estimate the average original depths relative to the outer banks of 14 oxbows, whose average radius of curvature we measured using 2004 aerial photos.

In the field, we measured the elevation difference between the outer bank of an oxbow and its water surface, water depth, and the fine-sedimentary (sand, silt, and clay) thickness. With an estimate of its original depth, we were then able to estimate the average gravel thickness within the oxbow. The results reveal a statistically significant and negative correlation between the average gravel thickness and diversion angle (Figure 59). We also found a significant and positive correlation between the amount that an oxbow has been filled and its average gravel thickness (Figure 60), reflecting the fact that the sedimentation rates are most rapid immediately following the cutoff when the channel is still flowing—and thus low diversion angles would have greater total sediment accumulation and higher gravel content. Infilling by finer-grained sediment would occur more slowly in subsequent years.

Using historical aerial photos of the reach, we were able to date the time of formation for 12 of the 14 studied oxbows. This allowed us to estimate average infilling rates, measured as the total thickness of sedimentary fill (gravel, sand, silt, and clay) divided by the number of years since cutoff. Consistent with our hypothesis, we found a significant and negative correlation between average infilling rates and the diversion angle (Figure 61).

We then examined sedimentation rate (cm/yr), measured in the field from our coring and probing, as a function of geometric channel type, as distinguished from our aerial photo analysis (Figure 62).

Our comparison of sedimentation rate among the four geometric channel types did not show any clear trends (Figure 62). When we distinguished points in the plot of sedimentation rate against the age of the former channels (Figure 9) by channel type, no differences were evident for M1, M2 and S1 types (Figure 63). However, S2 channel types, with more dynamic hydraulic conditions, tended to have somewhat lower sedimentation rates (Figure 63). We then developed a log-log regression model relating sedimentation rate, y , to the age of the unit, x (Figure 64). The regression equation, explaining 37 percent of the variance, is:

$$\text{Log } y = 1.82 - 0.7 \log x \quad r^2 = 0.37$$

Kopta Slough is clearly an outlier, with almost no fine sediment. This may be explained by past dredging for a boat launch.

5.2 Water Quality

The water quality parameters measured at the sites can provide information on the hydrological connectivity to the main channel, a general indication of habitat quality for aquatic species, and information on potential water pollutant sources. Some sites require more sampling to provide adequate data for analysis. However, the results provide preliminary information on overall water quality at the OCWB sites.

Dissolved oxygen in water is critical for supporting respiration of most aquatic organisms. Those OCWB sites with relatively low percent dissolved oxygen rates (i.e., less than 90%) may not provide suitable habitat for aquatic life. As stated in the results section, 11 of the 28 sites in Table 8 show an average % dissolved oxygen rate of over 90%. Many sites fall just below 90%, but some sites appear to have alarmingly low % dissolved oxygen rates of 50% or less. Dissolved oxygen may be a limiting factor in habitat quality for aquatic organisms at these sites.

Conductivity is a measure of water's ability to conduct electrical current and can also provide a general indication of water quality. Polluted runoff into an OCWB can affect conductivity rates, especially if the pollutants include inorganic dissolved solids such as bicarbonate, sulfate, chloride, calcium, magnesium, sodium, potassium, and phosphate ions. High conductivity in an OCWB adjacent to agricultural land may indicate that agricultural runoff is entering the water body since agricultural runoff typically has high levels of dissolved salts. According to the Environmental Protection Agency (EPA), streams supporting good mixed fisheries have conductivity measurements ranging from 150 to 500 $\mu\text{mhos/cm}$ (EPA 2006). Five OCWB sites have average conductivity measurements greater than 500 $\mu\text{mhos/cm}$, and five have average conductivity measurements of less than 150 $\mu\text{mhos/cm}$. Conductivity measurements at these sites indicate that water quality may limit species diversity of aquatic organisms. Water temperature also affects conductivity measurements.

To understand the effects of water quality on overall habitat quality of the OCWB sites, we also recommend that on-going water quality data collection occur in order to assess data, for example, at a range of river discharges. As Figure 20 indicates, water quality parameters such as conductivity can vary according to the discharge of the main channel. Thus, water quality may change seasonally within OCWB sites, responding to main channel flows.

5.3 Inundation of Scour Channels on Point Bars

5.3.1 Inundated area

This study was designed to identify the flows that connect scour channels on point bars with the mainstem and quantify how the extent of inundated habitat varies with flow. The left panels of Figures 65 to 68 depict how cumulative inundated area varies with discharge for sites associated with each flow gauge (Figure 65 to 67), and for all sites combined (Figure 68). The right panels of Figures 65 to 68 show the same relationships for the average normalized area of inundation, where normalized area is calculated for each site by dividing the observed inundated area by the total area available for inundation (see Section 3.8.3.4). This helps produce an average that gives equal weight to each study site, irrespective of site-to-site differences in total potentially inundated area. This makes for comparisons that are unaffected by the potentially confounding influence of study sites with large areas.

The five sites associated with the Ord Ferry gauge indicate there are two ranges of discharge that are important for changes in inundated area: 7,600–8,600 cfs and 12,000–14,000 cfs (Figure 65). Below 8,600 cfs, inundated areas of scour channels are contracting, isolated pools are drying up, inlets are disconnecting from the mainstem in type 3 channels (i.e., on the outsides of meander bends), and disconnected perennial pools are multiplying as riffles and gravel bars are becoming sub-aerially exposed. In contrast, 12,000 cfs appears to be a threshold for significant expansion in connected wetted area, with inlets to type 1 channels (i.e., probe channels that cross point bars)

beginning to connect, and water levels in type 2 channels (i.e., sloughs) beginning to rise and eventually providing connections among previously isolated pools.

The two sites associated with the Hamilton City gauge show a similar two-step change in inundated area as a function of discharge (Figure 66). Inundated area declines sharply below 7,600 cfs and increases substantially between 10,900 and 12,300 cfs. Only 2 sites are associated with the Hamilton City gauge. Discharges of interest are 7,600 cfs, when the inlet disconnects from the mainstem at site 23 (a type 2 channel) and 12,300 cfs, when the inlet connects to the mainstem of site 22 (a type 1 probe channel). Areas that are inundated but disconnected are minimal, because the majority of the axial length of the study sites was connected to the mainstem at the outlet for all flows observed in this study (Figure 66).

Study sites associated with the Vina Woodson Bridge gauge also appear to have two flow ranges where changes in inundated areas are most substantial. Study sites begin to go dry (i.e., show a substantial decrease in inundated area) at about 9,000 cfs. Further declines occur below 8,000 cfs, when inlets begin to disconnect (e.g., at sites 25 and 41) and pools show significant contraction. Once flow levels reach about 12,000 cfs, the study sites begin to show significant expansion, with a decreasing percentage of area that is inundated but disconnected from the channel, and increasing connectivity of type 1 inlets to the mainstem (e.g., at site 44).

The area-flow relationship for all sites combined highlights an additional potentially important flow threshold. When flow drops in the range of 8,600 to 7,600 cfs, inlets appear to become disconnected from the mainstem, and pools contract and become increasingly isolated (Figure 68).

During thermograph retrieval on 4/25 and 4/26/2007, pools were contracting and the mainstem was becoming disconnected from inlets at sites associated with the Hamilton City and Ord Ferry gauges, downstream of RM 206, where substantial flow was being diverted for irrigation at GCID. In contrast, at study sites upstream of RM 206 (i.e., those associated with the Vina Woodson gauge), pool water levels were stable. A contracting pool can generally be identified in the field from evidence of changes in water levels; observed water level is typically several centimeters below recently wetted water lines in the surrounding sediment (see Photo 4). In contrast, former water lines are not present in stable or expanding pools. Gauging station records indicate that average discharge on 4/25 and 4/26 was 8,800 at Vina Woodson Bridges (RM 218), 6,800 at Hamilton City (RM 199), and 7,700 cfs at Ord Ferry (RM 184). The average GCID (RM 206) diversion was 2,200 cfs over the same 2-day period. The concurrence of pronounced losses in inundated area and relatively lower flows downstream of GCID is suggestive of a cause-effect relationship; the diversion at GCID appears to have been sufficient to push the downstream study sites below their lower thresholds for inundation. Diversion-related losses in inundated area would presumably be more pronounced during spring months in relatively dry years, when GCID begins diverting at near maximum capacity, even though releases from Shasta-Keswick (the primary source of flow after the winter, in the absence of storm events) remain relatively low and steady, before being ramped up for summer irrigation releases. Further data on the relationship between discharge and inundation area will be necessary to verify whether this is the case.

5.3.2 Inlet connection flows

The morphology of scour channels on point bars appears to be an important regulator of the threshold for connectivity between inlets and the mainstem. Connectivity with the mainstem requires higher flows for Type 1 (probe channels) inlets than it does for Type 3 (outside of

meander bends) inlets. This probably reflects the fact that probe channels are typically perched well above low flow channel, whereas the inlets of scour channels on point bars on the outsides of meander bends tend to be more at grade with the mainstem channel (Figure 4). None of the Type 2 scour channel on point bar inlets connected to the mainstem via surface flow during the study period. This probably reflects the fact that Type 2 channel inlets are plugged with sediment. Type 2 did nevertheless exhibit water level fluctuations due to influxes of groundwater from elevated water tables and peak flow events. Inlets to prototypical probe channels (e.g., at sites 15, 22, and 44) have inlet channels that are easily discernible due to annual scour. They connected to the mainstem at discharges ranging from 11,300 to 12,200 cfs. Where probe channel inlets were less well-defined, due to vegetative growth or sediment deposition (e.g., sites 17, 39, and 40), connection with the mainstem did not occur during the study period. Inlets to the three Type 3 channels (at sites 16, 23, and 41) all became disconnected from the mainstem at similar discharges, ranging from 7,600 to 8,100 cfs.

In addition to affecting inundated area, inlet connectivity is an important regulator of water temperature in scour channels on point bars. Water temperatures were higher within units that lacked inlet connectivity than they were at those that had inlet connectivity, irrespective of whether the outlet was connected to the mainstem at the time of the measurement. For all 55 days analyzed, the average maximum water temperature for thermographs in study sites that lacked inlet connectivity was higher (by 1.6 to 6.4°C; average = 4.6°C) than it was for those that were connected at their inlets to the mainstem (Figure 69). We focused specifically on variations in maximum daily water temperatures because they are a readily assessable proxy for thermal stress on the aquatic species of interest. Study sites with persistently disconnected inlets were, in most cases, connected to the mainstem at their outlets throughout the monitoring period. This indicates that the cooling effects of mainstem flow are minimal, unless there is a direct connection to the study site at its inlet; for outlet-connected study sites, flow-related effects on temperature are probably limited to the immediate vicinity of the outlet. Also evidenced in Figure 69, is the strong affect of air temperature on the maximum daily water temperatures in the scour channels on point bars, which is presumable more pronounced in these shallower water bodies than the mainstem.

Temperature is a primary limiting factor for juvenile Chinook salmon, which strongly affects growth and survival. For Central Valley fall-run Chinook fry, optimal temperatures for growth and survival are 13 to 18°C, and around 22 to 23°C major mortality is expected (Moyle 2002). During the study period, 7 out of the 13 thermographs with disconnected inlets exceeded 22°C, and 12 of 13 exceeded 20°C while inundated. In contrast, none of the inundated thermographs with connected inlets exceeded 22°C, and only 1 of 6 exceeded 20°C while inundated. Although our data illustrate that temperatures were warmer in sites without inlet connection, the cumulative effect of the warmer temperatures on growth and survival for juvenile Chinook salmon is inconclusive. Sommer et al. (2001) found higher growth and survival rates for juvenile Chinook salmon in the warmer Yolo Bypass than the mainstem Sacramento, largely due to significantly higher prey consumption and food availability in the bypass that exceeded the increased metabolic costs of rearing in the significantly warmer floodplain. For our study sites that were warmer water at sites with inlet disconnection, the temperature effects may not have deleterious to for juvenile Chinook salmon as long as the outlet of the water bodies remained connected and fish could escape to the mainstem as temperatures approached survival thresholds around 22 to 23°C. Additional data evaluating food production would be necessary in order to fully evaluate the benefits and costs of the higher water temperatures on growth and survival for juvenile Chinook salmon.

Temperature strongly affects growth and survival of juvenile Chinook salmon. For Central Valley fall-run Chinook fry, optimal temperatures for growth and survival range from 13 to 18°C, and at around 22 to 23°C mortality is expected to occur (Moyle 2002). During the study period, water temperatures at 7 out of the 13 thermographs with disconnected inlets exceeded 22°C, and temperatures at 12 of 13 exceeded 20°C. In contrast, water temperatures never exceeded 22°C at connected inlets, and exceeded 20°C at only 1 of 6 connected inlets. Although our data illustrate that temperatures were warmer in sites without inlet connection, the cumulative effect of warmer temperatures on growth and survival for of juvenile Chinook salmon is inconclusive. Sommer et al. (2001) found higher growth and survival rates for juvenile Chinook salmon in the warmer Yolo Bypass than the mainstem Sacramento, largely due to significantly higher prey consumption and food availability in the bypass that exceeded the increased metabolic costs of rearing in the significantly warmer floodplain. For our study sites with inlet disconnection, warmer temperatures may not be deleterious to juvenile Chinook salmon as long as the outlet of the water bodies remains connected and fish can escape to the mainstem if temperatures approach survival thresholds around 22 to 23°C. Additional data evaluating food production would be necessary in order to fully evaluate the benefits and costs of the higher water temperatures in sites with disconnected inlets on growth and survival for juvenile Chinook salmon.

5.3.3 Stage-discharge relationships in scour channels on point bars

Quantifying how water depth (i.e., stage) changes as a function of discharge in the mainstem is important for evaluating aquatic habitat within the study sites at varying flow levels. To construct stage-discharge relationships for our study sites, we used our thermograph observations to identify when points of known elevation (i.e., stage) at surveyed cross-sections became wet (or dry) due to changes in discharge on the mainstem. We were able to develop stage-discharge relationships with 3 or more observations for three sites (Figures 35, 40, and 50). The slopes of the stage-discharge relationships are consistent at these sites, at about 0.10 m (0.34 ft) of stage change per 1,000 cfs change in discharge (Figures 35, 40, and 50).

We collected stage-discharge observations at surveyed cross-sections other than those depicted in Figures 35, 40, and 50. However, we were not able to gather more than two observations at these other sites, because some thermographs never became inundated and/or some thermographs never became dry. Figure 43 shows an example stage-discharge plot from such a site. Although the slopes of the stage-discharge relationships are not as well constrained as they are at sites with 3 or more observations, data from plots such as Figure 43 still provide insight into how stage changes with mainstem discharge across our sites. Utilizing all available stage-discharge observations, we grouped the stage discharge slopes by study unit type and plotted them as a function of River Mile in Figure 70. Slopes were not calculated for changes in discharge <1,000 cfs when discharges errors on the order of 100 cfs will substantially alter the calculated stage-discharge slope, due to uncertainties associated with determining discharges (which require extrapolation across multiple river miles from nearby gauges). Eighty percent (16 out of 20) of stage-discharge slopes in Figure 70 are based on changes in discharge >3,300 cfs. We suggest that errors associated with extrapolating changes in discharges of this magnitude from nearby flow gauge data are minimal.

The mean rate of change in stage per 1,000 cfs change in discharge was 0.10 m (0.32 ft) (Figure 70). The range of stage changes one standard deviation from the mean are between 0.13 m (0.42 ft) and 0.07 m (0.22 ft) change in stage per 1,000 cfs (Figure 70). The mean for the 20 slopes analyzed is very similar to the slopes from the three sites with 3 or more observations. Figure 70 shows that stage-discharge slope shows no clear trend with distance downstream from RM 240 to

187 ($R^2 = 0.01$ for a linear fit comparing rates with distance). Nor do any clear correlations emerge when the data are grouped by study unit type; this could be due, in part, to the small number of observations for type 2 and 3 channels. Stage-discharge slopes presented herein were sampled during discharges ranging from 7,000 to 15,000 cfs in the mainstem Sacramento. Extrapolating them outside the 7,000 to 15,000 cfs range would result in significant uncertainty. They are more likely to be applicable when the study sites remain a distinct feature separated from the mainstem by a sediment deposit or landform, and less likely to be applicable during higher flows when the study sites and their separating landforms are completely submerged (such that the study sites function as the edge of the mainstem channel).

5.3.4 Data uncertainty

In this study, we used indirect methods and assumptions to determine when points of interest became wet (or dry), to estimate local flow conditions, and to quantify inundated areas. We also made direct observations of inundated area during thermograph deployment and retrieval. The accuracy of the temperature readings of the thermographs ($\pm 0.2^\circ\text{C}$) was more than adequate for the study needs. Determining whether a thermograph was submerged or aerially exposed drew upon several lines of evidence, including patterns (see Section 3.8.3.2) that were anticipated during study inception, as well as some that were determined after analyzing several thermograph records. In general, we were able to develop a high level of confidence about when thermographs became wet (or dry) because we (i) deployed arrays of thermographs in areas with both wet and dry conditions, (ii) sampled a period that included multiple cycles of inundation and aerial exposure, and (iii) in many cases had several independent methods for deducing whether thermographs were wet or dry at any given time. Uncertainties were generally greater for thermographs that were installed wet and became dry during low flow periods (i.e., flows $< 8,500$ cfs). This was because many of the thermographs in question were located in pools that were not receiving flow inputs from the inlet. As the pools shrank, their water temperatures approached ambient air temperatures, making it relatively difficult precisely identify the timing of complete sub-aerial exposure and errors are estimated as high as 4 hours for determining desiccation (see Section 3.8.3.2 for details on how these instances were resolved). Errors of order ± 4 hours on the arrival of flows should have minimal implications for our estimated flow thresholds during these low flow periods of relatively stable hydrographs, because we report them to the nearest 100 cfs, and because stage and flows fluctuated at slow rates during low flow periods. We calculated that 30 cfs is about the average change of discharge over a 4 hour window at the Vina Woodson Bridge gauge during low flow periods of this study.

To correlate thermograph data with flow data from the nearest, most appropriate gauging station, we had to adjust the time stamp of the flow data to account for the distance between the gauge and the study site. We used an average speed of 4.5 mi/hr (± 0.5 mi/hr, $n = 15$), based on the time lag for the arrival of flow peaks for each of the three peak flows during the 2/22/07 to 3/1/07 interval. This adjustment speed is not expected to be universally applicable to flow data series on the middle Sacramento River, because the watershed is large enough and storm patterns are variable enough that the timing of tributary inputs is likely to vary from storm to storm. When this is considered along with the likely variability in antecedent ground saturation conditions, and variations in reservoir and diversion operations, it seems clear that the speed of flow peaks is likely to vary considerably on the river. In this case, however, the 4.5 mi/hr is specific to 2/22/07 to 3/1/07, which was also the period when sub-aerially installed thermographs became inundated during our study as all high flows occurred during this time period. We can therefore be reasonably certain that the adjustment is approximately correct over the short timescale of the study. Nevertheless, the further a given study site is from a gauge, the larger is the adjustment

and degree of uncertainty in the adjustments of the flow time stamps. We expect that adjustments for sites within 9 miles of a flow gauge (i.e., with a ≤ 2 hour time stamp adjustment) should be reliable. Study sites 39, 40, 41, and 44 are located between RM 233 and 240 (Table 4); this makes them the only sites that are >9 miles from a gauge (Vina-Woodson Bridge is at RM 218). Site 44 was the farthest from its gauge, requiring a 4.75 hour time-stamp offset. Although the time-stamp offsets for sites 39, 40, 41 and 44 are substantial, we can be reasonably certain that they did not introduce significant errors into our analysis, because, for each thermograph, the timing of submersion consistently matches a similar flow magnitude when the average 4.5 mi/hr offset speed is used to adjust the flow timing. The consistency from flow to flow (at a given thermograph) justifies the use of a constant average speed over the brief timescale of the study. Although the Red Bluff Diversion Dam gauge (RM 243) could have provided a better discharge association for these sites, it currently only provides stage data and is not rated for flow and therefore could not provide the data needed for our study.

We made a series of assumptions to estimate inundated areas for discharges other than those observed during field visits (see Section 3.8.3.4 for assumptions). This introduced the most significant, but difficult to quantify uncertainties in this study. In light of these uncertainties, data presented in Figures 65–68 should be viewed as depicting general inundation patterns rather than precise inundated areas. In Figures 65–68, the right panel depicts how the inundation changes with flow for normalized areas, in which each study site is given equal weight regardless of aerial extent. This makes it perhaps the most robust indicator of how inundation changes with flow, because it would not be overly distorted if a few areas were in error due to flaws in the assumptions in Section 3.8.3.4. In contrast, in the left panel, errors at larger sites will have a much greater effect on the overall relationship than errors at small sites.

6 MANAGEMENT IMPLICATIONS/CONCLUSIONS

6.1 Off-Channel Water Bodies

- Long-term conservation and restoration strategies for former channels must consider evolutionary trends, such as the pattern and rate of infilling/terrestrialization, depth of fine sediment deposited, and likely long-term future sedimentation rates.
- If in the future it is determined that it would be worthwhile to take steps to prevent or slow terrestrialization by deepening a partially-filled oxbow lake (or to restore hyporheic connectivity by excavating down to the channel gravel layer), any such effort should be informed by the history and pattern of sedimentation, notably the thickness of fine-grained material to remove, as well as the probable rate of future infilling and expected caliber of sediment.
- At a larger scale, we must consider not only the processes of how former channels evolve once they form (our study) but also the processes of meander cut-off, and the rate at which new cutoffs occur. Cutoff rates are being addressed in parallel studies, but one fundamental threat to maintaining a diverse assemblage of former channel habitats is the progressive decrease in sinuosity of the system (Micheli and Larsen, in prep.). As more and more outside bends are stabilized with riprap, fewer sites will have the potential to cut off.

6.2 Scour Channels on Point Bars

- Mainstem Sacramento River discharges $\geq 12,000$ cfs appear to provide substantial increase in inundated areas and connection to the mainstem for scour channels on point bars. Approximately 12,000 cfs is also the threshold discharge for inlet connection of Type 1 scour channels on point bars (Figure 3a).
- Mainstem Sacramento River discharges $\leq 8,500$ cfs appear to define another flow of concern: inlets of scour channels on point bars near grade with the edge of the mainstem disconnect (Figure 3b) and isolated pools within all scour channels on point bars show significant contraction and/or complete desiccation.
- For mainstem flows in the range of 7,000 to 15,000 cfs, stage-discharge slope within scour channels on point bars is 0.10 m (0.34 ft) of stage change per 1,000 cfs change in mainstem discharge.
- Water temperatures in scour channels on point bars without inlet connection to the mainstem are significantly higher than those with inlet connection. During this study period, the average difference between inlet connected and disconnected max daily temperatures was 4.6°C (range 1.6 to 6.4°C). During the study period, 7 out of the 13 thermographs with disconnected inlets exceeded 22°C (22 to 23°C is the threshold for major mortality in Central Valley fall-run Chinook fry [Moyle 2002]); in contrast, none of the inundated thermographs with connected inlets exceeded 22°C. Overall effects of the increased temperatures on growth and survival of juvenile Chinook salmon are inconclusive.

6.3 Future Research Needs

- Develop better relationships between OCWB water quality and such factors as surrounding land use, drainage pathways, and connectivity of the OCWB with the mainstem, so that we can better understand the factors limiting ecological potential in OCWBs.
- Collect sediment cores to document sedimentation history in greater detail and to analyze samples for radiometric dating. These data would refine our understanding of sedimentation history, especially for OCWBs that become cut off prior to our earliest map record in the late 19th century.
- Improve the gauging network, in both the mainstem and OCWBs, to document hydrologic interactions between OCWBs and mainstem.
- Inventory and analyze the length of rocked vs. unprotected bank (i.e., open to channel migration) on the mainstem Sacramento River, in order to assess future potential for meander bend cutoff (and thus a generation of new OCWBs).

7 REFERENCES

Bjornn T. C. and D. W. Reiser. 1991. Habitat requirements of salmonids in streams. American Fisheries Society Special Publication 19:83–138.

EPA. 2006. "Monitoring and Assessing Water Quality."
<http://www.epa.gov/volunteer/stream/vms59.html>

Hager, W. H. 1984. An approximate treatment of flow in branches and bends: Proceedings of the Institute of Mechanical Engineers, v. 198, 63–69.

Kelley, R. 1989. *Battling the Inland Sea: Floods, Public Policy, and the Sacramento Valley*. Berkeley: University of California Press.

Law, S. W. and A. J. Reynolds. 1966. Dividing flow in an open channel: Journal of the Hydraulics Division, American Society of Civil Engineers, v. 92, 207–231.

Limm, M. P., and M. P. Marchetti. 2003. Contrasting patterns of juvenile Chinook salmon (*Oncorhynchus tshawytscha*) growth, diet, and prey densities in off-channel and main stem habitats on the Sacramento River. Prepared for The Nature Conservancy, Chico, California.

Lister, D. B., and H. S. Genoe. 1970. Stream habitat utilization of cohabiting underyearlings of Chinook (*Oncorhynchus tshawytscha*) and coho (*O. kisutch*) salmon in the Big Qualicum River, British Columbia. Journal of the Fisheries Research Board of Canada 27: 1215–1224.

Micheli, E. R., and E. W. Larsen. In preparation. River channel cutoff dynamics, Sacramento River, California, USA.

Moyle, P. B. 2002. *Inland Fishes of California*. University of California Press, Berkeley and Los Angeles, California.

Sommer, T. R., M. L. Nobriga, W. C. Harrell, W. Batham, and W. J. Kimmerer. 2001. Floodplain rearing of juvenile Chinook salmon: evidence of enhanced growth and survival: Canadian Journal Fisheries Aquatic Sciences, v. 58, 325–333.

Stillwater Sciences and W. E. Dietrich. 2002. Napa River Basin Limiting Factors Analysis. Prepared for San Francisco Bay Water Quality Control Board and California State Coastal Conservancy by Stillwater Sciences, Berkeley, California and W. E. Dietrich, Department of Earth and Planetary Sciences, University of California, Berkeley.

Sullivan, D. G. 1982. Prehistoric flooding in the Sacramento Valley: Stratigraphic evidence from Little Packer Lake, Glenn County, California: University of California, Berkeley, Master's Thesis, 90 p.

Stokes, S. and D. E. Walling. 2003. Radiogenic and isotopic methods for direct dating of fluvial sediments. pp. 233–267 in G. M. Kondolf and H. Piégay (eds.) *Tools in Fluvial Geomorphology*, John Wiley & Sons, Chichester UK.

Thomas, J. 2000. A physical model of meander migration on the central Sacramento River. Master's thesis. University of California, Davis.

Vanoni, V. A. 1975. Sedimentation Engineering. New York: American Society of Civil Engineers.

Wagner, R. J., H. C. Mattraw, G. F. Ritz, and B. A. Smith. 2000. Guidelines and standard procedures for continuous water-quality monitors: site-selection, field operation, calibration, record computation, and reporting. USGS Water-Resources Investigations Report 00-4252. U.S. Geological Survey, Reston, Virginia.

Acknowledgements

Greg Golet, Mike Roberts, and Ryan Luster with The Nature Conservancy's Sacramento River Project provided direction, logistical support, and comments on the study design and implementation. Daryl Peterson, formerly with TNC's Sacramento River Project, helped to plan and launch this study. Steve Greco of UC Davis kindly provided access to an extraordinary collection of aerial photographs. Mia Roberts, Kate Huxster, Albert Rovira, and Will Stockard scanned prints of aerial photos at UC Davis. Joe Silveira of the U.S. Fish and Wildlife Service Sacramento National Wildlife Refuge provided sampling permits, access to study sites, and encouragement. Henry Lomeli of the California Department of Fish and Game provided access to the DFG sites. Koll Buer assisted with the deployment and recovery of the miniature water temperature recorders.

Figures

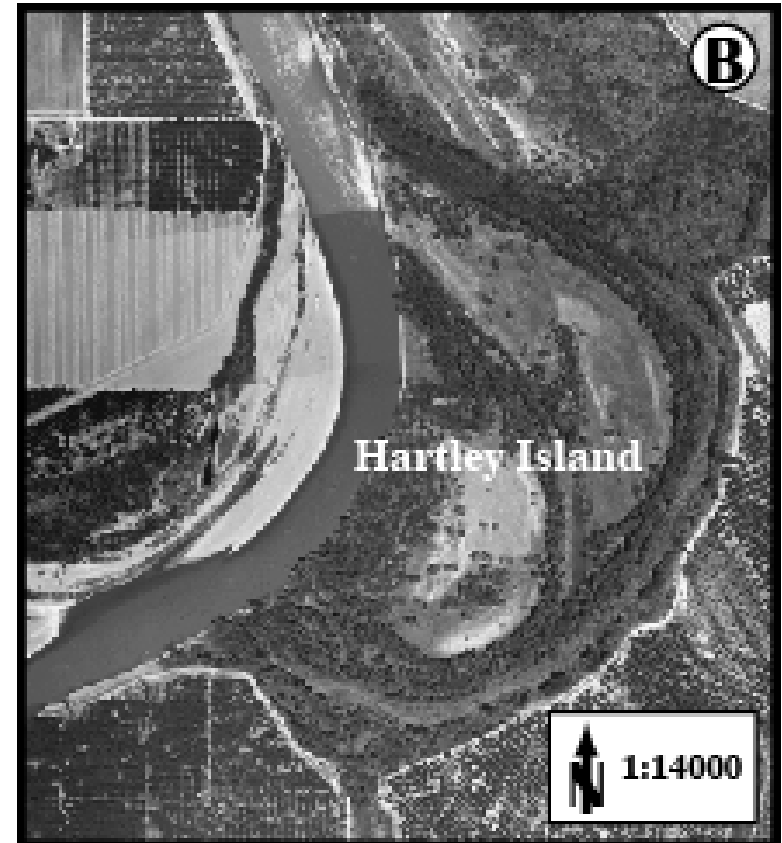
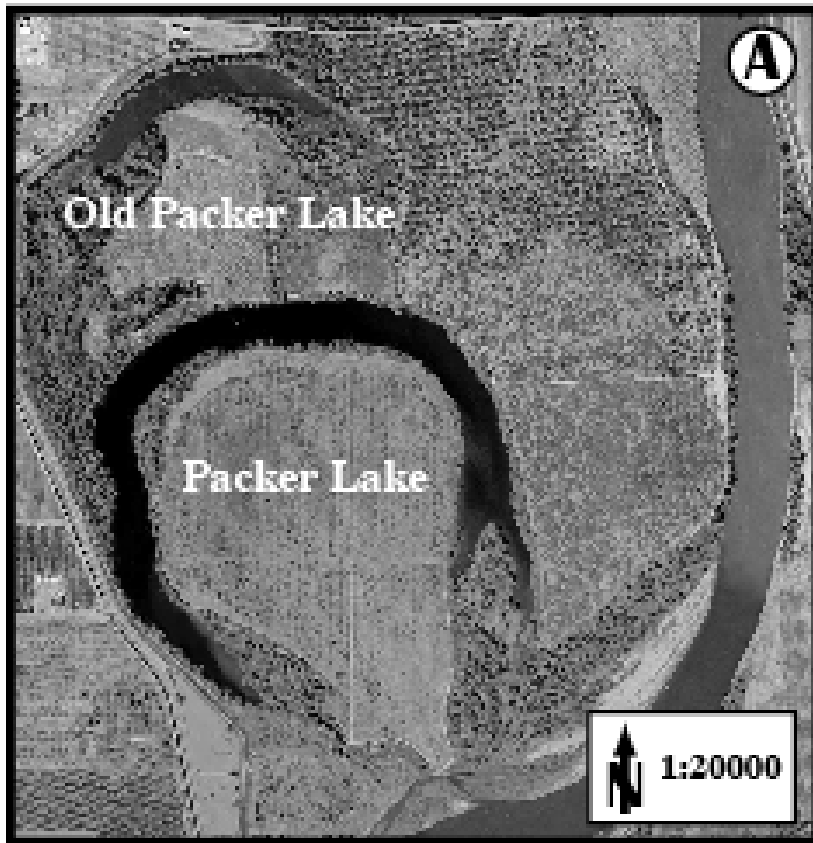


Figure 1. (A) Aerial photo of floodplain near river mile 167 taken in 2004. Based on radiocarbon data, Old Packer Lake is estimated to have formed over 800 years ago (Sullivan 1982). Historical maps of the vicinity show the formation of Packer Lake in 1874. (B) Aerial photo of floodplain near river mile 175 taken in 1997. Historical aerial photos show that Hartley Island formed in the late 1950's.



Figure 2. Example of a scour channel that forms on the downstream end of a point bar, providing seasonally inundated, shallow-water habitat that can support rearing of salmonid fry. (Photo Source: CDWR 1999)

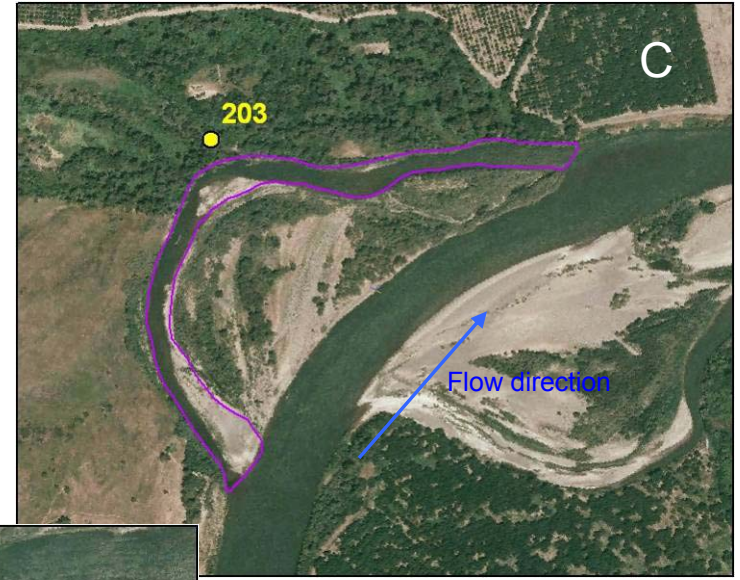
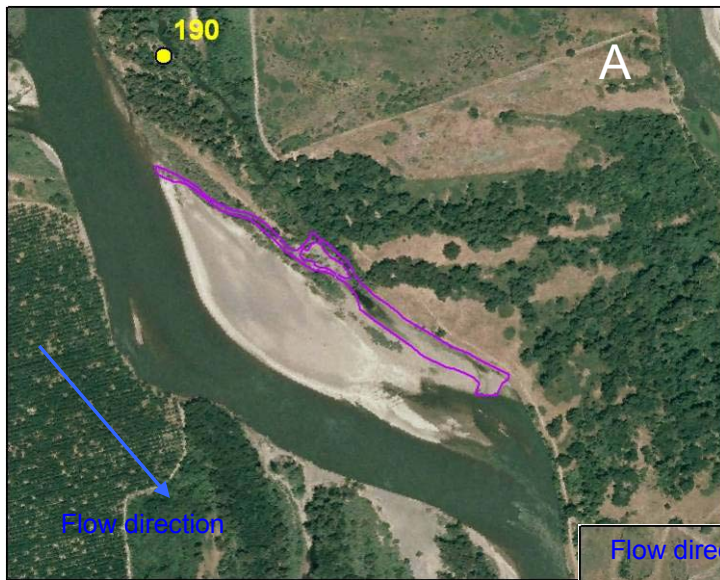
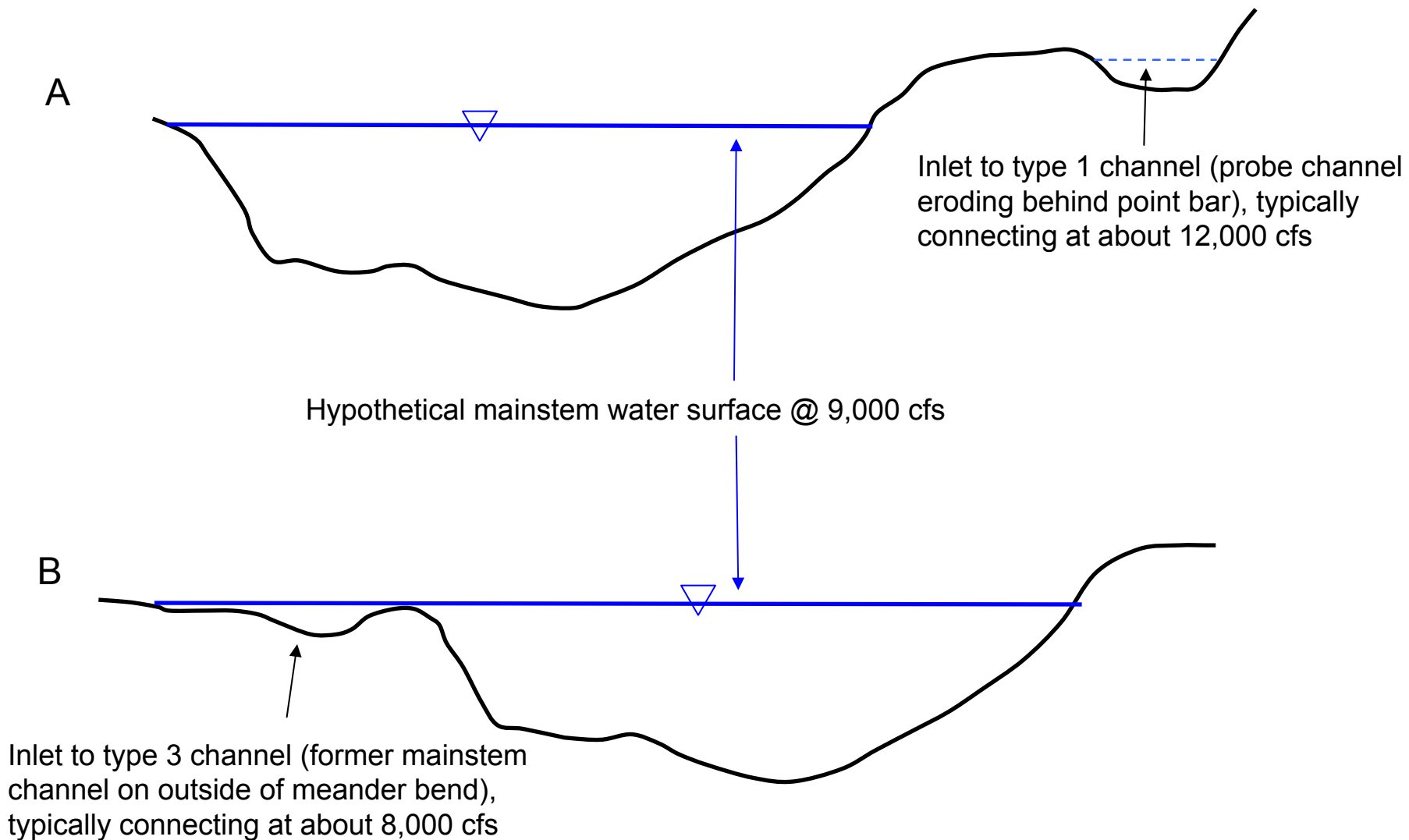


Figure 3. Examples of off channel water bodies studied for inundation flows on the Sacramento River: (A) Type 1- probe channel eroding behind an active point bar, (B) Type 2- an abandoned channel on the inside of a meander bend as the mainstem continues to erode outward, and (C) Type 3- a former main channel position on the outside of a bend that is abandoned as the main channel cuts behind a point bar.



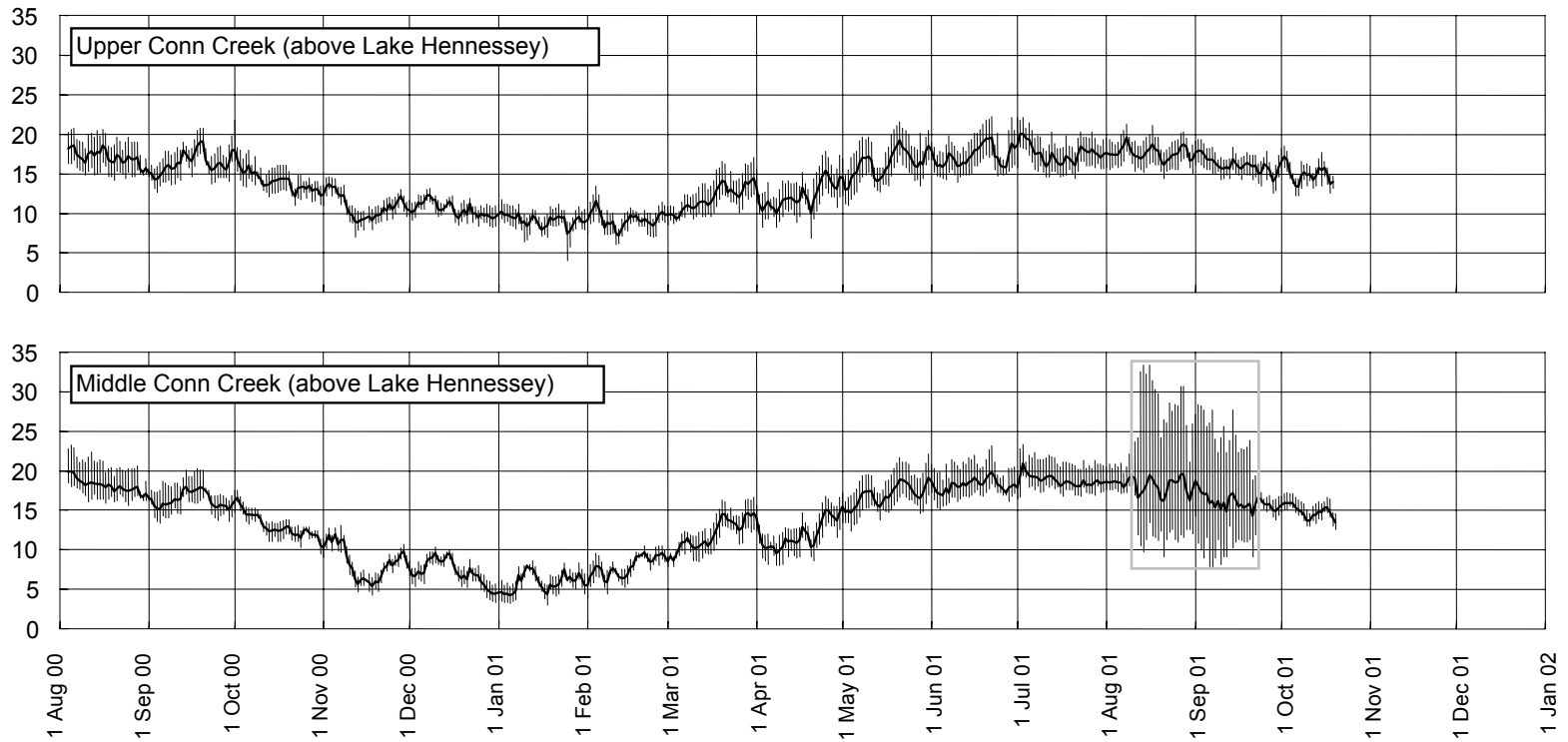


Figure 5. Miniature water temperature recorders can be used to identify periods of inundation and desiccation. Diurnal temperature fluctuations are generally muted during periods of inundation, and more pronounced when they are exposed to the open air (gray box).

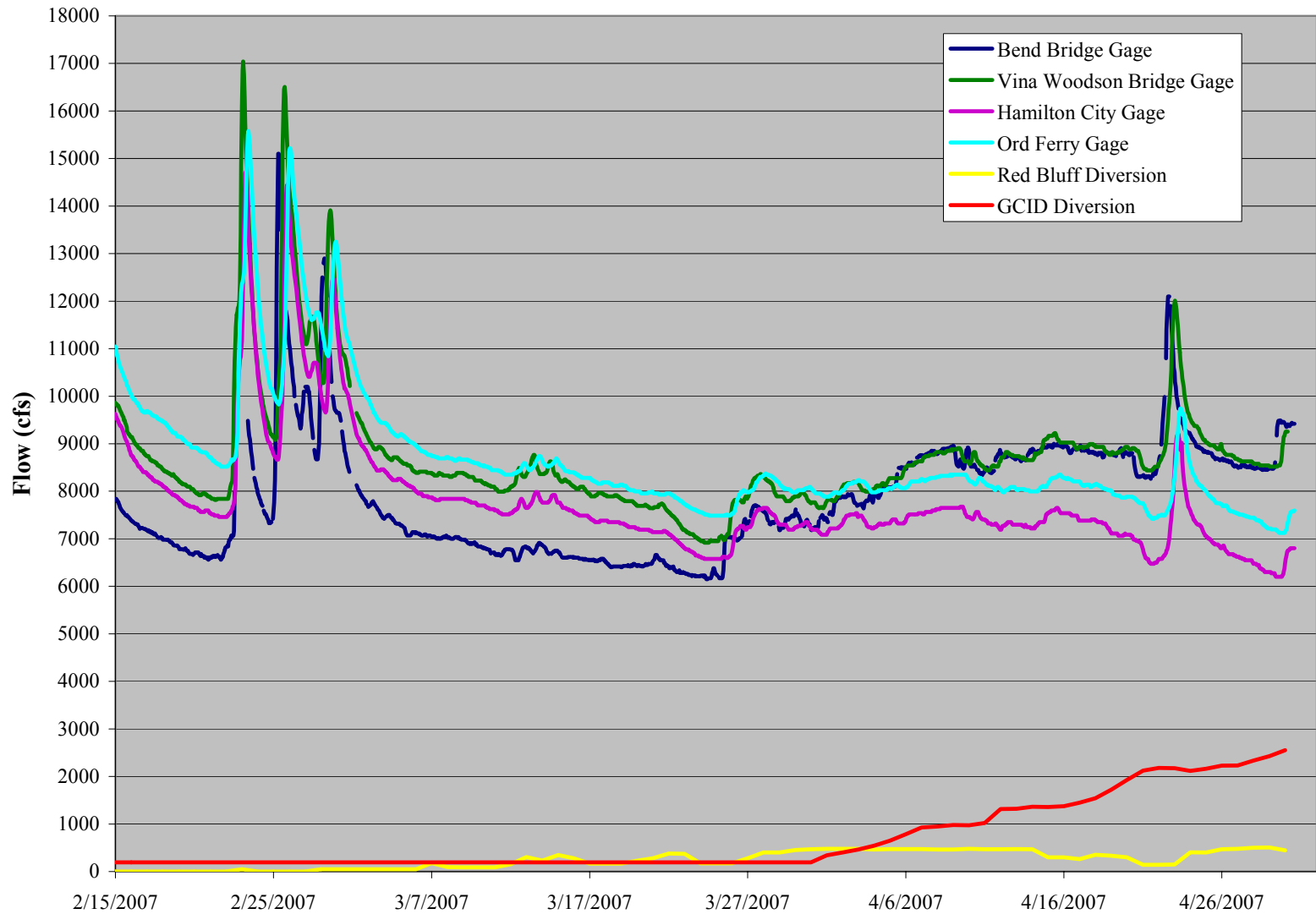
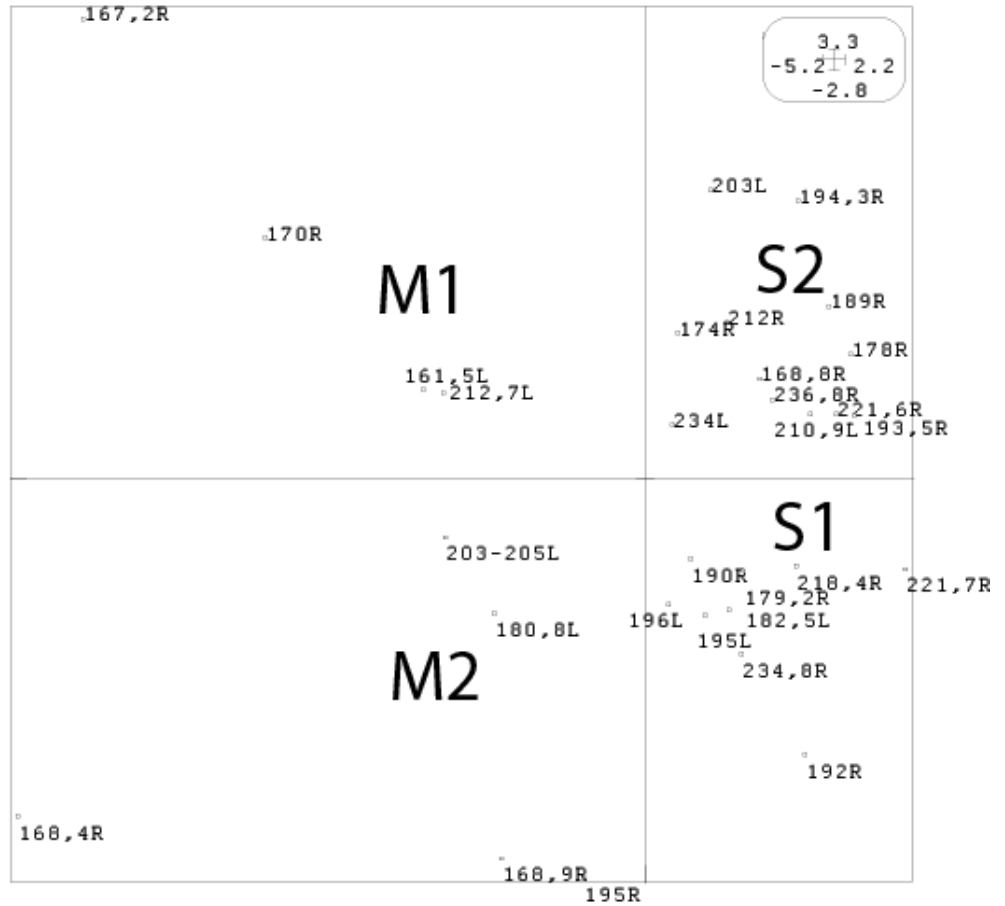
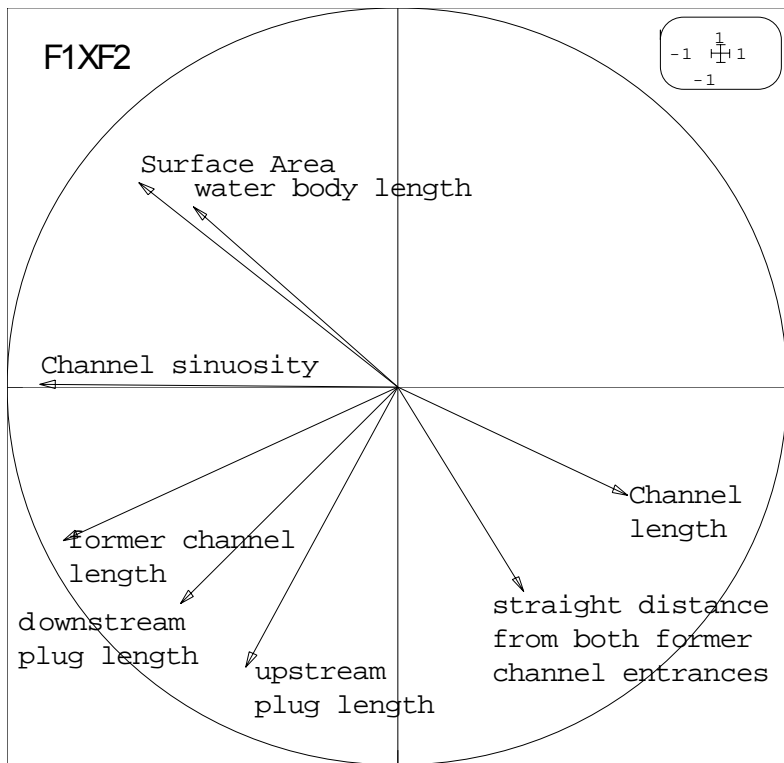


Figure 6. CA DWR flow gauges and flow diversions on the Sacramento River used to analyze OCWB study sites from 2/15/2007 to 4/30/2007.



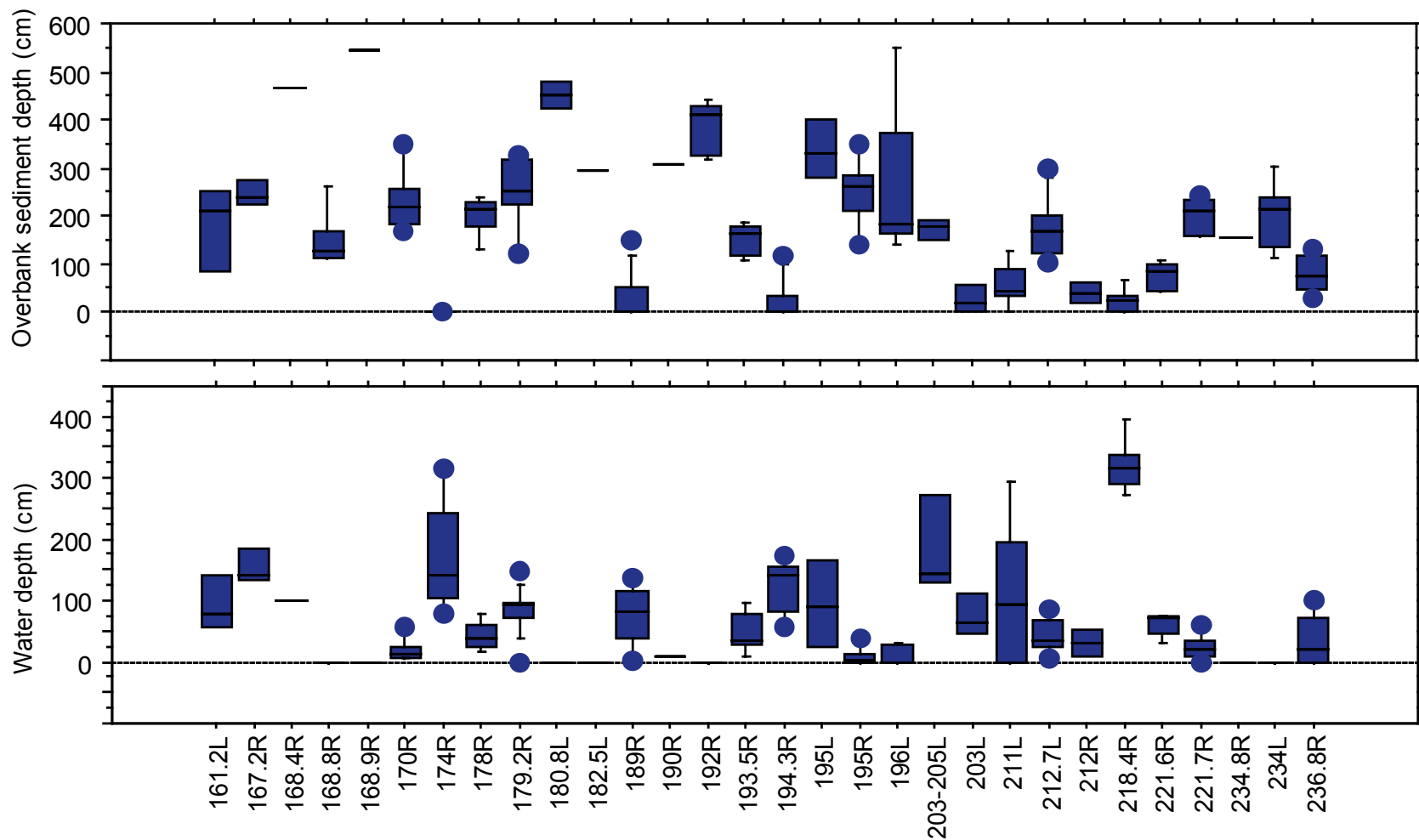


Figure 8. Sediment thicknesses and water depths measured in OCWBs of the Sacramento River, presented as box-and-whisker plots (Tukey 1977), in which the spread of the middle 50% of the data is shown by the box, and upper and lower outliers indicated by points connected to the box by lines (whiskers).

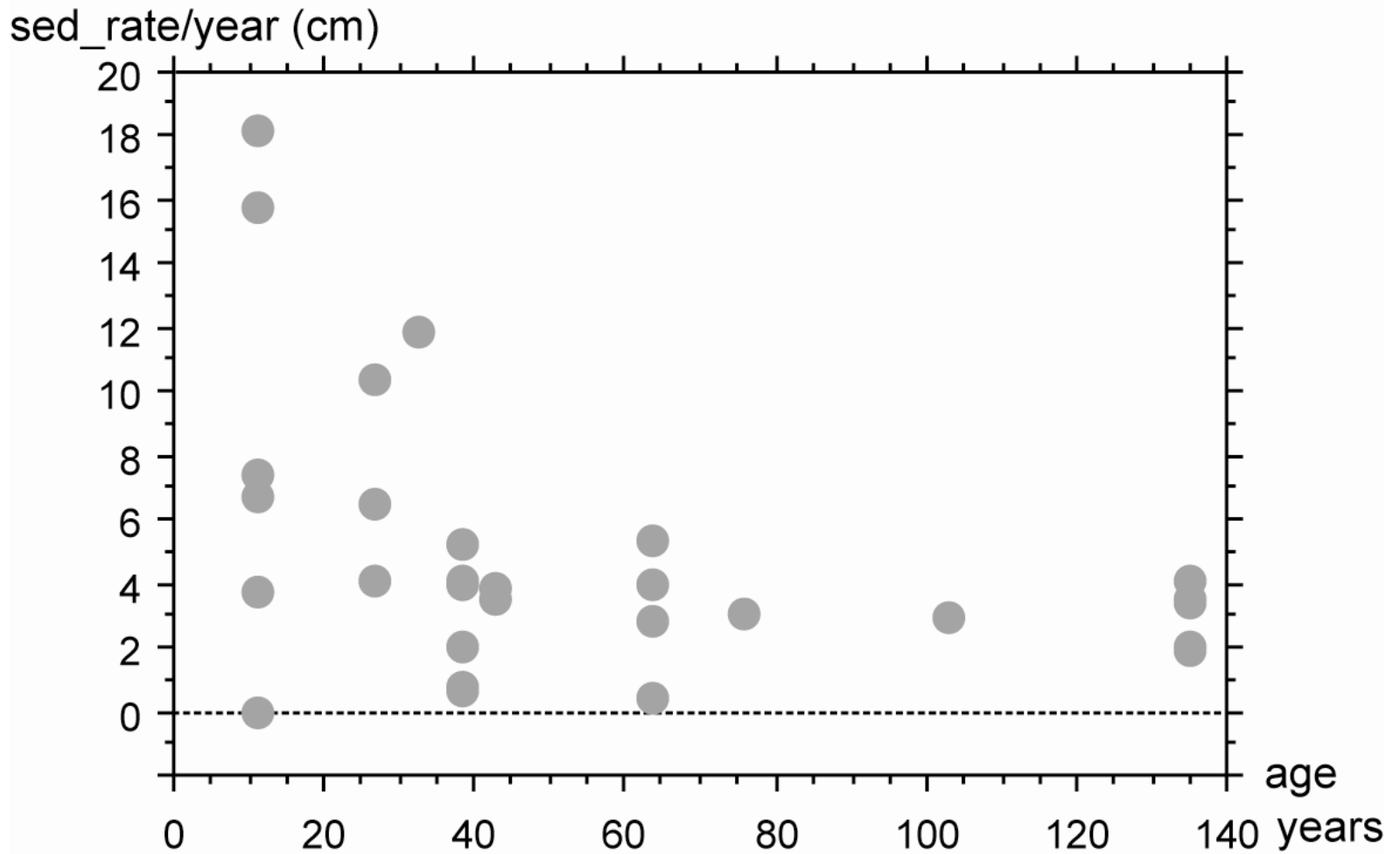


Figure 9. Sedimentation rates measured in OCWBs plotted against age of the channel being cut off from the mainstem Sacramento River.

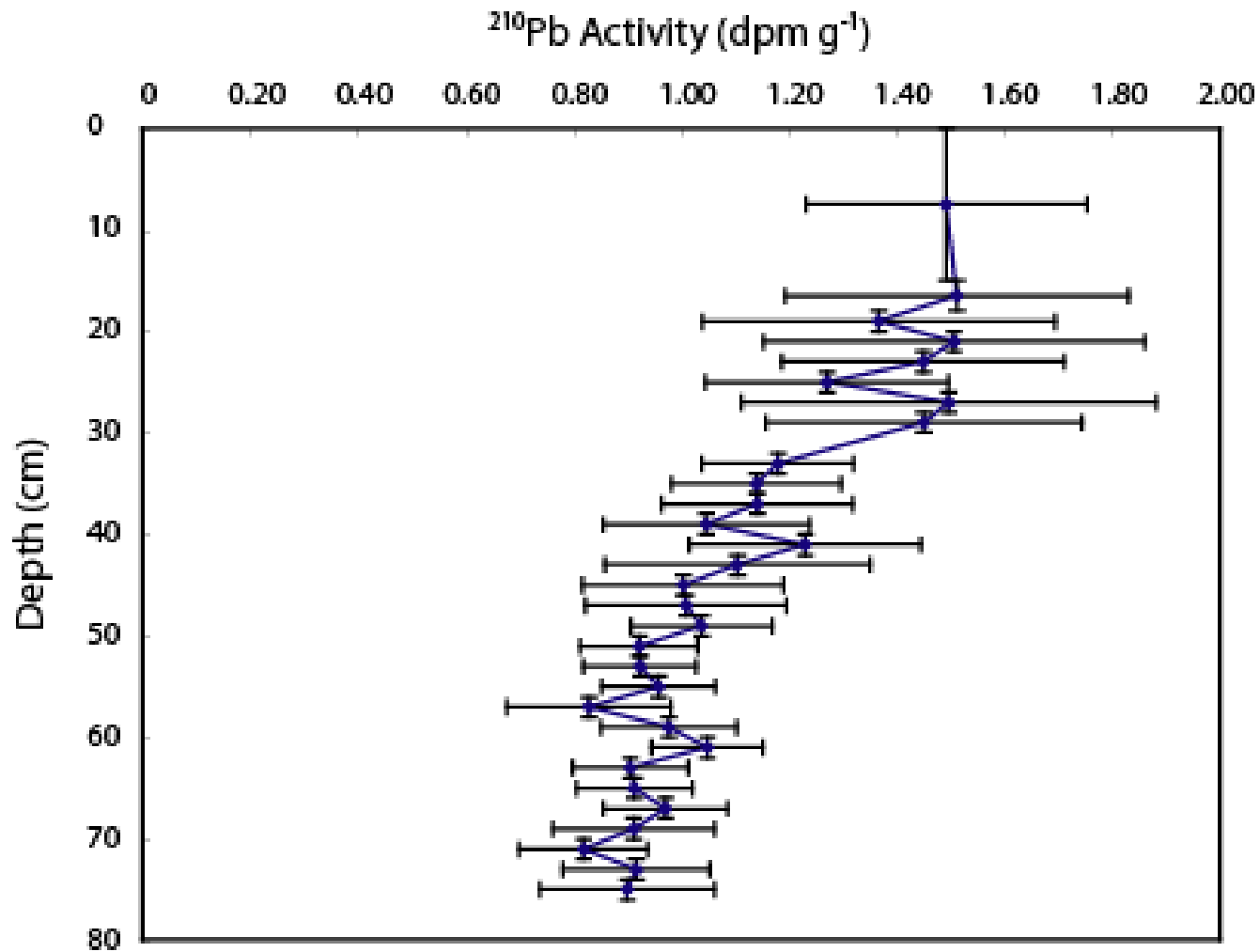


Figure 10. Activity of ^{210}Pb in units of decays per minute per gram, through the depth of a sediment core from Packer Lake. The core was taken near the apex of the lake.

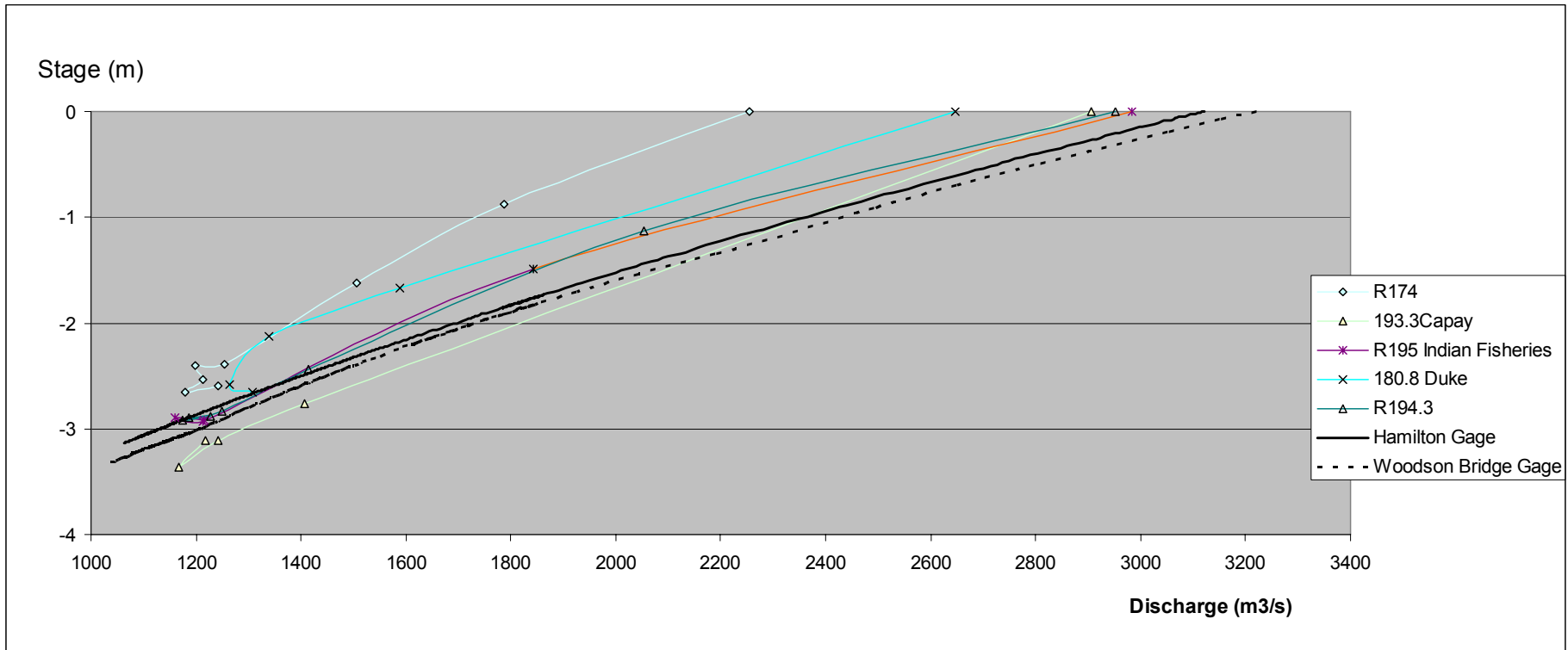


Figure 11. Stage-discharge relations during recession limb of the March 2006 for the mainstem at Woodson Bridge and Hamilton City, and for five OCWBs. For each site shown, the point along the zero line at the top of the figure represents the highest reading (at the beginning of our period of measurement during the flood's recession limb). The later observations are along the line descending to the left. The mainstem lines show linear declines. The OCWBs with straight lines reflect good connection between side channel and mainstem, while the non-linear traces reflect poor connection to the main channel.

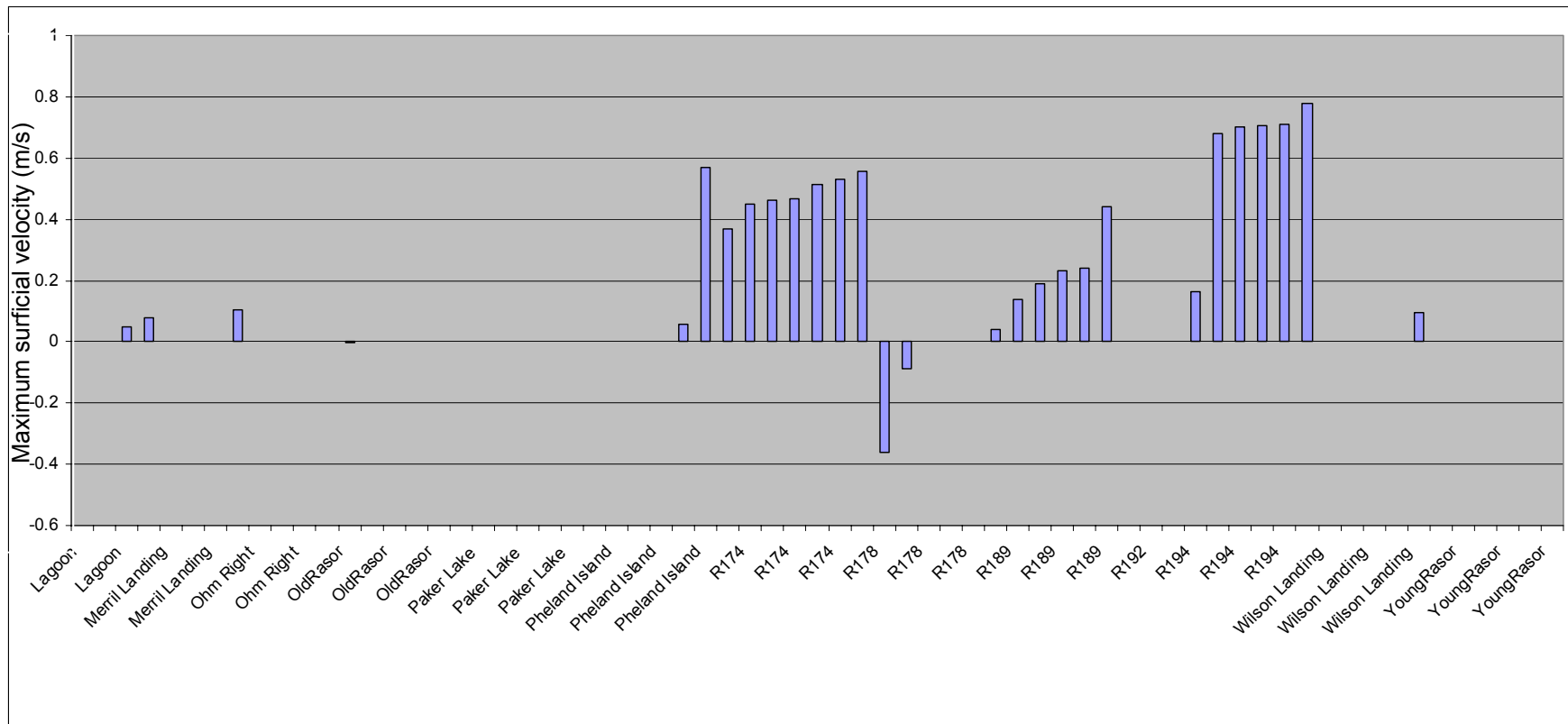


Figure 12b. Surface velocity measurements during the recession limb of the March 2006 flood for Lagoon, Merrills Landing, Old Razor Slough, Packer lake, Pheland Island, R174, R178, R189, R192, R194, Wilson Landing, and Young Razor Slough. The x-axis is labeled with the name of the OCWB for each velocity measurement. If the velocity was zero, no bar is visible. If velocity was negative (i.e., in the upstream direction), the bar extends downward from the zero line. If velocity was positive (i.e., downstream), the bar extends upward.

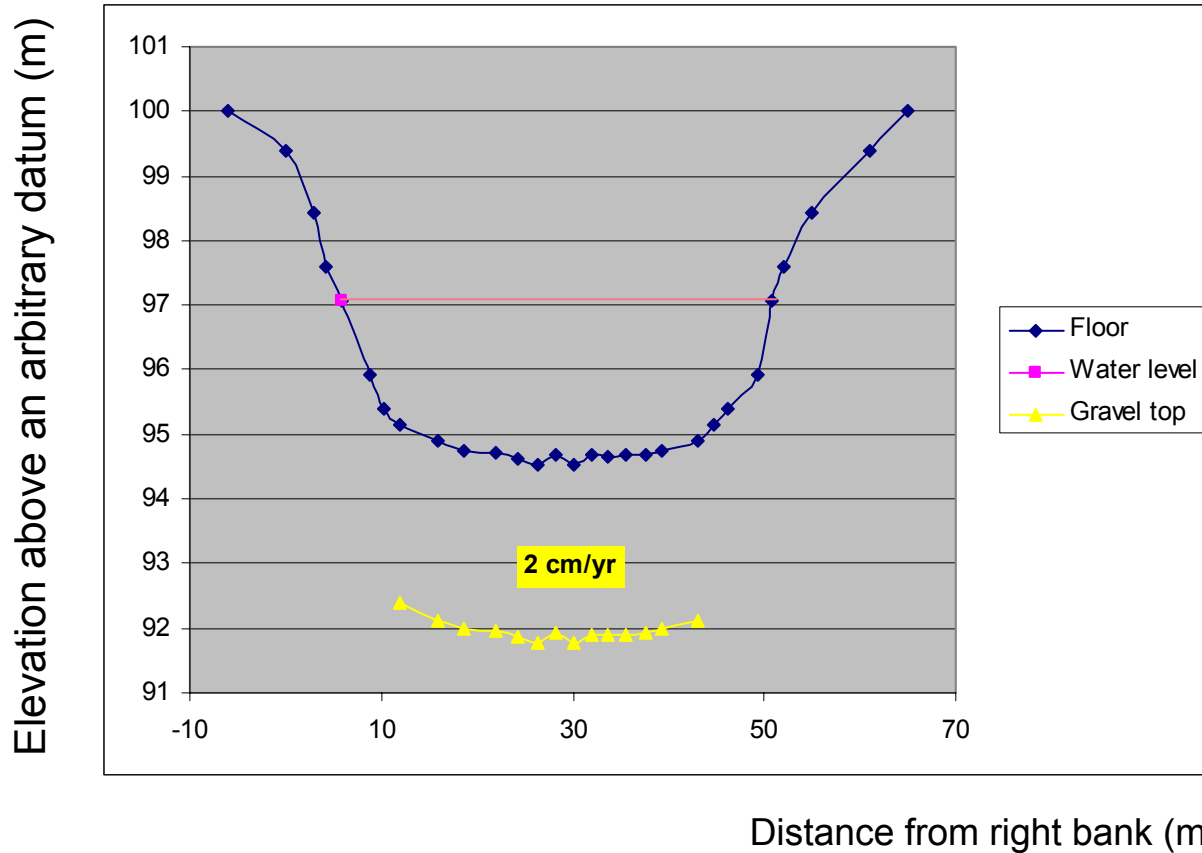


Figure 13. Cross section of Phelan Island OCWB.

Elevation above an arbitrary datum (m)

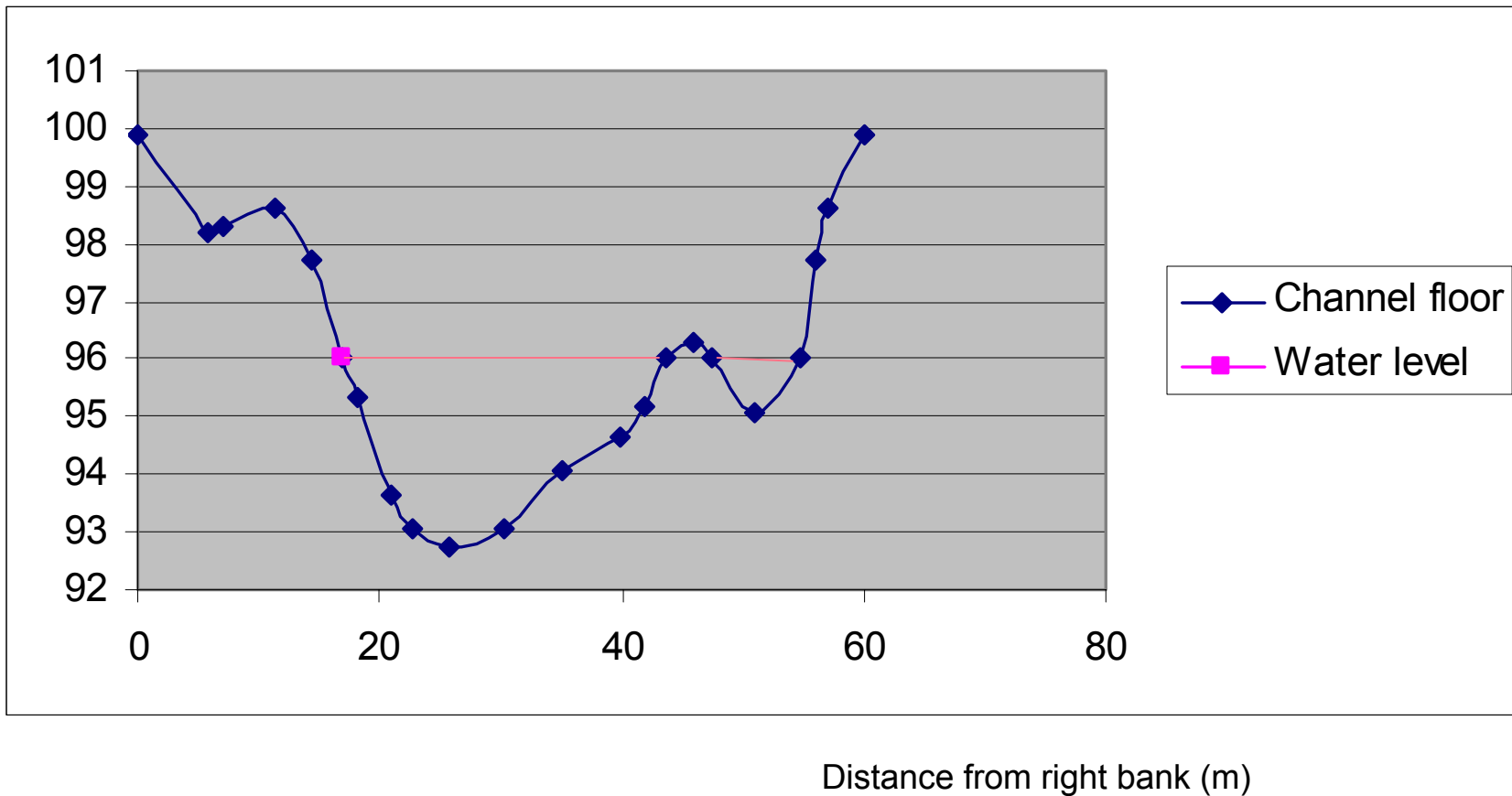
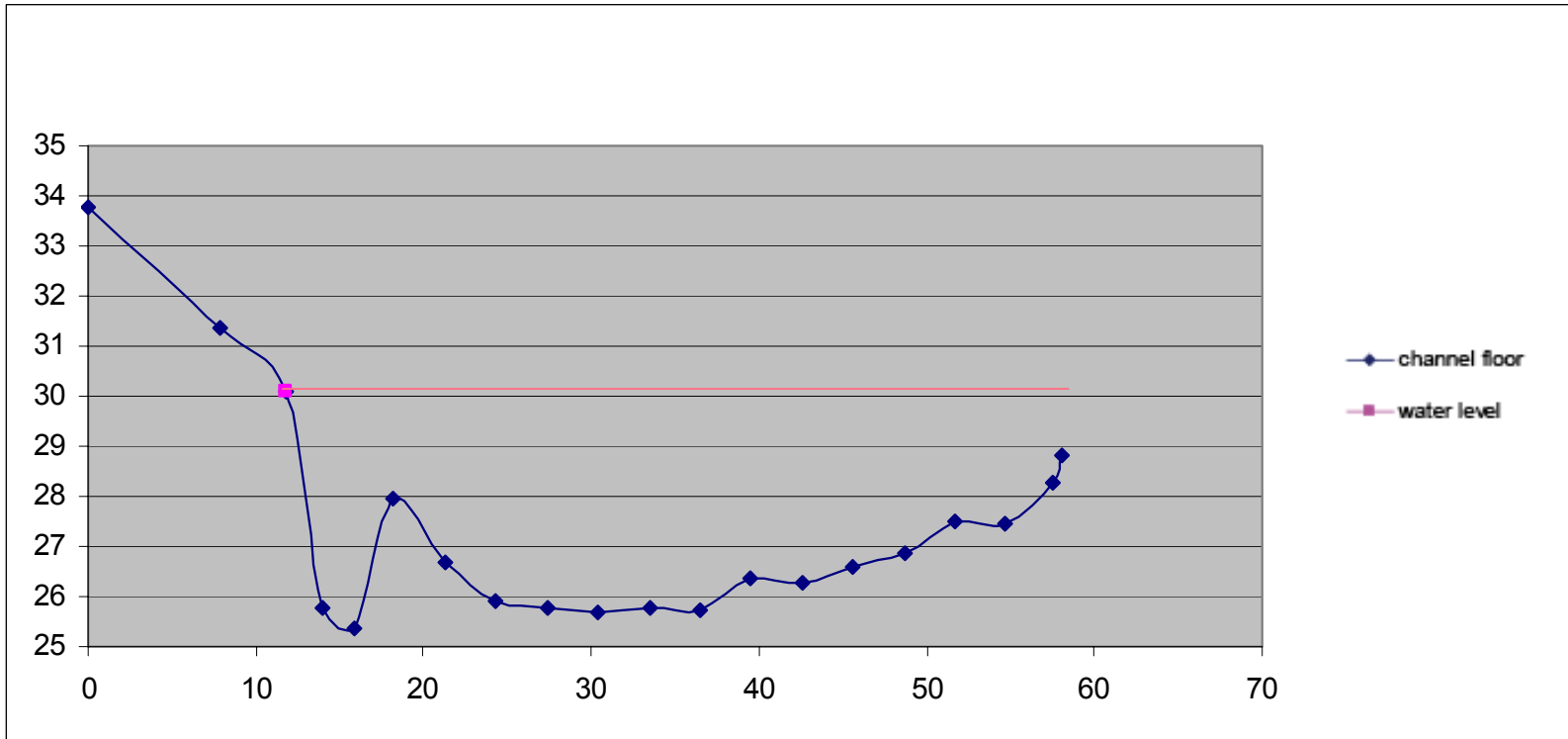


Figure 14. Cross section of Capay OCWB.

Elevation above an arbitrary datum (m)



Distance from right bank (m)



Stillwater Sciences

Figure 15. Cross section of Jacinto OCWB.

Elevation above an arbitrary datum (m)

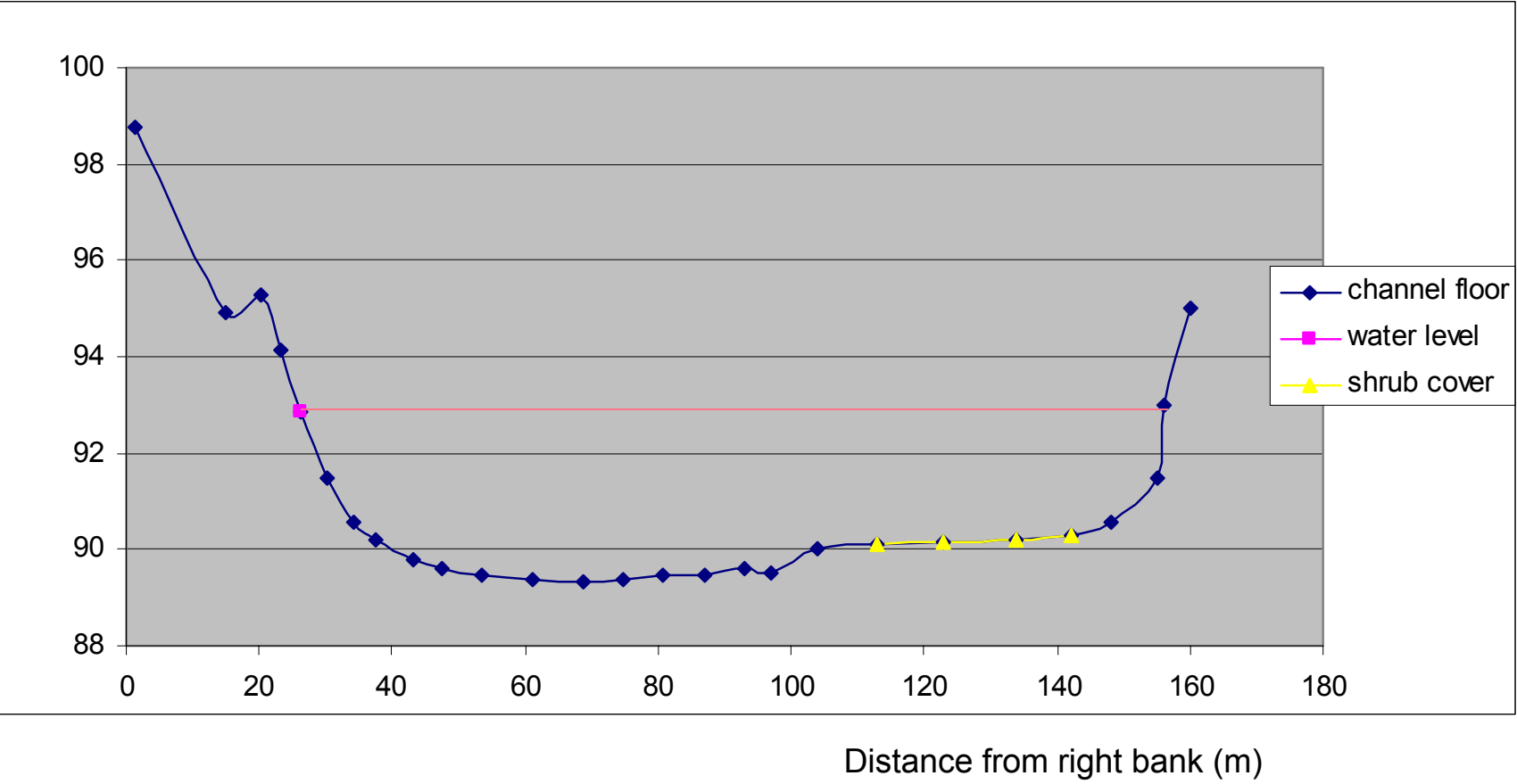


Figure 16. Cross section of Old Rasor OCWB.

Elevation above an arbitrary datum (m)

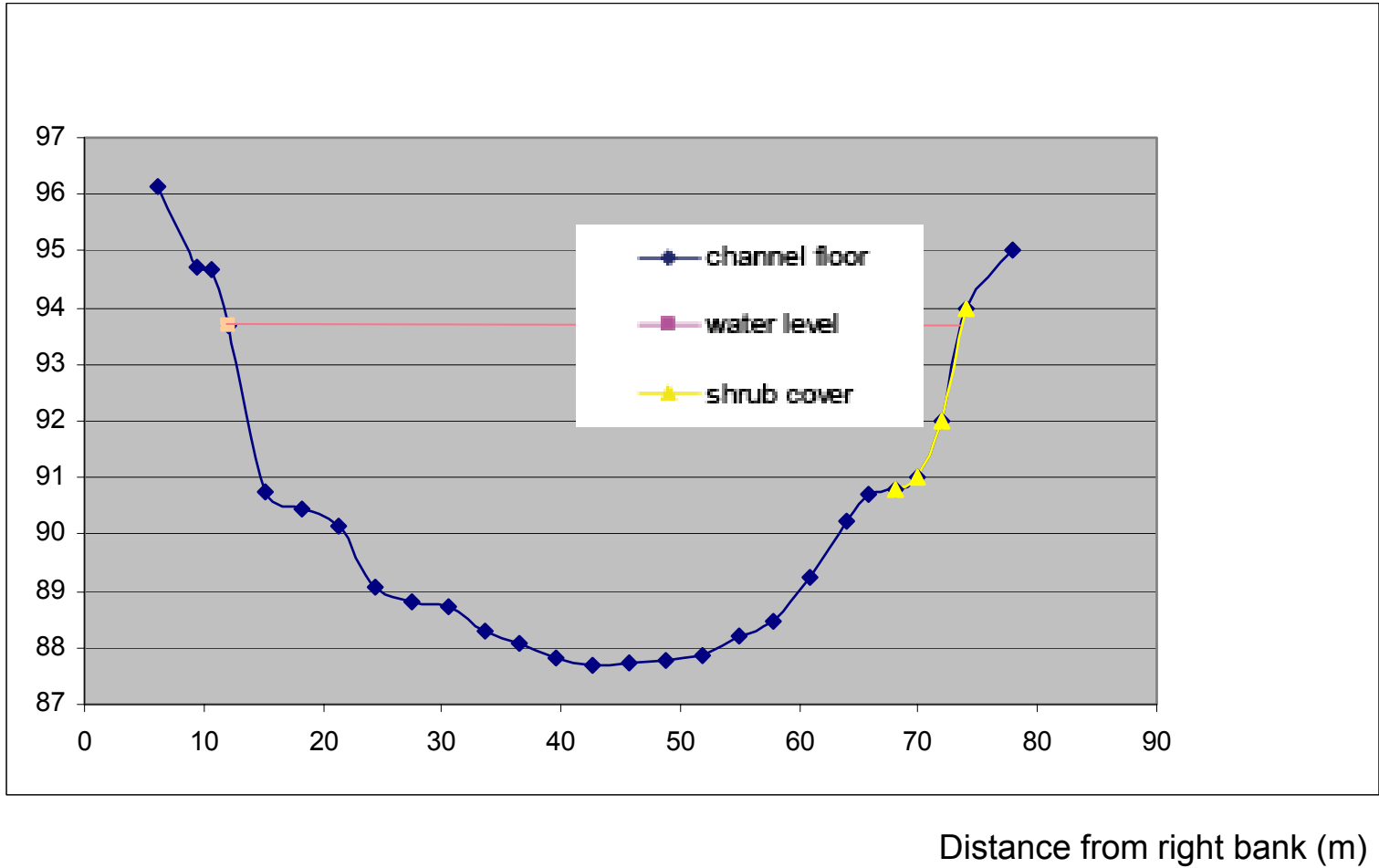


Figure 17. Cross section of Kopta main OCWB.

Elevation above an arbitrary datum (m)

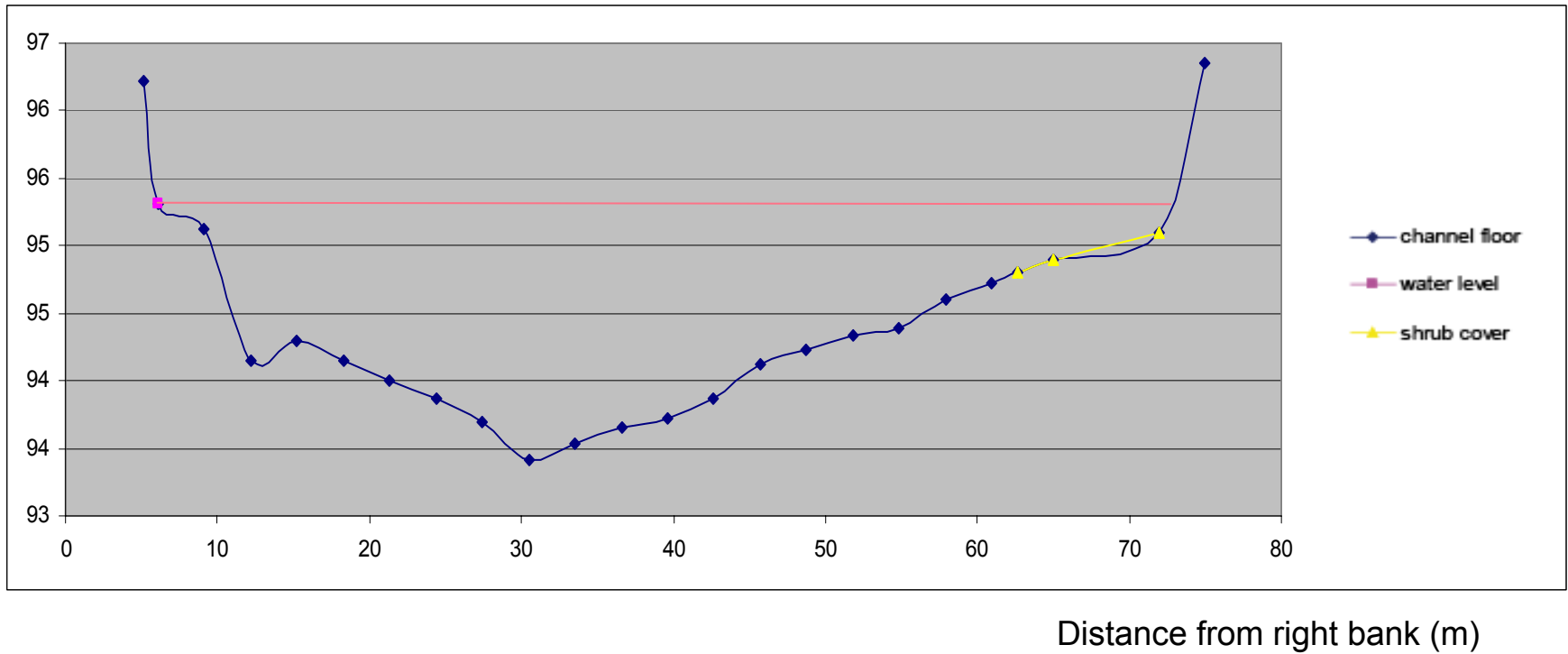


Figure 18. Cross section of Jenny Lind Bend OCWB.

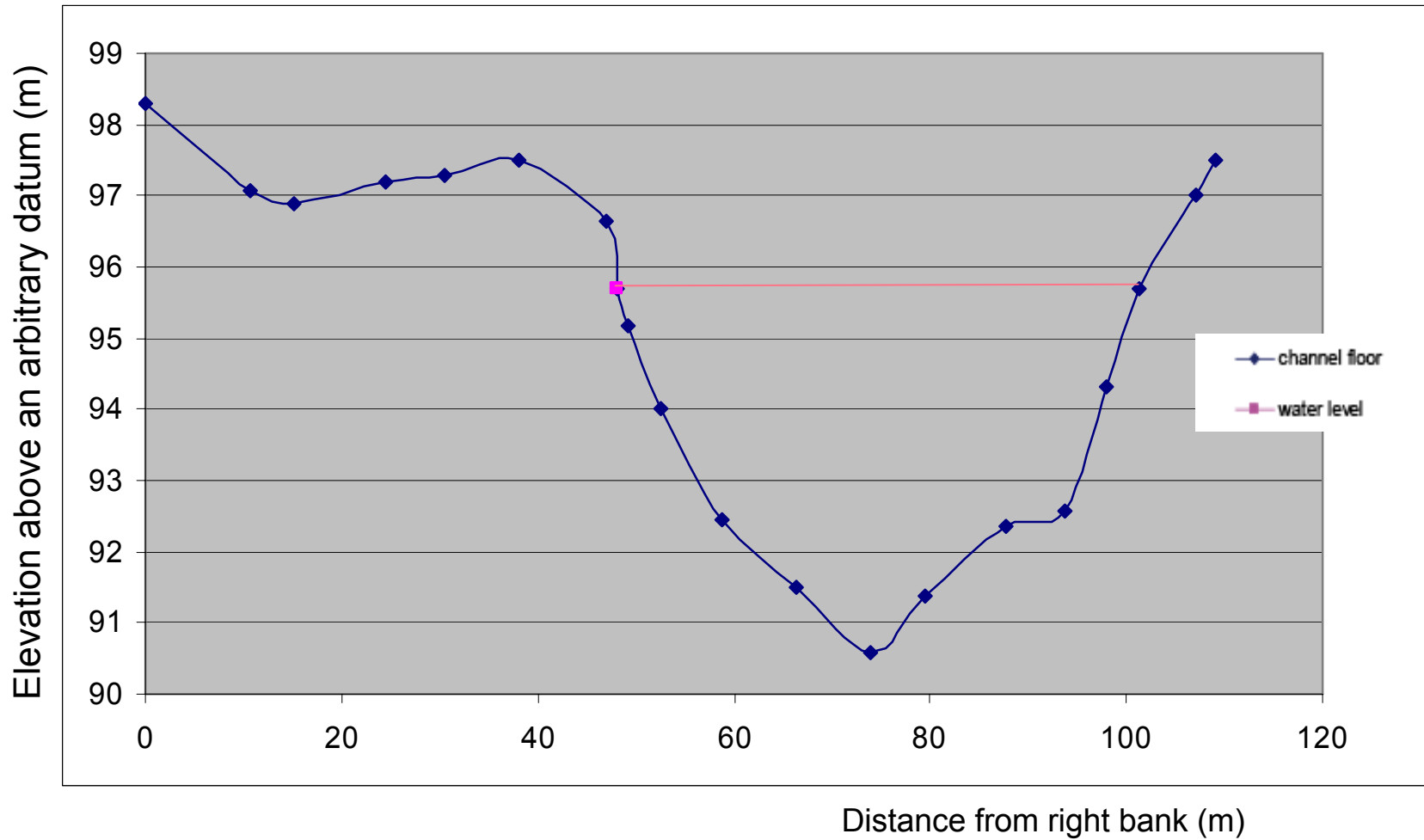


Figure 19. Cross section of Young Razor slough OCWB.

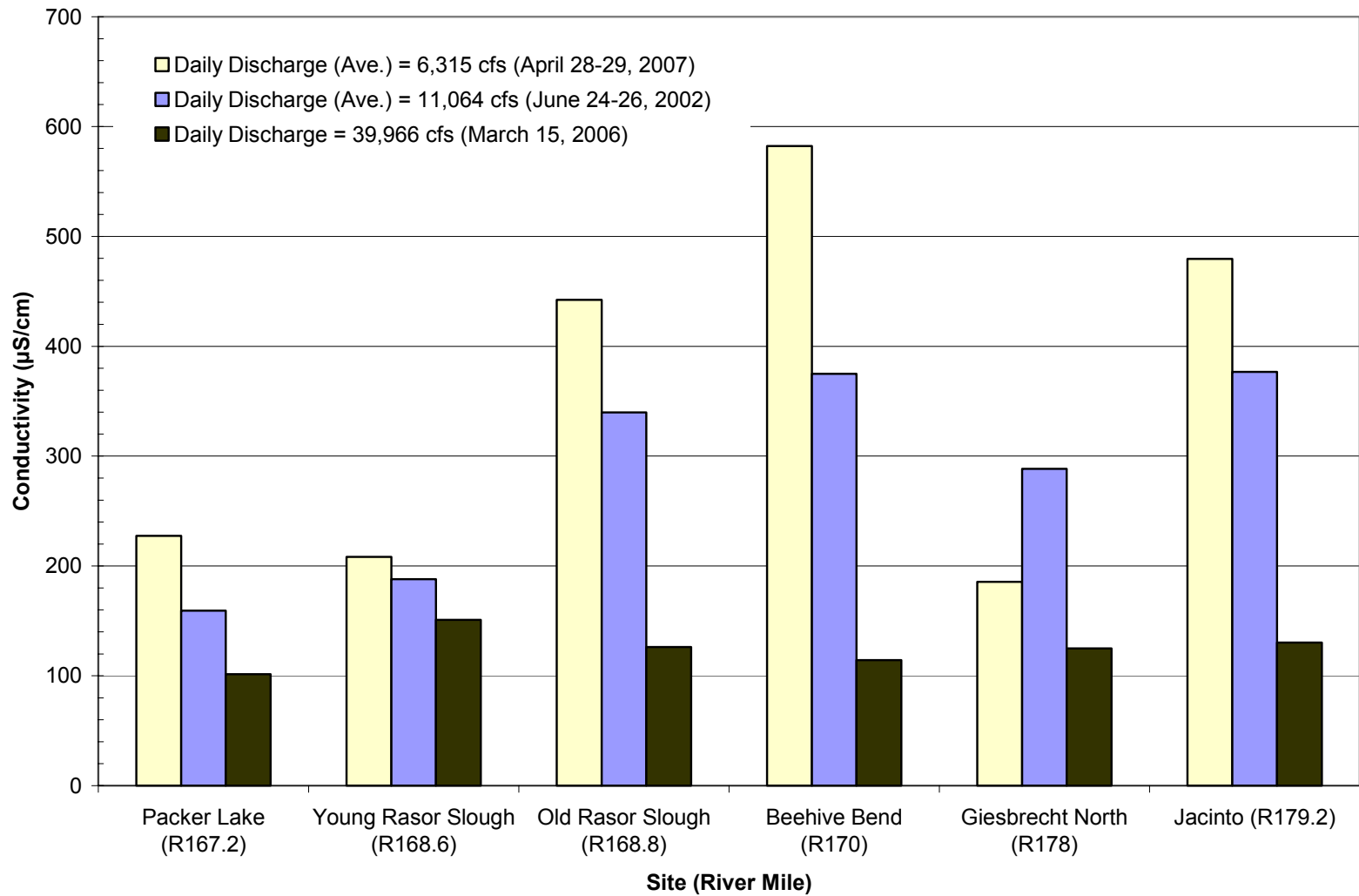
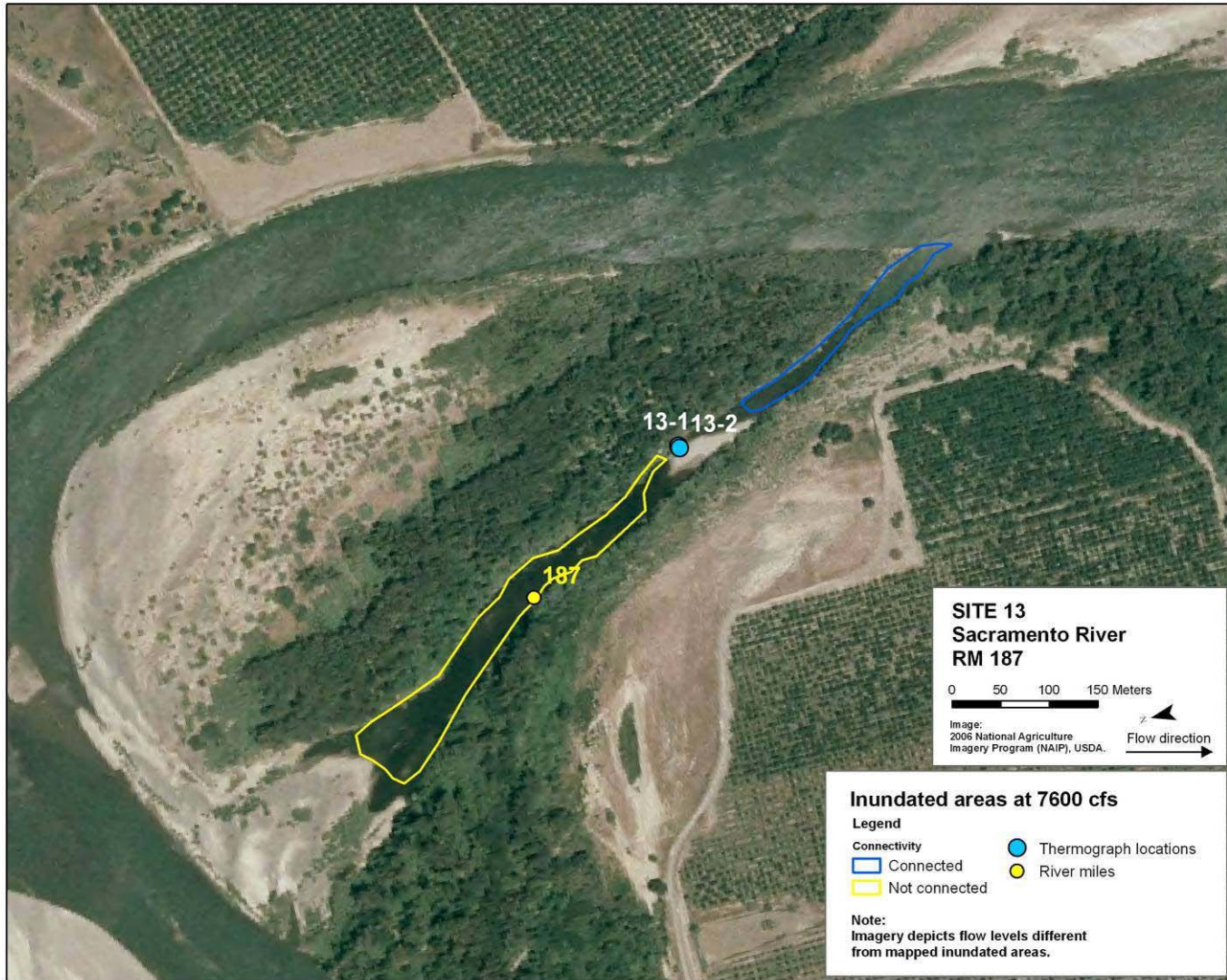


Figure 20. Conductivity measurements for selected OCWB sites taken during a range of Sacramento River discharge rates.



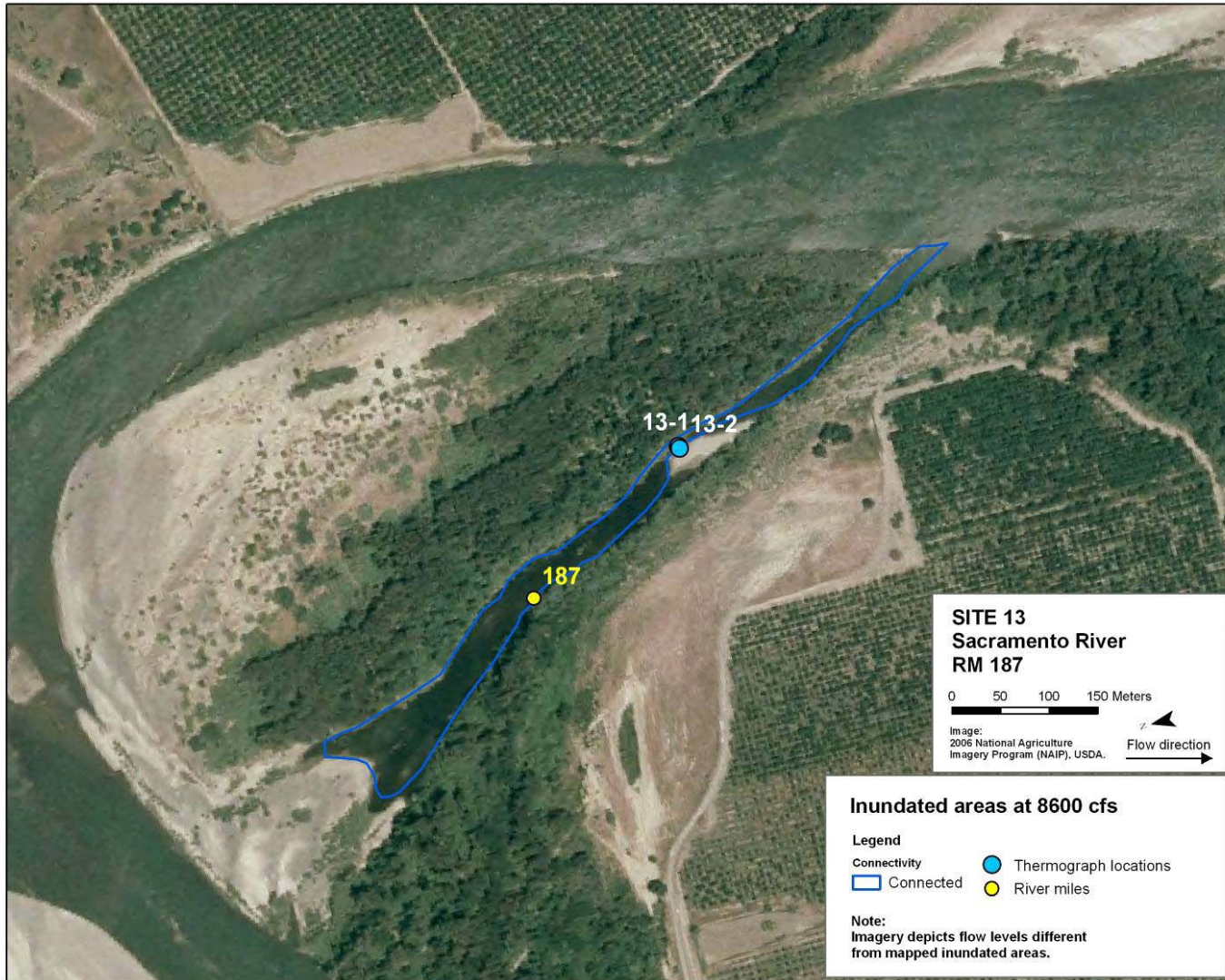
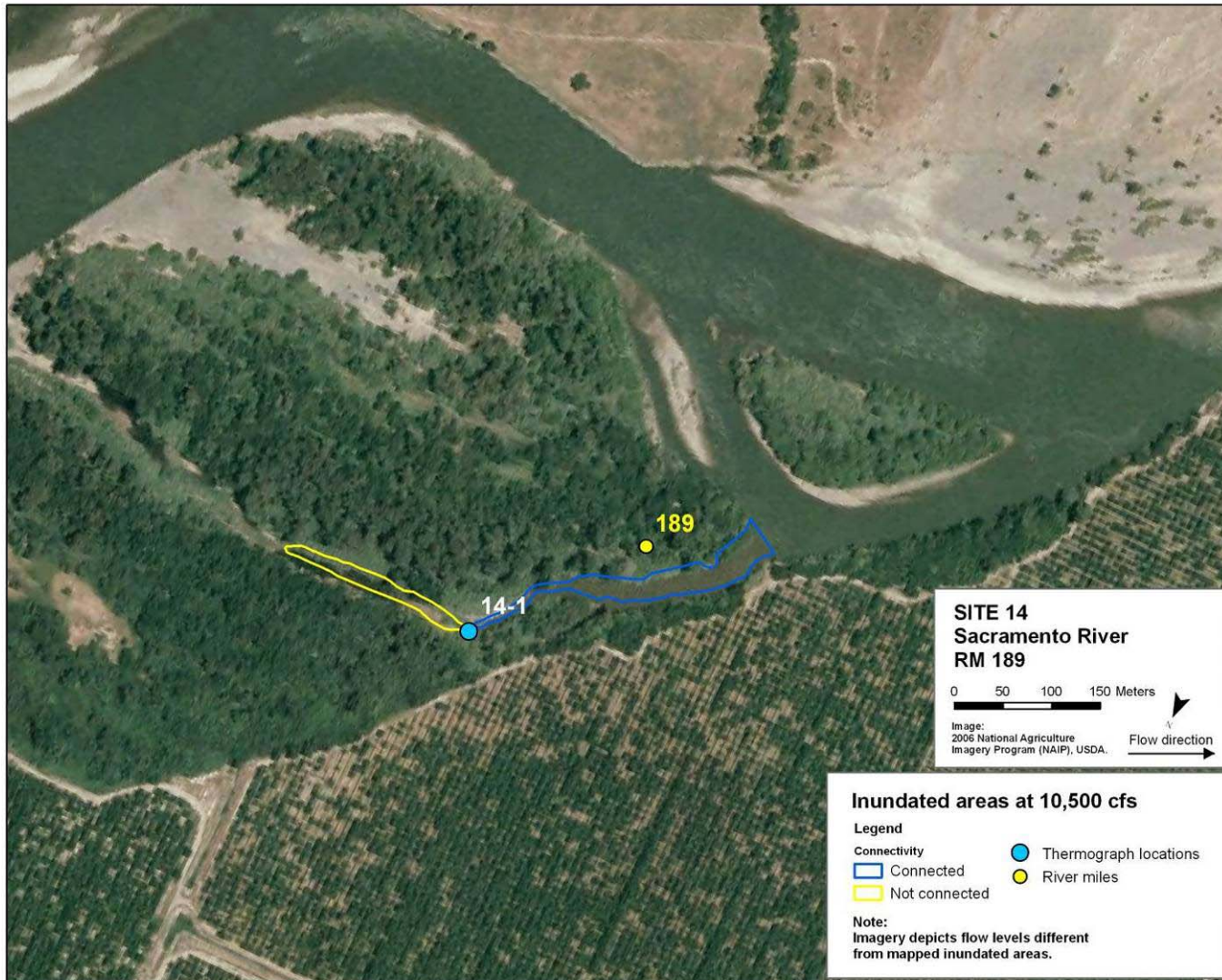


Figure 21b. Inundated areas at site 13 (RM 187R) with flows of 8,600 cfs, areas observed and drawn during field mapping.



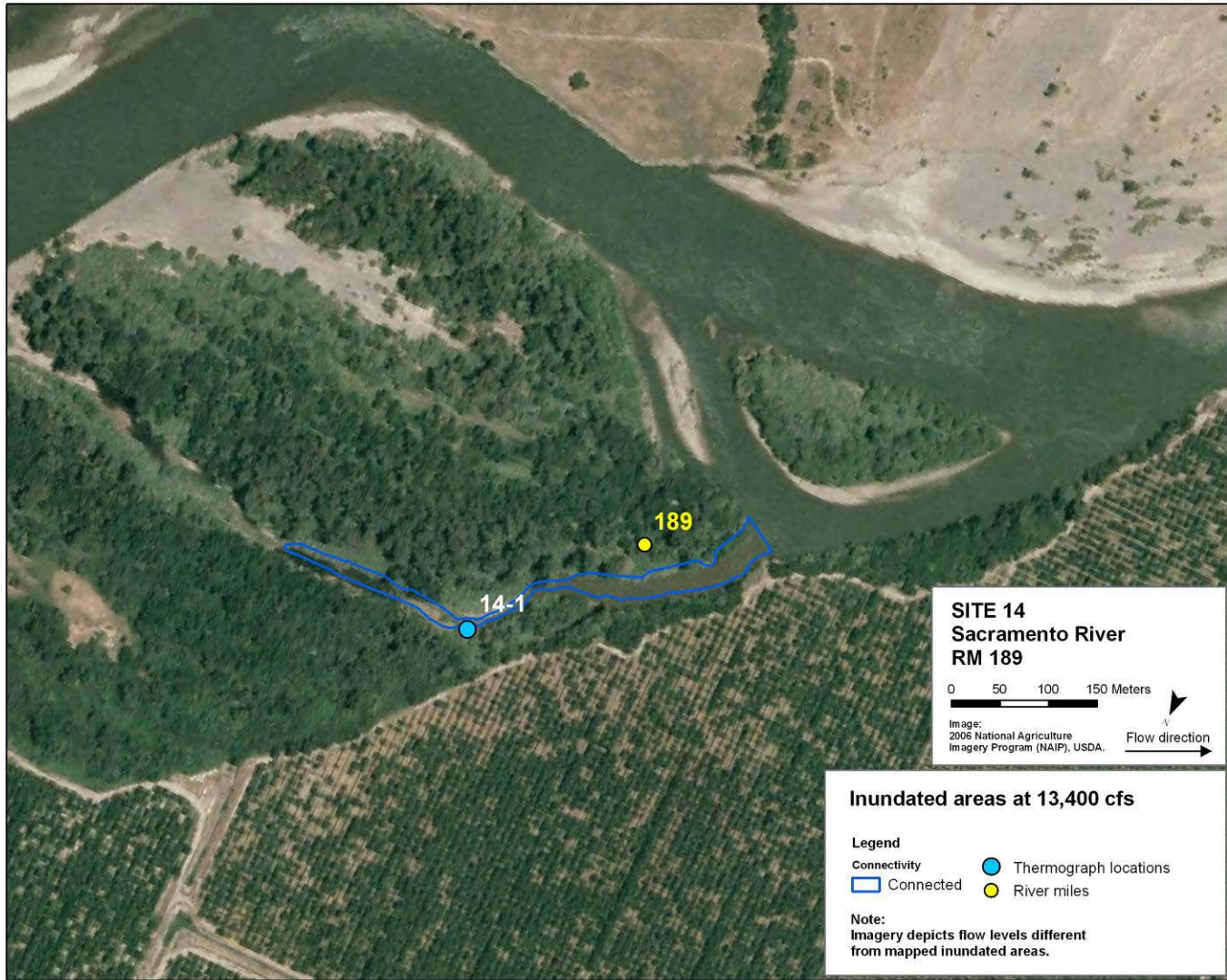


Figure 22b. Inundated areas at site 14 (RM 189R) with flows of 13,400 cfs, areas based on thermograph temperature records and field surveys.

Site 14

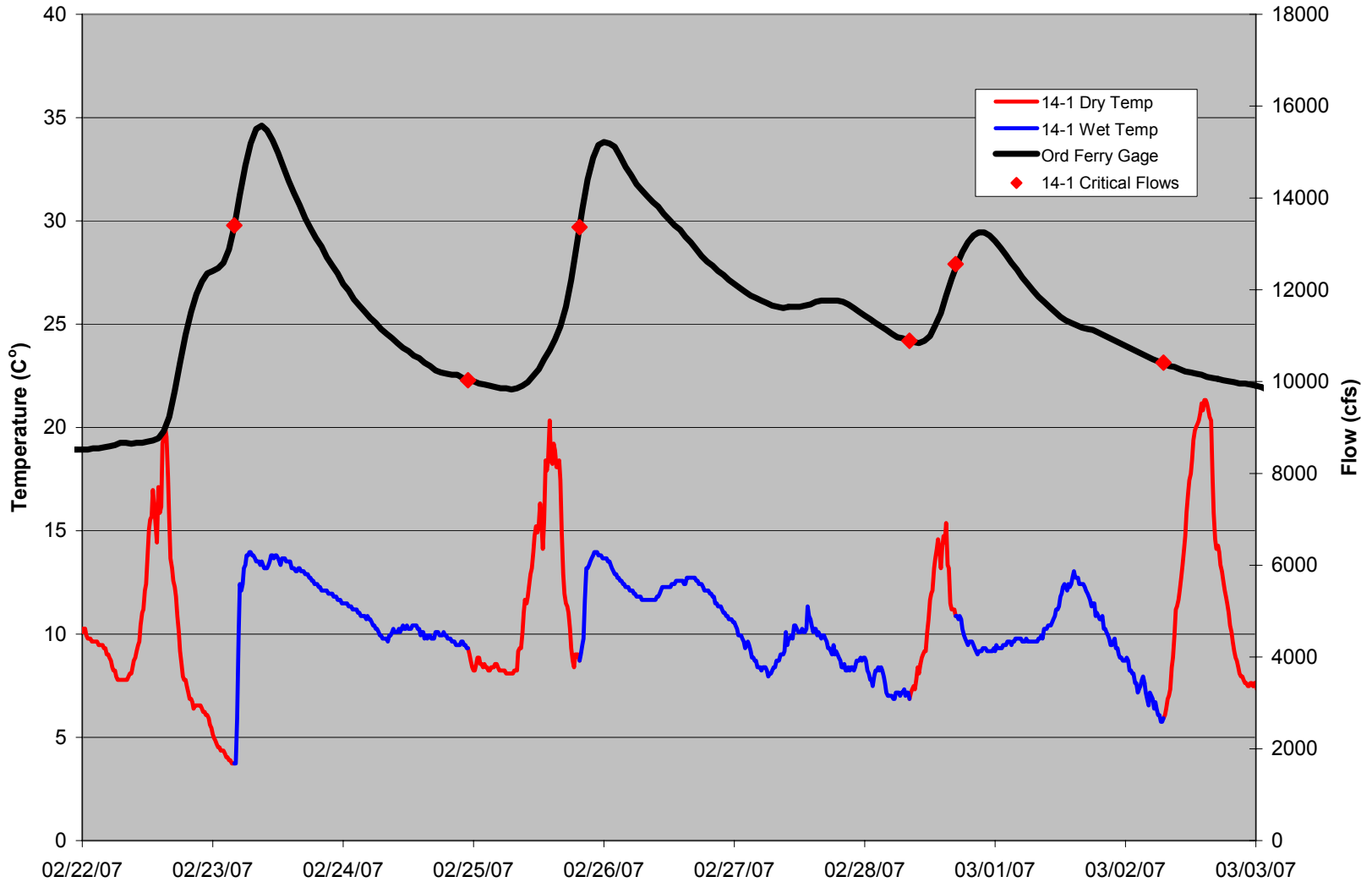
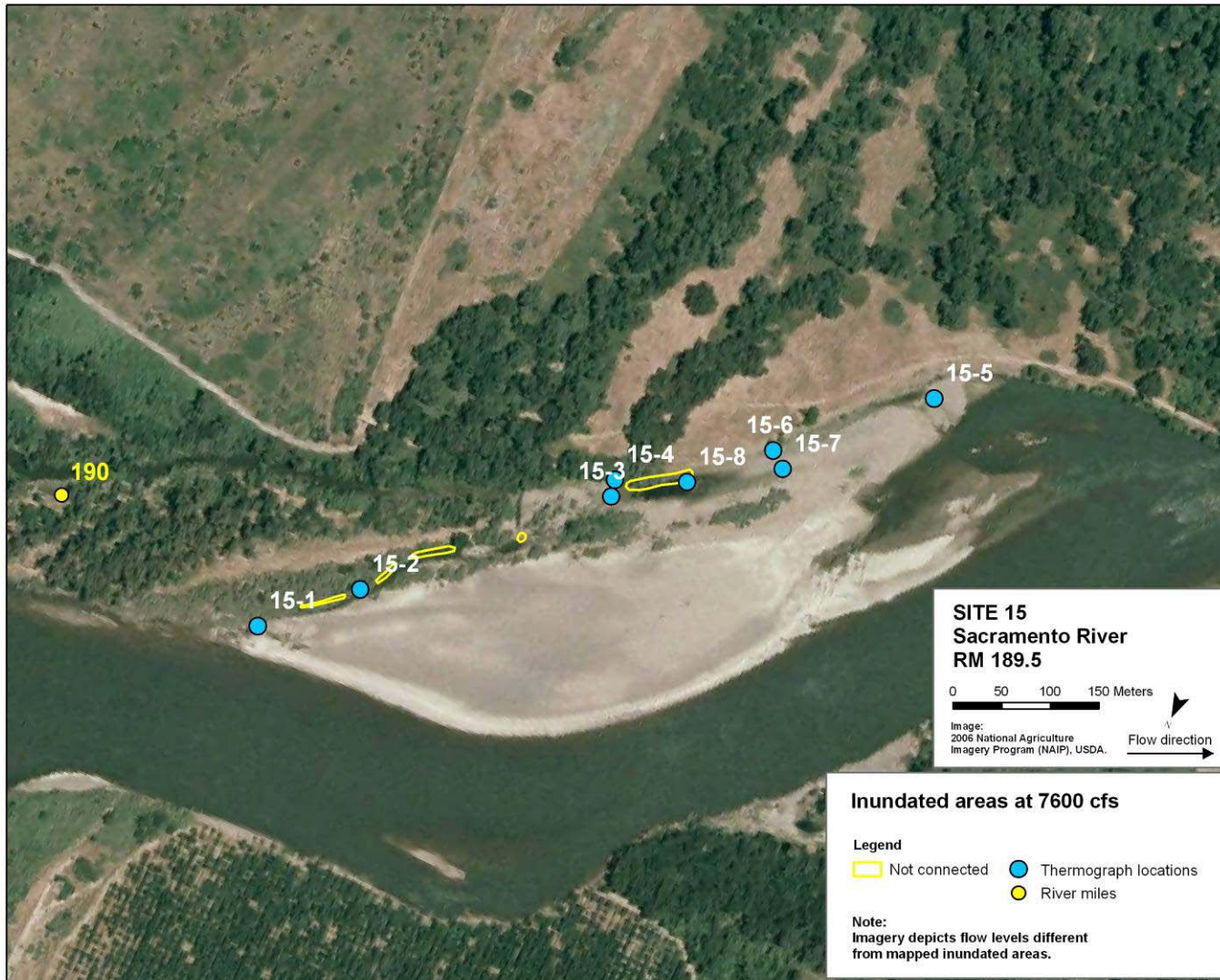
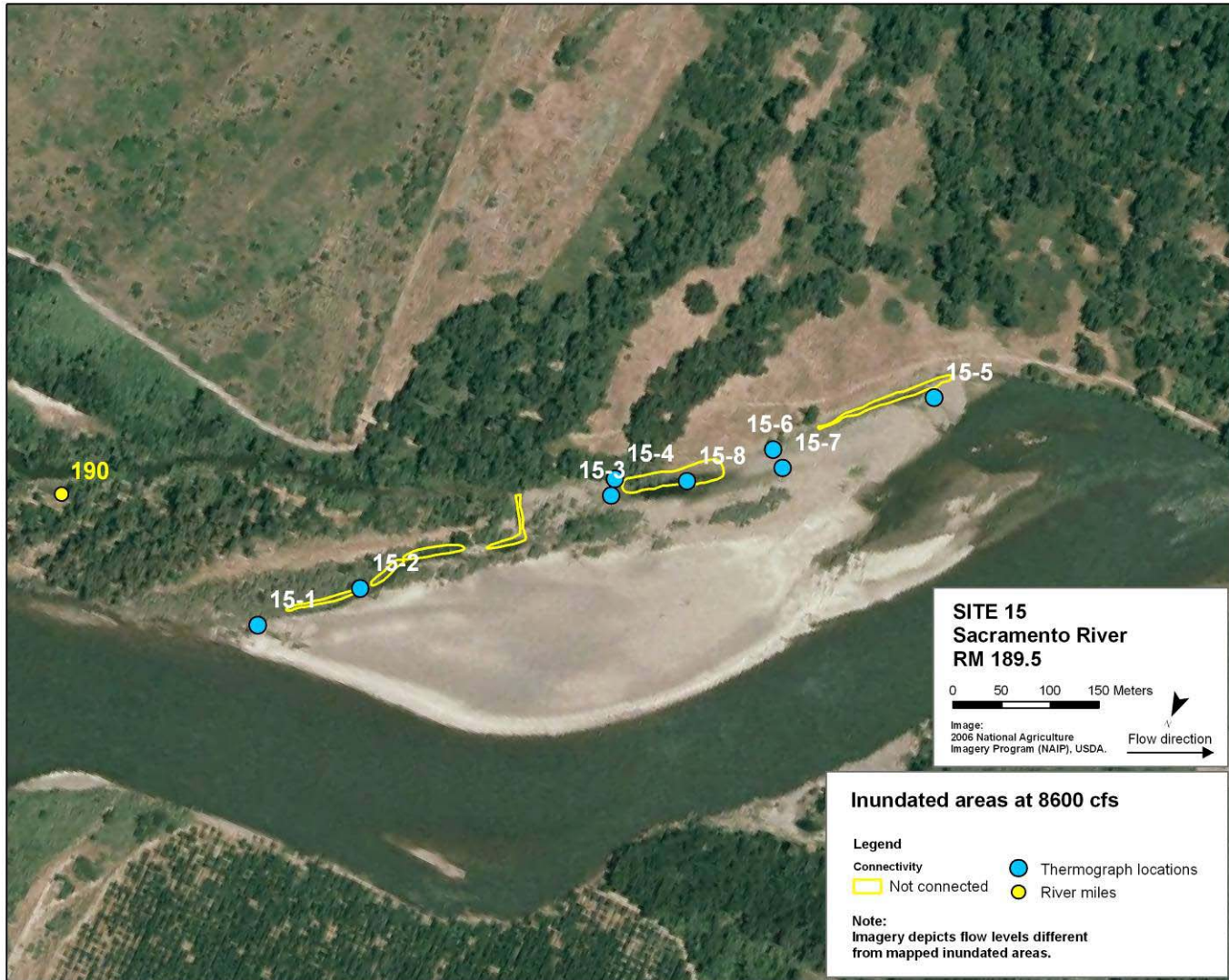


Figure 23. Thermograph data for site 14 (RM 189R) and discharge at Ord Ferry between 2/22/07 and 3/3/07. Critical flow points depict thermograph changes between dry and wet status.





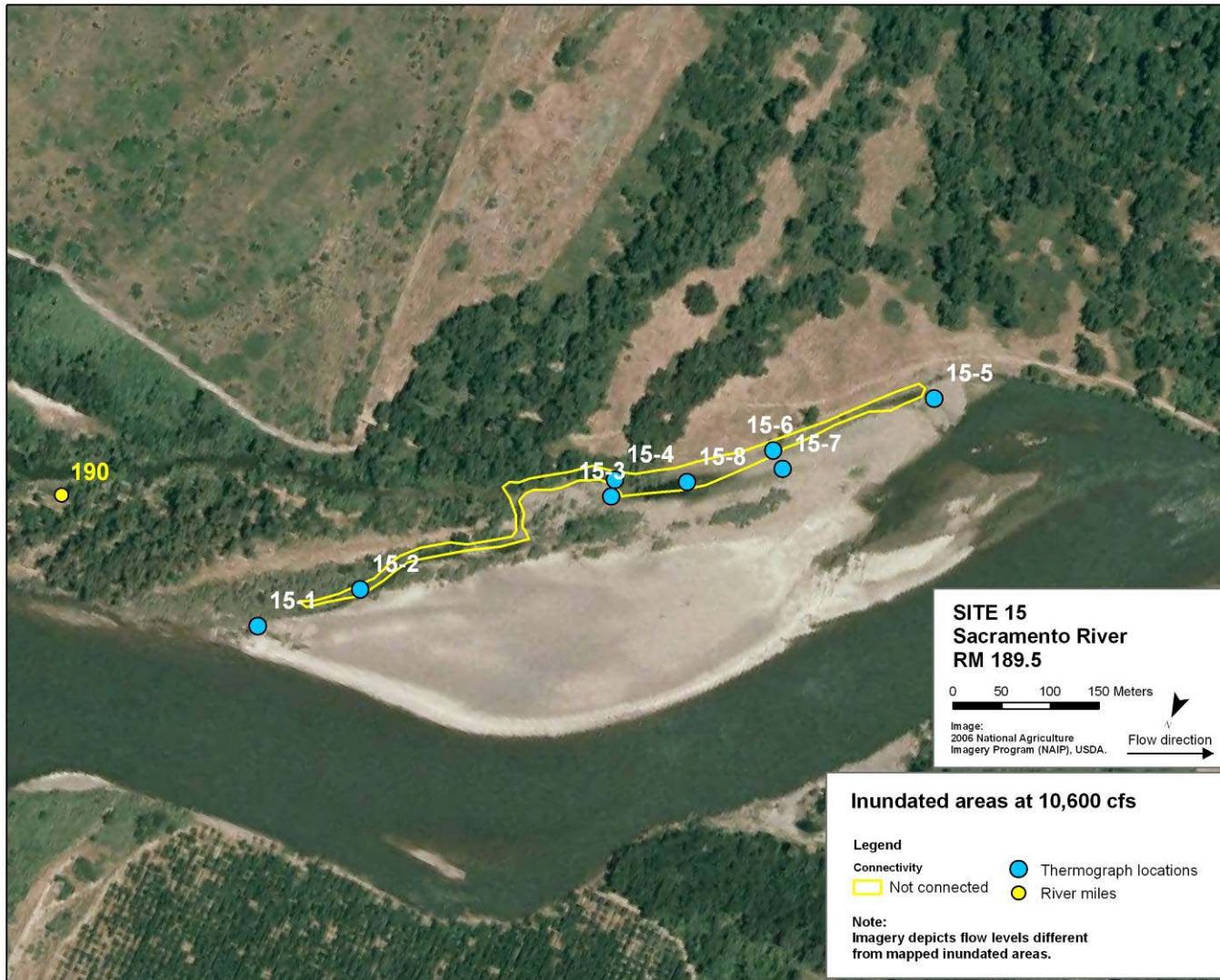




Figure 24d. Inundated areas of site 15 (RM 189.5L) at flows of 12,200 cfs , areas based on thermograph temperature records and field surveys.

Site 15

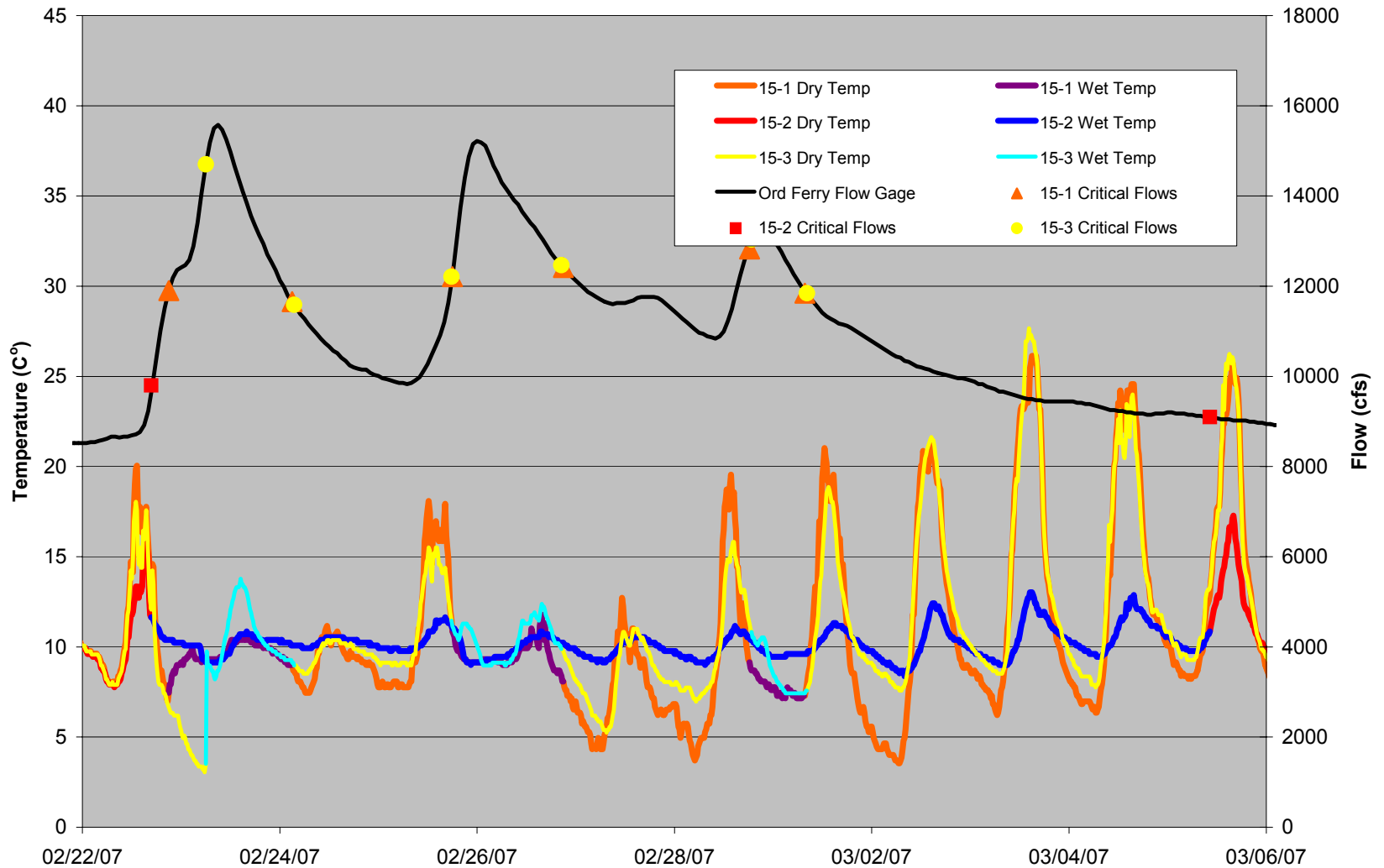


Figure 25a. Thermograph data for site 15 (RM 189.5L) and discharge at Ord Ferry between 2/22/07 and 3/6/07. Critical flow points depict thermograph changes between dry and wet status.

Site 15

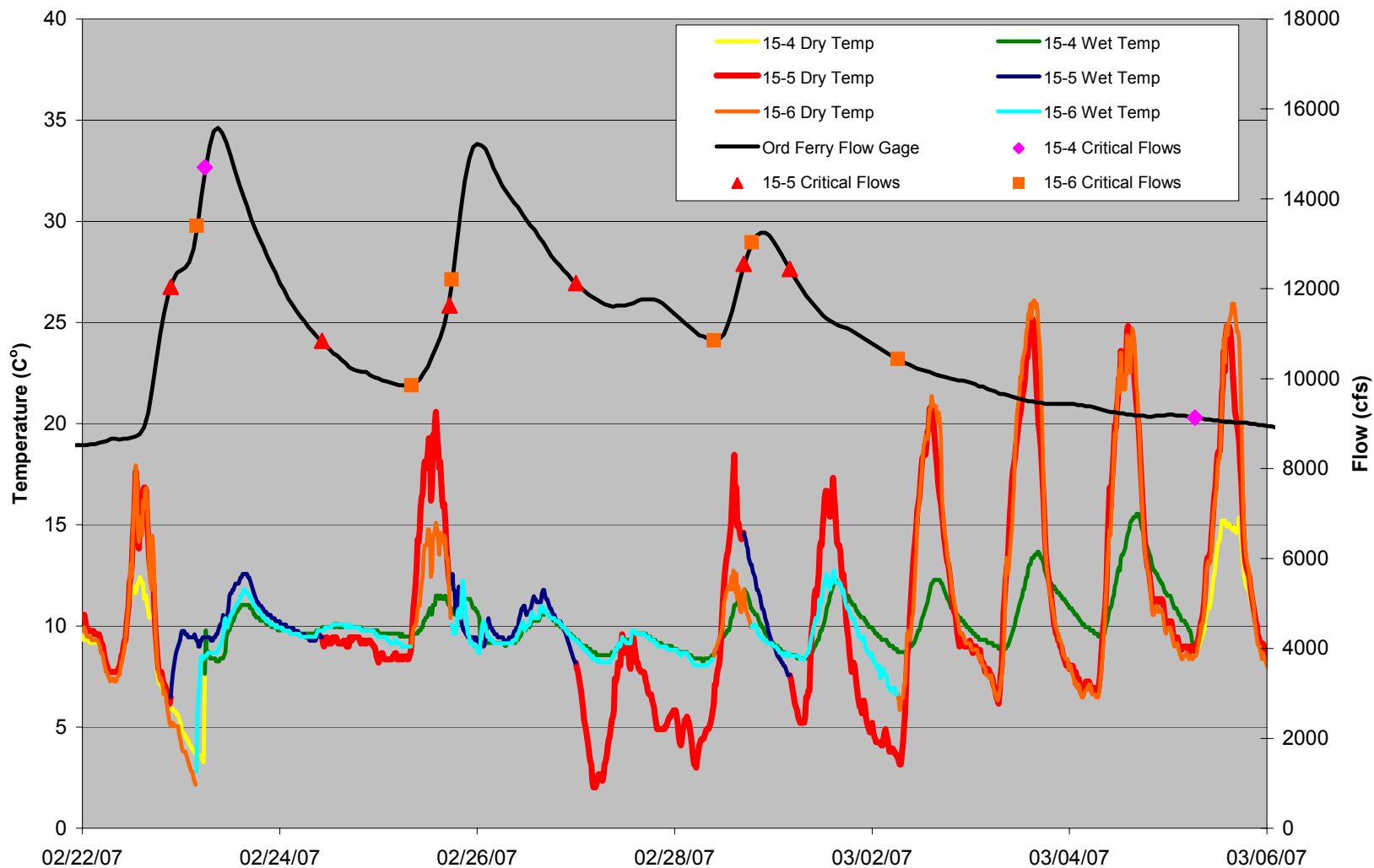


Figure 25b. Thermograph data for site 15 (RM 189.5L) and discharge at Ord Ferry between 2/22/07 and 3/6/07. Critical flow points depict thermograph changes between dry and wet status.



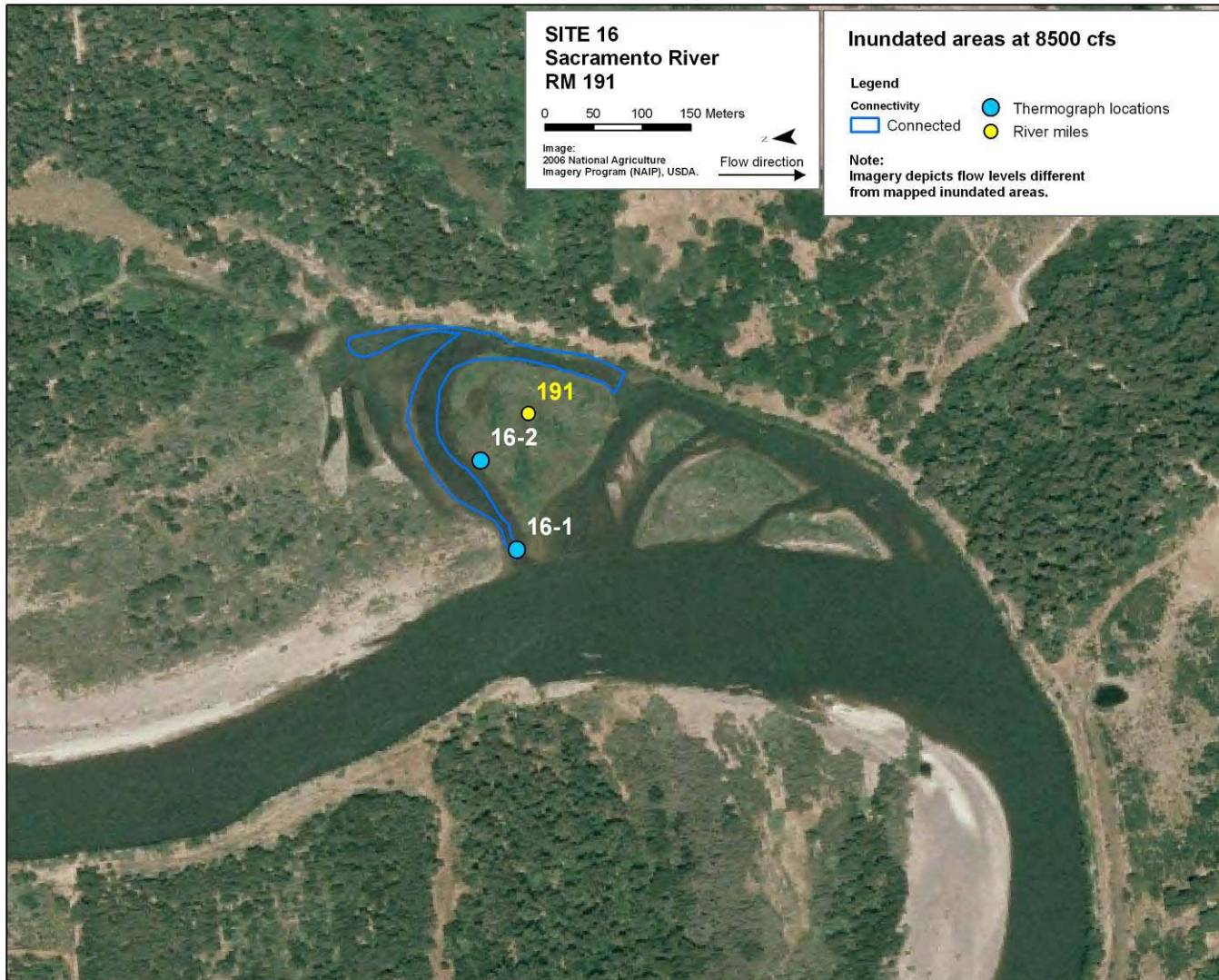


Figure 26b. Inundated areas of site 16 (RM 191L) at flows of 8,500 cfs, areas observed and drawn during field mapping.

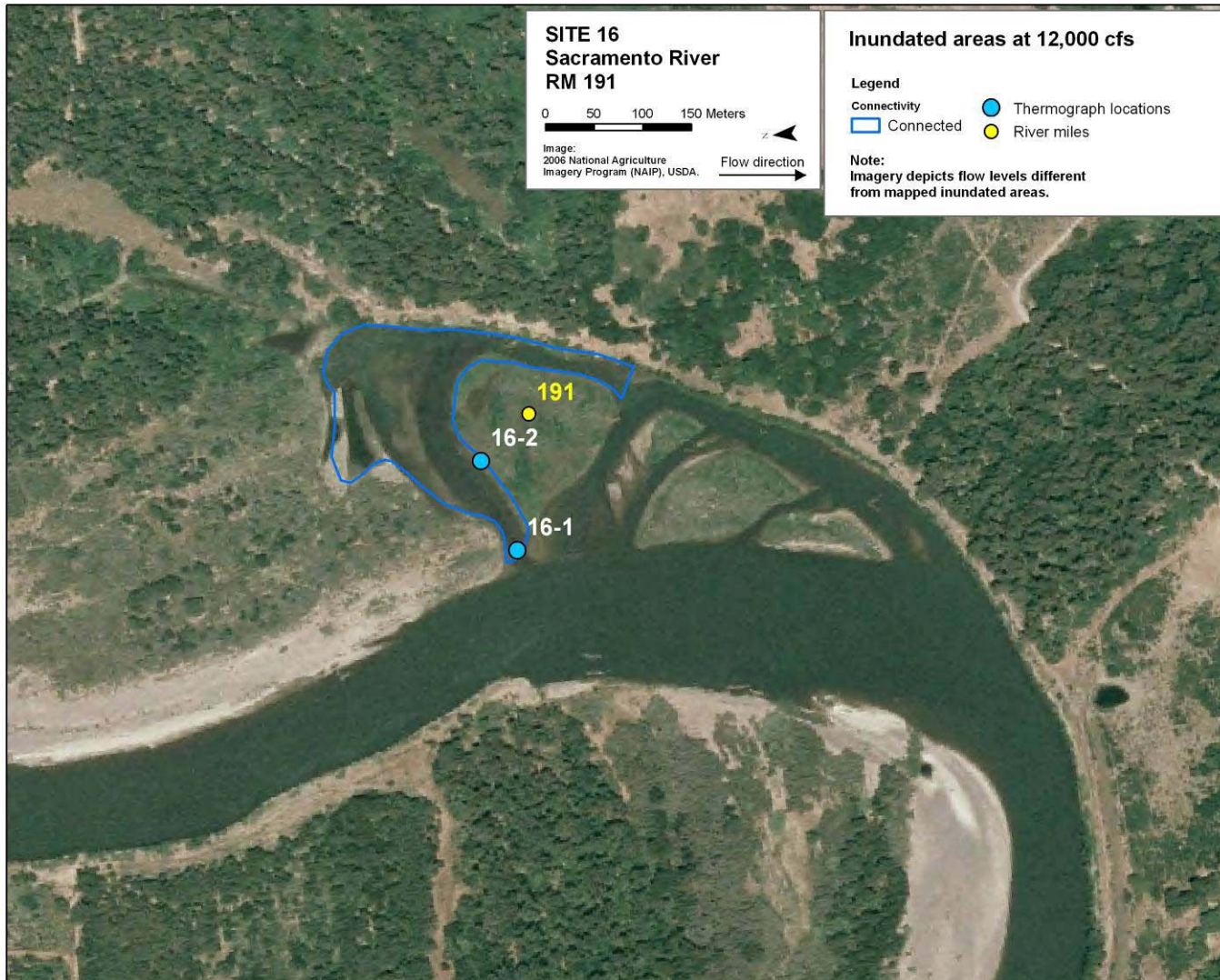


Figure 26c. Inundated areas of site 16 (RM 191L) at flows of 12,000 cfs , areas based on thermograph temperature records and field surveys.

Site 16

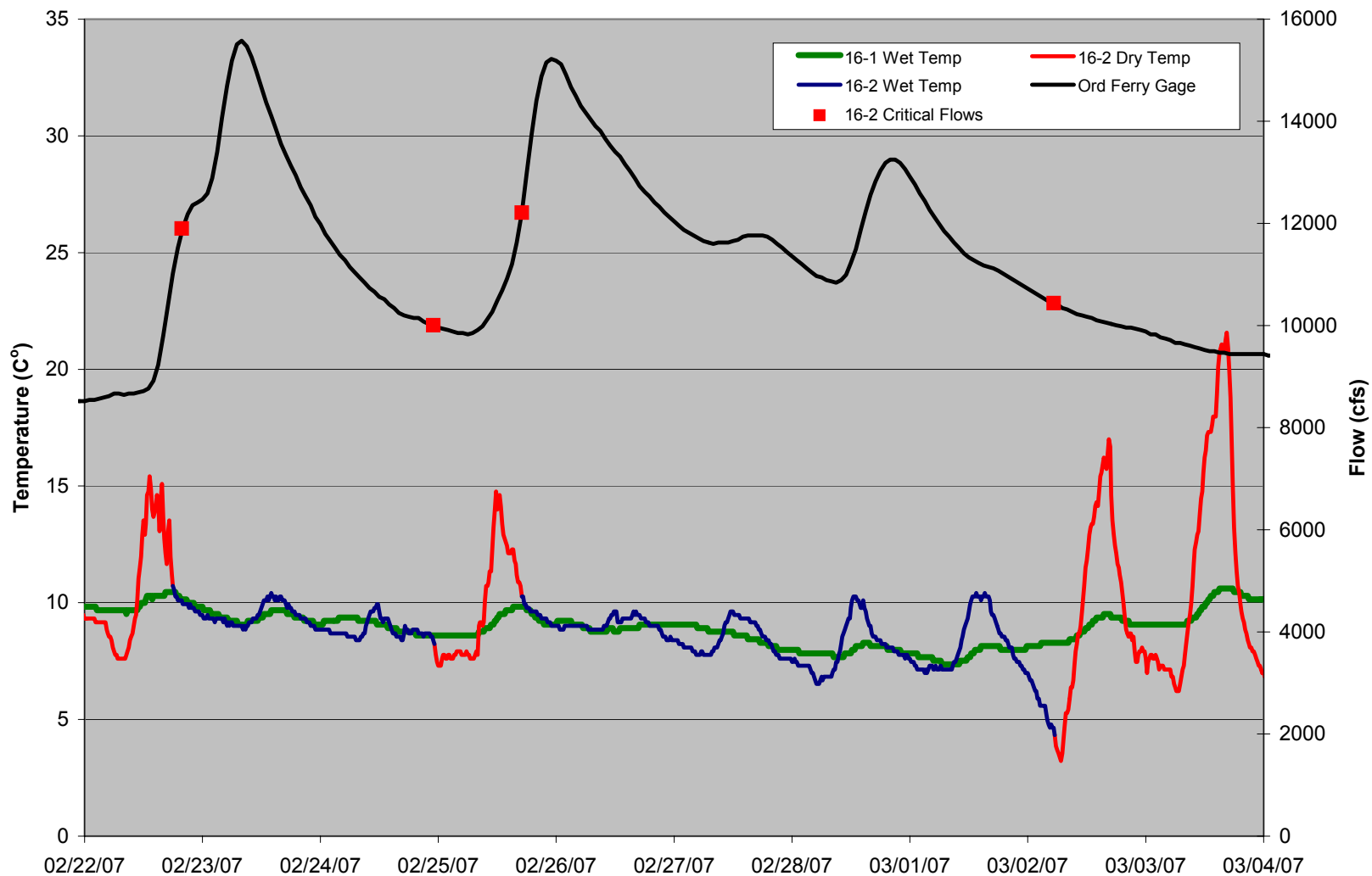


Figure 27. Thermograph data for site 16 (RM 191L) and discharge at Ord Ferry between 2/22/07 and 3/4/07. Critical flow points depict thermograph changes between dry and wet status.

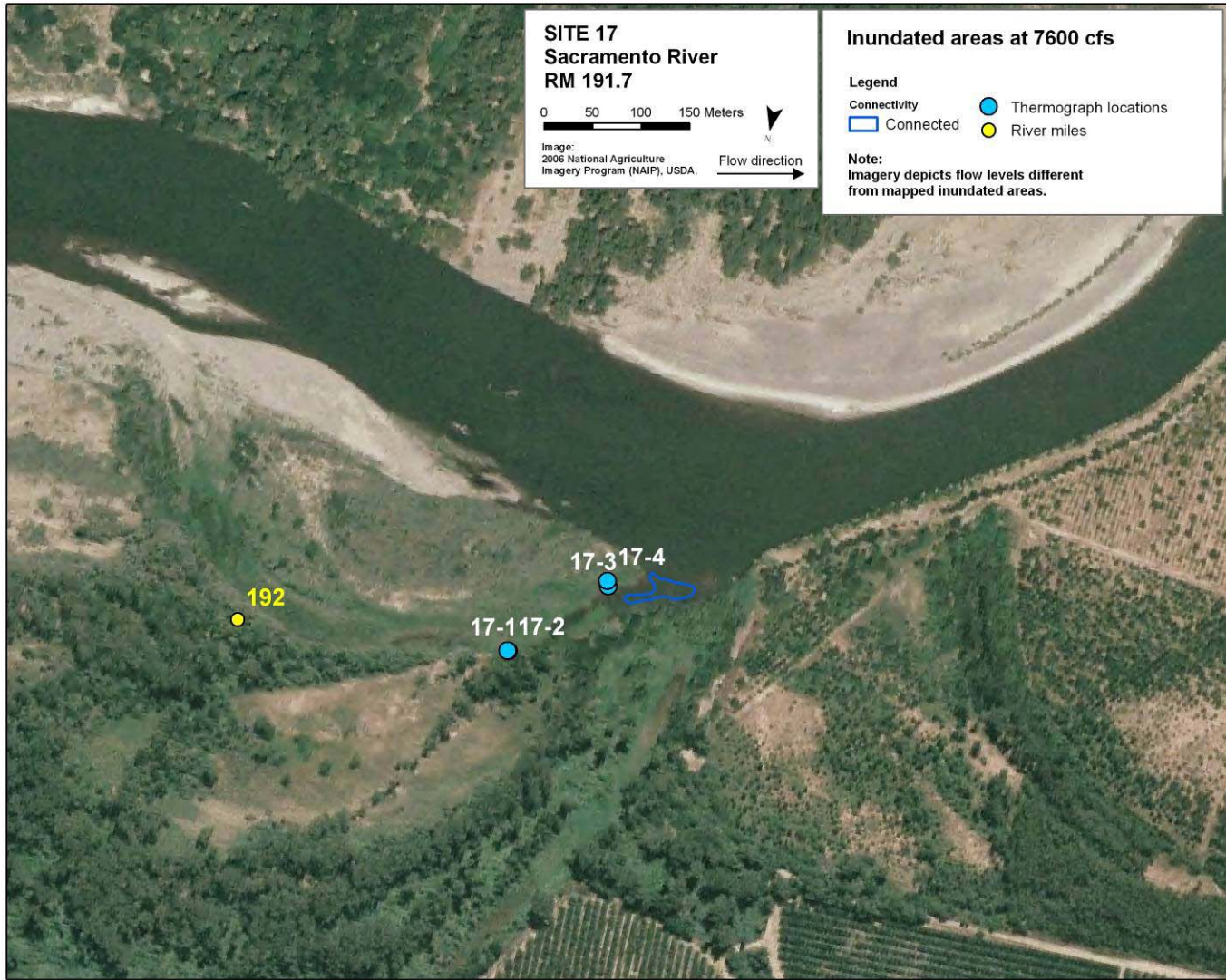
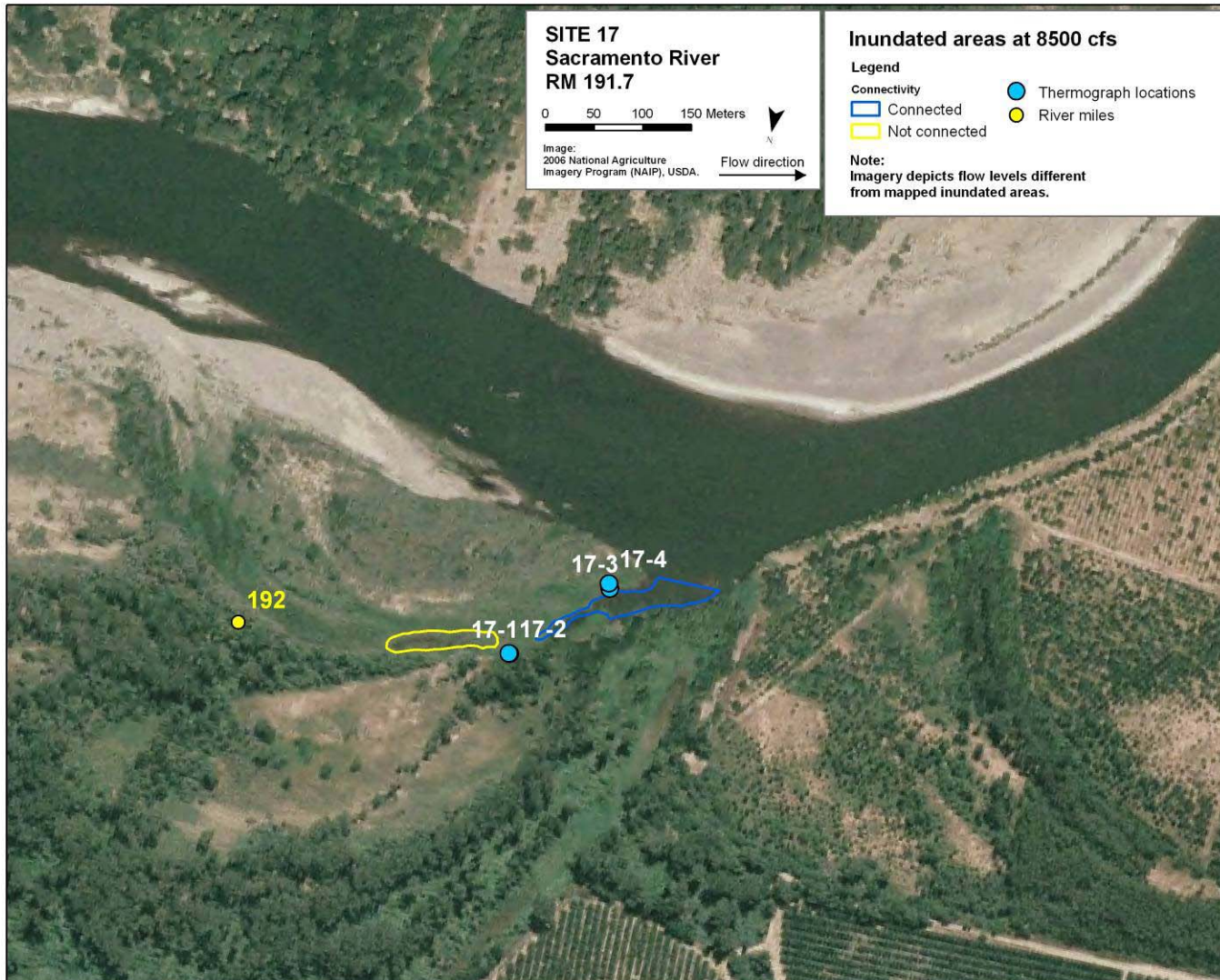
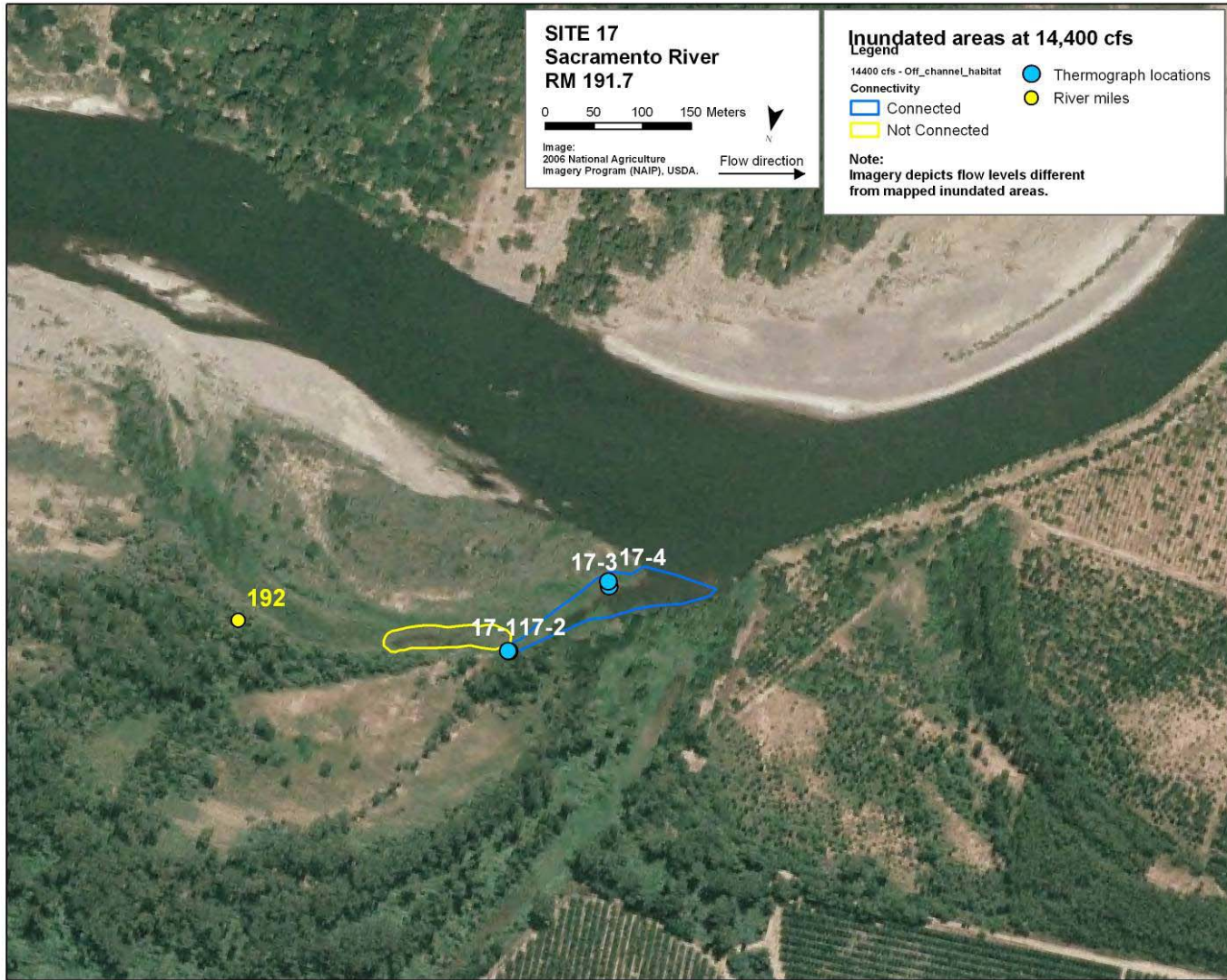


Figure 28a. Inundated areas of site 17 (RM 191.7R) at flows of 7,600 cfs, areas observed and drawn during field mapping.





Site 17

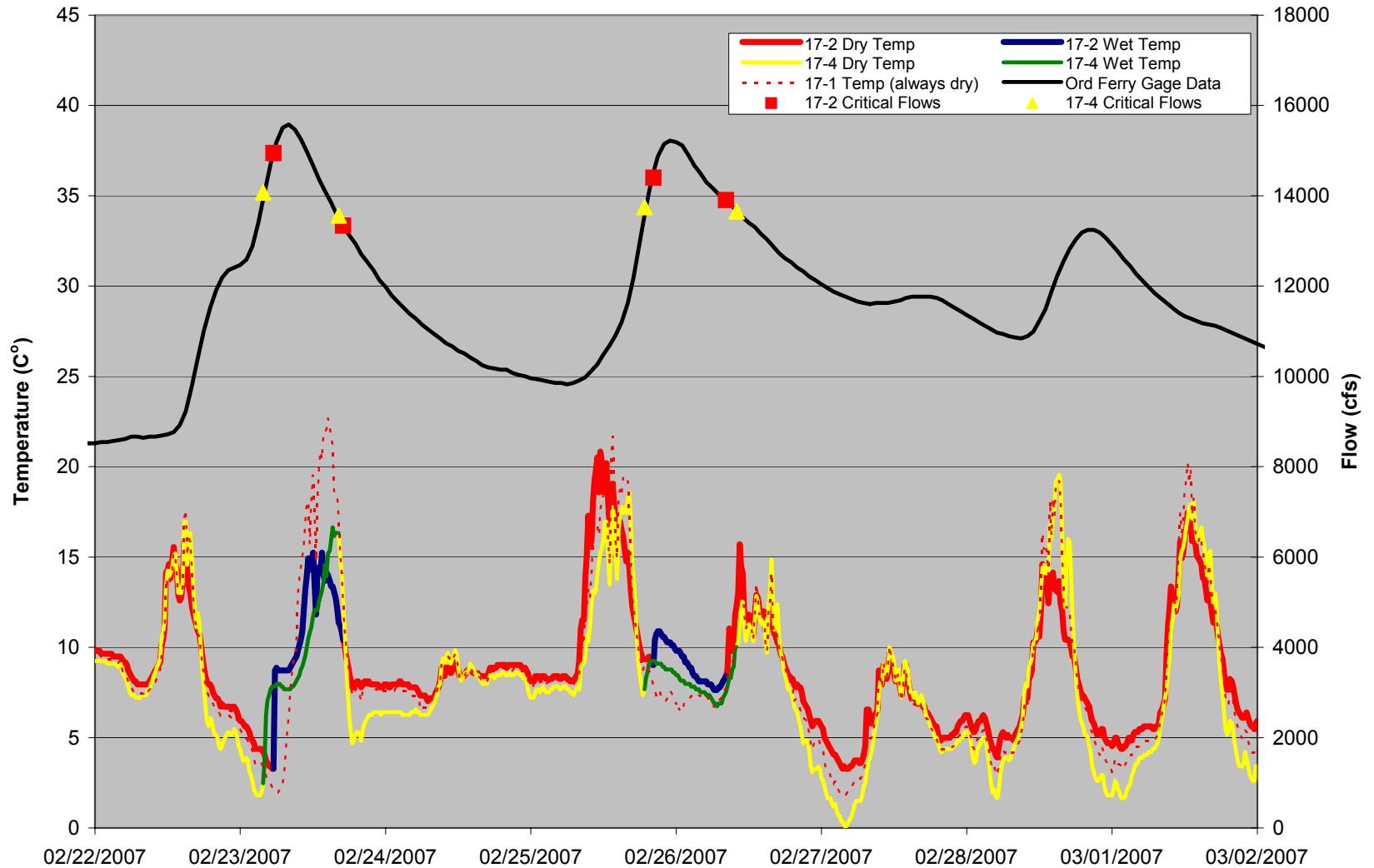
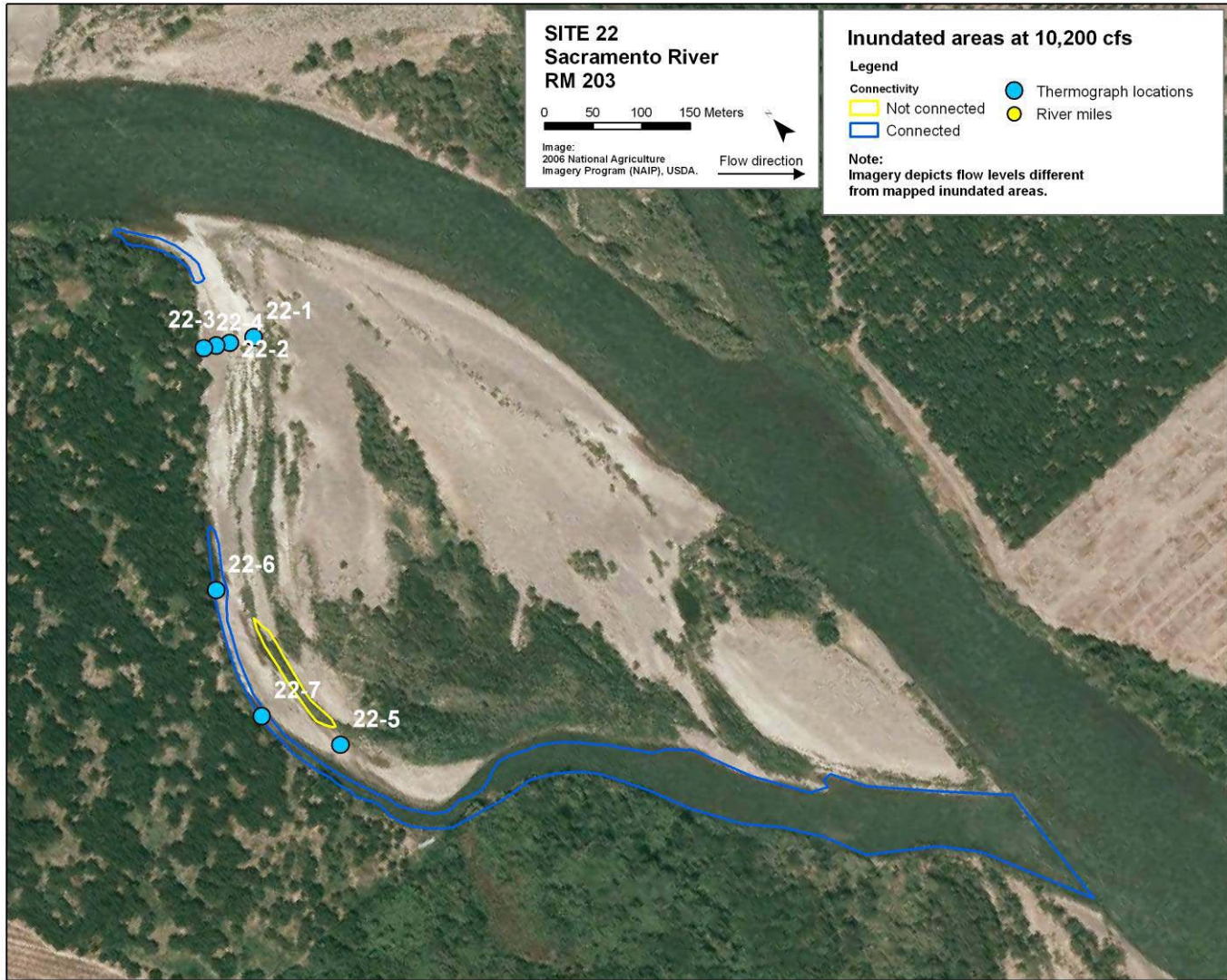
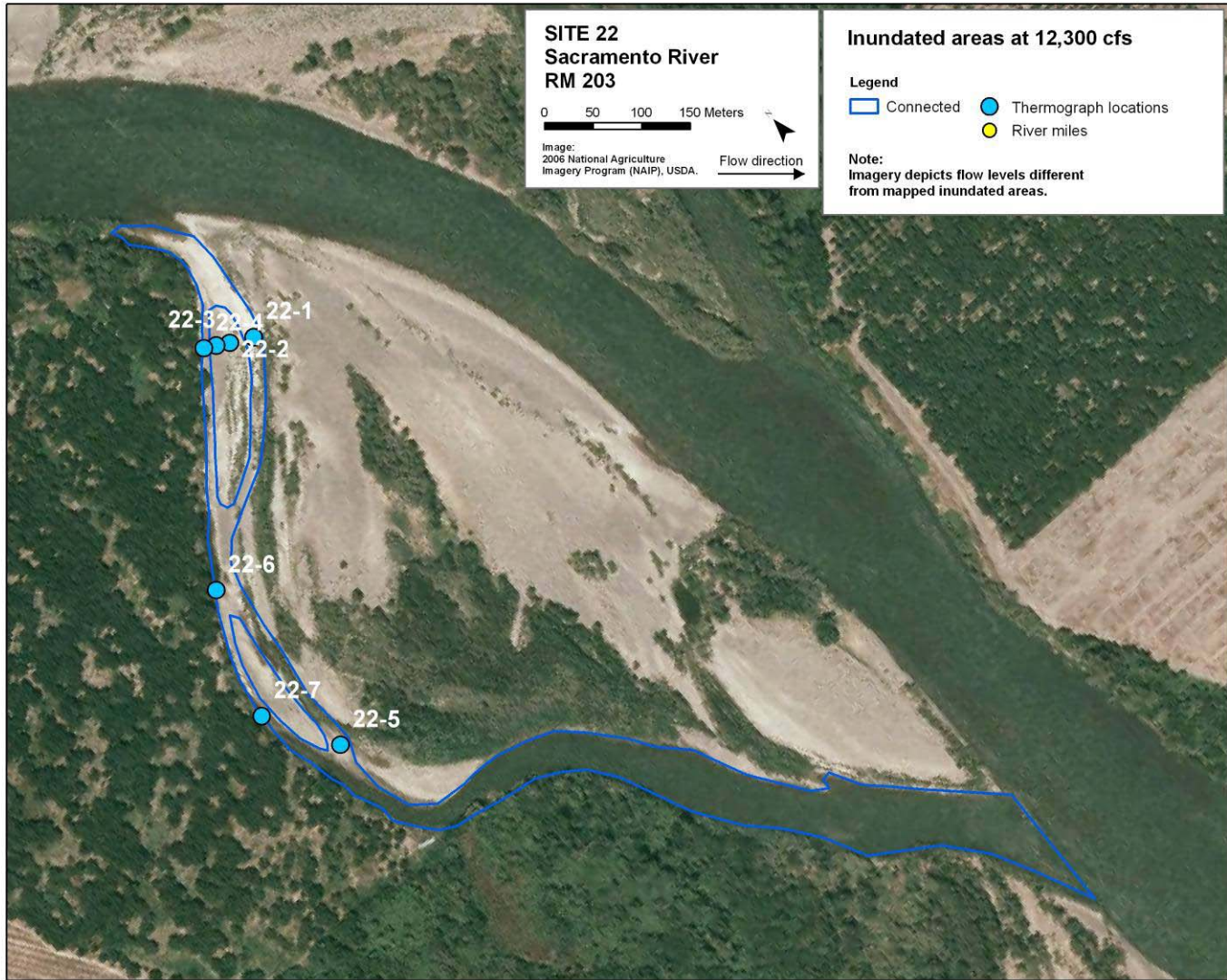


Figure 29. Thermograph data for site 17 (RM 191.7R) and discharge at Ord Ferry between 2/22/07 and 3/2/07. Critical flow points depict thermograph changes between dry and wet status.







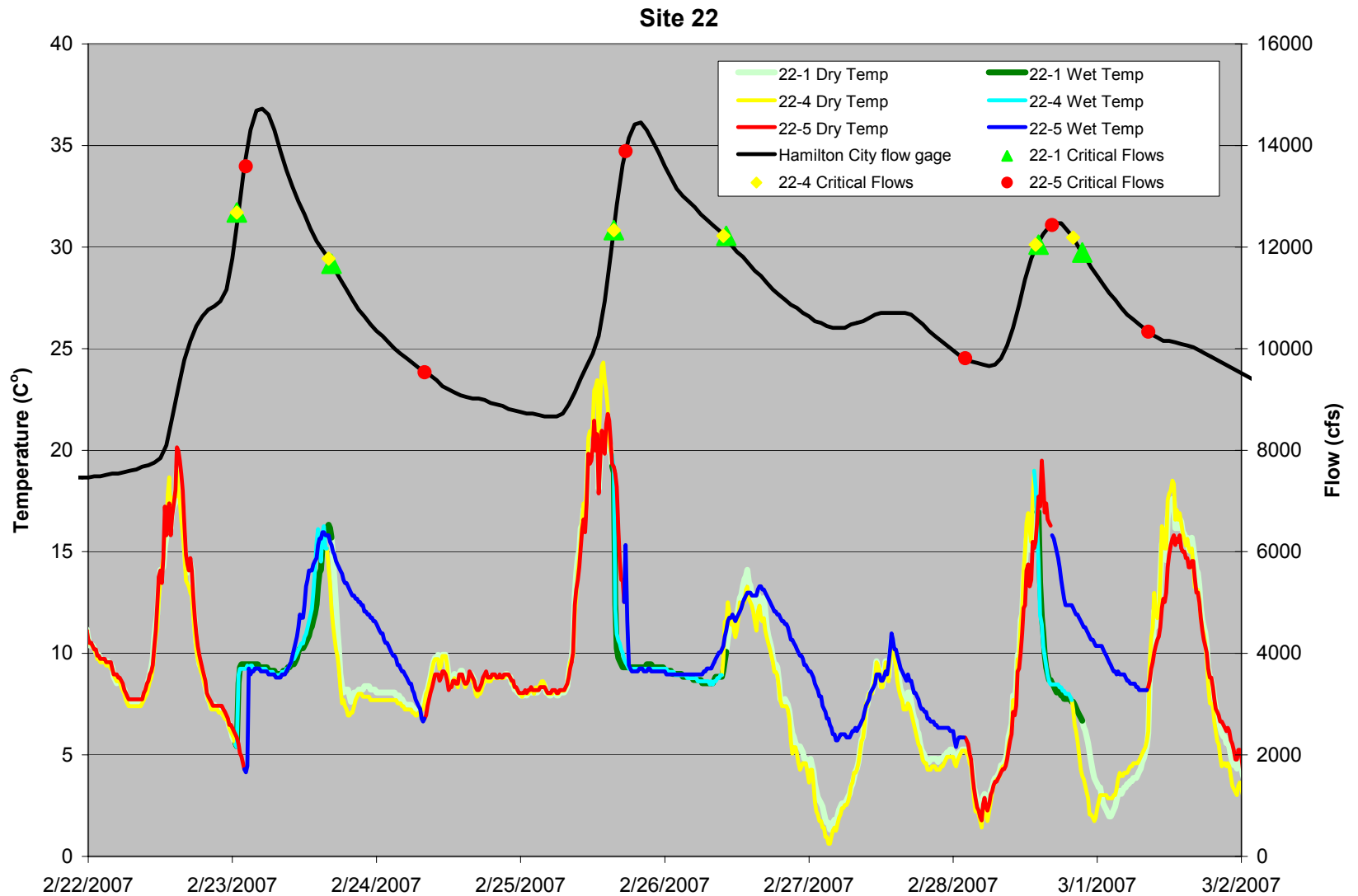
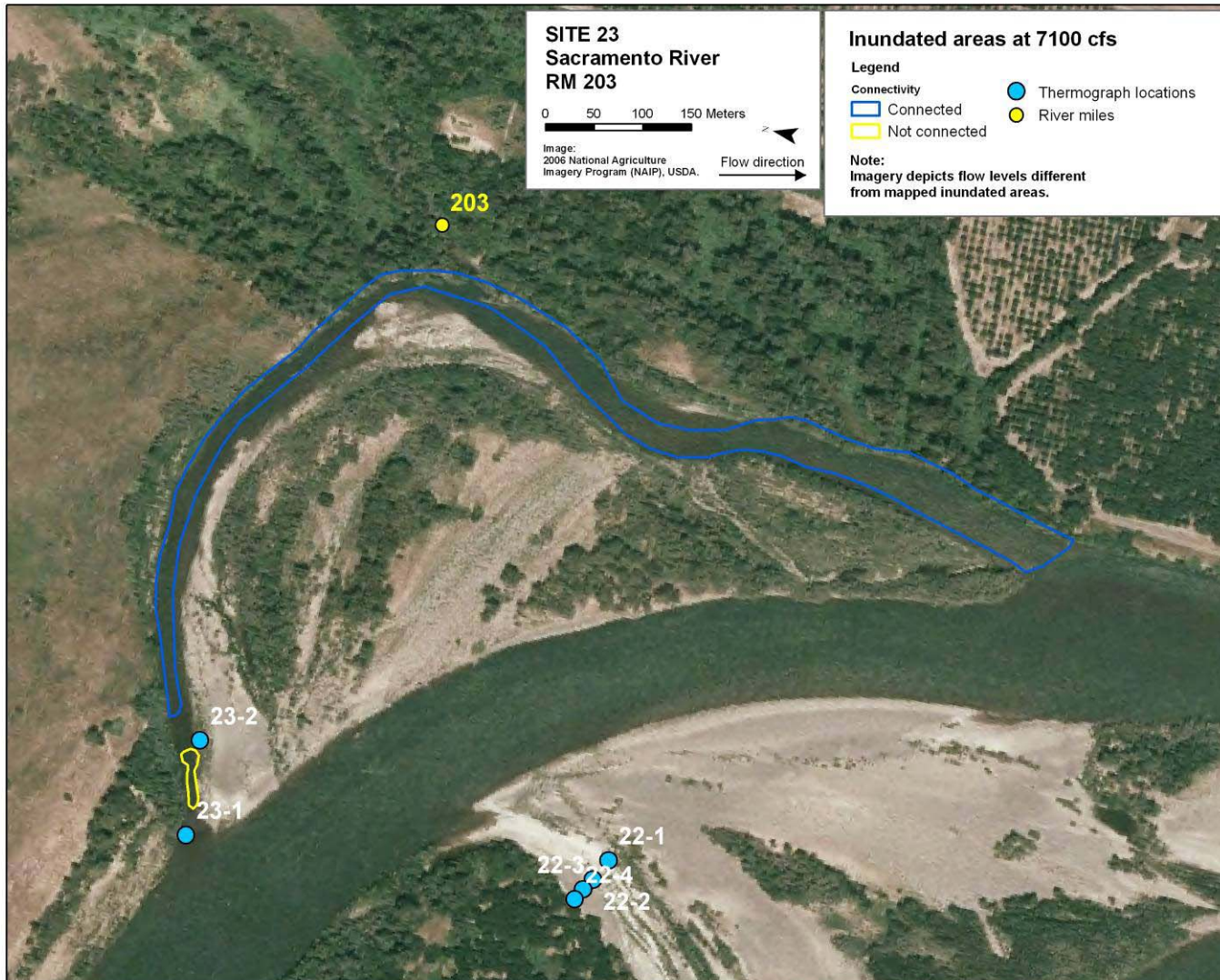
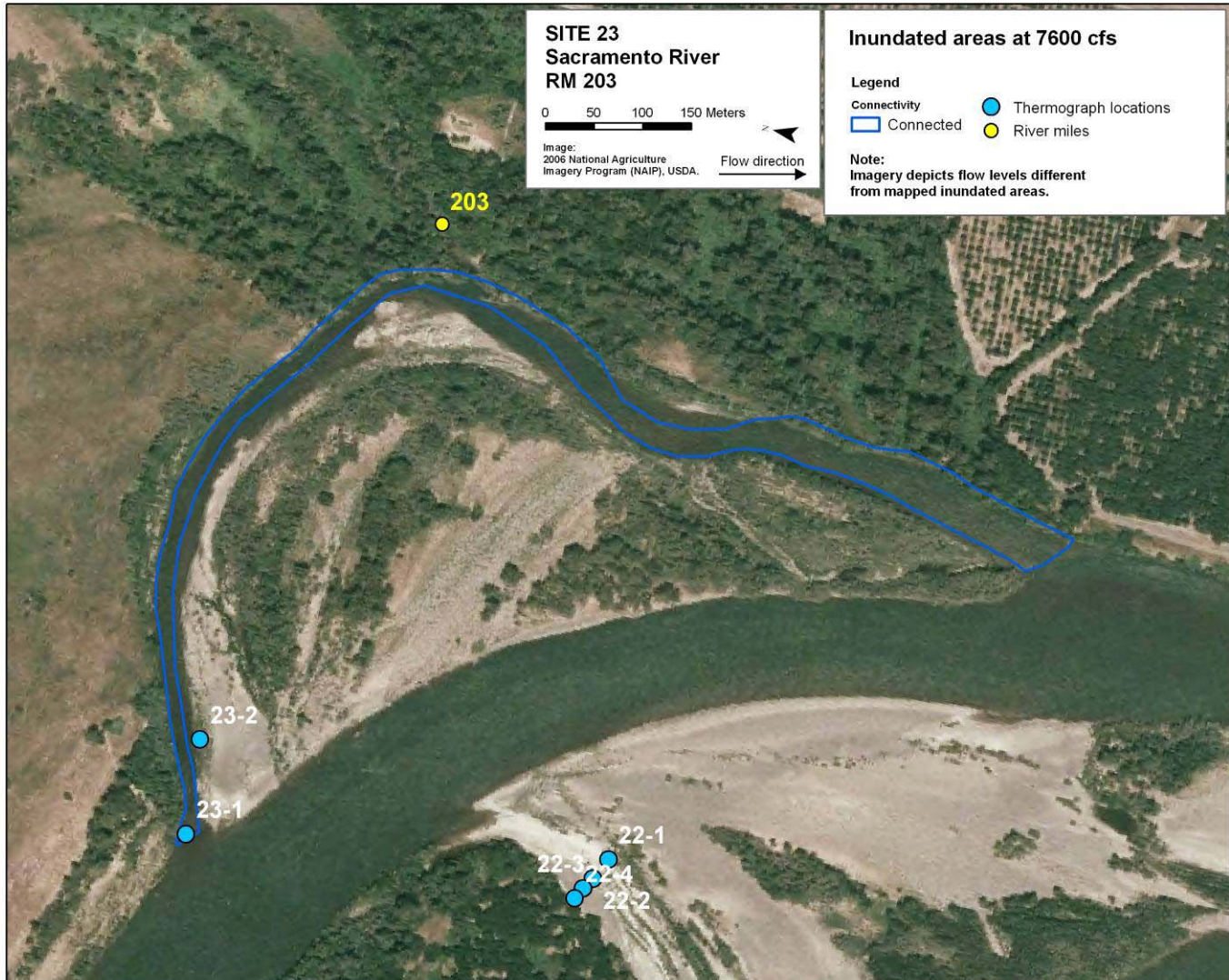
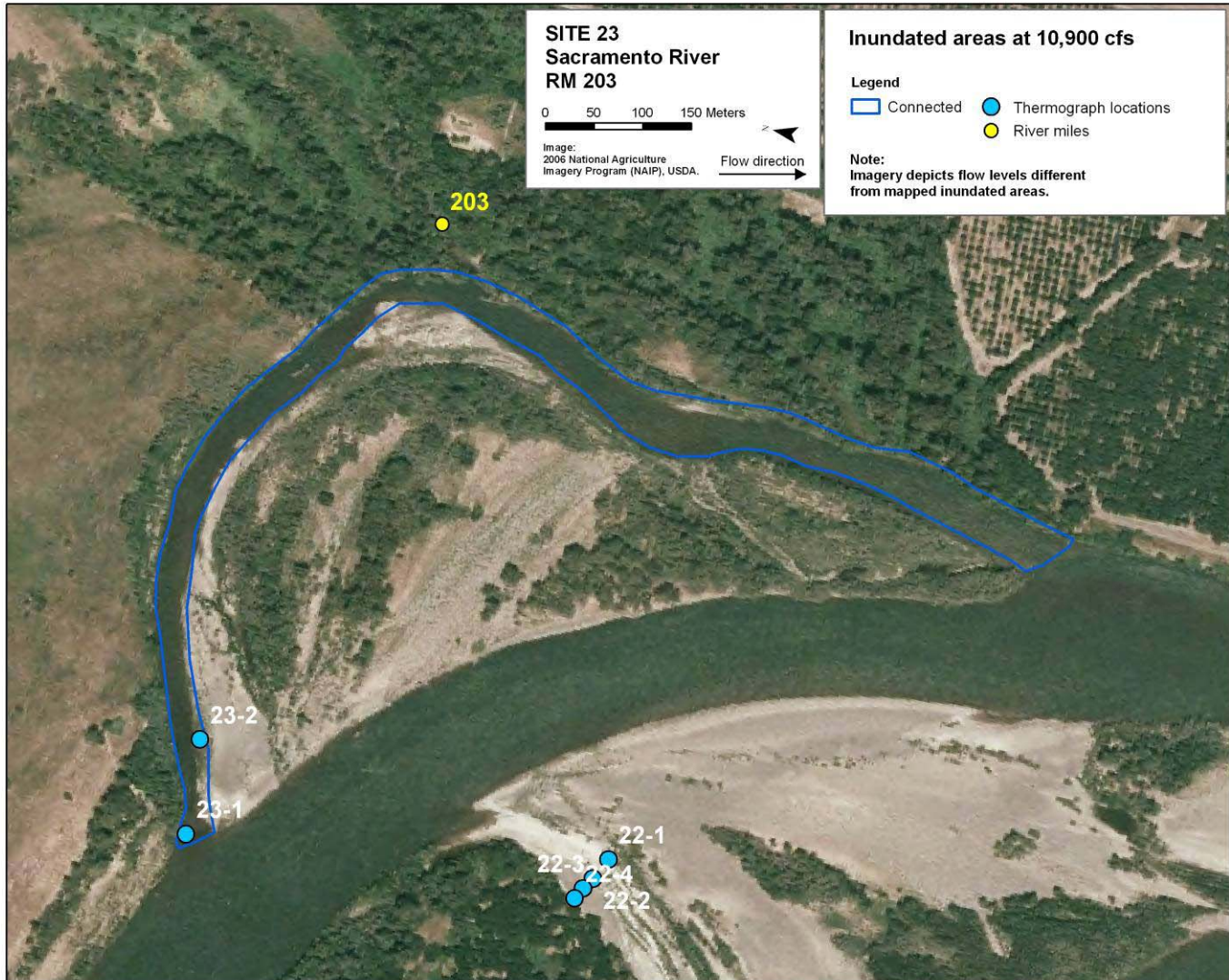


Figure 31. Thermograph data for site 22 (RM 203R) and discharge at Hamilton City between 2/22/07 and 3/2/07. Critical flow points depict thermograph changes between dry and wet status.







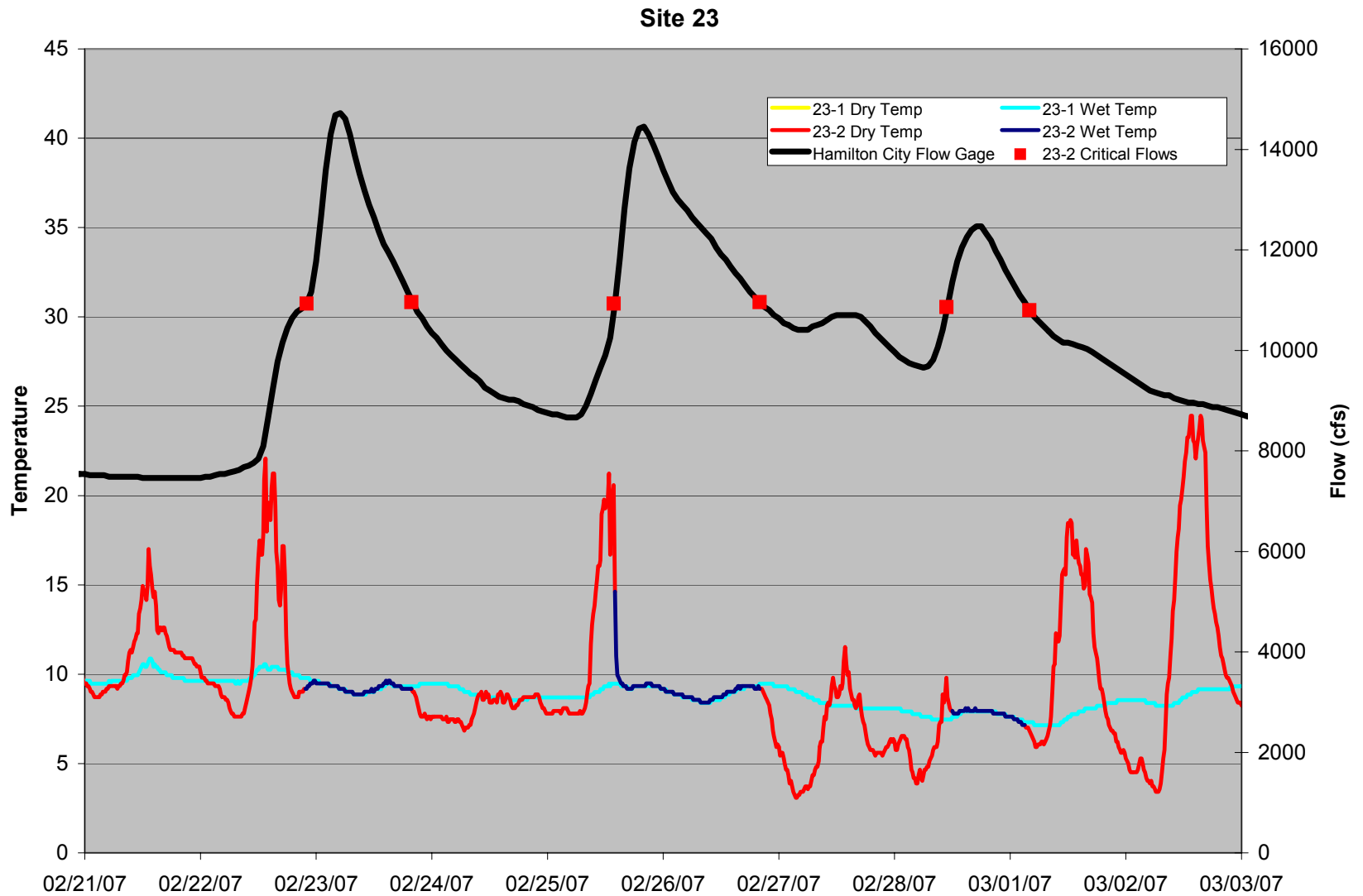


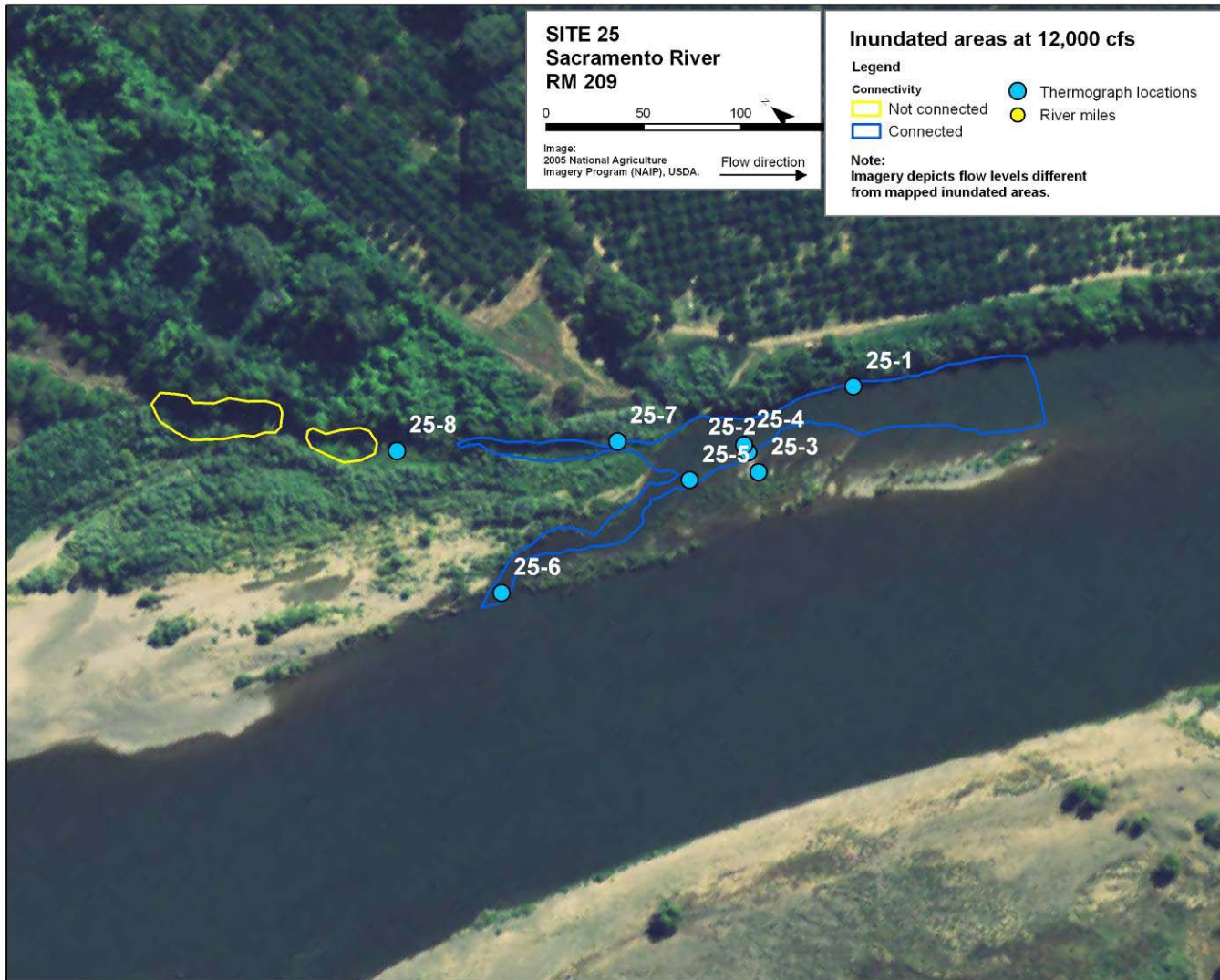
Figure 33. Thermograph data for site 23 (RM 203L) and discharge at Hamilton City between 2/21/07 and 3/3/07. Critical flow points depict thermograph changes between dry and wet status.



Figure 34a. Inundated areas of site 25 (RM 209L) at flows of 7,900 cfs, areas observed and drawn during field mapping.



Figure 34b. Inundated areas of site 25 (RM 209L) at flows of 8,700 cfs, areas observed and drawn during field mapping.



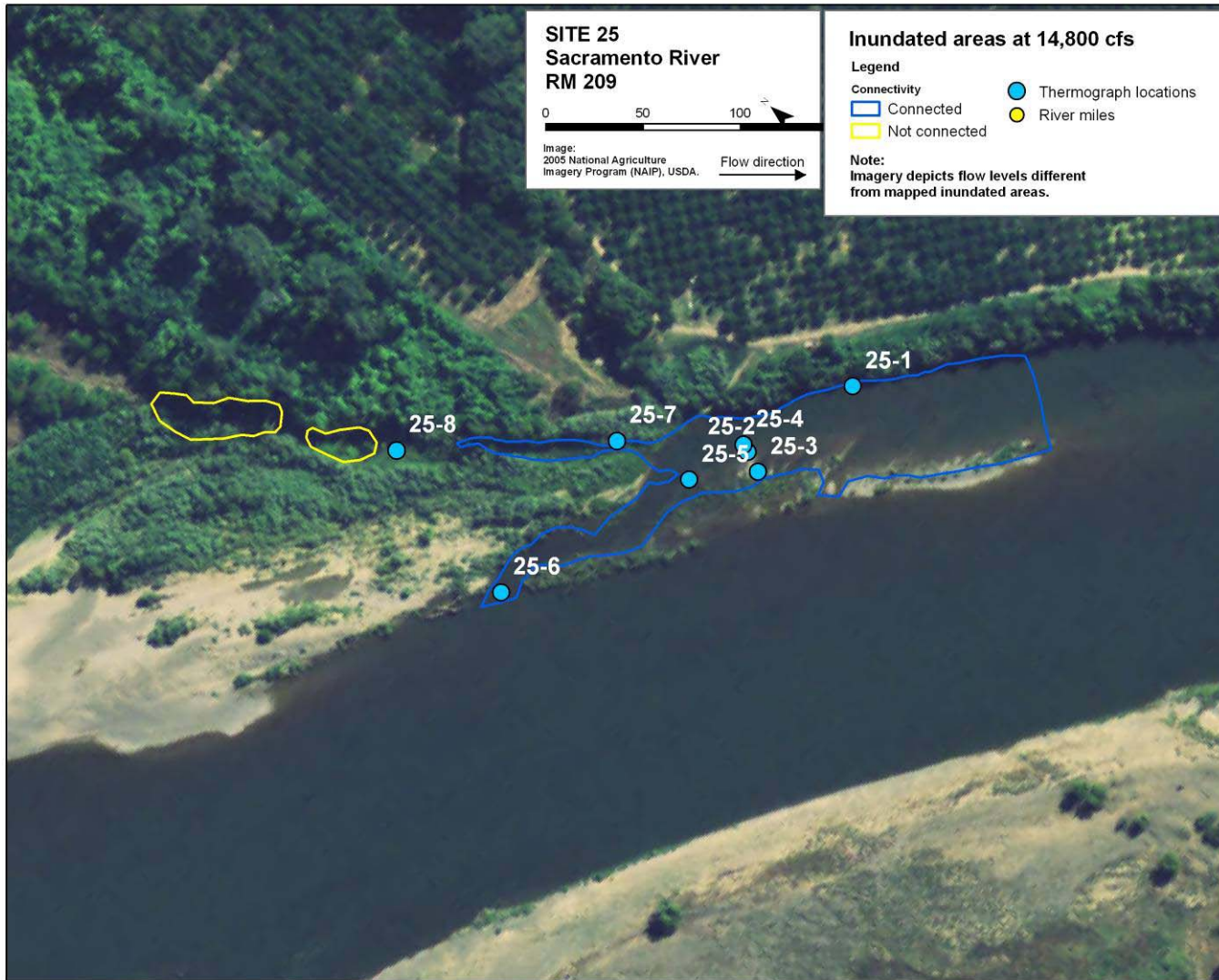


Figure 34d. Inundated areas of site 25 (RM 209L) at flows of 14,800 cfs , areas based on thermograph temperature records and field surveys.

XS Plot for OCWB Study Site 25, Sacramento River RM 208.9

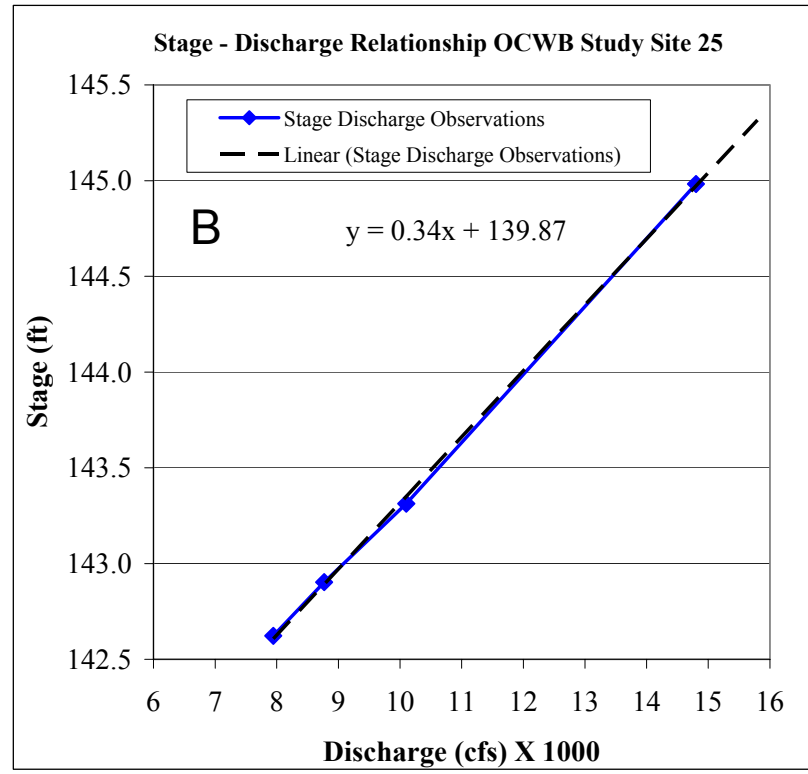
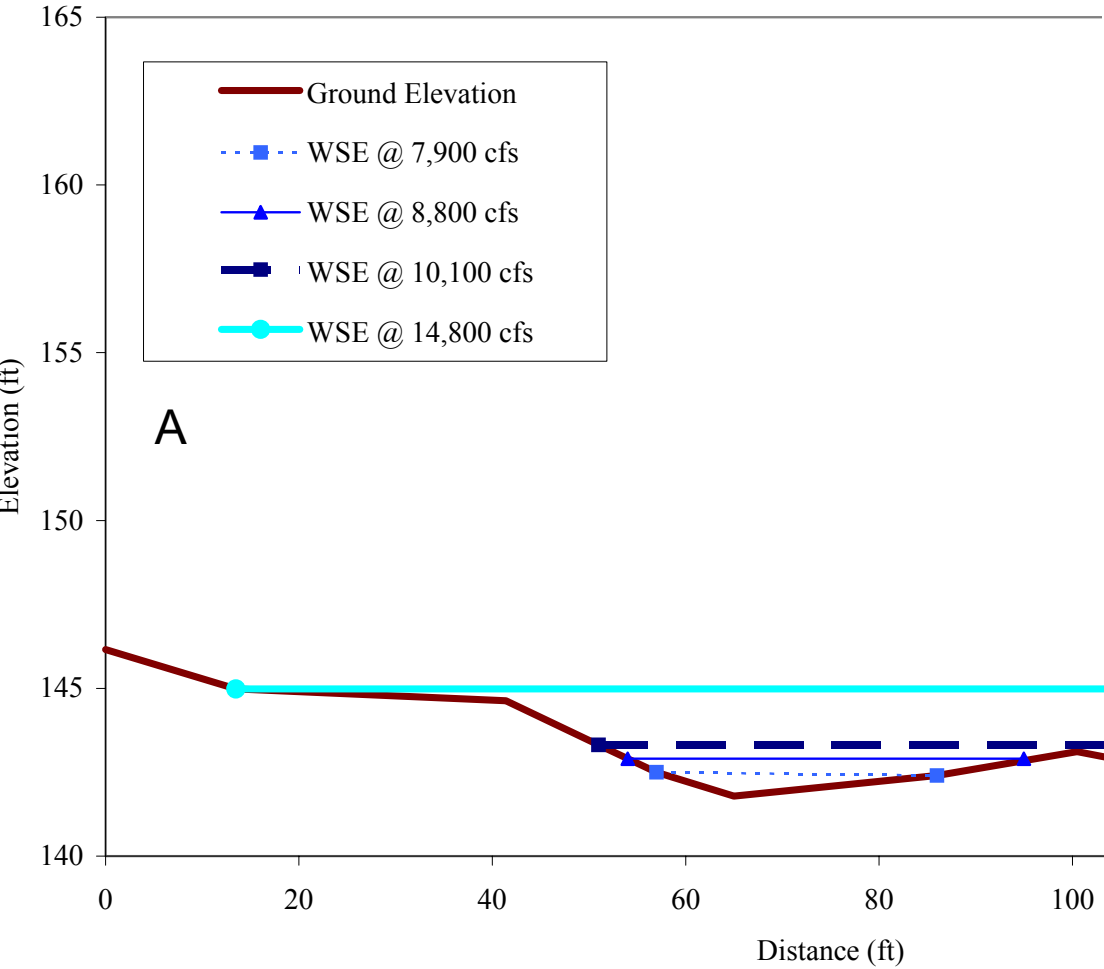


Figure 35. Study site 25, (A) cross section plot with known water surface elevations, and (B) plot of stage – discharge relationships at cross section.

Site 25

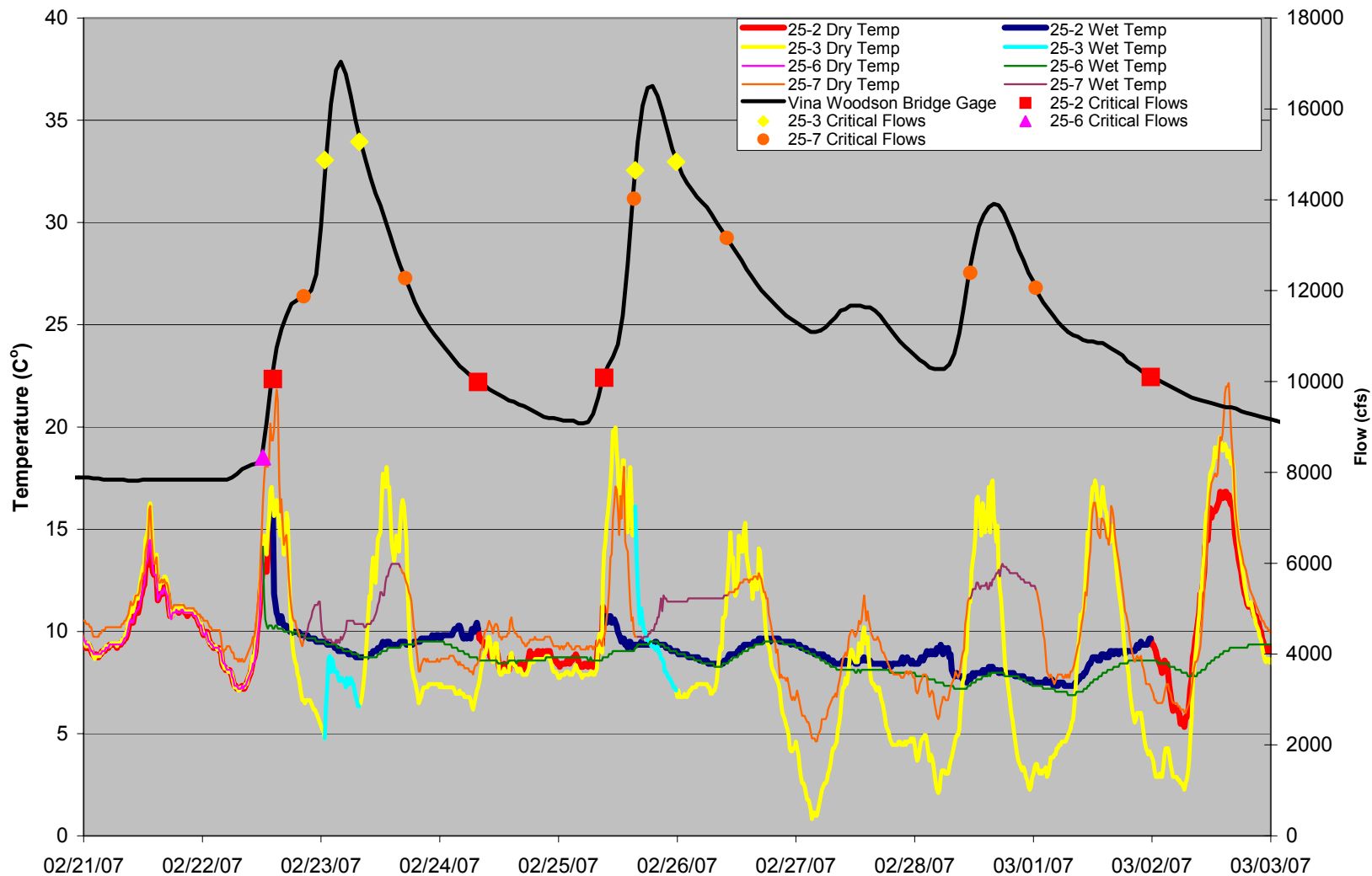
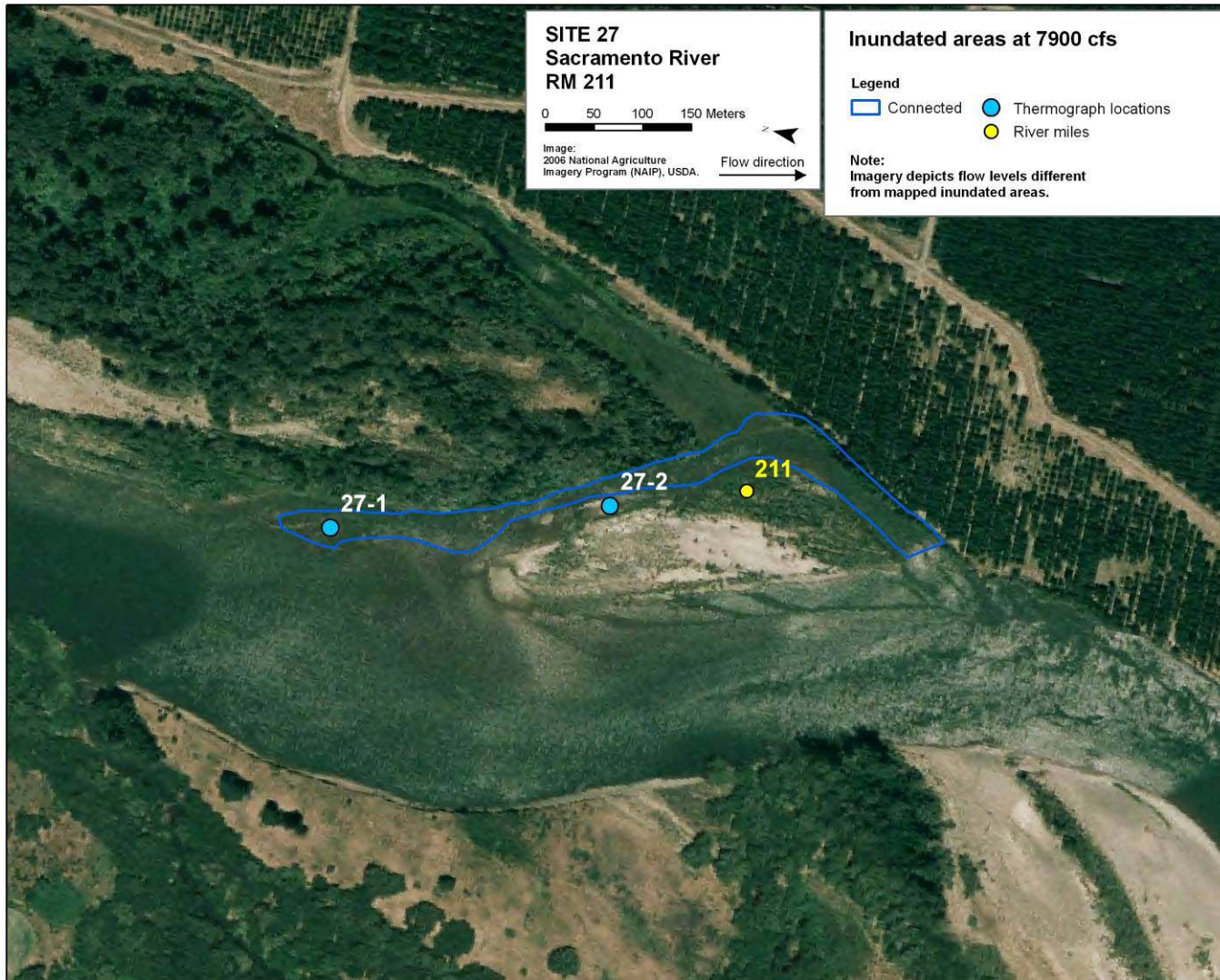
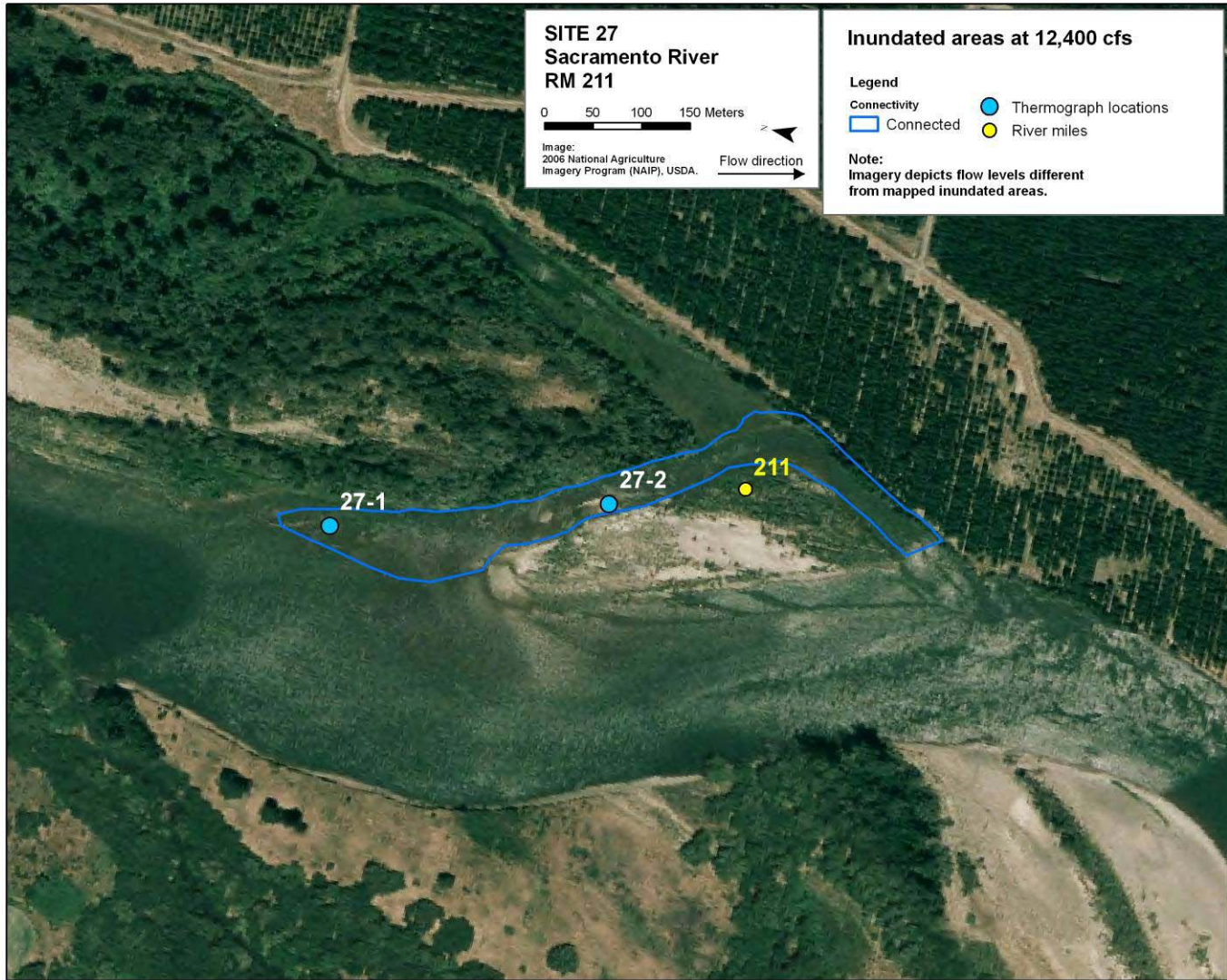


Figure 36. Thermograph data for site 25 (RM 209L) and discharge at Vina Woodson Bridge between 2/21/07 and 3/3/07. Critical flow points depict thermograph changes between dry and wet status.





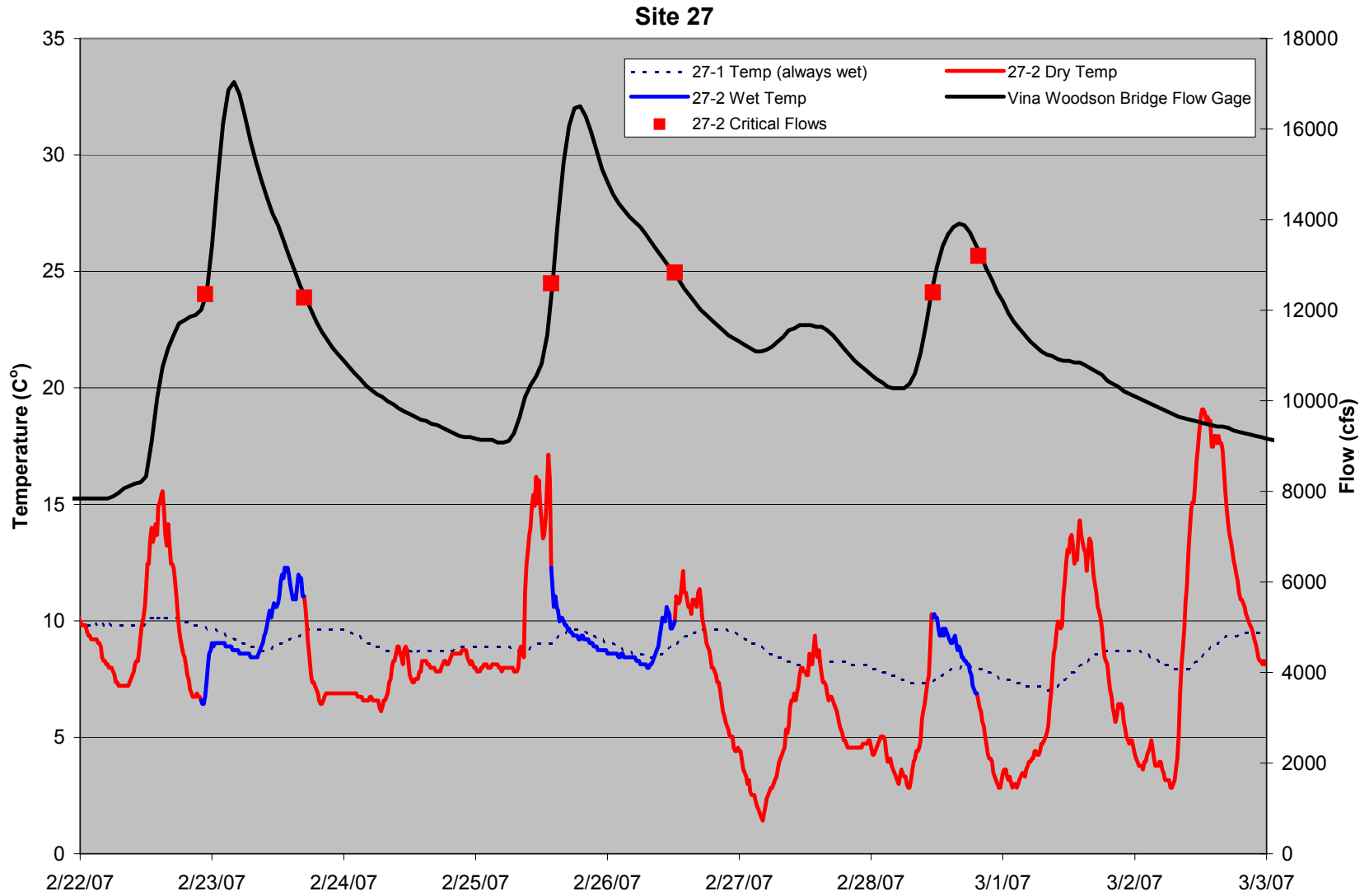


Figure 38. Thermograph data for site 27 (RM 211L) and discharge at Vina Woodson Bridge between 2/22/07 and 3/3/07. Critical flow points depict thermograph changes between dry and wet status.

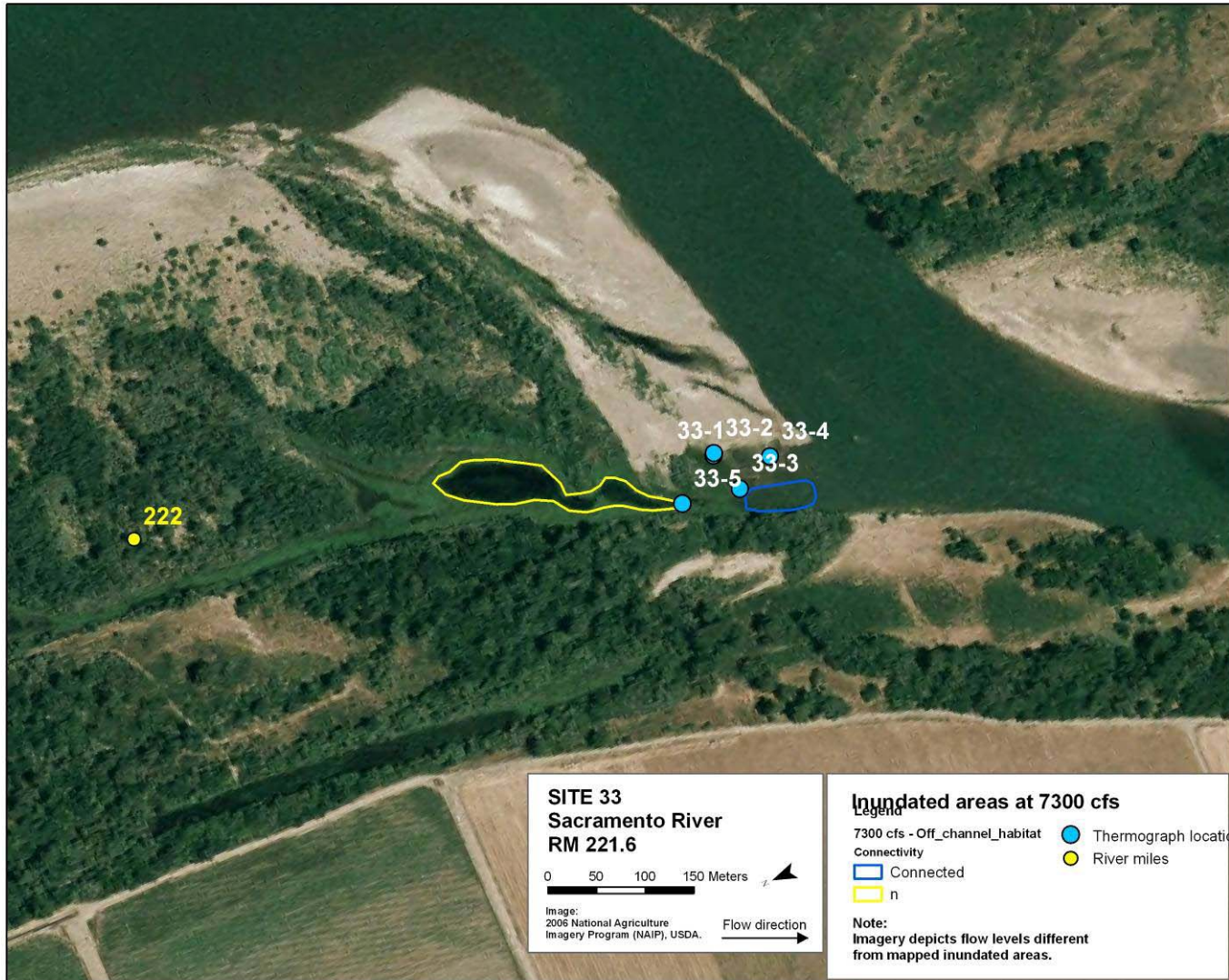
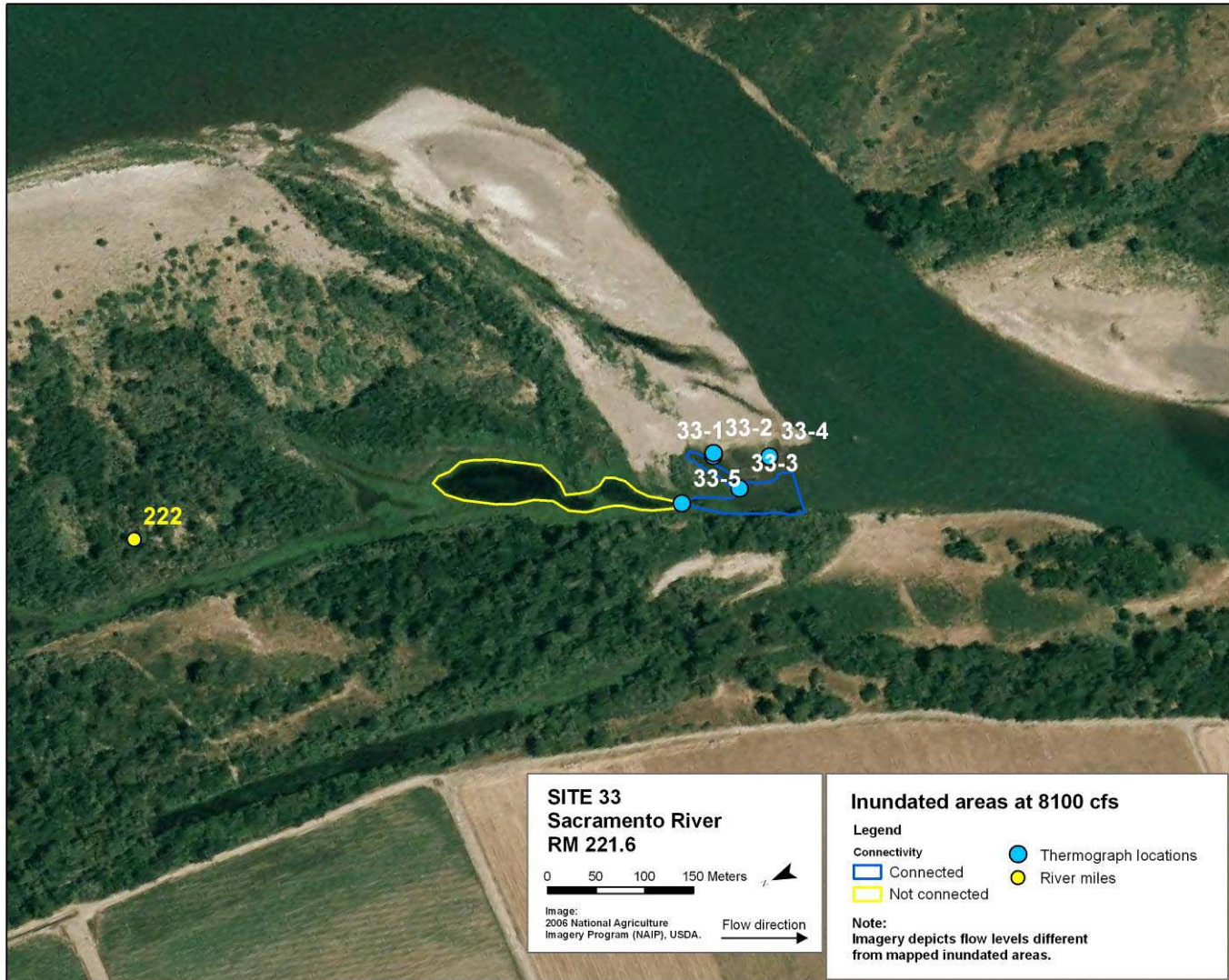
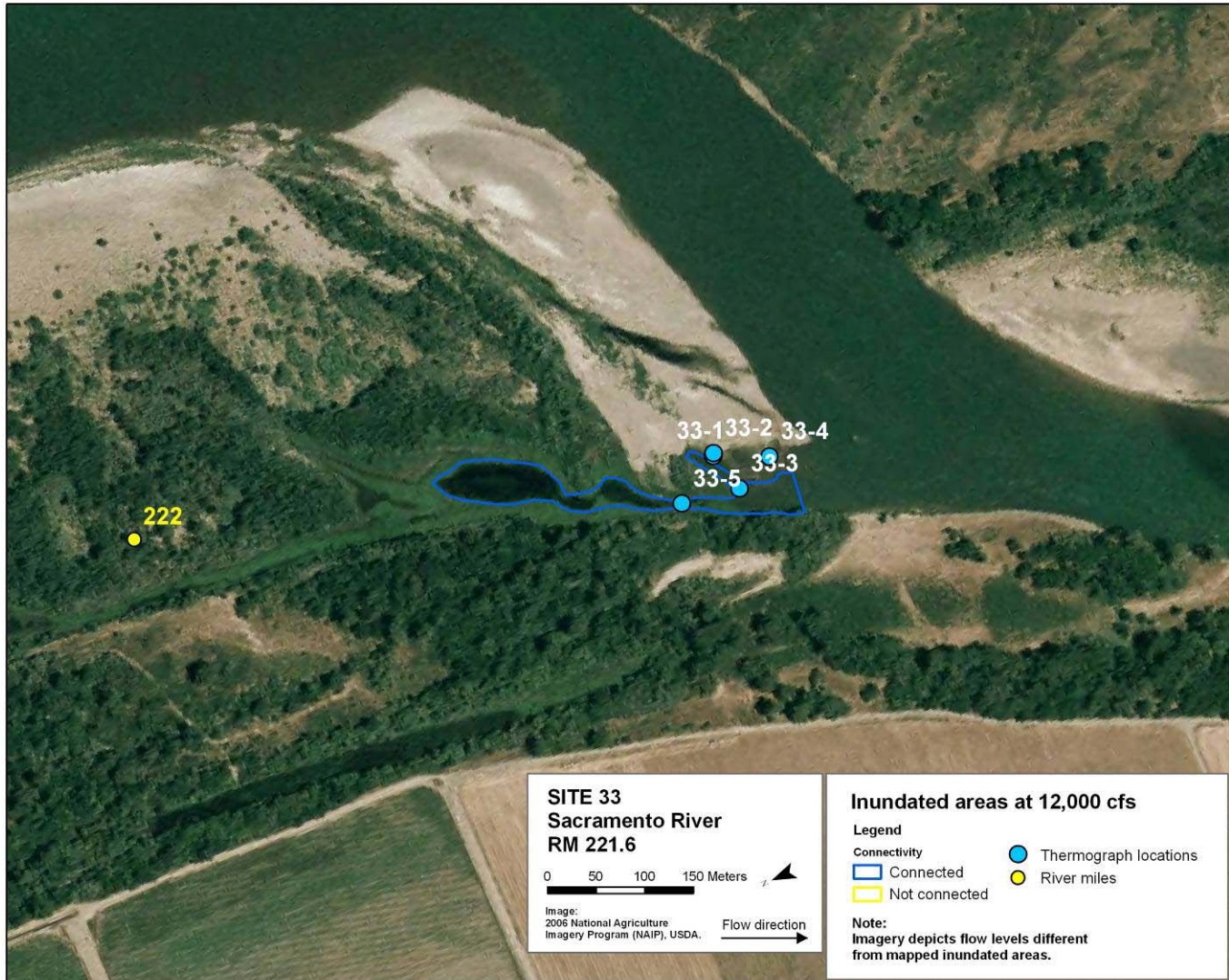


Figure 39a. Inundated areas of site 33 (RM 221.6R) at flows of 7,300 cfs , areas based on thermograph temperature records and field surveys.





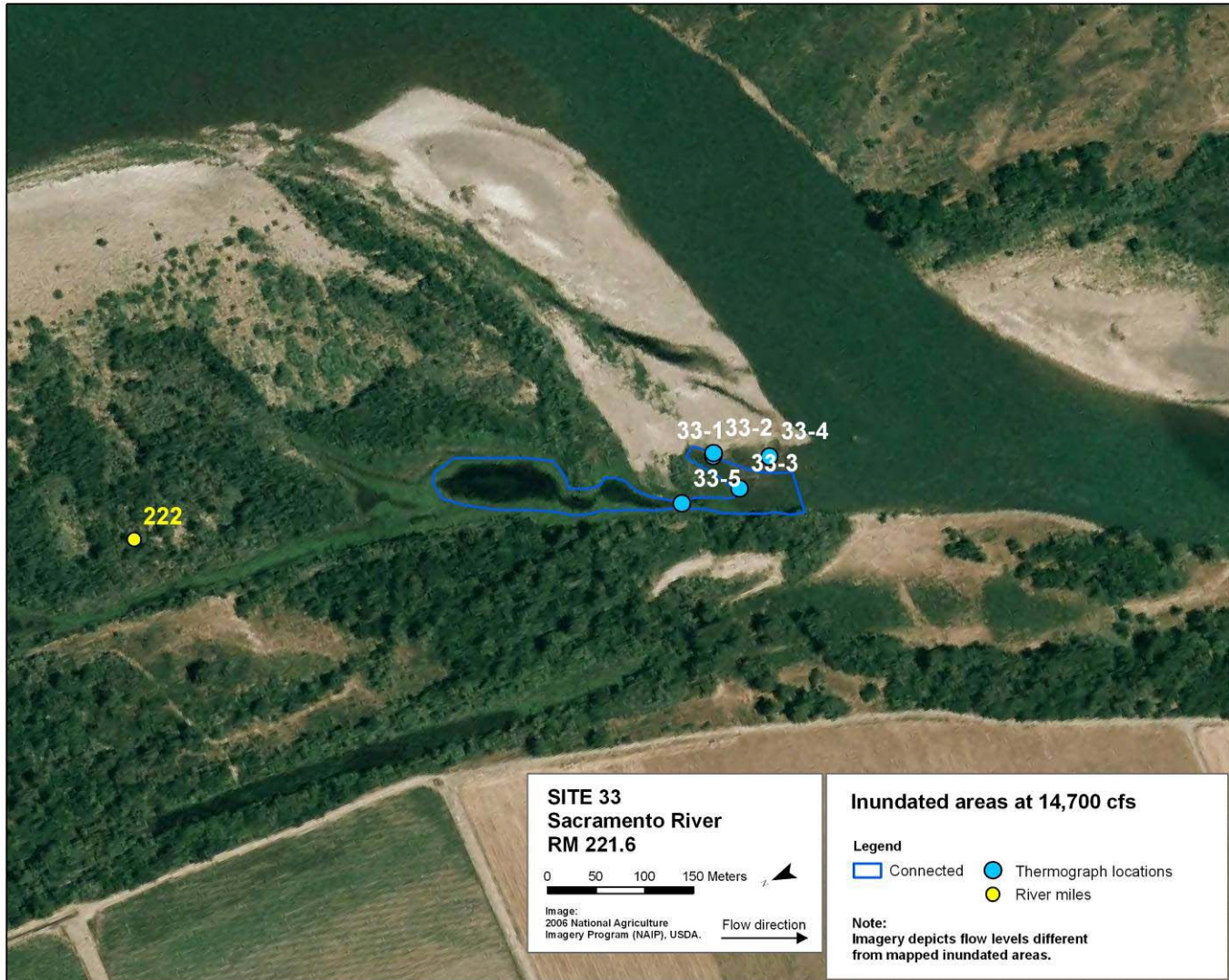


Figure 39d. Inundated areas of site 33 (RM 221.6R) at flows of 14,700 cfs , areas based on thermograph temperature records and field surveys.

XS Plot for OCWB Study Site 33, Sacramento River RM 235.3

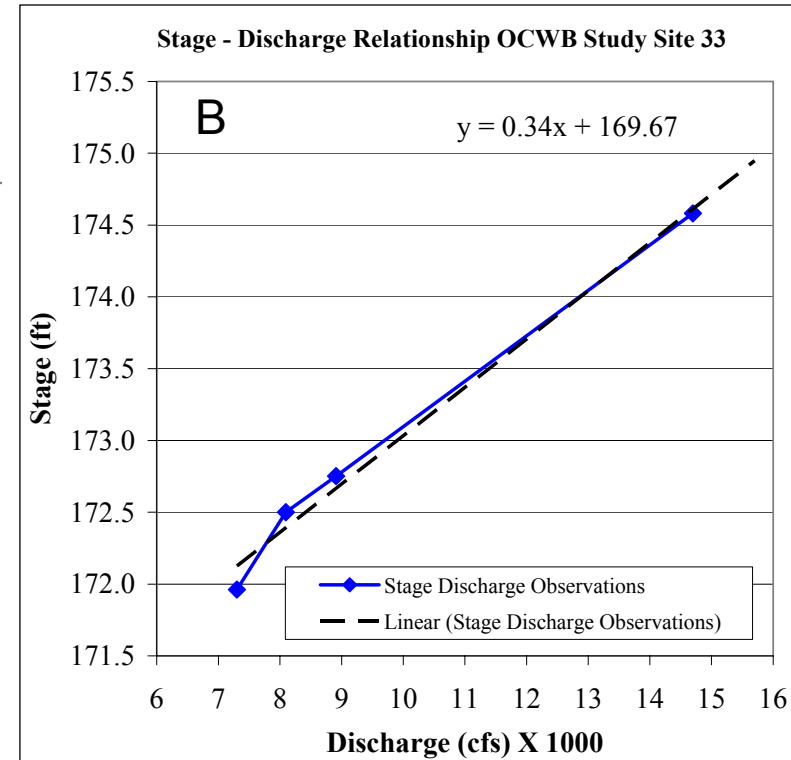
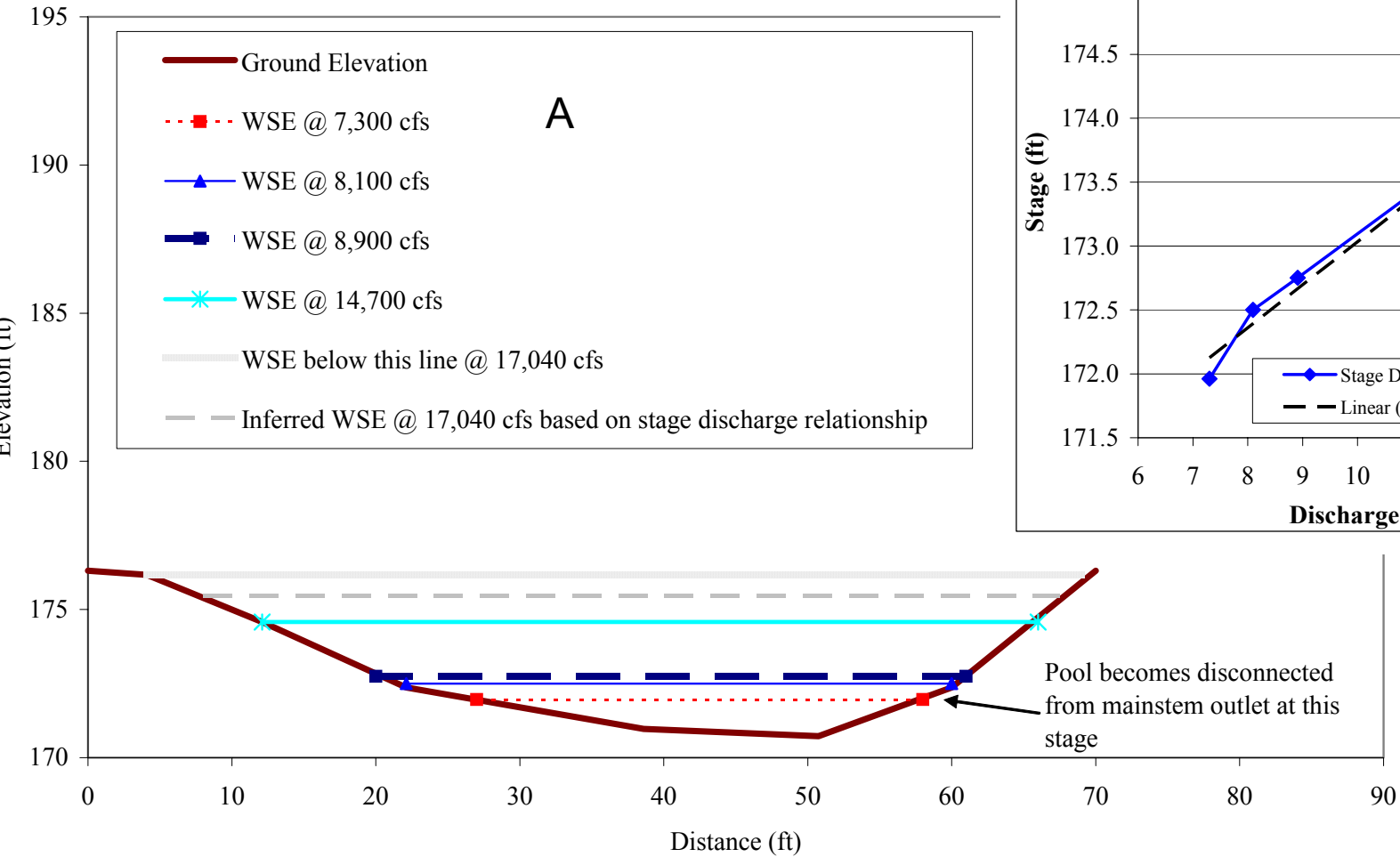


Figure 40. Study site 33 (RM 221.6R) , (A) cross section plot with known water surface elevations, and (B) plot of stage – discharge relationships at cross section.

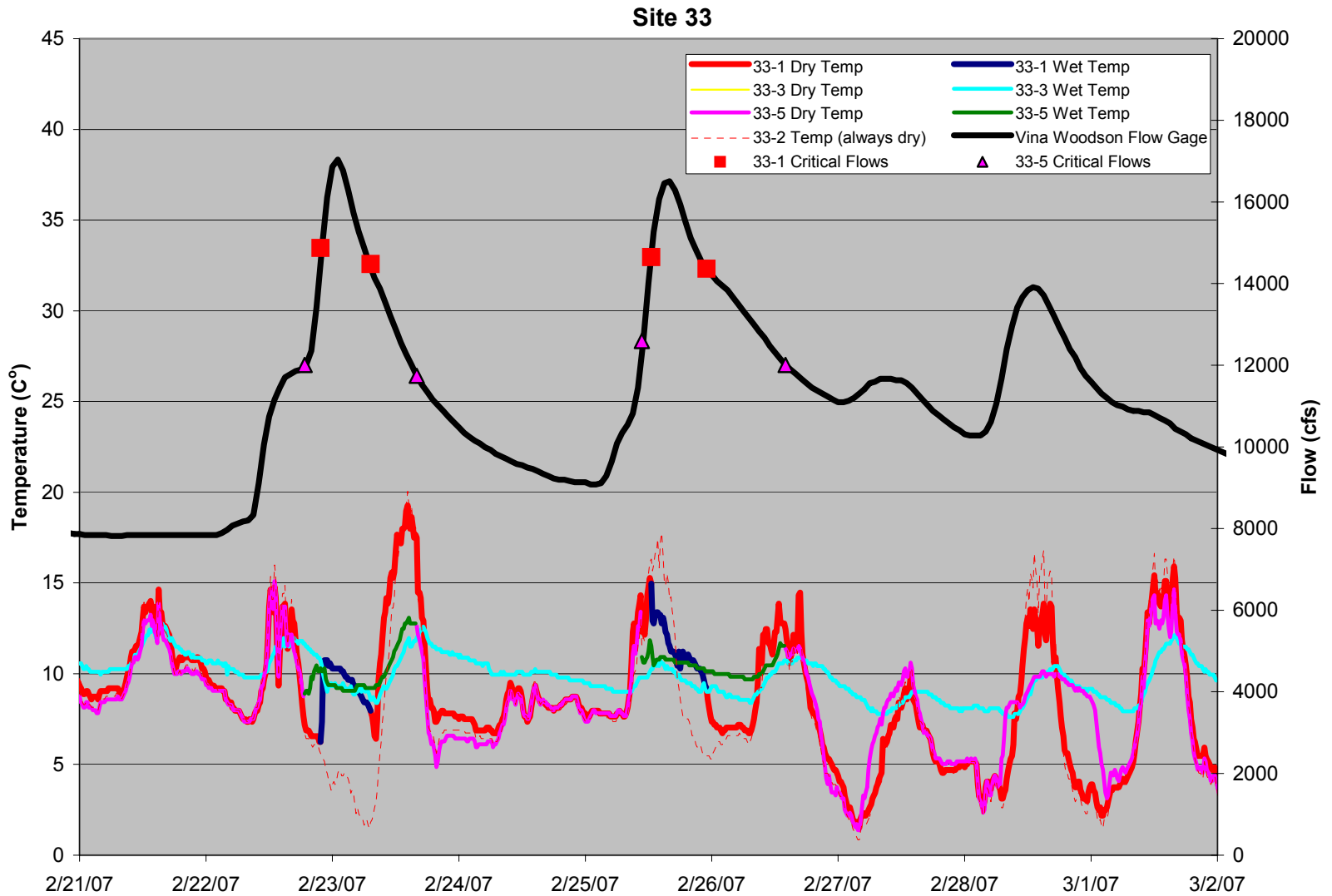
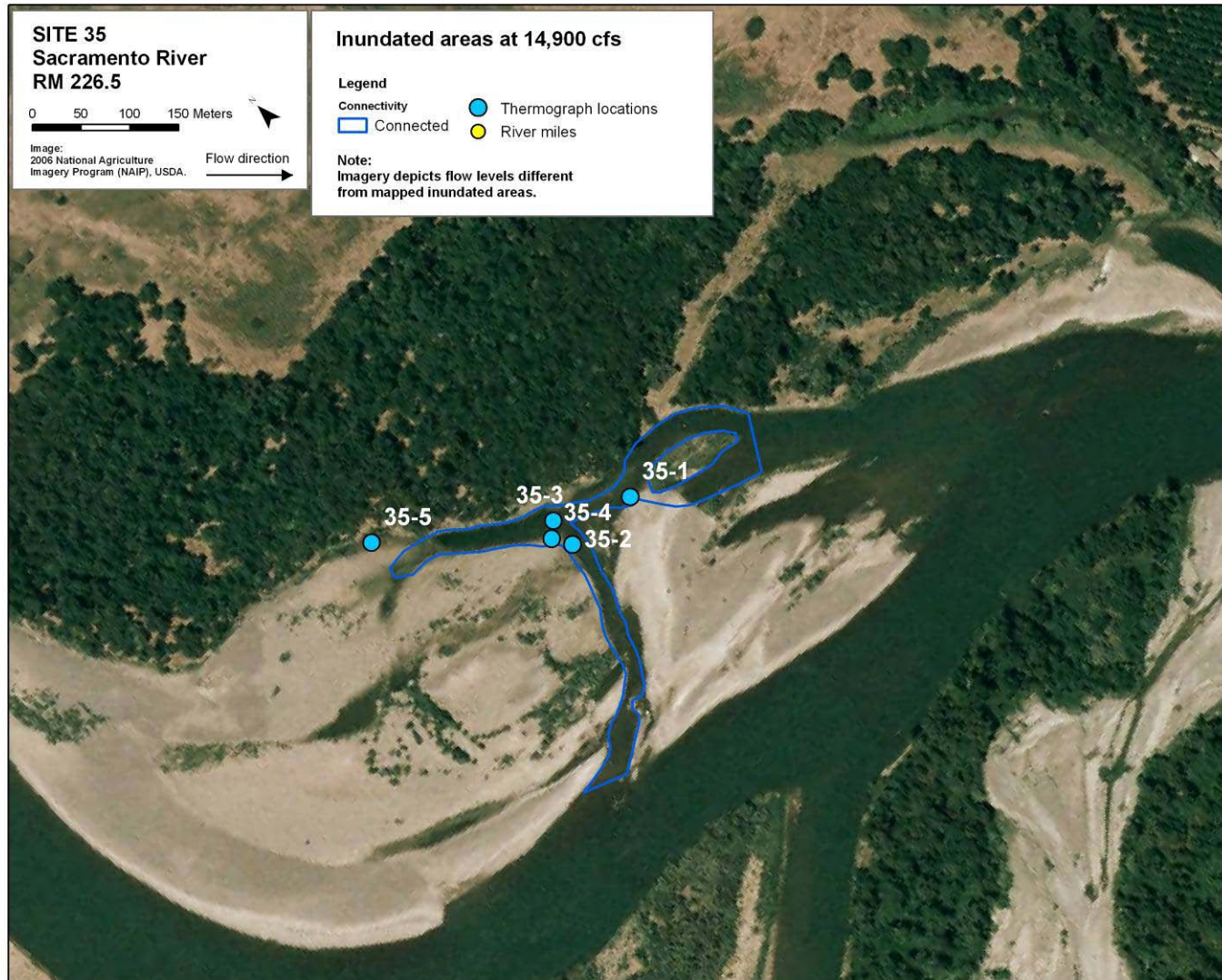


Figure 41. Thermograph data for site 33 (RM 221.6R) and discharge at Vina Woodson Bridge between 2/21/07 and 3/2/07. Critical flow points depict thermograph changes between dry and wet status.







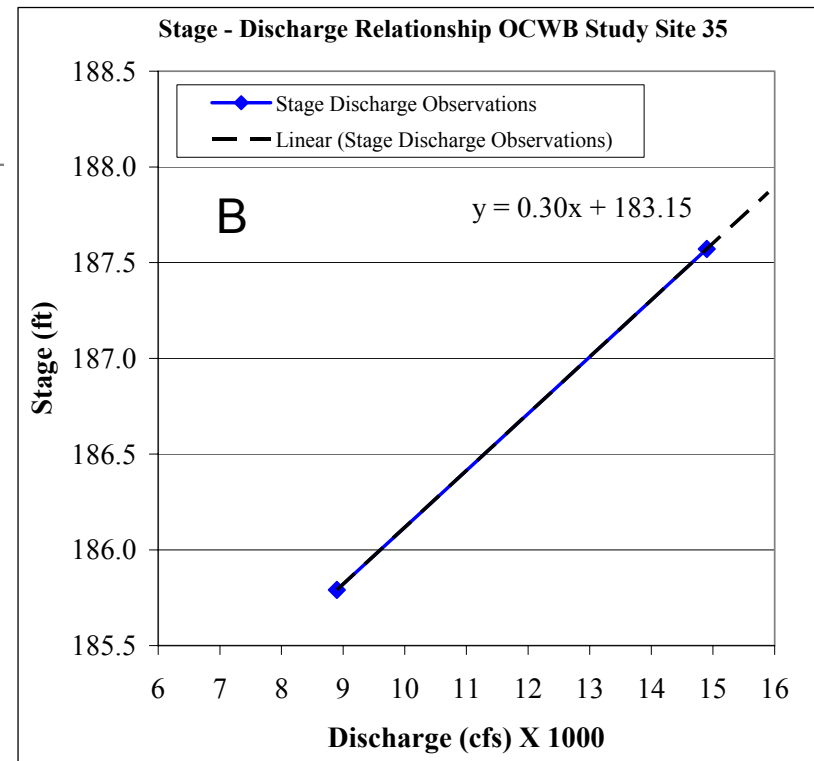
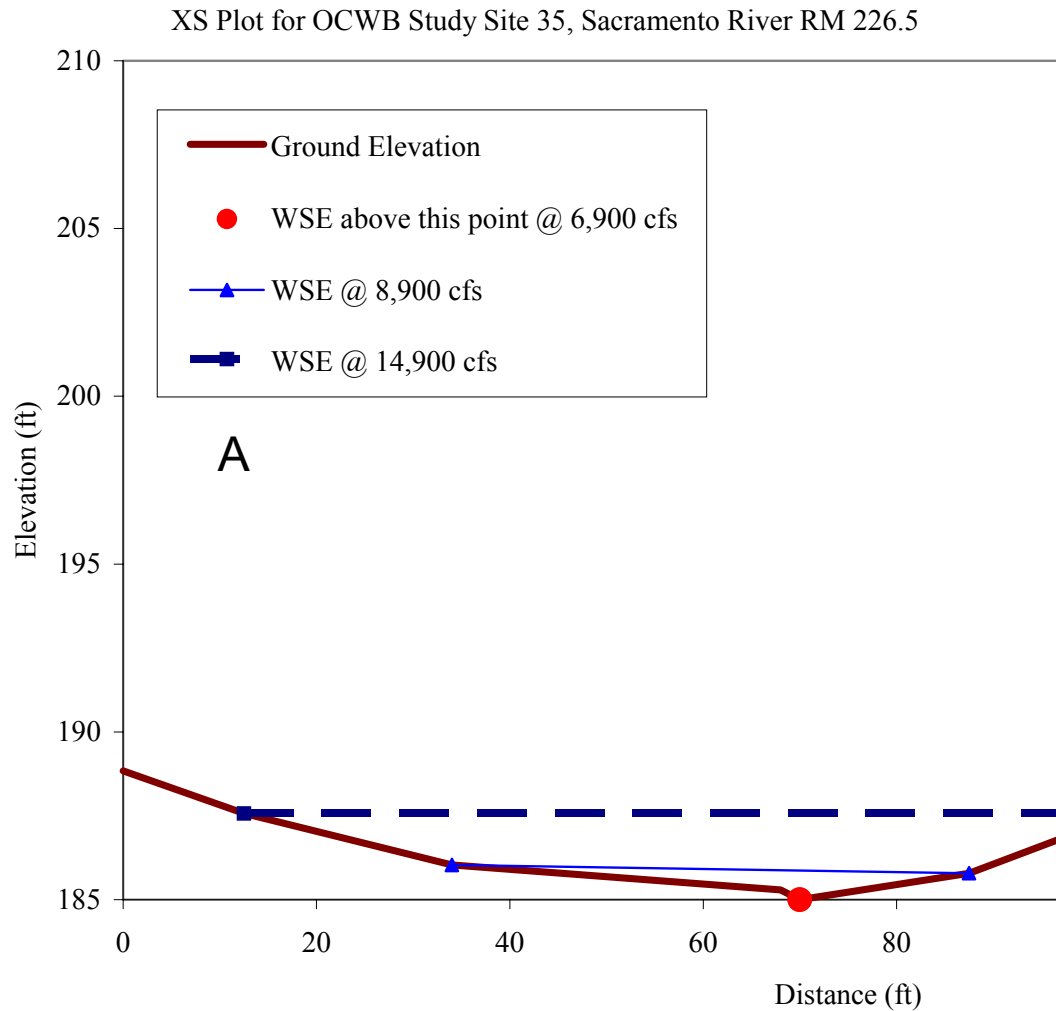


Figure 43. Study site 35 (RM 226.5L), (A) cross section plot with known water surface elevations, and (B) plot of stage – discharge relationships at cross section.

Site 35

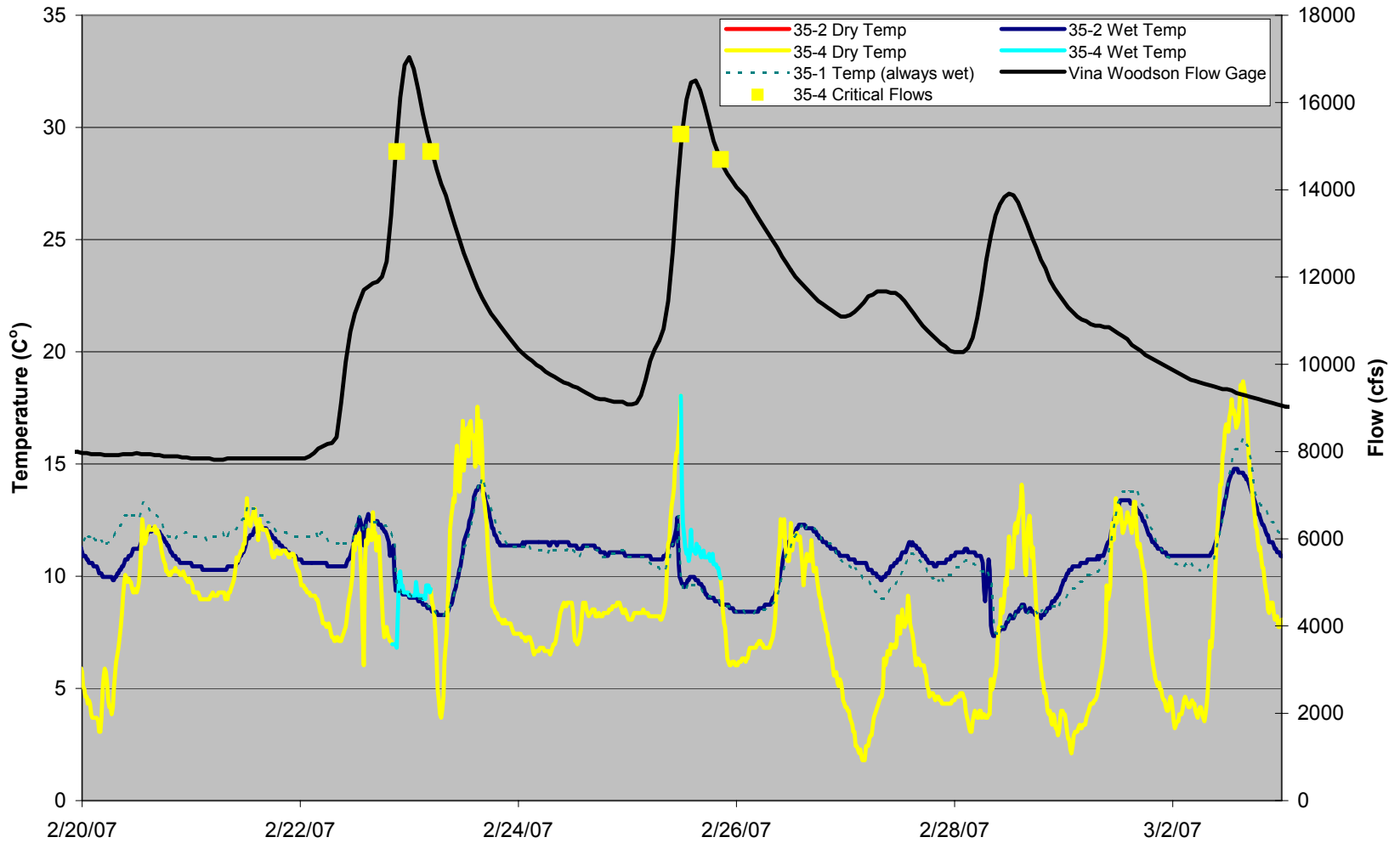


Figure 44. Thermograph data for site 35 (RM 226.5L) and discharge at Vina Woodson Bridge between 2/20/07 and 3/3/07. Critical flow points depict thermograph changes between dry and wet status.





Site 39

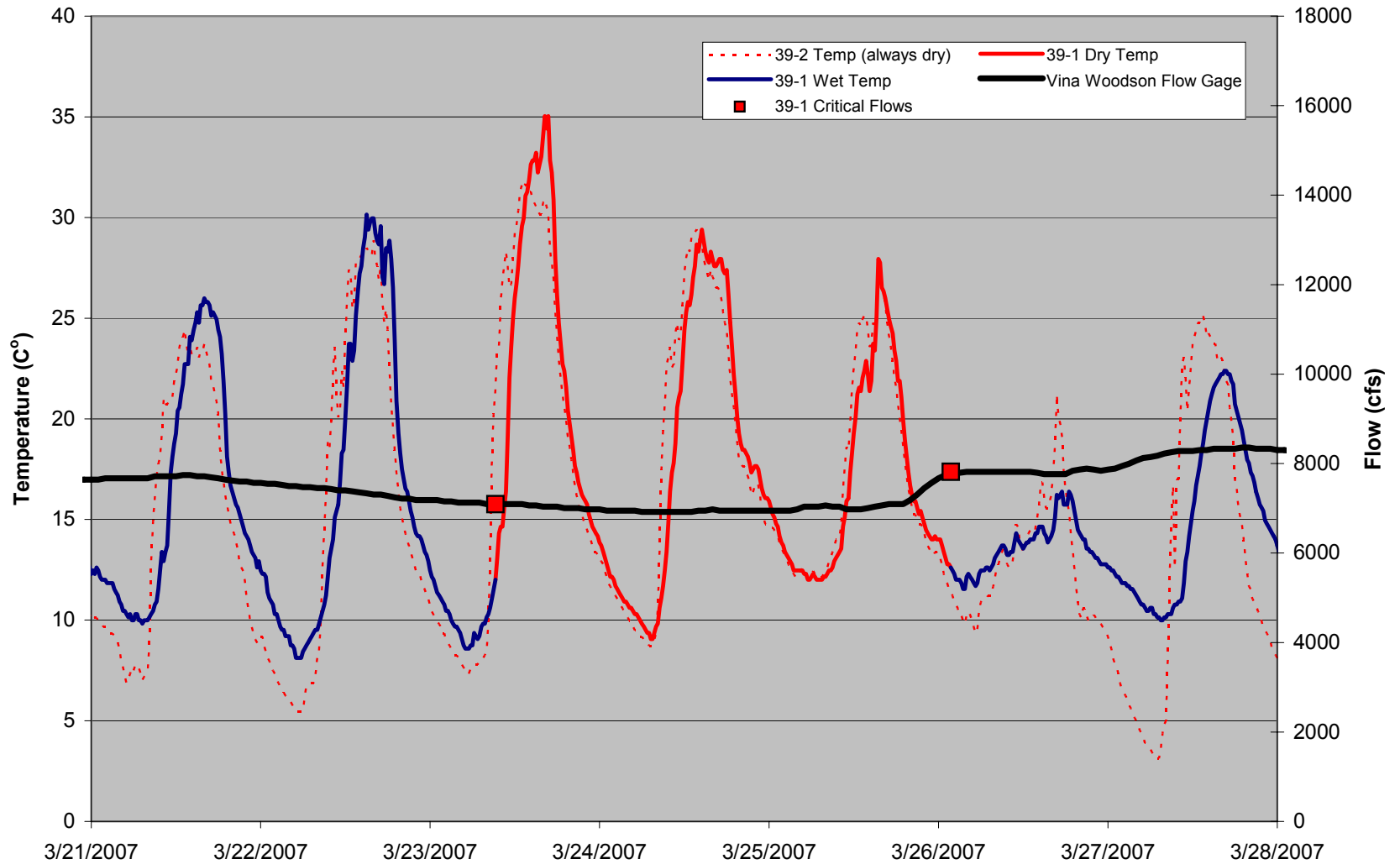


Figure 46. Thermograph data for site 39 (RM 232.8L) and discharge at Vina Woodson Bridge between 3/21/07 and 3/28/07. Critical flow points depict thermograph changes between dry and wet status.



Figure 47a. Inundated areas of site 40 (RM 233.5R) at flows of 8,900 cfs , areas observed and drawn during field mapping.



Figure 47b. Inundated areas of site 40 (RM 233.5R) at flows of 13,500 cfs , areas based on thermograph temperature records and field surveys.

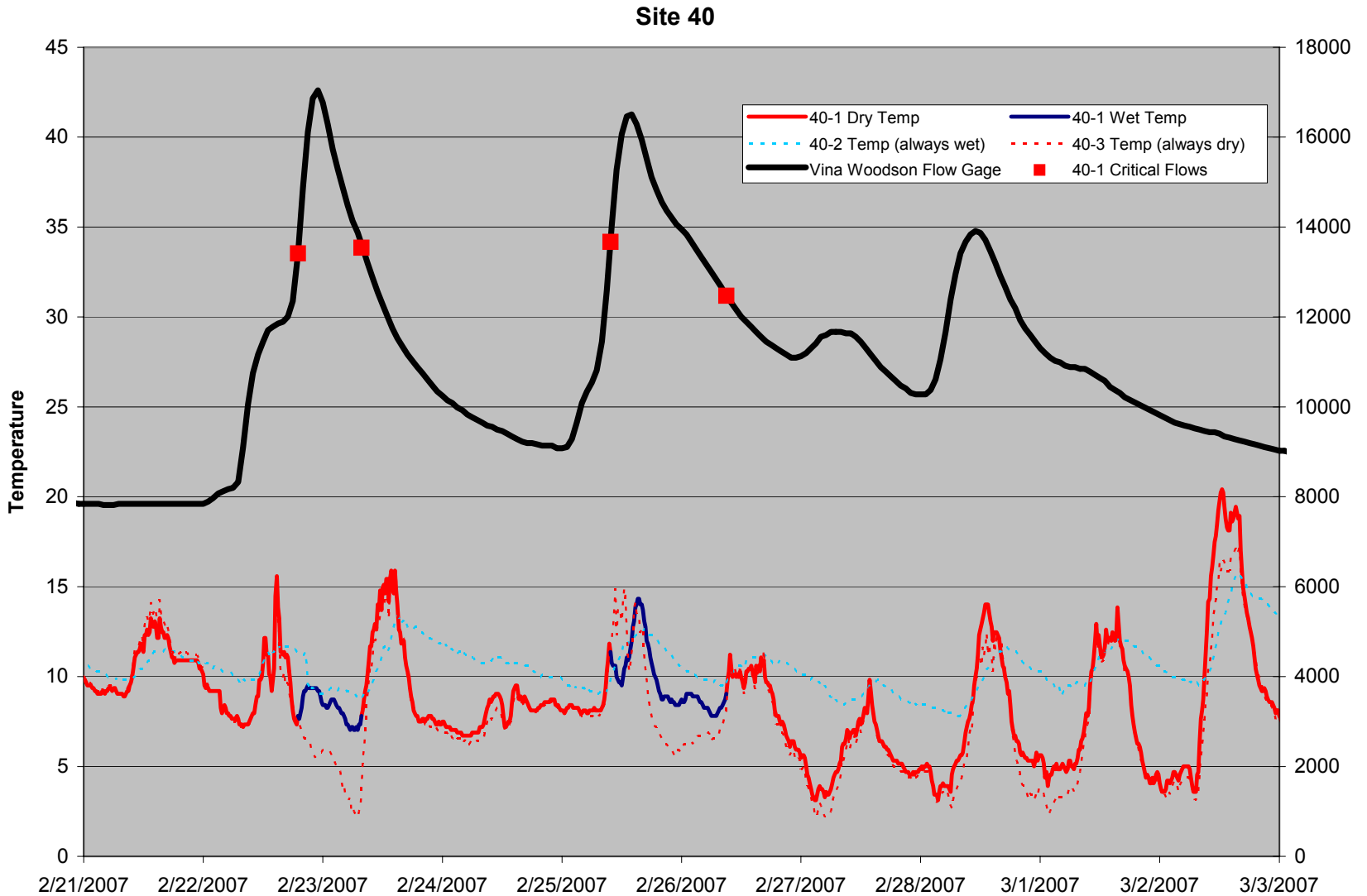
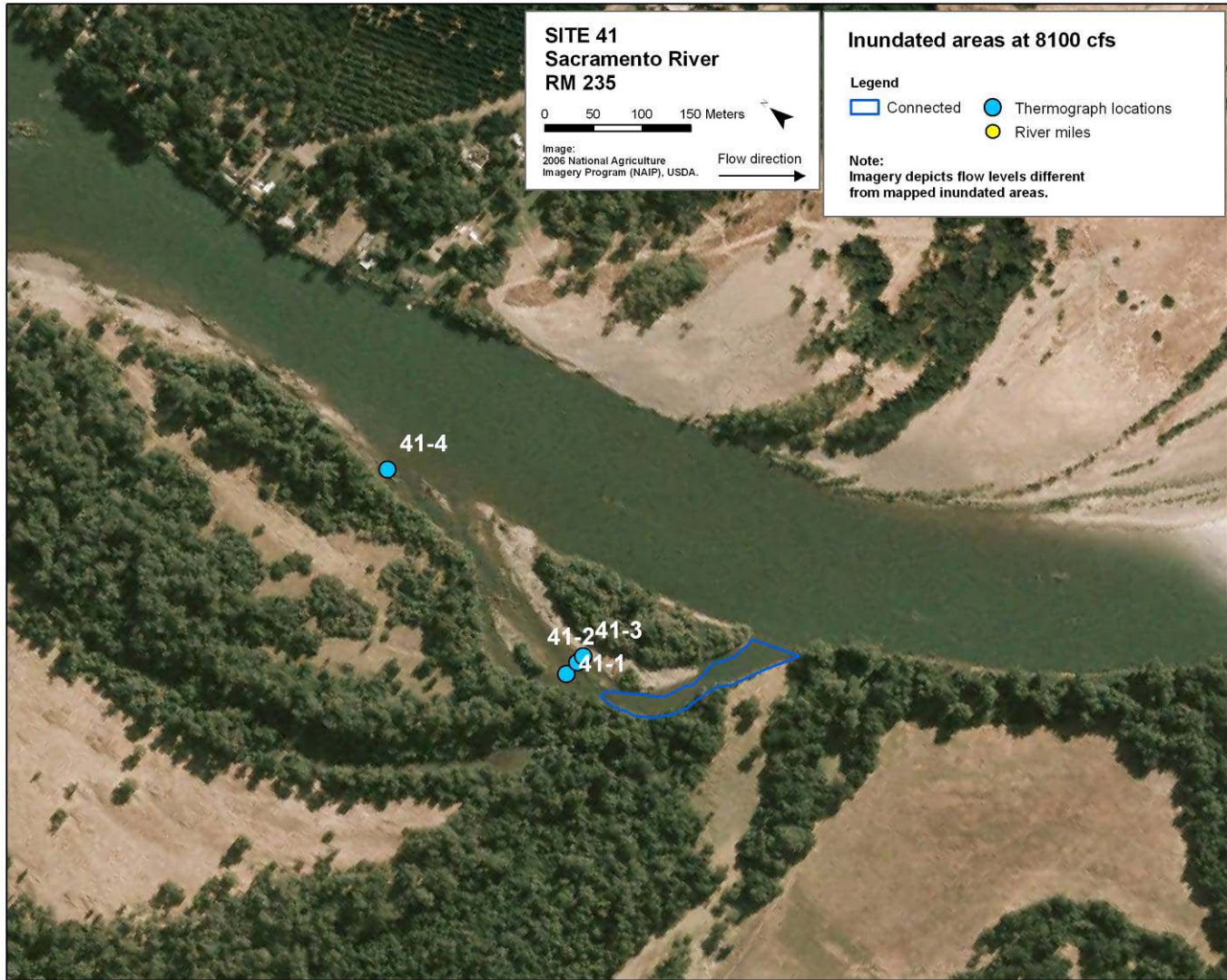


Figure 48. Thermograph data for site 40 (RM 233.5R) and discharge at Vina Woodson Bridge between 2/21/07 and 3/3/07. Critical flow points depict thermograph changes between dry and wet status.



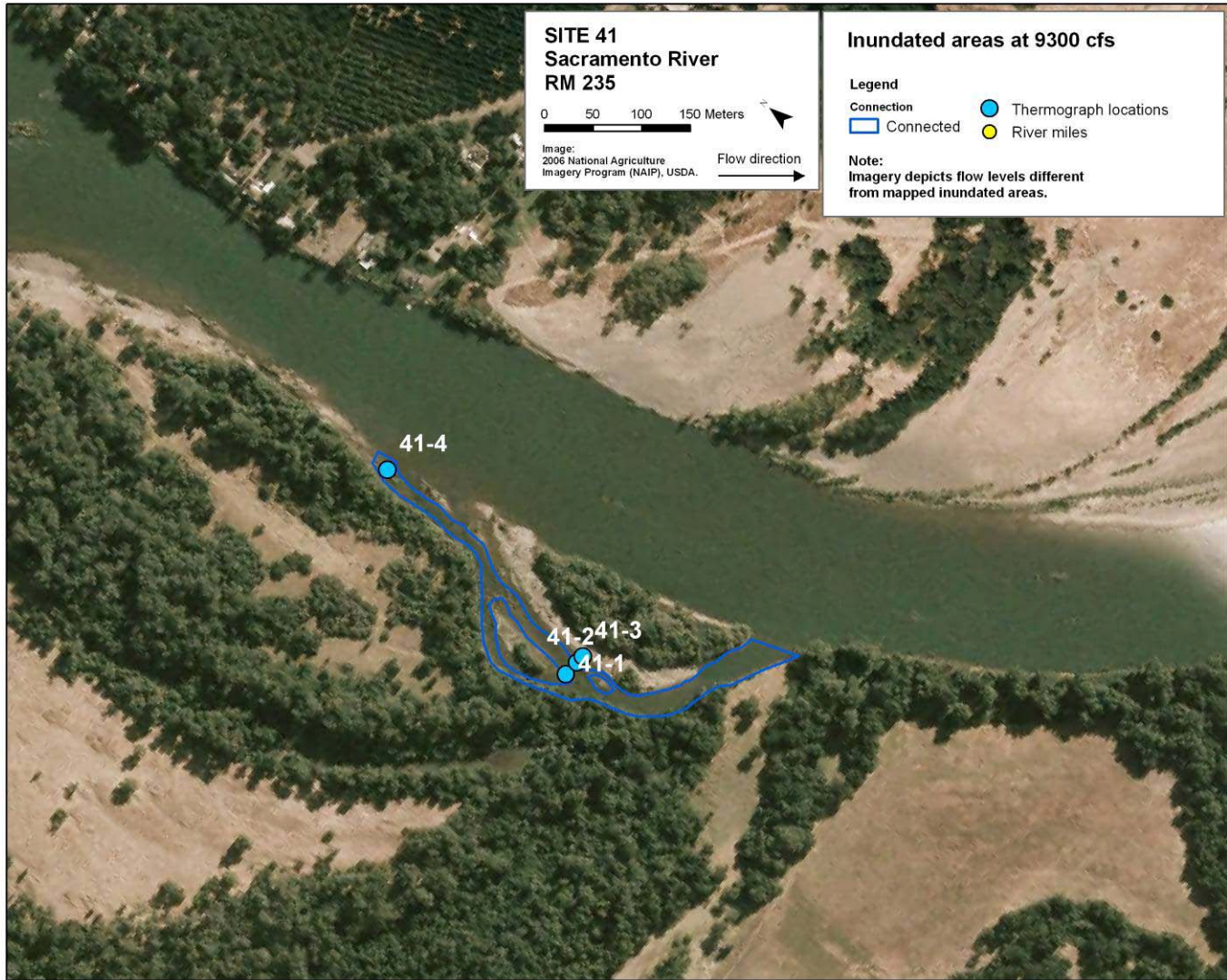
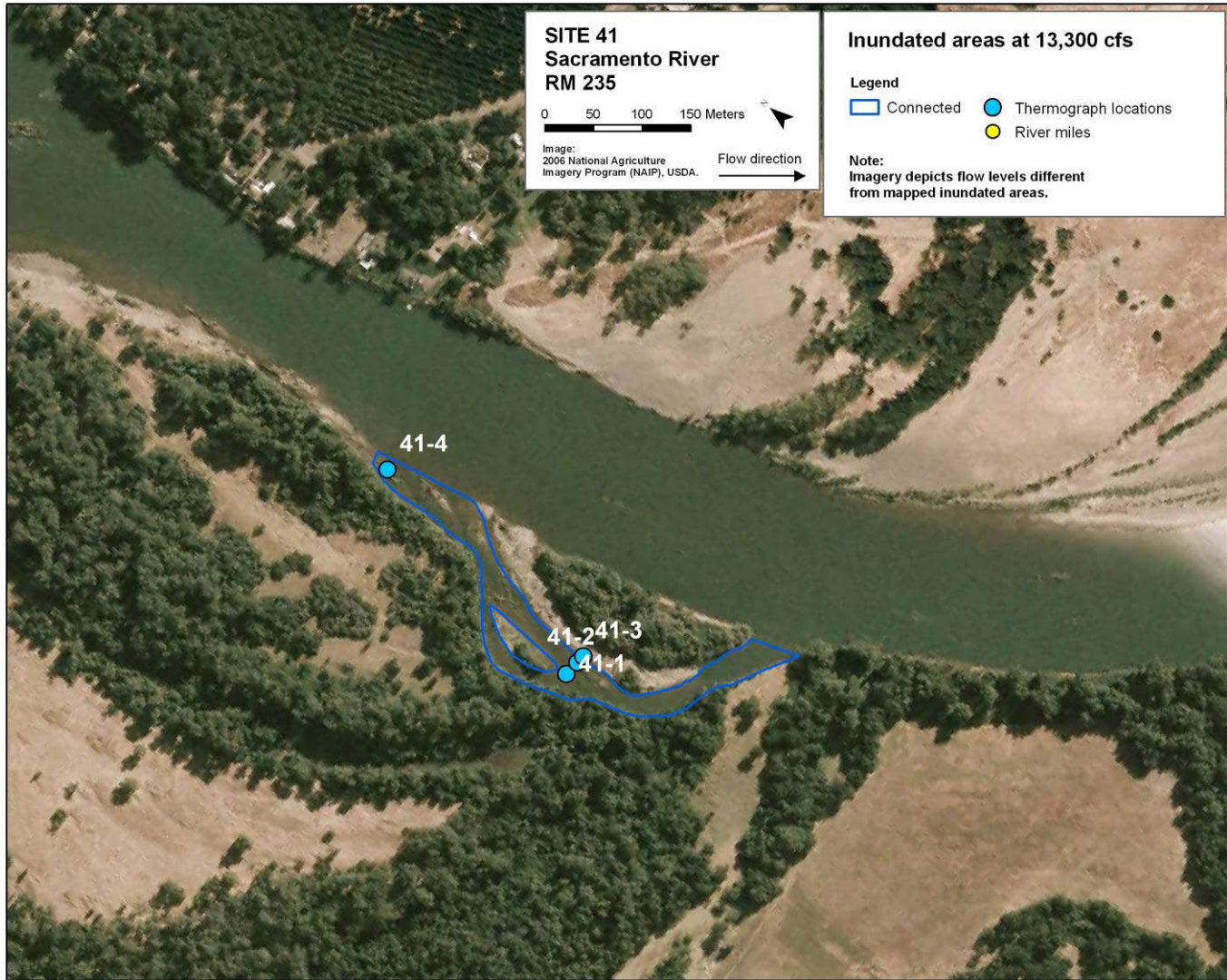


Figure 49b. Inundated areas of site 41 (RM 235.3R) at flows of 9,300 cfs, areas observed and drawn during field mapping.



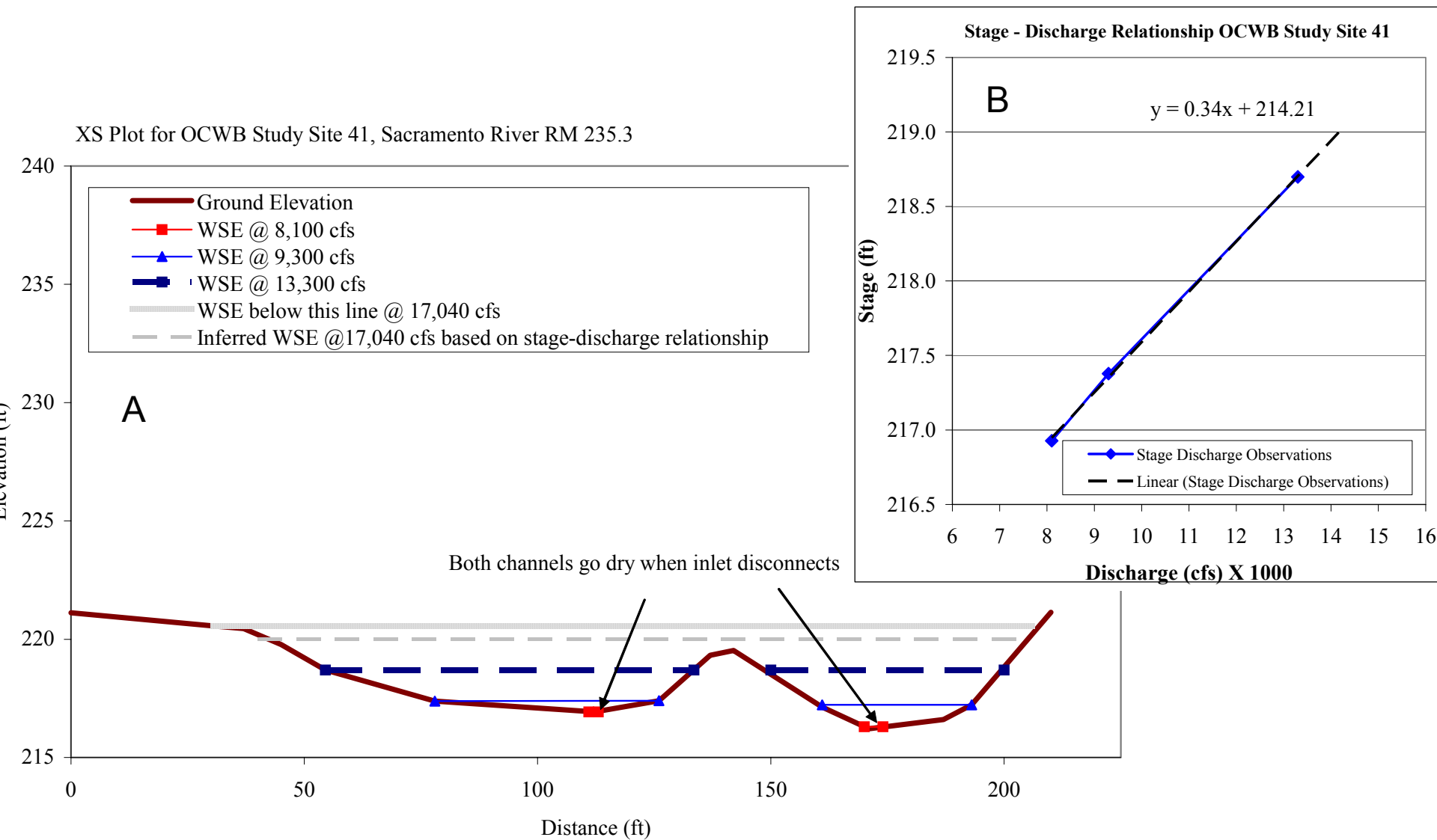


Figure 50. Study site 41 (RM 235.3R) , (A) cross section plot with known water surface elevations, and (B) plot of stage – discharge relationships at cross section.

Site 41

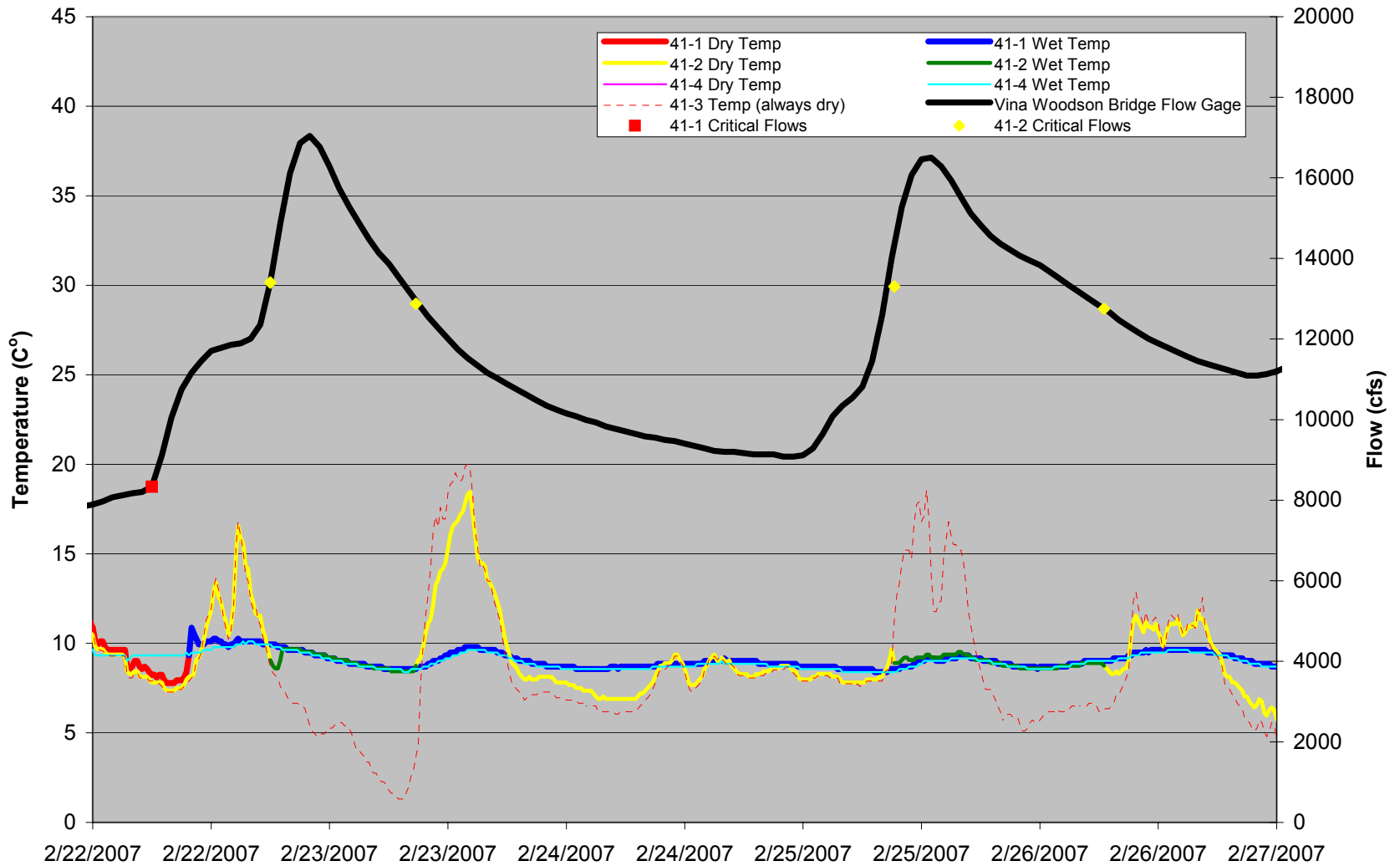
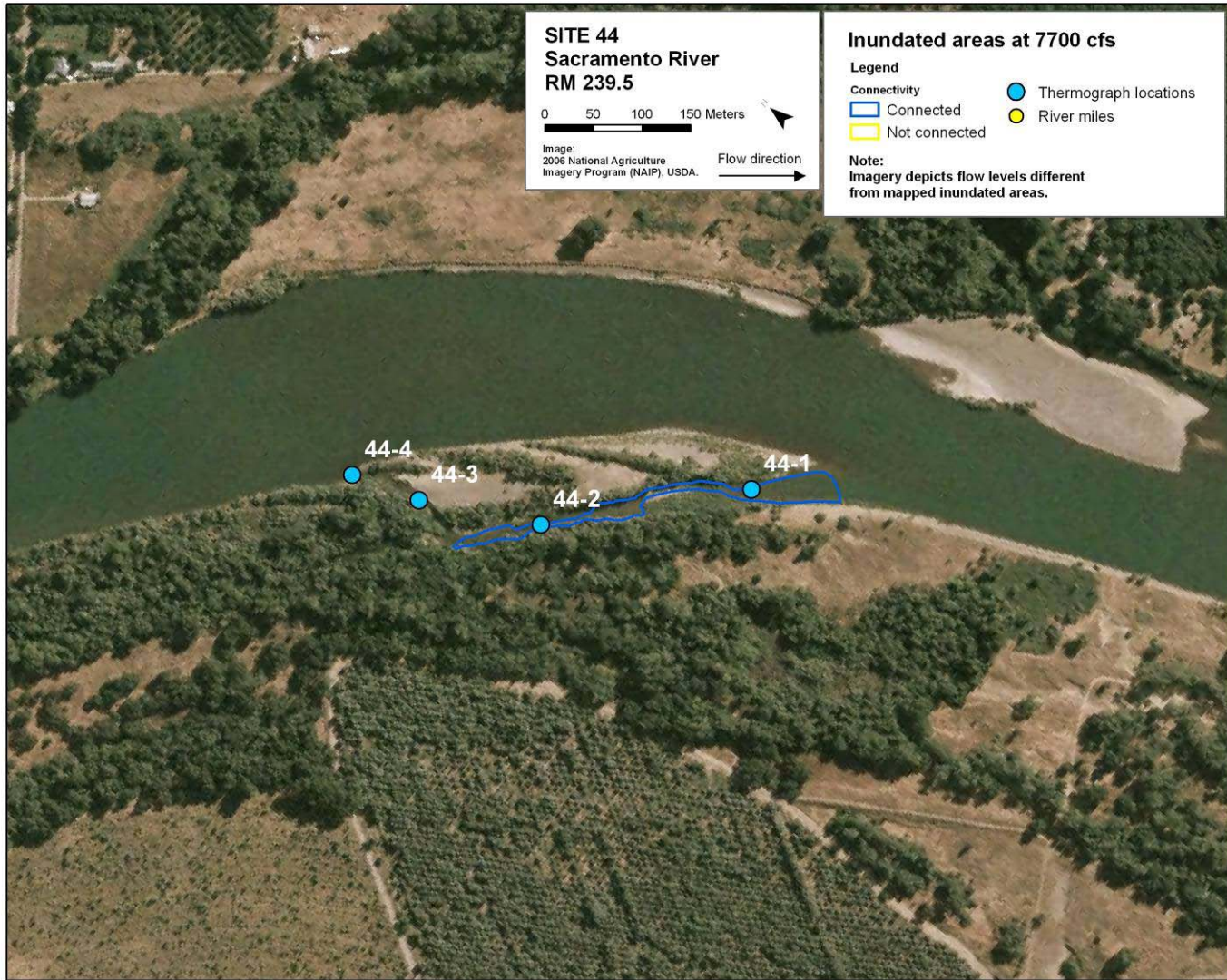
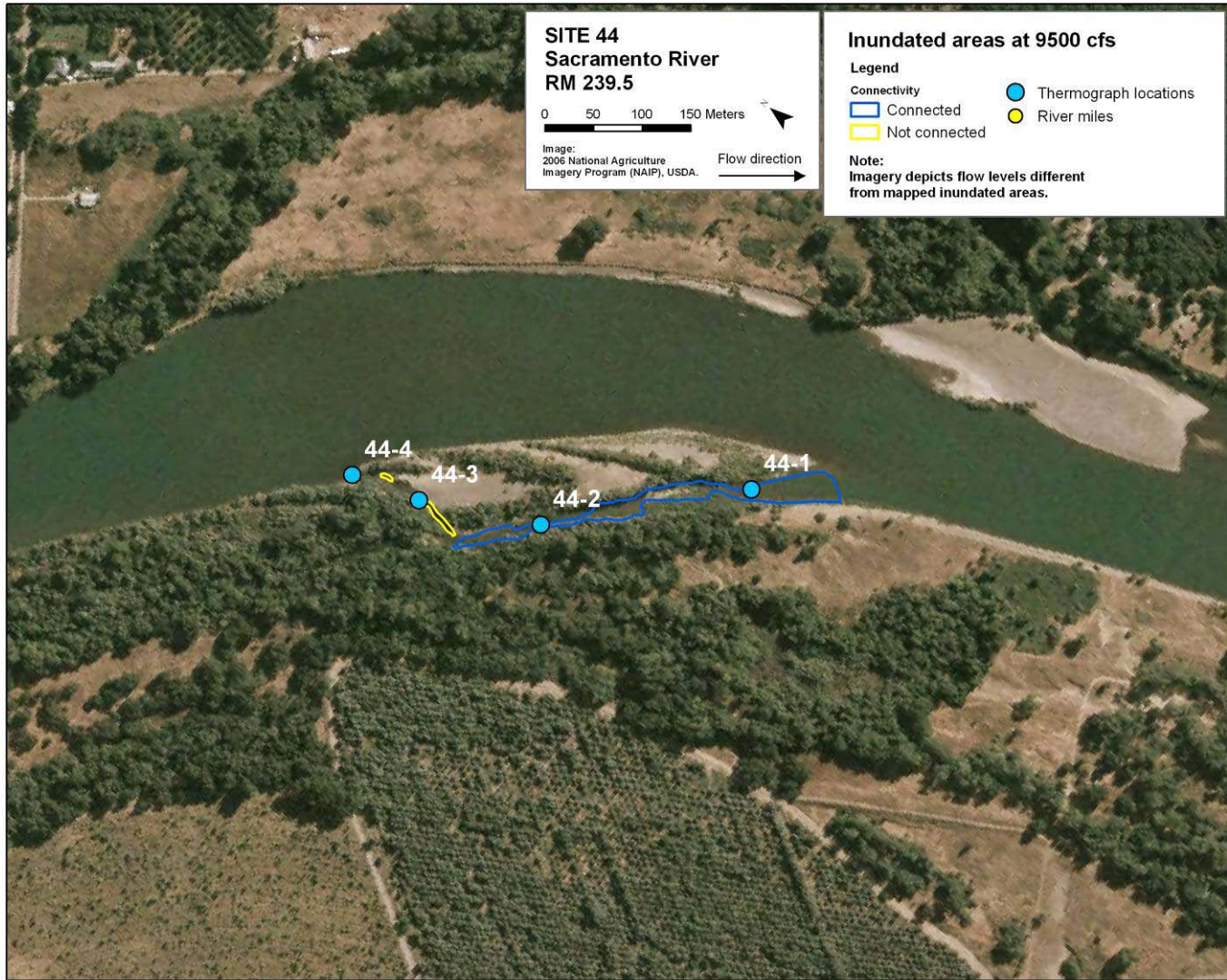


Figure 51. Thermograph data for site 41 (RM 235.3R) and discharge at Vina Woodson Bridge between 2/22/07 and 2/27/07. Critical flow points depict thermograph changes between dry and wet status.







Site 44

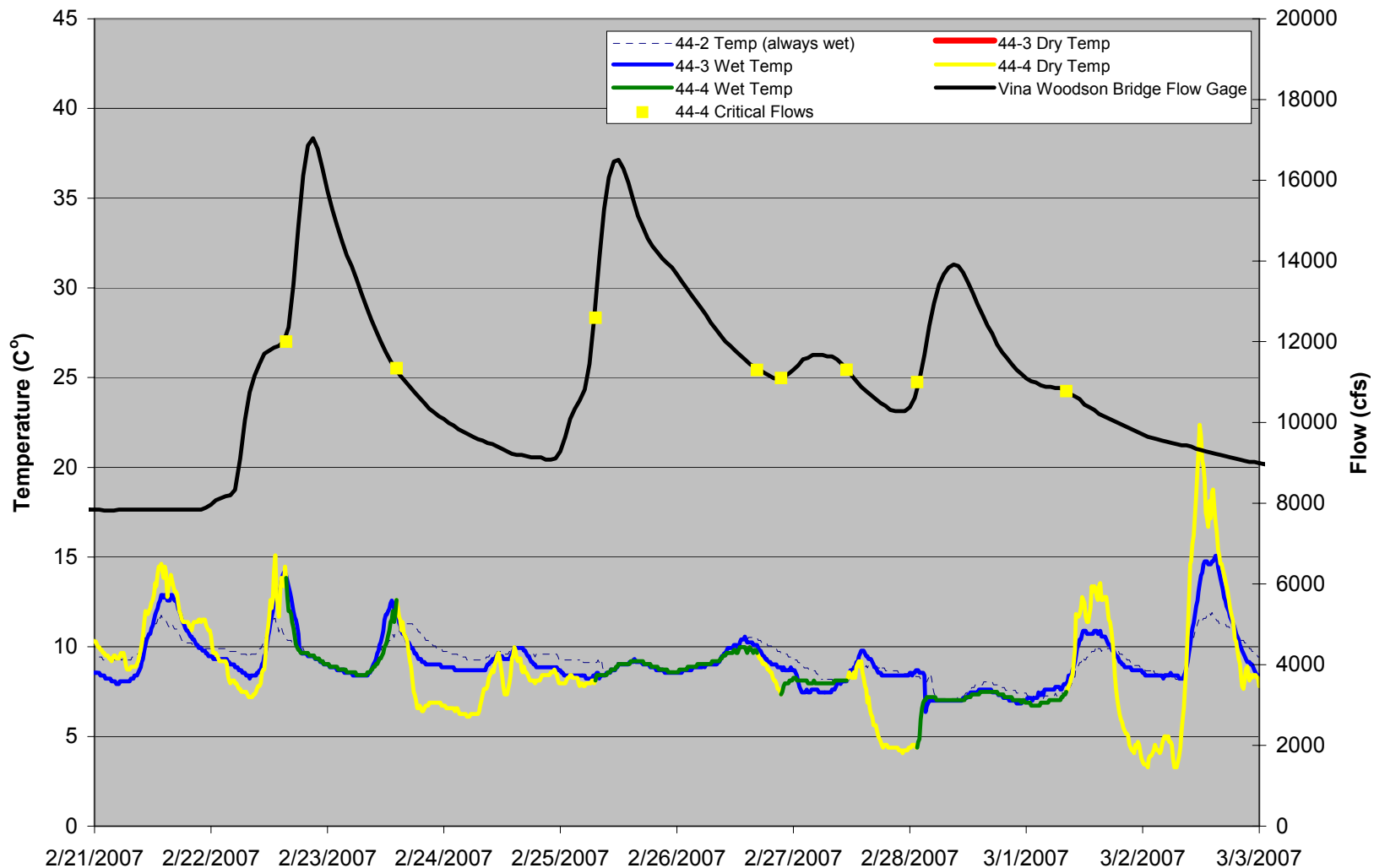


Figure 53. Thermograph data for site 44 (RM 239.5R) and discharge at Vina Woodson Bridge between 2/21/07 and 3/3/07. Critical flow points depict thermograph changes between dry and wet status.

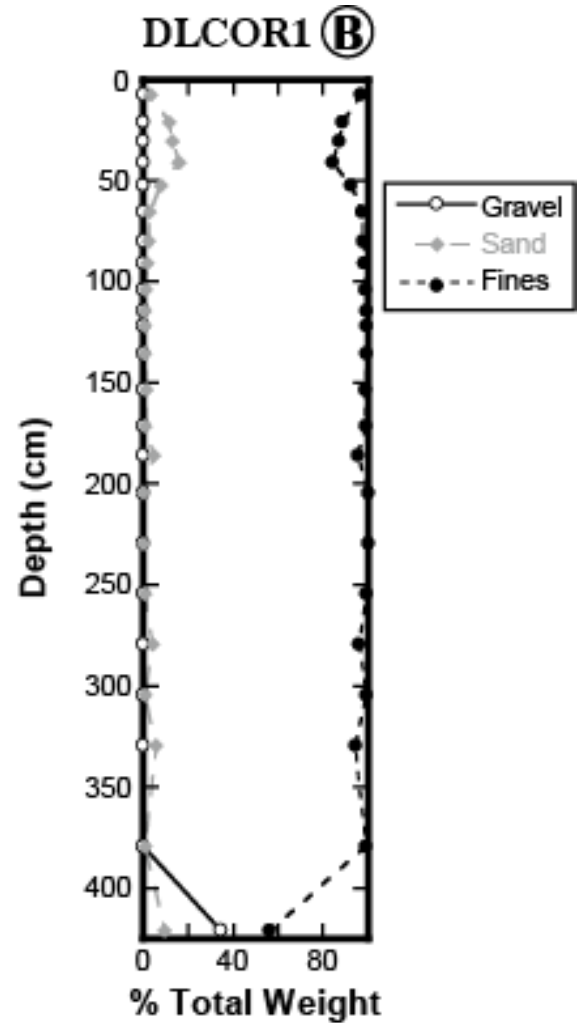
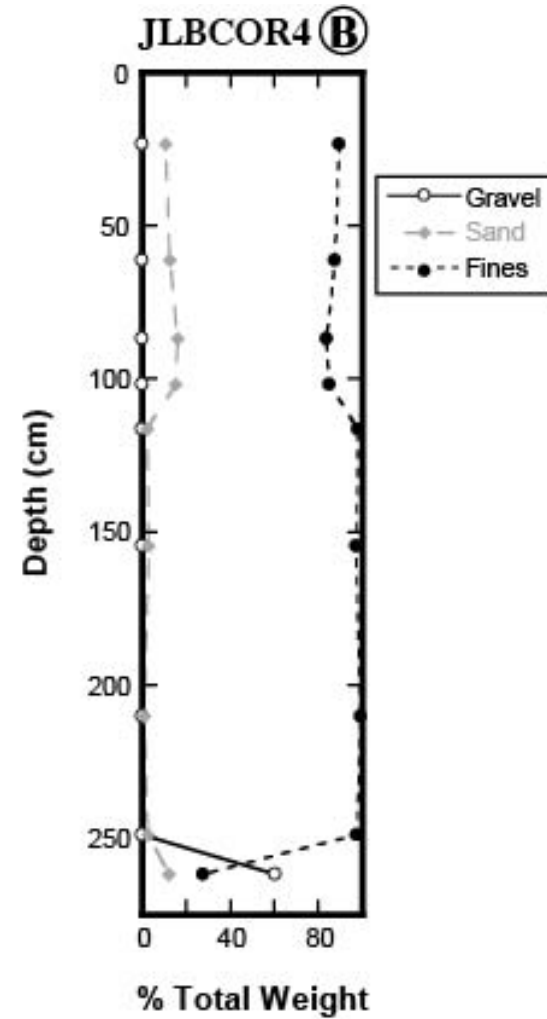


Figure 54. (A) Aerial photo of Duck Lake near river mile 181 taken in 2004. The diversion angle and core locations are shown within the photo. (B) Granulometric profile for core DLCOR1.



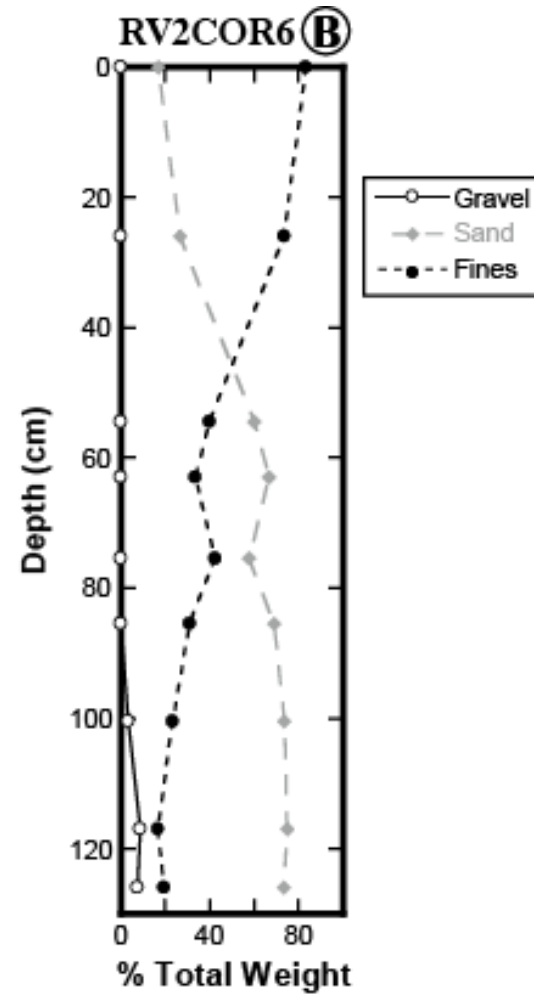
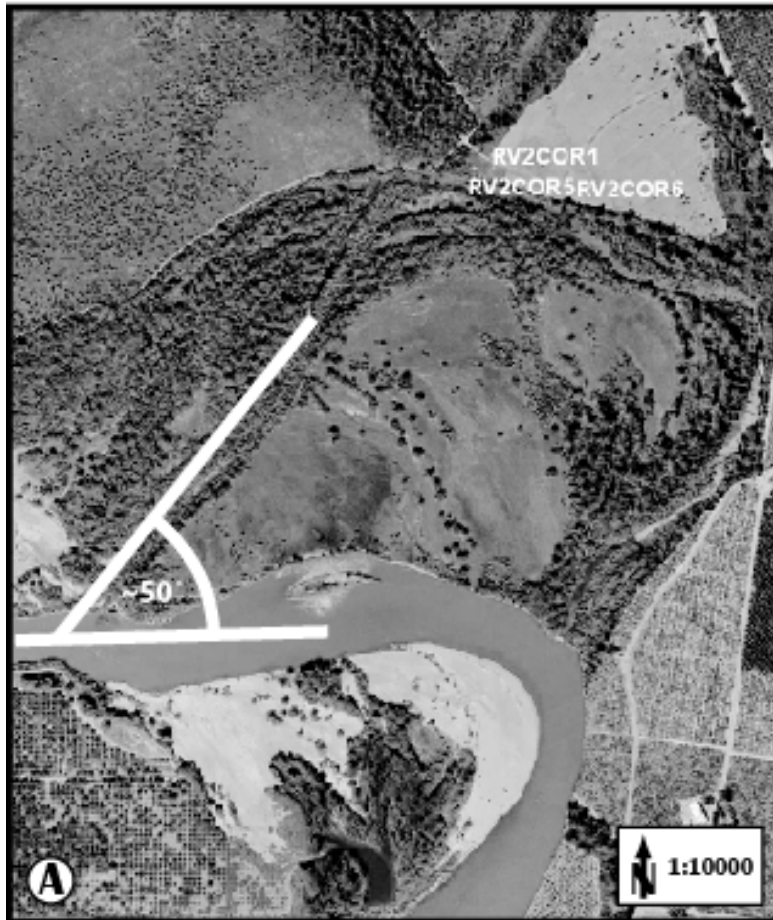


Figure 56. (A) Aerial photo of Rio Vista near river mile 214 taken in 2004. The diversion angle and core locations are shown within the photo. (B) Granulometric profile for core RV2COR6.

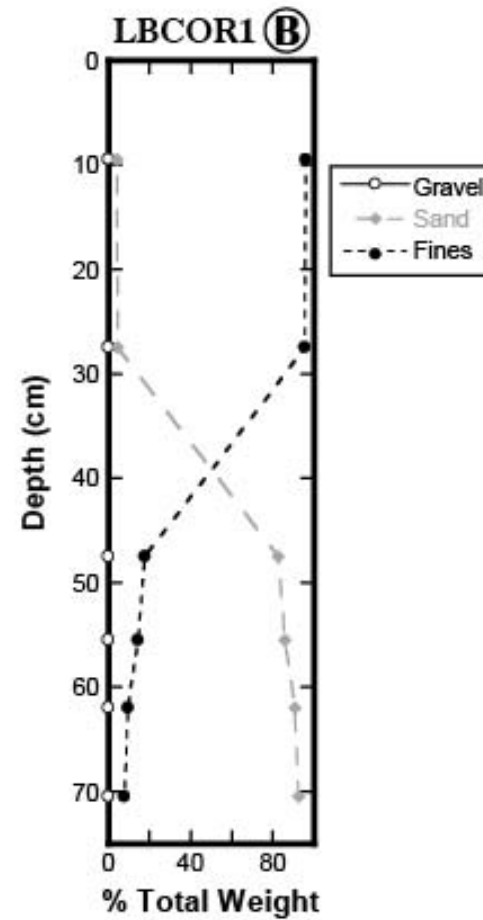


Figure 57. (A) Aerial photo of La Barranca near river mile 237 taken in 2004. The diversion angle and the core location are shown within the photo. (B) Granulometric profile for core LBCOR1.

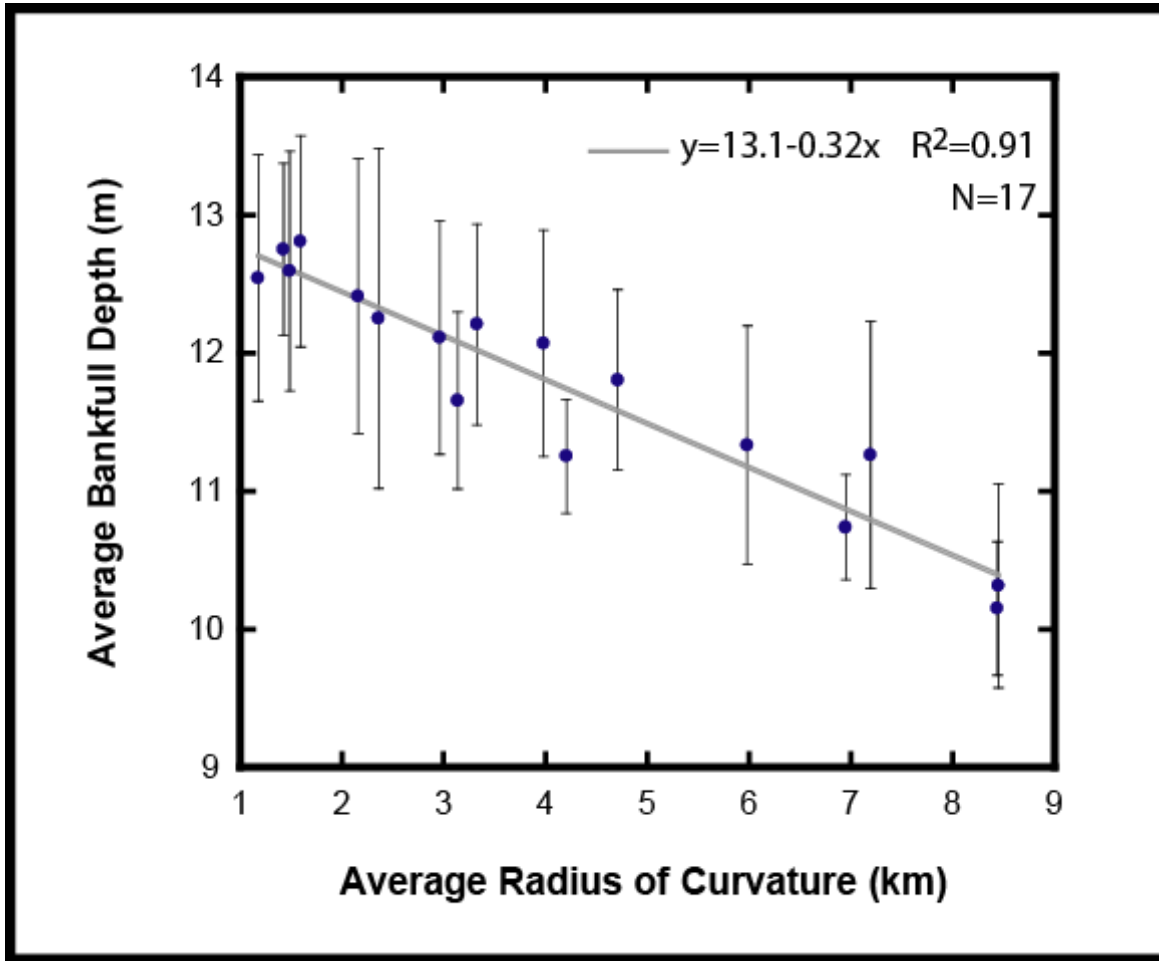
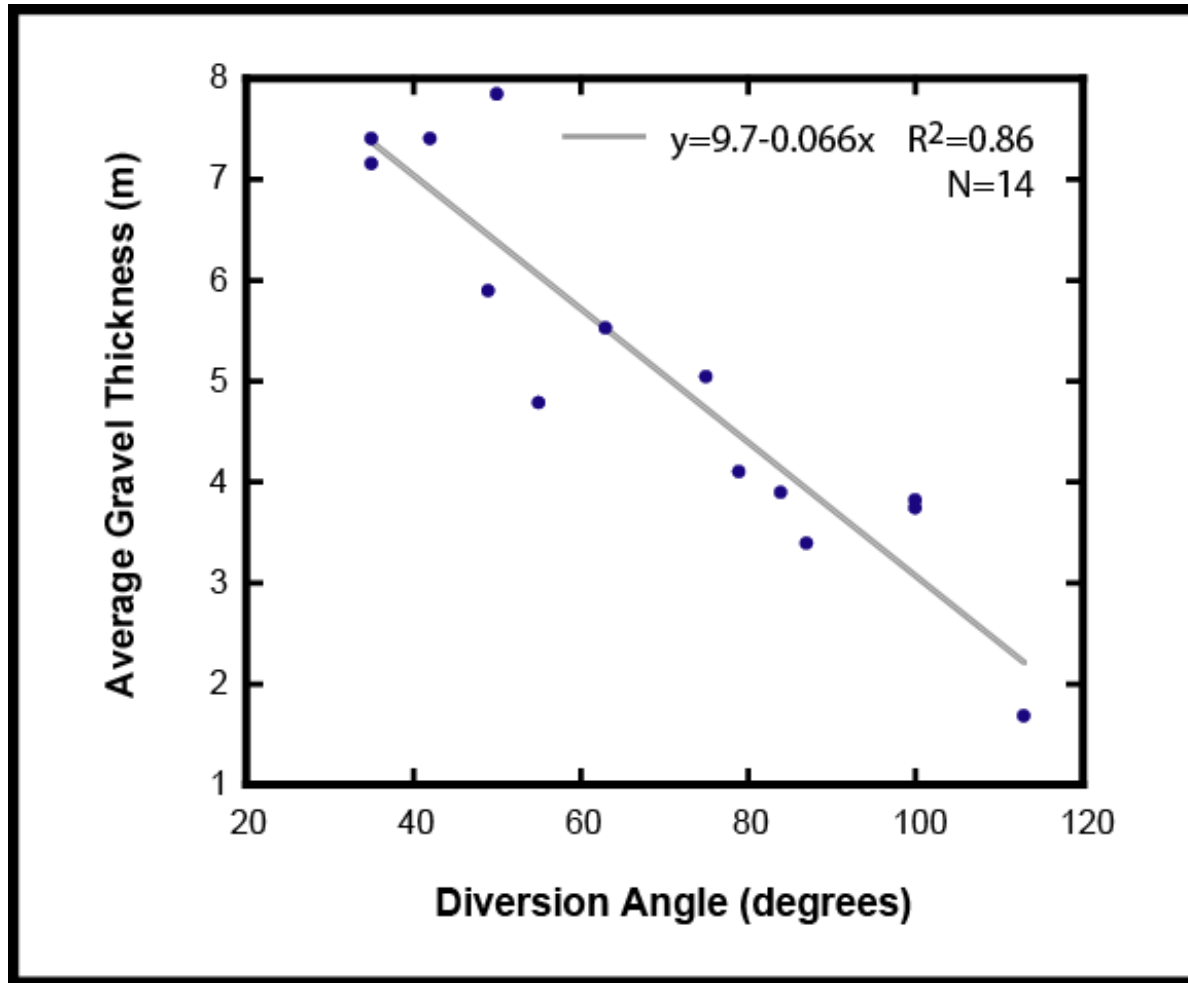


Figure 58. The average bankfull depth of meanders comprising the 1997 Sacramento River versus the average radius of curvature of each meander. Error bars represent one standard deviation.



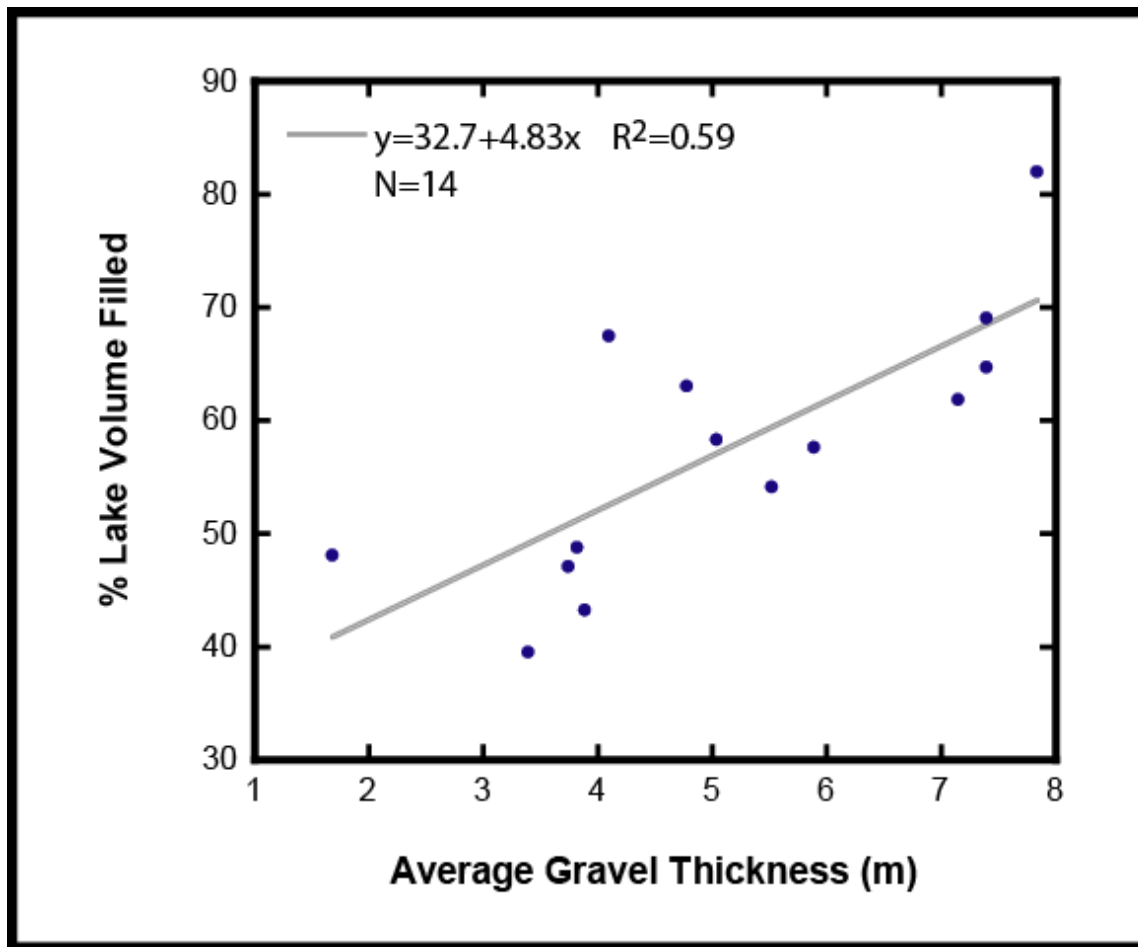


Figure 60. The percentage that an oxbow has been filled, measured as the total thickness of sedimentary fill divided by its average original depth, versus average gravel thickness.

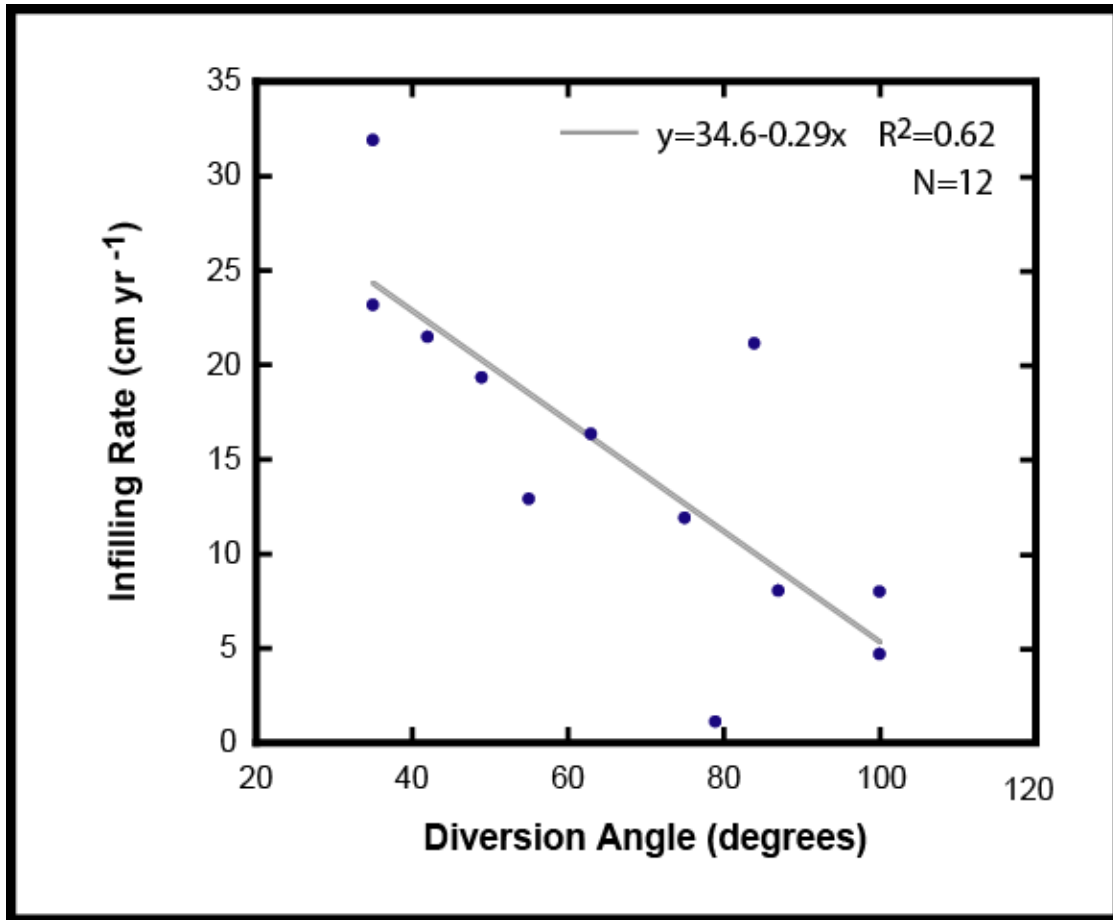


Figure 61. The percentage that an oxbow has been filled, measured as the total thickness of sedimentary fill divided by its average original depth, versus average gravel thickness.

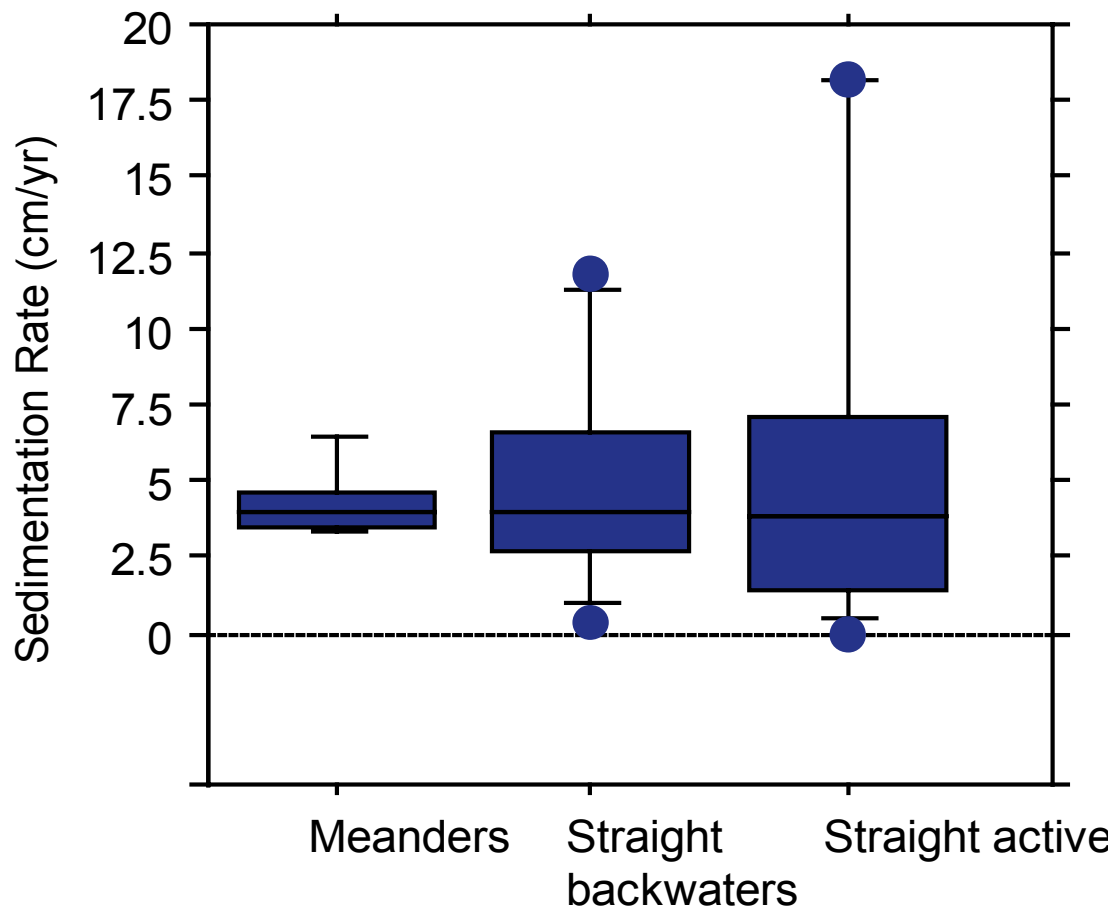


Figure 62. Sedimentation rates (in cm per yr) grouped by geometric former channel type as distinguished from features measured on aerial photographs.

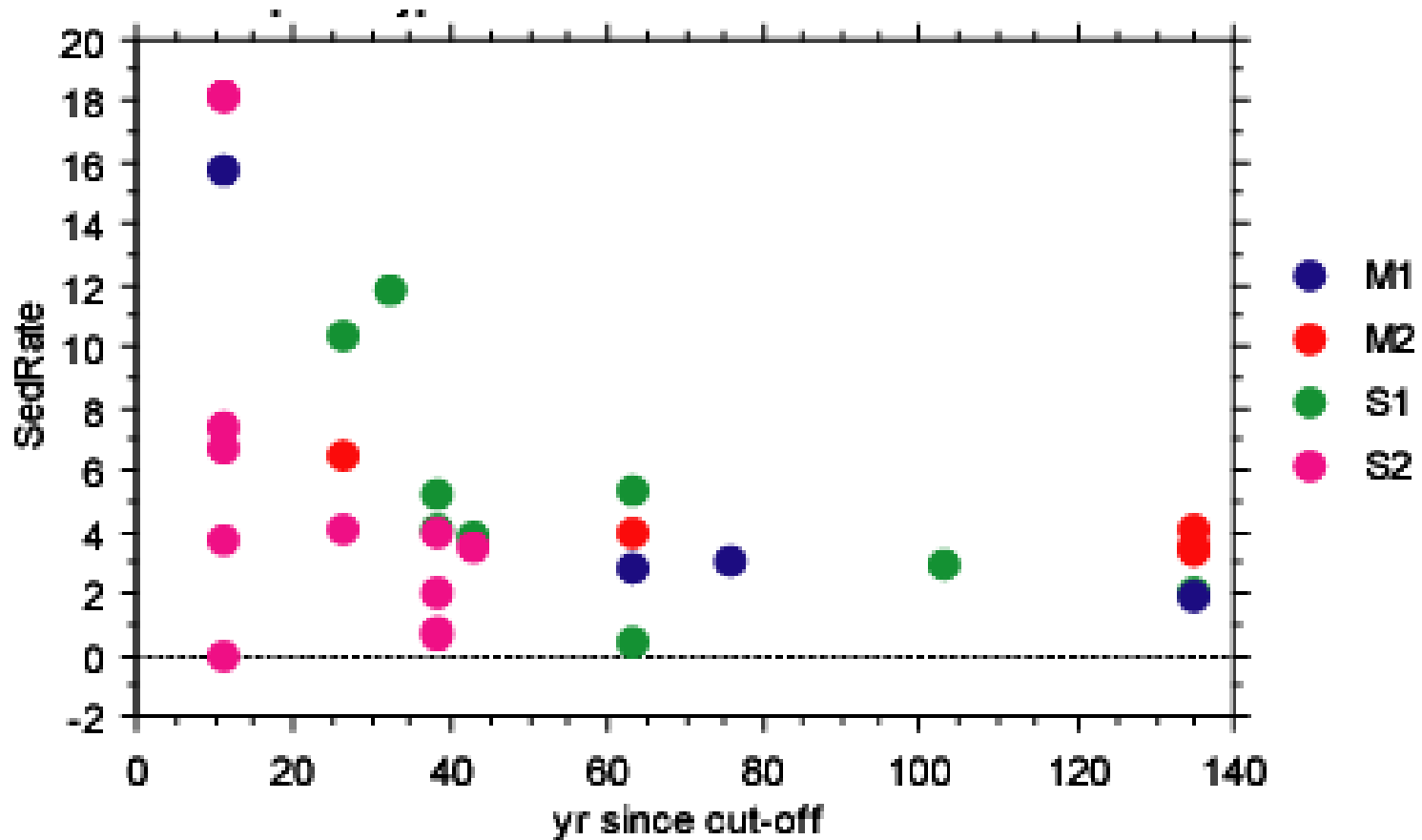


Figure 63. OCWB sedimentation rate (in cm per yr) plotted against age of OCWB, with geometric channel type (from aerial photo analysis) identified. (Same as Figure 9 but with channel types identified.)

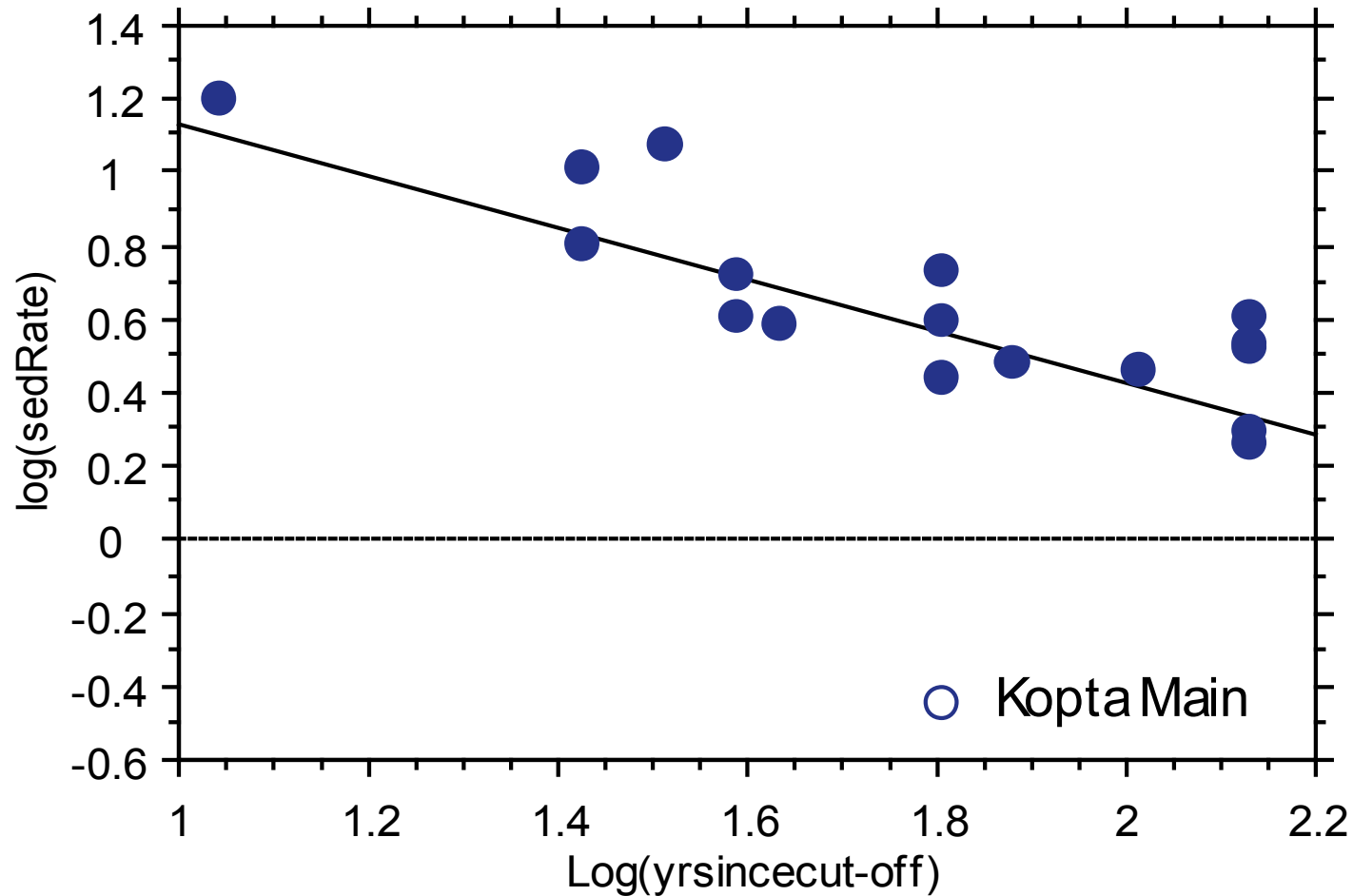


Figure 64. Log-log scale regression model relating sedimentation rate to the age of the OCWB unit. The regression equation is $\text{Log } y = 1.92 - 0.72 \text{ log } x$; $R^2 = 0.78$ (Kopta outlier excluded)

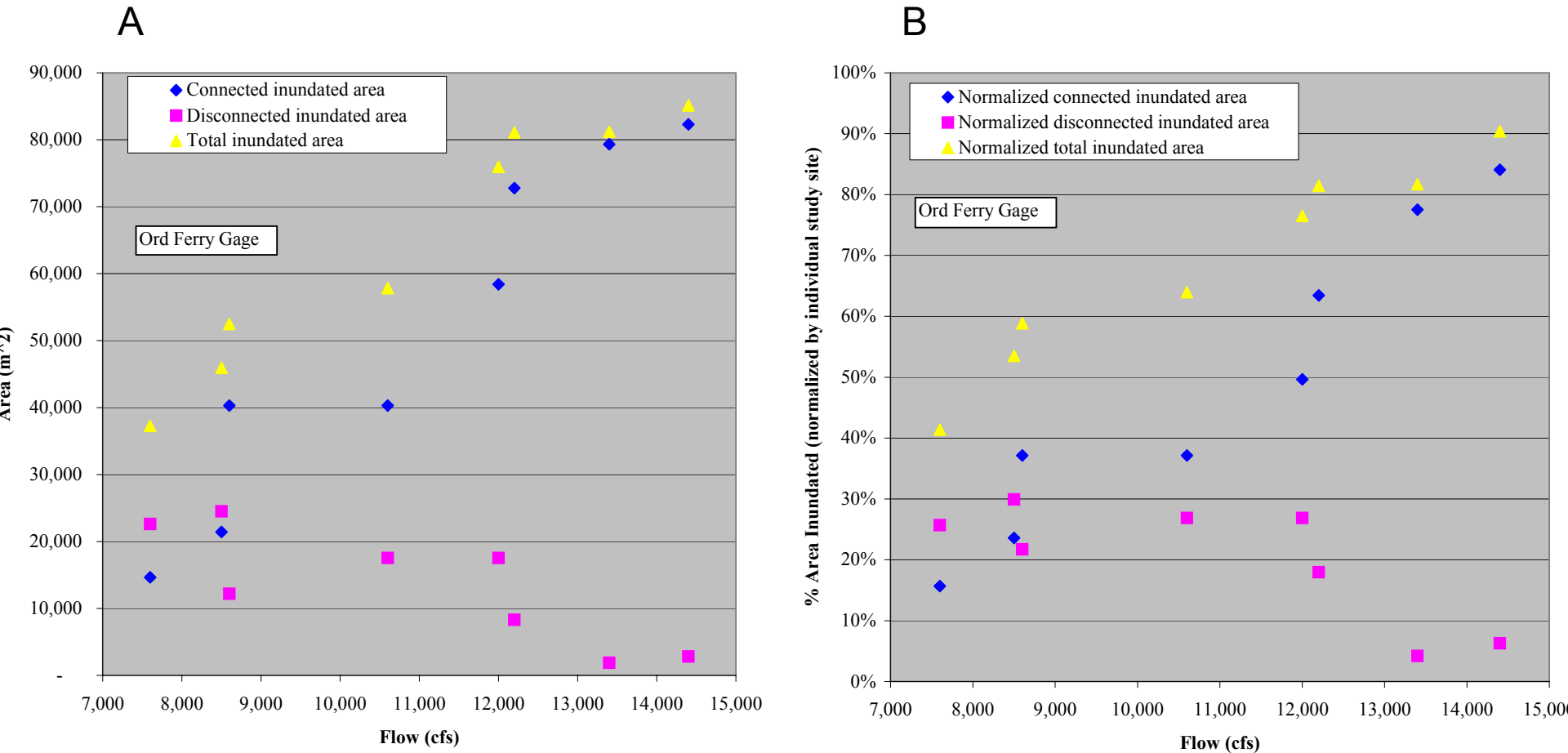


Figure 65. (A) Cumulative connected, disconnected, and total inundated area at 5 study sites related to the Ord Ferry gauge on the Sacramento River. **(B)** Normalized connected, disconnected, and total inundated area at study sites related to Ord Ferry gauge on the Sacramento River. Each site is normalized by its maximum potential inundated area that could be characterized by the thermograph deployment, such that each site has equal weight in determining the % inundated area.

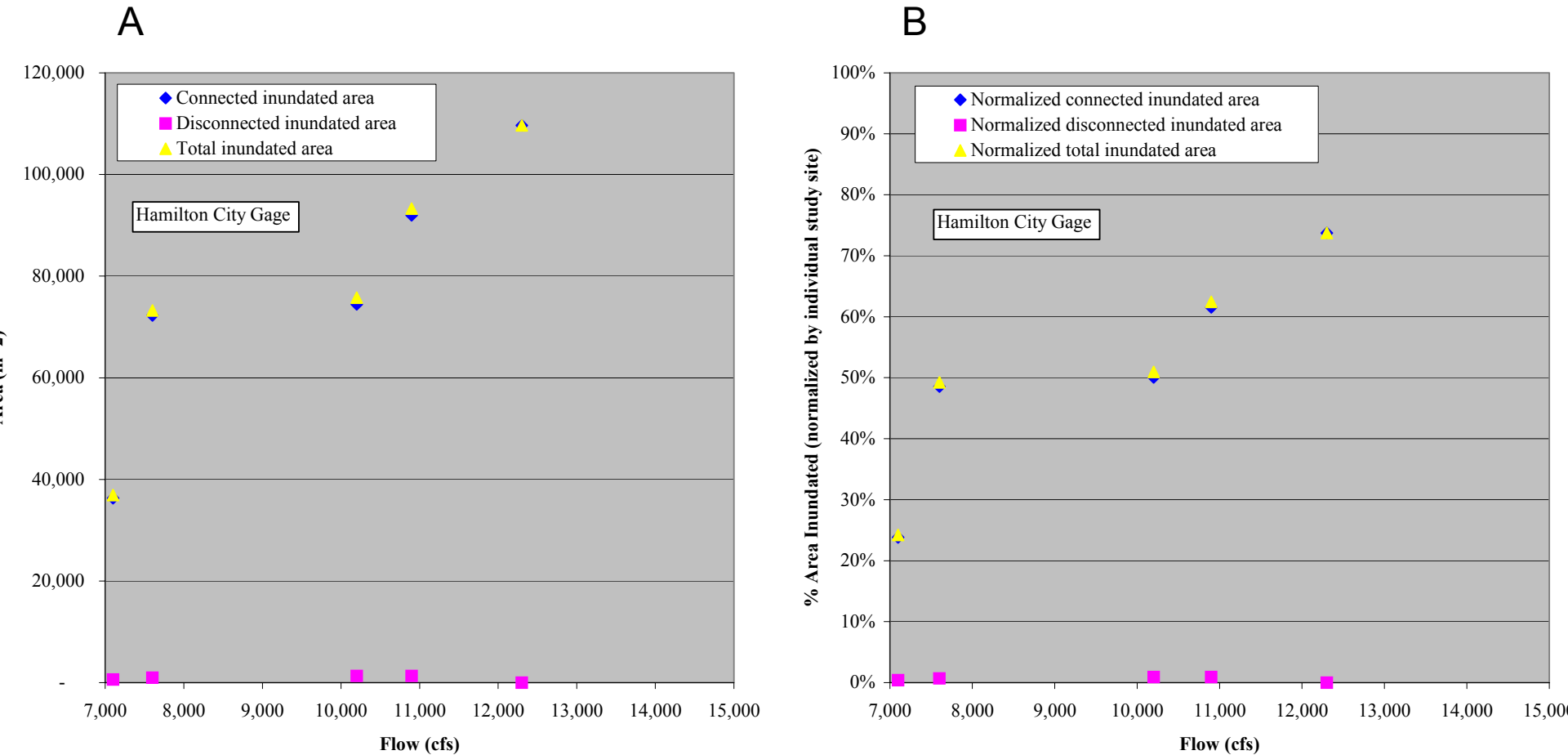


Figure 66. (A) Cumulative connected, disconnected, and total inundated area at 2 study sites related to the Hamilton City gauge on the Sacramento River. **(B)** Normalized connected, disconnected, and total inundated area at study sites related to Hamilton City gauge on the Sacramento River. Each site is normalized by its maximum potential inundated area that could be characterized by the thermograph deployment, such that each site has equal weight in determining the % inundated area.

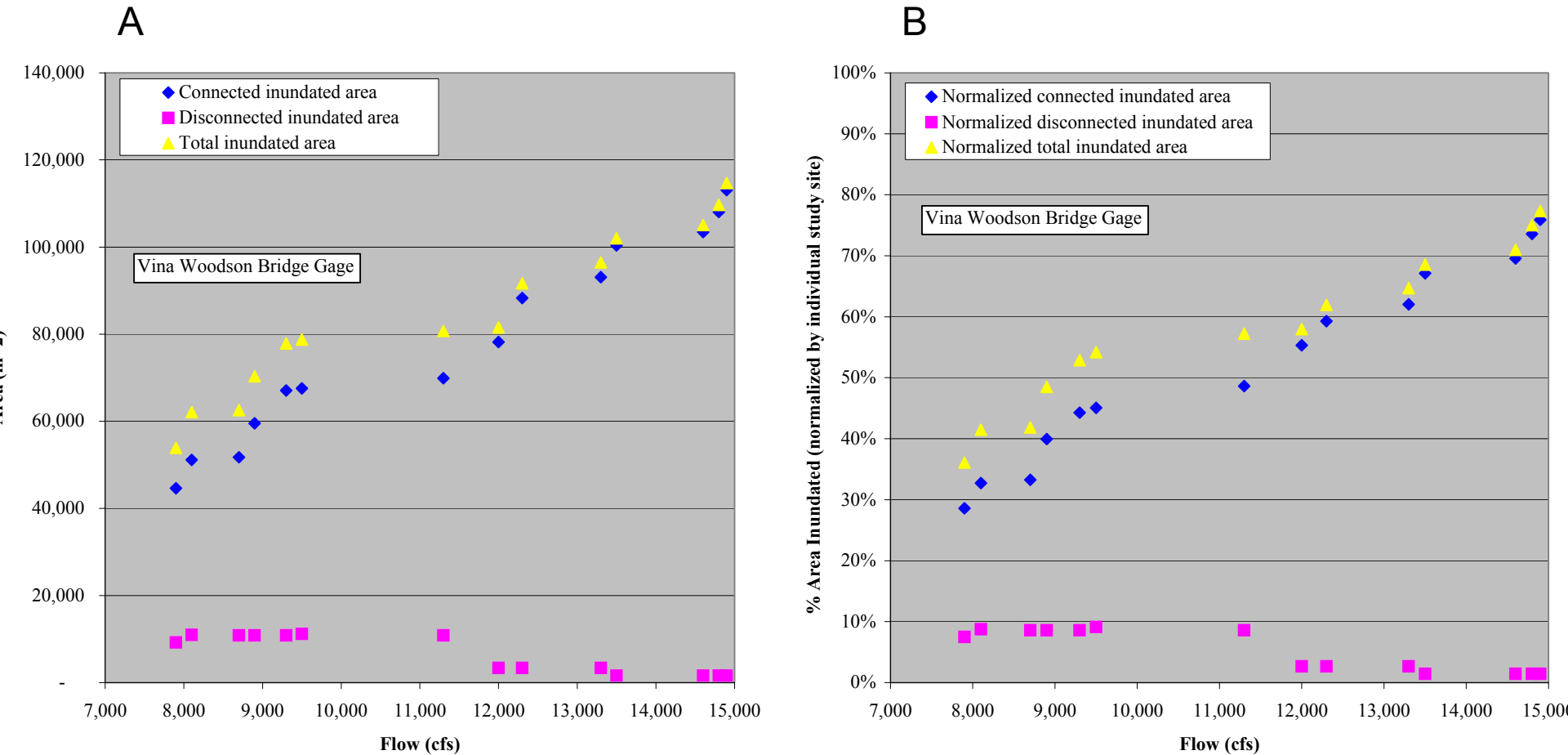


Figure 67. (A) Cumulative connected, disconnected, and total inundated area at 8 study sites related to the Vina Woodson Bridge gauge on the Sacramento River. **(B)** Normalized connected, disconnected, and total inundated area at study sites related to Vina Woodson Bridge gauge on the Sacramento River. Each site is normalized by its maximum potential inundated area that could be characterized by the thermograph deployment, such that each site has equal weight in determining the % inundated area.

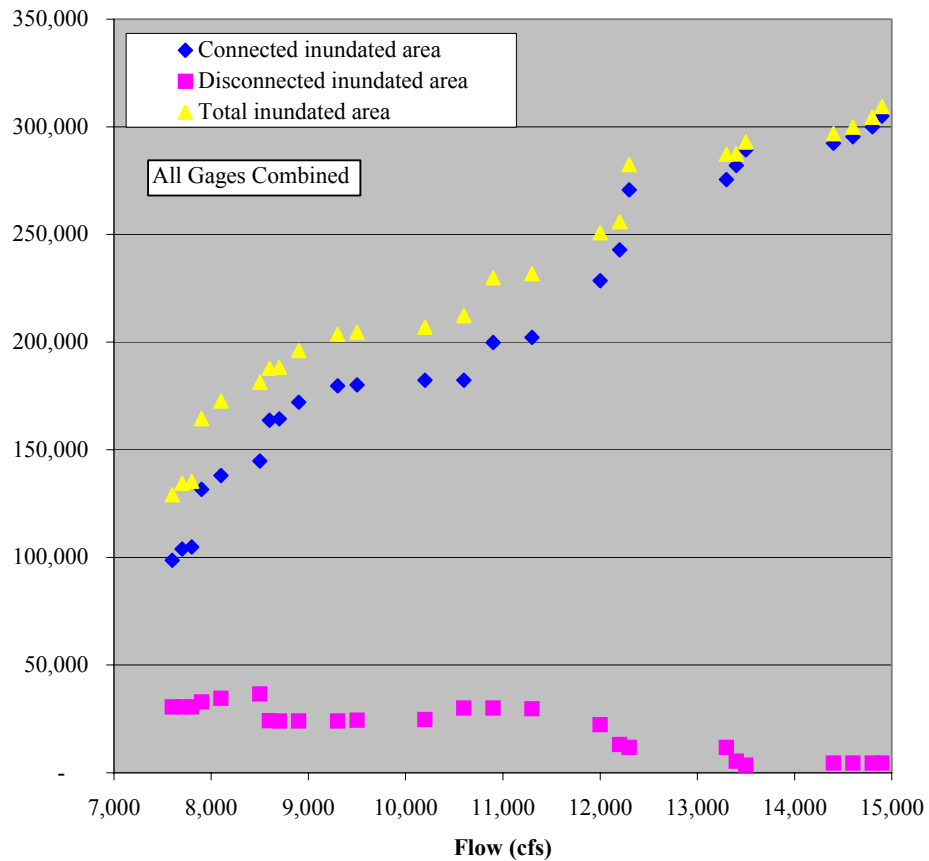
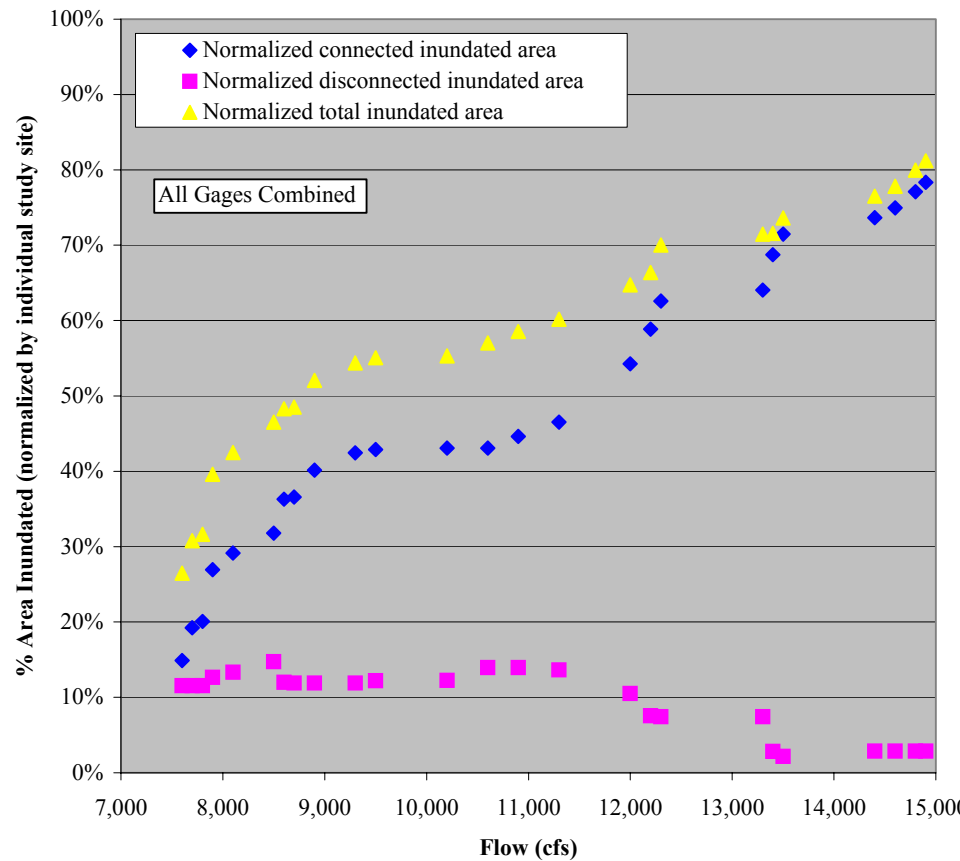
A**B**

Figure 68. (A) Cumulative connected, disconnected, and total inundated area at all study sites (15) at varying flows on the Sacramento River. (B) Normalized connected, disconnected, and total inundated area at all study sites at varying flows on the Sacramento River. Each site is normalized by its maximum potential inundated area that could be characterized by the thermograph deployment, such that each site has equal weight in determining the % inundated area.

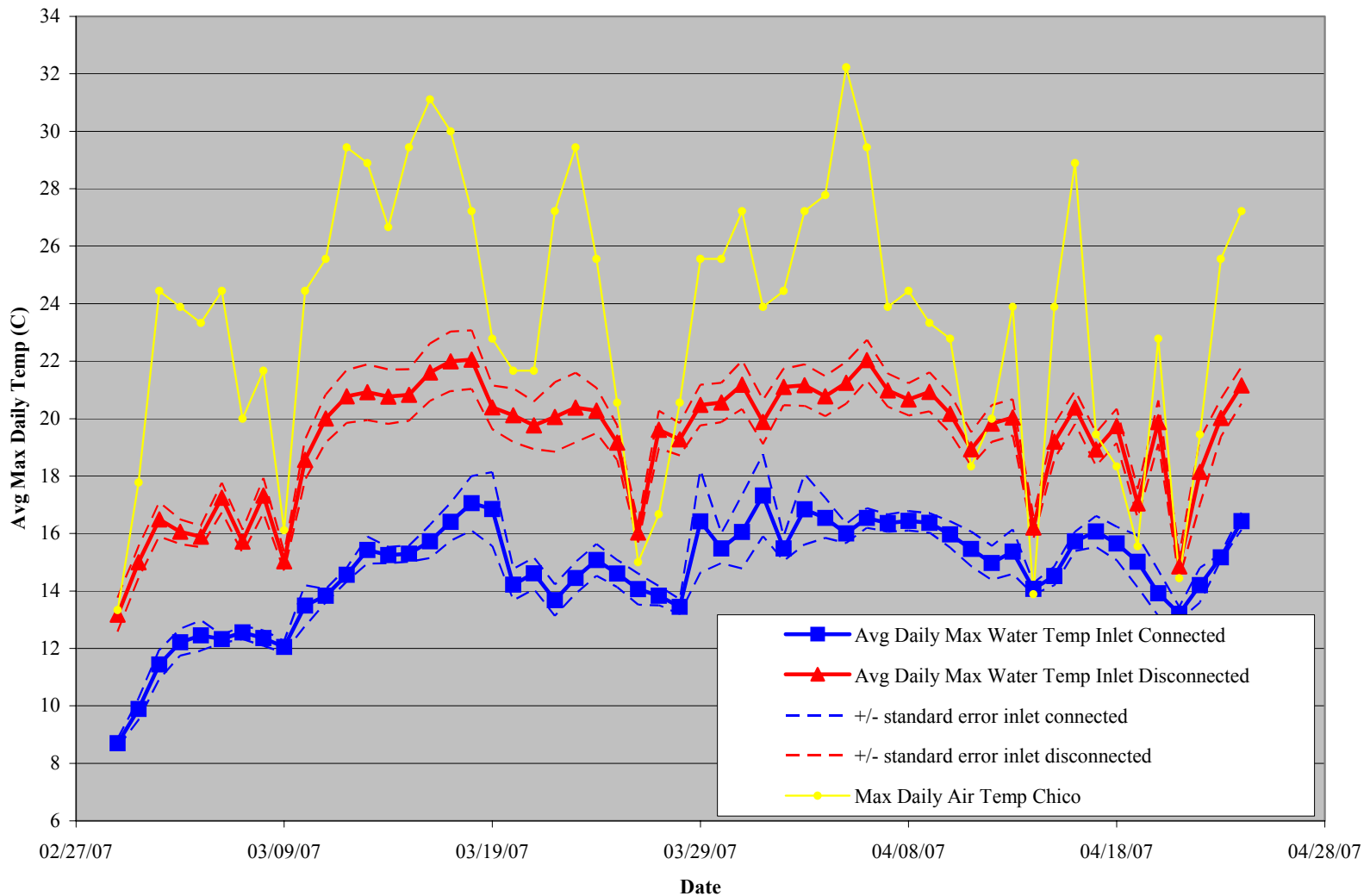


Figure 69. Average maximum daily water temperatures for submerged thermographs with inlets connected and disconnected to the mainstem. The maximum daily air temperature from Chico, CA (site maintained by CDF) is also displayed.

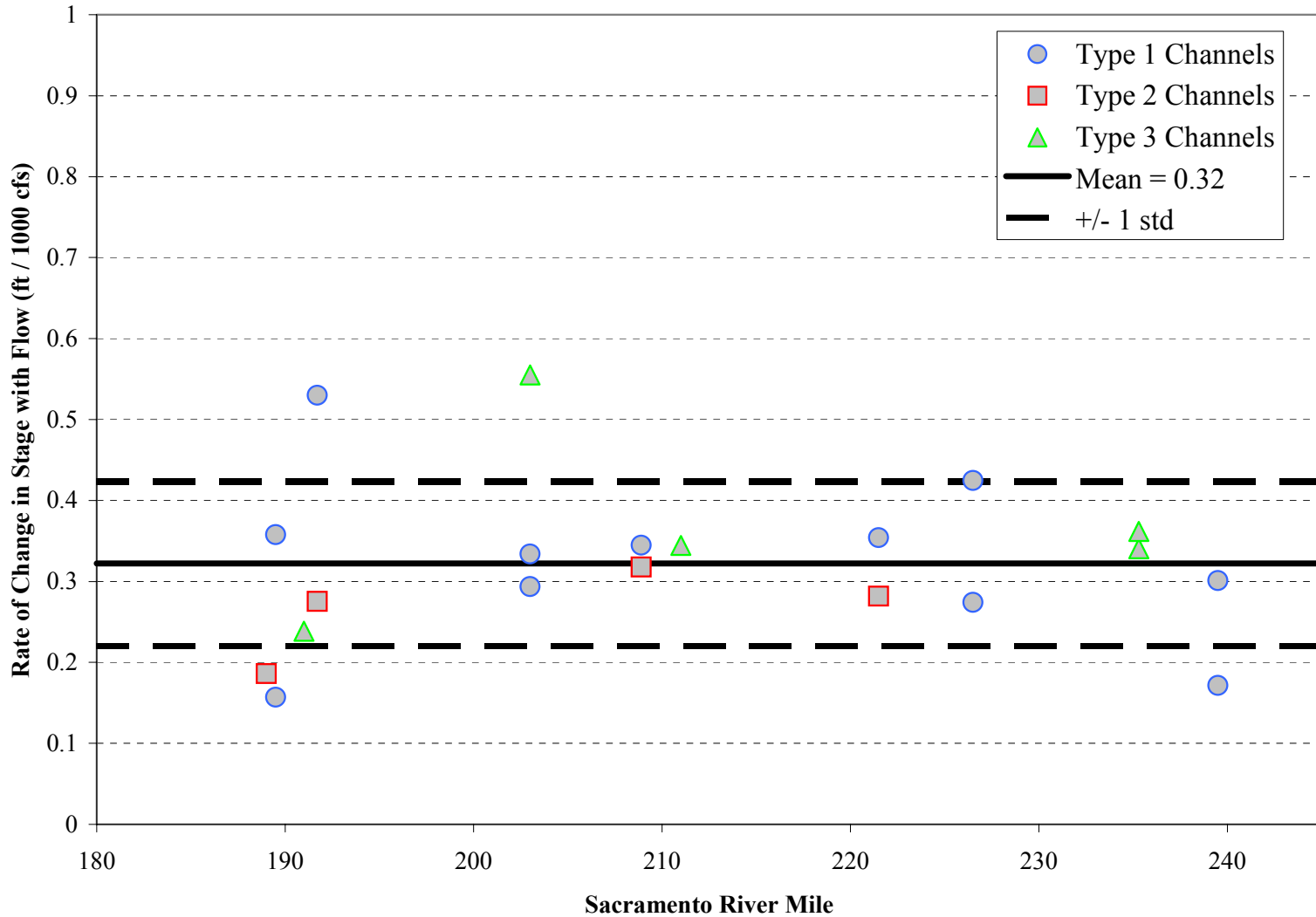


Figure 70. Rates of stage change (ft) within OCWB study sites per 1,000 cfs changes in mainstem Sacramento River discharge for type 1, 2, and 3 OCWB channels.

Photos



A

thermograph (13-1) installation



B

thermograph not recovered









Appendices

APPENDIX A Detailed Description of Sites and Results for Scour Channels on Point Bars

River Mile 187R

Study site 13 is located at RM 187L of the Sacramento River, at the downstream end of Shannon Slough (Figure 21). Site 13 is a former main channel flow scar, likely abandoned as the main channel bend at RM 187 continued to erode eastward. Under the classification scheme outlined in Section 2.2.2, site 13 is a type 2 channel, which we expect should generally exhibit good hydraulic connectivity at the outlet, and limited or no connectivity at the inlet. Thermographs were installed on 2/21/2007, when flow was 8,600 cfs (based on data from the Ord Ferry gauge). The inlet was disconnected from the river by a sediment plug, while the outlet was more or less at grade with and thus connected to the mainstem (Figure 21b). The thermographs were installed at two points (one wet and one dry) designed to investigate (i) whether flow would recede enough to disconnect the site's primary pool from the outlet and the mainstem, and (ii) whether flow levels would expand to submerge gravel bars that were sub-aerially exposed at the time of installation.

No fish were observed at site 13. High turbidities made observations difficult in water depths greater than two feet. The site is composed mostly of gravel (55%) and sand (35%), with 5 percent of the wetted area containing emergent vegetation which may provide useful cover for fish. During thermograph removal, 50–100 green sunfish were observed protecting redds near the outlet of the primary pool, upstream of the outlet.

None of the thermographs deployed at site 13 were recovered. However, the primary pool upstream of the outlet became disconnected by the time we arrived to remove the thermographs, (Figure 21a and Photo 2), indicating that flow at the threshold of connectivity occurred at some point between 8,600 and 7,600 cfs.

River Mile 189R

Study site 14 is located at RM 189R, on the west bank of the Sacramento River. Site 14 is an abandoned channel arm which has two large pools separated by a short shallow riffle that was dry during thermograph installation (Figure 22a). Using the classification scheme outlined in Section 2.2.2, site 14 is a type 2 unit, which we expect should generally exhibit good hydraulic connectivity at the outlet, and limited or no connectivity at the inlet. One thermograph was installed in a dry riffle below the study site's primary pool to investigate the pool's connectivity with the mainstem (Figure 22a). Installation occurred on 2/21/2007, when flow was of 8,600 cfs. The thermograph was dry upon retrieval on 4/26/2007, when the Sacramento River was at a flow of 7,600 cfs.

The substrate at site 14 is dominated by silt and sand, with little gravel present. The riparian area adjacent to the margin consists of a dense thicket of bamboo, which appears to rule out competition from other vegetation. No fish were observed during the site visit, but this may have been due, in part, to high turbidities that made it difficult to see deeper than two feet. The maximum water depth was one meter. Average water depth was 0.3 meter.

The thermograph data and direct observations of inundation from the site indicate that the upstream pool connected and disconnected with both the lower pool and the mainstem channel three times during the triple peak storm event in late February (Figure 22b). The upstream pool became connected at a flow of about 13,400 cfs and disconnected after flows levels dropped to

between 10,000 to 11,000 cfs (Figure 23). Hydrologic connectivity between the pools is associated with elevated water tables and increased groundwater flow as the inlet to the pools was connected to the mainstem. Disconnection likely has a time lag relative to changes in flow on the mainstem due to groundwater tables receding slower than the stage in the mainstem. This would explain why the range of estimated discharges during disconnection spans a wider range than the flows associated with inundation.

River Mile 191L

Study site 16 is located on the east bank at RM 191L of the Sacramento River, and is considered a type 3 unit under the classification scheme outlined in Section 2.2.2. Two thermographs were installed on 2/21/2007 at a flow of 8,500 cfs when the inlet was connected. The thermographs were installed in pattern to investigate when (i) the inlet is connected and (ii) the wetted width expands to a maximum channel width of the study site (Figure 26b). Both thermographs were recovered dry on 4/26/2007 at a flow of 7,600 cfs when the inlet was disconnected (Figure 26a).

No fish were observed in site 16. The visibility was poor in this site due to the water depth, turbidity, and time of day the site was sampled. This site is dominated by silt and sand, with willow comprising the majority of the vegetation adjacent to the watercourse. *Ludwigia* (water primrose) was observed at this site, although not in abundance.

The inlet to site 16 disconnected 4 times during the study period, all at approximately 8,000 cfs (Figure 26b, Photo 4). Thermograph 16-2 at the outer edge (break in slope between channel and perennial vegetation that was continuous around the entire circumference of the study site) became inundated twice during the study period at approximately 12,000 cfs (Figures 26c and 27). However, the precise time signal for each inundation was slightly ambiguous and 12,000 cfs was the overlapping discharge between the two inundation cycles and was selected as the critical discharge. Thermograph 16-2 went dry at a lower discharge (10,200 cfs) than when it became inundated.

River Mile 191.7R

Study site 17 is located on the west bank at RM 191.7R of the Sacramento River. Site 17 is located at the downstream end of an active point bar, but the channel geometry and planform location suggest that it is also an abandoned main channel position, and is classified as both a type 1 and 3 unit (Figure 28a). Thermographs were installed on 2/21/2007 at a flow of 8,500 cfs (Figure 28b), at which time the outlet was connected to the mainstem but the inlet was disconnected. Four thermographs were installed in an array to investigate lateral channel expansion and connection of upstream pools that were disconnected at the time of installation. Three thermographs were recovered on 4/26/2007 at a flow of 7,600 cfs (Figure 28a).

The channel substrate at site 17 is primarily composed of silt and sand. The turbidity was high which made fish observation difficult and no fish were observed. *Ludwigia* thoroughly covers the wetted and non-wetted surfaces of this site. It appears to be the dominant aquatic vegetation at this site in the summer season, out-competing other native plant species. An active beaver dam is located between the two pools and contributes to the disconnection of the upstream pool.

The connected pool at the outlet expanded to its maximum channel width at a flow of about 13,800 cfs (Figure 29), and was presumably receiving the additional flow from increased backwater from the mainstem as the thermograph (17-1) placed at the connection point with the

upstream pool never became inundated during the study period. Thus the upstream pool remains disconnected from the mainstem up to a flow of at least 15,600 cfs. However, thermograph 17-2, which was 0.23 m below 17-1, became inundated at 14,400 (Figure 28c). Thermograph 17-2 becoming inundated illustrated when the upstream pool expanded to its maximum width, likely via groundwater associated with the increased water table in the mainstem. During thermograph removal the upstream pool was found completely dry.

River Mile 203L

Study site 23 is located on the east bank at RM 203L of the Sacramento River. Site 23 is a type 3 channel where we would expect a higher degree of inlet and outlet connectivity (Figure 32a). Two thermographs were installed on 2/20/2007 at a flow of 7,600 cfs (Hamilton City gauge) at which time both the outlet and the inlet were connected to the mainstem (Figure 32b). Thermographs were installed in an array to investigate the inlet connection with the mainstem and at which flows the depth and width within the pool increase. Two thermographs were recovered on 4/26/2007 at a flow of 7,100 cfs, and both of the thermograph sites were dry (Figure 32a).

Site 23 consisted of wide, shallow, gravel-dominated pools connected by shallow riffles. Large tree stumps reside in the wetted area and provided excellent cover near the inlet. The average depth was 0.2 m with a maximum depth of 0.4 m. No fish were observed. Infrequent grasses were located on the dry sand and gravel bars.

The inlet to site 23 disconnected 4 times during the study period, consistently between flows of 7,100 and 7,200 cfs (Figure 32a). The thermograph at the outer edge of the channel of the study site became inundated twice during the study period at about 10,900 cfs (Figures 32c and 33), which represented a 50% increase in available habitat relative to the amount available when the inlet disconnects.

River Mile 211L

Study site 27 is located on the east bank at RM 211L of the Sacramento River. Site 27 functions similarly to a type 3 channel as described in Section 2.2.2; although, it may not be an abandoned former mainstem channel but rather a former probe channel that cut across the downstream end of a point bar and has established a more perennial connection than a typical type 1 channel and formed an island by dissection the point bar (Figure 37a). Site 27 likely stays perennially connected to the mainstem at the outlet and an additional slough is also likely perennially connected to the study site at the downstream end. Two thermographs were installed on 2/20/2007 at a flow of 7,900 cfs (Figure 37a) at which time both the inlet and outlet were connected to the mainstem. Thermographs were installed in an array to investigate (i) connectivity of the inlet and (ii) lateral expansion of available habitat. Both thermographs were recovered on 4/26/2007 at a flow of 8,800 cfs.

At the time of installation, study site 27 maintained an average width of 30 m and had a maximum depth of 1.2 m. The cloudy sky conditions and high turbidity made fish observations difficult, and no fish were observed. The substrate consisted of a mix of sand (55%) and gravel (35%) throughout the site with some cobble intermixed. Large woody debris settled near the inlet to site 27 and provides habitat for fish when flows come up. Submerged *Ludwigia* was observed in sparse accumulations near the inlet as well.

The inlet remained connected to the mainstem for the duration of the study period. The channel width expanded to the maximum channel width (break in slope between exposed substrate and established perennial vegetation) at about 12,400 cfs, and rapidly dewatered during the receding flow limbs (Figures 37b and 38).

River Mile 221.6R

Study site 33 is located on the west bank at RM 221.6R of the Sacramento River. Site 33 is a combination of both a probe channel eroding behind an active point bar (type 1 unit) and a former main channel flow scar (type 2 channel that currently functions as a slough) that converge at the downstream end of site 33 (Figure 39a). Kopta Slough North (RM 221.7, Table 1) is located slightly west of the outlet of site 33, and the slough that enters site 33 is referred to as Kopta Slough Backwater in Table 1. Five thermographs were installed on 2/19/2007 at a flow of 8,100 cfs at which time a wide, shallow backwater pool existed at the outlet that was not connected to Kopta Slough Backwater (Figure 39b). Thermograph placement was designed to investigate (i) the discharge Kopta Slough Backwater connected to site 33 and the mainstem, and (ii) the lateral and longitudinal connectivity of the portion of site 33 that extends up the probe channel across the point bar. Five thermographs were recovered on 4/25/2007 at a flow of 8,900 cfs.

No fish were observed in site 33. The channel substrate consists of sand (100%) throughout, with large portions of the sand bars covered in grasses. In areas that appear to be wetted throughout the summer, *Ludwigia* covers the channel. The current wetted portion of site 33 had 25% coverage of floating vegetation, 20% submerged (most likely *Ludwigia*), and 10% emergent, with a total of 55 percent of its area covered in vegetated. Little to none vegetative canopy cover existed at the pool. An active beaver dam contributed to the disconnection of Kopta Slough Backwater.

Kopta Slough Backwater connected and disconnected from site 33 three times during the study period, connecting around 12,000 cfs and disconnecting at about 11,300 cfs (Figures 39c and 41). Stage within the portion of site 33 classified as a type 1 channel increased at a rate of approximately 0.1 m (0.34 ft) per 1,000 cfs increase in discharge, but never expanded to its full channel width (Figure 40). Stage increases were likely a product of backwater from the mainstem as the site never received surface flow from the inlet. The deepest portion of the scour channel (thermograph 33-3) did go dry around 7,300 cfs, after which likely only a small pool at the outlet remained (Figure 39a). Thermograph 33-3 also exhibited high water temps (25°C) while submerged at low flows.

River Mile 226.5L

Study site 35 is located on the east bank at RM 226.5L of the Sacramento River. Site 35 is a type 1 channel with additional high flow channels that cut laterally across the bar and enter site 35 (Figure 42). Five thermographs were installed on 2/16/2007 at a flow of 8,900 cfs (Figure 42b) at which time the inlet was disconnected and the outlet connected to the mainstem. Thermographs were installed in an array to investigate (i) the connectivity of the inlet and outlet, (ii) the extent of lateral and longitudinal inundation, and (iii) when an additional lateral high flow channel connects to the site. Four thermographs were recovered on 4/25/2007 at a flow of 8,900 cfs. During both installation and removal the lateral high flow channel was receiving input through groundwater as it was flowing into to site 35 but not connected at its inlet to the main channel (Figure 42b).

The maximum depth at the site is 1.8 m and the average depth is 0.7 m. Some vegetation and LWD existed in the arms providing fish habitat, although none were observed. Water depth and turbidity limited fish observations in the deeper pools. The substrate composition at the site is sand (85%) with small patches of gravel (15%). *Ludwigia* and other aquatic vegetation were present in 15 % of the unit and sparsely distributed.

Thermograph 35-5 was placed to investigate when the inlet to the main probe channel became connected with the mainstem, and this thermograph was not recovered. However, based on field evidence indicating a lack of surface and thermographs placed at other study sites at similar elevations above the water surface that did not become inundated, the inlet to the main probe channel likely did not connect during the study period. At 14,900 cfs, the primary pool in the main probe channel had increased its depth by 0.5 m (1.7 ft) to a maximum depth of 1.3 m (4.1 ft) (Figures 42c and 43). Because the inlet to site 35 did not connect to the mainstem, stage increases within the main pool are likely due to increased flow inputs from the lateral high flow channel and backwater from the mainstem. During the monitoring period, the pools in the main probe channel did not go dry (thermographs 35-1 and 35-3). The lateral high flow channel that was wet and connected to site 35 at 8,900 cfs did go dry at about 7,100 cfs (Figure 42a).

River Mile 232.8L

Study site 39 is located on the east bank at RM 232.8L of the Sacramento River. Site 39 is a type 1 channel that erodes behind a point bar that significantly increased in size between the 2005 and 2006 aerial photography images. Two thermographs were installed on 2/16/2007 at a flow of 8,900 cfs, and the inlet was disconnected and the outlet connected to the mainstem (Figure 45b). Thermographs were deployed in a manner to investigate (i) lateral channel expansion and (ii) when pools in the study site dried. Two thermographs were recovered on 4/25/2007 at a flow of 9,000 cfs.

In a shallow portion of the wetted area, 50 Sacramento pike minnow were observed using overhanging vegetation as cover. Small woody debris and large woody debris were sparsely located in the unit. The outlet of the unit exceeded two meters of depth which presented problems for fish observations in the outlet pool. Turbidities were also relatively high and no additional fish species were observed. Sand is the dominant substrate (100%) and 10% of the wetted area is covered with aquatic vegetation, one of three species present being *Ludwigia*.

Shallower pools along the longitudinal axis of site 39 went dry at about 7,100 cfs and became inundated at 7,800 cfs (Figures 45a and 46). During low flow periods, water temperatures in the pools were very high when thermographs were submerged, reaching a maximum of 30°C. During the study period, flows were insufficient to induce water level rises outside the thalweg area of the probe channel and submerge thermograph 39-2. During thermograph removal, three small pools near LWD that were disconnected from the study site appeared to be going dry and had high potential for fish stranding (no fish were observed in the pools). These pools were not present during thermograph deployment, which was at a flow about 100 cfs less than when the pools were observed during retrieval.

River Mile 233.3L

Study site 40 is located on the west bank at RM 233.3L of the Sacramento River. Site 40 is type 1 channel where we would expect low degrees of connectivity at the inlet and outlet. Thermographs were installed on 2/16/2007 at a flow of 8,900 cfs. At 8,900 cfs the inlet and

outlet were disconnected, the outlet was connected to the mainstem, and a long shallow disconnected pool provided the majority of fish habitat (Figure 47a). Four thermographs were installed in an array to investigate when the inlet, isolated pool, and outlet were connected to the mainstem and the overall longitudinal connectivity within the site. Four thermographs were recovered on 4/25/2007 at a flow of 8,900 cfs.

No fish were observed in the long, shallow pool in Study site 40. The maximum depth in the pool was 1 m, with an average depth of 0.3 m. The substrate consisted of 100% sand, with *ludwigia* and willow growing throughout.

The isolated pool connected and disconnected twice from the mainstem during the study period at approximately 13,500 cfs (Figures 47b and 48). The inlet did not connect to the mainstem during the study period nor did the primary pool go completely dry. Water temperatures within the pool were high (maximum of 26°C) when the study site was disconnected from the mainstem. During the study period, flows were insufficient to induce water level rises outside the shallower portion of the primary pool and submerge thermograph 40-3.

River Mile 235.3R

Study site 41 is located on the west bank at RM 235.3R of the Sacramento River. Site 41 is located in an ephemeral channel flowing around an island and may have been a former main channel location (Figure 49). Site 41 is considered a type 3 channel according to the classification scheme outlined in Section 2.2.2, where we would expect higher degrees of inlet and outlet connectivity. Four thermographs were installed on 2/15/2007 at a flow of 9,300 cfs at which time both the inlet and outlet were connected to the mainstem (Figure 49b). Thermographs were installed in a pattern to investigate when the inlet disconnected and three were placed in cross-section array to investigate lateral and longitudinal connectivity. All four thermographs were recovered on 4/25/2007 at a flow of 8,900 cfs.

No fish were observed in Study site 41. A majority of the site consisted of broad, shallow braided channels and willow-vegetated sand bars. Most wetted areas were shallow with the average depth being 0.5 m and a maximum depth of 1.3 m. Small and large woody debris was interspersed throughout the site primarily located in the upstream portion of the site. The bed material was composed of sand (85%) and gravel (15%). Sparse amounts of aquatic vegetation were present including *Ludwigia*.

The inlet disconnected from the mainstem at about 8,100 cfs and the thermograph (41-1) placed in the thalweg of the scour channel went dry about 10 hours prior to this at about 8,150 cfs (Figures 49a and 50). Thermographs in the cross-section array were placed in the thalweg, atop mid-elevation bench, and on a higher elevation bench that would reflect the maximum channel width (Figure 50). During the study period the mid-elevation bench became inundated 4 times, typically around 13,300 cfs (Figures 49c, 50, and 51) and the upper elevation bench that characterized the maximum channel width never became inundated. The stage discharge relationship at the cross-section indicated that the rate of stage change relative to mainstem discharge was 0.1 m (0.34 ft) per 1,000 cfs change in discharge (Figure 50), which is consistent with the rate of stage change observed at cross-sections in study sites 25 and 33.

APPENDIX B List of Researchers and Institutional Affiliations

Principal Investigators:	Affiliation
G. Matt Kondolf kondolf@berkeley.edu	Dept of Landscape Architecture and Environmental Planning, University of California, Berkeley 94720
Hervé Piégay herve.piegay@ens-lsh.fr	Centre National de la Recherche Scientifique UMR 5600 Environnement - Ville - Société Site ENS-Lsh, 15 Parvis René Descartes BP 7000, 69342 Lyon cedex 07, France
Bruce Orr bruce@stillwatersci.com	Stillwater Sciences 2855 Telegraph Ave Berkeley, CA 94705
Researchers:	Affiliation
Ingrid Morken Dave Shaw Kate Huxster (undergrad assistant)	Dept of Landscape Architecture and Environmental Planning, University of California, Berkeley 94720
Jose Constantine	Dept of Earth Science, University of California, Santa Barbara
Mike Singer	U.S. Geological Survey, Menlo Park, CA
Julien Levrat	University of Lyon 3, CNRS UMR 5600, Lyon, France
Gudrun Bornette, Sara Puijalón	University of Lyon 1, CNRS UMR5023, France
Simon Dufour	Université of Aix-en-Provence and CNRS UMR 5600 of Lyon, France
Adrien Alber, Vincent Gaertner, Kristelle Michel, Marie-Laure Tremelo, Monika Michalkova	CNRS UMR 5600, Lyon, France
John Wooster, Yantao Cui, Michael Fainter	Stillwater Sciences, 2855 Telegraph Ave, Berkeley, CA 94705

APPENDIX C Lessons from Chute-Cutoff Modeling Exercises

Introduction

As part of the Sacramento River Ecological Flow Study, Stillwater Sciences attempted to develop a numerical, mechanistically-based, chute-cutoff numerical model for prediction of the discharge required to form a chute cutoff channel. Unfortunately we have been unsuccessful in producing a workable model due to the complexity of the physical process and the associated numerical difficulties. This appendix briefly reexamines the hypothesis we outlined in our scope of work and discusses the main technical difficulties that we encountered during model development. Our aim is to provide useful information for future research.

Reexamination of hypotheses and recommendations for future research

The proposed hypotheses in the scope of work are as follows:

- Hypothesis 1. The shorter (and thus steeper) passage for flow along the potential cutoff route creates a significantly higher friction slope, relative to conditions in the main channel, and is a key regulator of cutoff.
- Hypothesis 2. Chute-cutoff can be simulated with a one-dimensional approximation of flow in which water bifurcates through the main channel and the potential cutoff route as soon as it inundates the potential cutoff route.
- Hypothesis 3. Cutoff initiates when the shear stresses over the potential cutoff route exceed the "critical" shear stress for erosion of the riparian layer.
- Hypothesis 4. Once a cutoff is initiated, such that flow cuts through the more erosion-resistant riparian layer, sediment transport in the incipient cutoff will be similar to fluvial sediment transport in rivers (such that it can be simulated by conventional sediment transport modeling).
- Hypothesis 5. The initiation of a cutoff channel will allow for more concentrated flow and thus increased shear stresses and accelerated cutoff progress.

Below we consider each hypothesis, to provide some insights about what didn't work in this case and what might work in future efforts.

Hypothesis 1

We were unable to fully test this hypothesis because we were unable to produce a workable numerical model. We believe this hypothesis is likely true as agreed upon by several experts working in the area of sediment transport and river mechanics during a mini technical workshop held in Berkeley in July 2005.

The simulated shear stress distribution in the Sacramento River near RM 172 corroborates the hypothesis. Figure 1 shows the River-2D simulated shear velocity, defined as

$$u_* = \sqrt{\tau / \rho}$$

(in which u^* denotes shear velocity, τ denotes shear stress, and ρ denotes density of water), indicating substantially higher shear velocities near the dashed line (marking the potential cutoff route), as compared to the surrounding area for a flow of 3,400 m³/s (120,000 cfs). River-2D simulations of higher discharge events revealed similar patterns.

Hypothesis 2

We were unable to test this hypothesis because we could not produce a workable numerical model. Even so, we suspect that this hypothesis may be valid; our difficulties in producing the model stemmed mostly from other technical issues, as discussed later in this memorandum. Unless technical difficulties of the model are solved in a separate research effort, however, we do not recommend any further effort to examine this hypothesis, because it will most likely be fruitless.

Hypothesis 3

Strictly speaking, this should not be treated as a hypothesis because it has been widely accepted that shear stress drives soil erosion. What is challenging and needs further research to improve chute-cutoff modeling, is quantifying the relationship between shear stress and the rate of erosion of stratified and heterogeneous sediment deposits that may be reinforced with dense root systems from trees, shrubs and grasses. Without further understanding of this relationship, any numerical modeling would at best be useful only as a gaming tool. On the other hand, a model with a good characterization of the relationship between shear stress and erosion rate will be far more useful. We did not attempt to quantify the relationship between shear stress and erosion rate in this research, as we were interested in a gaming tool as a first step.

Hypothesis 4

Similar to the other hypotheses, we did not have a chance to test this because the model was not successfully developed. The hypothesis is most likely valid, based on general observations in the field from cut-banks where surface sediment is usually seen to be more erosion resistant due to the presence of vegetative root system.

Hypothesis 5

This hypothesis was not tested because the model was not successfully developed.

Major difficulties in developing the numerical model

We encountered technical difficulties both in the simulation of water flow and the simulation of sediment transport. The difficulty in simulating water flow was caused by the fact that multiple solutions for water depth exist for a given total energy head in a compound channel (e.g., Chaudhry 1993) during the calculation for energy conservation. This makes it difficult to write a robust algorithm even for a relatively simple subcritical flow condition. The difficulties are compounded in the real world, where we are often faced with subcritical, supercritical, and transient flow conditions.

Moreover, it turns out that researchers have not yet developed a robust algorithm for transient flow conditions in complex compound channels. To the best of our knowledge, there is not even a robust algorithm for the simplest, subcritical conditions in compound channels. We actually thought we had produced a robust algorithm at one point because our initial testing with a specific topography produced reasonable results. However, when we modified the topography to reflect conditions at Sacramento River RM 172, however, the model produced very unrealistic results, revealing that our algorithm was not robust. Worst of all, this was not discovered until the later stages of the project, and repeated efforts to subsequently to fix the problem failed.

The first technical difficulty we faced in the sediment transport simulation was that we were unable to produce a quasi-equilibrium profile (i.e., one with minimal cumulative aggradation and degradation in the channel) near a bend by routing sediment through the reach. This is most likely an indication that the one-dimensional approximation was not adequate. The second

technical difficulty we faced in sediment transport simulation was that researchers had not yet developed a defensible theory for partitioning sediment transport at the point of bifurcation.

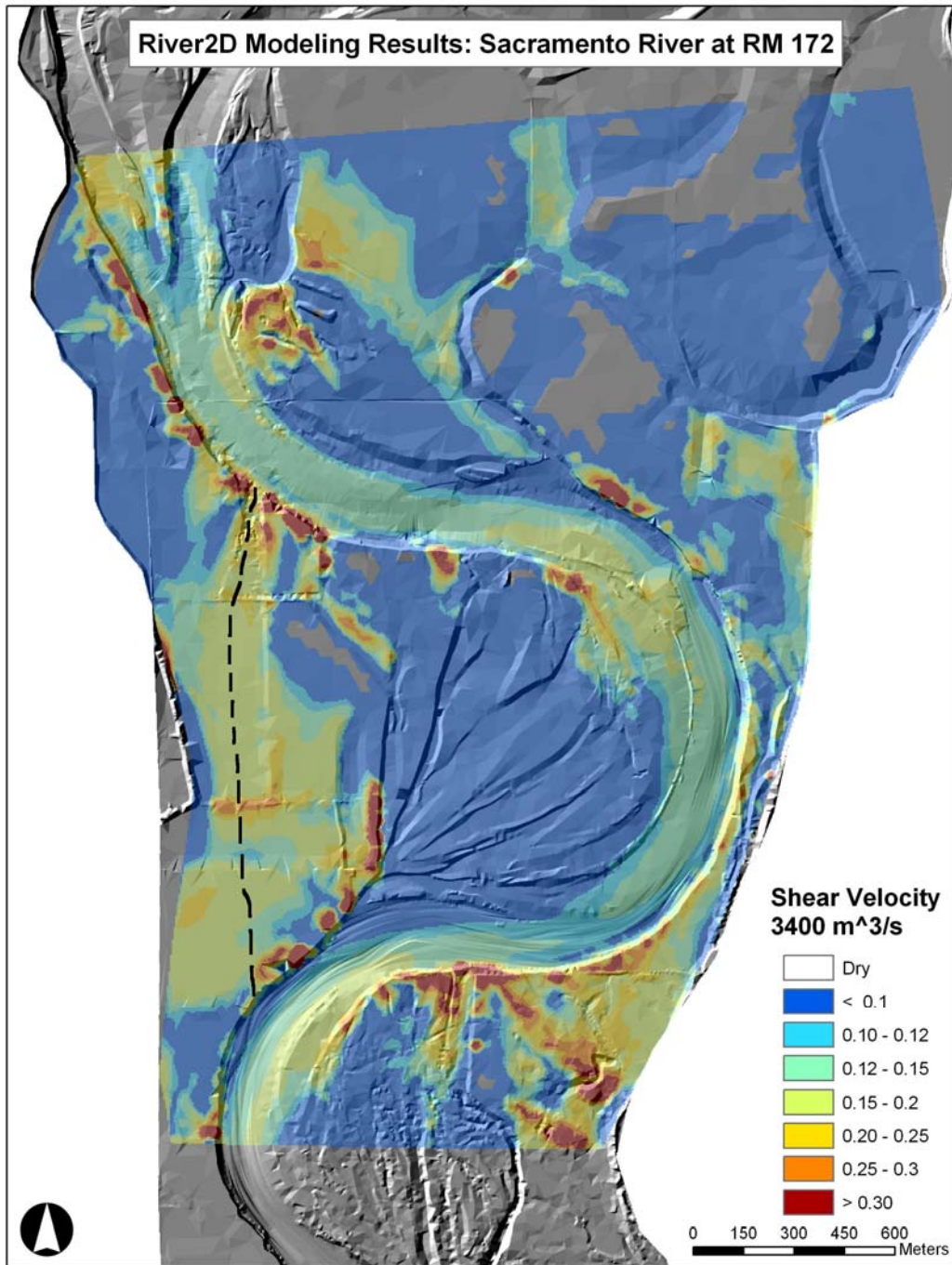
During study plan development, we assumed that we could overcome the technical difficulties in sediment transport modeling by making the following assumptions:

- the formation of the chute-cutoff channel is a purely erosional process, allowing us to ignore the other sediment transport process in the river and focusing only on sediment erosion within the cutoff channel; and
- the modeling can ignore the silting process in resultant oxbow lake once the cutoff channel is formed.

We were unable to test these assumptions after we discovered the problems with the flow algorithm (see discussion above) and were unable to fix it.

Reference

Chaudhry, M. H. 1993. *Open-Channel Flow*. Prentice-Hall, Inc., Englewood Cliffs, New Jersey 07632, ISBN 0-13-637141-8.



Appendix C, Figure 1. Simulated shear velocity at discharge = 3,400 m³/s (120,000 cfs), showing high shear stress along potential cutoff route (dashed line) compared to surrounding area.

APPENDIX D Off-Channel Habitats Study Plan



Sacramento River Ecological Flow Study

Off-Channel Habitat Study Plan

Prepared for
The Nature Conservancy
500 Main Street
Chico, CA 95928

Prepared by

Dr. G. Mathias Kondolf
2241 Ward Street
Berkeley, CA 94705

and

Stillwater Sciences
2855 Telegraph Avenue, Suite 400
Berkeley, CA 94705

Funded by
CALFED Ecosystem Restoration Program
and the Resources Legacy Fund Foundation

Sacramento Ecological Flow Study Off-Channel Habitat Study Plan

1. Introduction

Large rivers like the Sacramento River create a variety of secondary channels (e.g., oxbow lakes, side channels) that are formed by channel migration, cutoff, and avulsion. These secondary channels evolve over time, often as a function of sediment deposition and scour, vegetation colonization and succession, and the buildup of organic detritus from aquatic vegetation. Secondary channels in the Sacramento River corridor provide important habitat for a variety of native species, such as Western Pond Turtle (*Clemmys marmorata*), Sacramento sucker (*Catostomus occidentalis*), Sacramento pikeminnow (*Ptychocheilus grandis*), California roach (*Hesperoleucus symmetricus*) and Chinook salmon (*Oncorhynchus tshawytscha*).

Large rivers also create shallow-water, seasonally inundated habitats that form as a function of overbank flows (e.g., floodplains) and point bar dynamics (e.g., scour channels on point bars and edge habitat). Shallow-water areas provide important rearing habitat for juvenile salmon (Lister and Genoe 1970, Bjornn and Reiser 1991), including the runs of Chinook salmon that occur in the Sacramento River basin (Sommer et al. 2001).

As with most aquatic riverine habitats, the formation and maintenance of secondary channels is a function of flow and sediment dynamics, both of which have been altered dramatically in the Sacramento River by the construction and operation of water storage and delivery systems. Flow regulation often reduces the frequency and magnitude of high flow events that drive the fundamental processes of bank erosion and meander migration, which are essential for creating off-channel water bodies (OCWBs). Bank armoring activities are designed specifically to halt bank erosion and meander migration, thus preventing the creation of new OCWBs.

Similarly, human activities like bank armoring and flow regulation influence the seasonal inundation of shallow-water habitat in the Sacramento River basin. For example, flow regulation can reduce the magnitude and frequency of high flow events, thereby reducing the frequency, extent, and duration of floodplain inundation. Bank armoring often induces the scour of deeper pools on the outside of meanderbends where rip-rap is typically placed, which in turn causes channel cross sections to become steeper as the channel adjusts (Figure 1). These steeper cross-sections generally reduce the area of shallow water habitat associated with point bars opposite of the armored bank. By preventing bank erosion, armored banks can also deprive a reach of an important sediment supply, so that point bars located immediately downstream of armored banks become smaller than point bars that form downstream of eroding banks (CDWR 1994). The smaller size of point bars reduces the area of shallow-water edge habitat, and it often reduces the area of the eddy zone that forms downstream of point bars. These effects on point bars can reduce important rearing habitat for Chinook salmon fry, and they can reduce the area that supports the colonization of riparian vegetation.

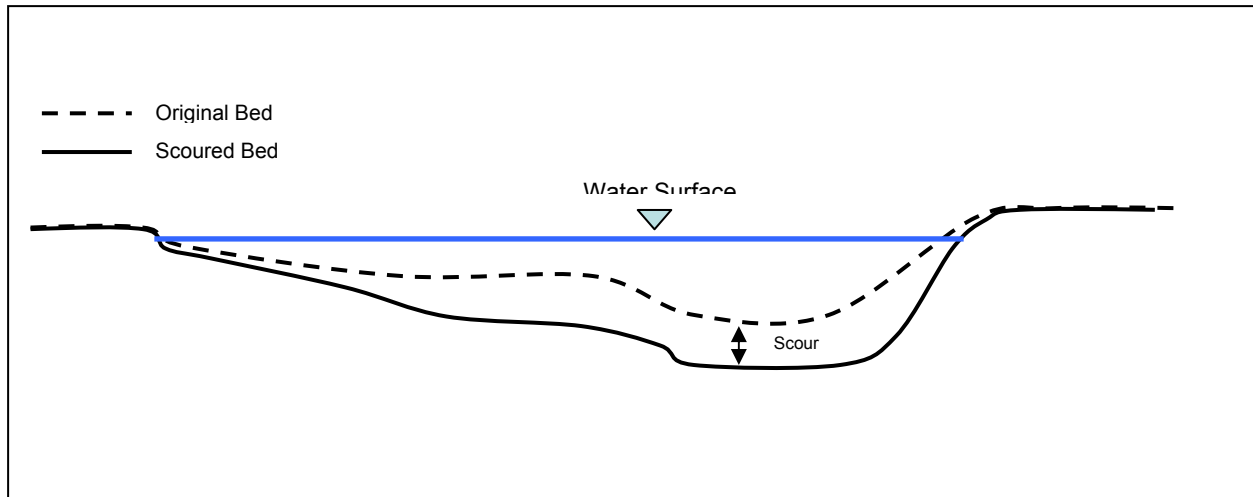


Figure 1. CDWR found thalweg depths in armored bends of the middle Sacramento River to be 6 ft deeper, on average, than those at eroding bank sites. Both CDFG(1983) and CDWR (1994) hypothesized that armored banks induce deeper scour of the bed and cause the cross-sectional slope of the channel to become more steep, thereby reducing the area of channel with suitable hydraulics to support salmonid spawning and rearing.

To develop effective strategies for the conservation and restoration of secondary channel and seasonally inundated habitats, it is important to understand the physical and ecological processes that create these habitats and drive their evolution over time. It is also important to better understand their ecological value in the Sacramento River ecosystem.

Key uncertainties remain in our understanding of the processes that drive the creation and evolution of secondary channel and seasonally inundated habitats in the Sacramento River, and the ecological response to human-induced changes to the physical processes and to water quality in secondary channels. Specifically, we need to understand:

- the mechanisms and flow triggers for meander bend development, cutoff and side channel sedimentation,
- the effects of land and water management on these processes,
- how the hydrologic connectivity of side channels changes with changing mainstem discharge,
- how water quality in side channels is affected by connectivity with the mainstem, by groundwater seepage, and by runoff from surrounding land uses, and
- flow magnitudes required to create shallow-water habitat within the bank full channel.

2. Study Objectives

The goal of this study is to identify potential management measures (e.g., changes in flow releases, changes in bank armoring, excavation of off-channel habitats) that can help to conserve and restore secondary channel habitats and maintain their ecological value for a number of species. To achieve this overarching goal, this study is guided by four primary objectives:

- 1) evaluate the physical processes that create chute cutoffs;
- 2) evaluate the life span of secondary channels as a function of flow and sedimentation;

- 3) survey aquatic vegetation and monitor water quality in secondary channels to identify factors affecting aquatic vegetation composition and distribution; and
- 4) identify flows that create shallow-water, seasonally inundated habitats within the bankfull channel to support juvenile salmonid rearing.

3. Field Studies

3.1 Sediment coring of former channels

In unregulated river systems, overbank flows that inundate former channels (e.g., oxbows, side channels) carry fine sediments that settle out in the lower velocity secondary channels. Over time, secondary channels can accumulate sediment and generally become more shallow and narrow, thereby altering the type of habitat through changes in vegetation, open water area, thermal stratification, etc. However, in river systems regulated by large water supply and flood control dams, it is unclear how changes in sediment supply and high flow events affect sedimentation rates in former channels. Large dams generally reduce the frequency and magnitude of high flow events, thus reducing the number of overbank flows capable of transporting fine sediment into former channels. Dams also tend to reduce the sediment supply by trapping sediment from the upper watershed, which may combine with the reduced frequency of overbank flooding to prolong the longevity of secondary channels by reducing sedimentation. However, land use changes downstream of large dams (e.g., conversion of floodplains to agriculture, timber production in tributaries) can increase the fine sediment supply, thus increasing the potential load of fine sediment that can be deposited in former channels during overbank flow events, even if they occur less frequently because of flow regulation. In the Sacramento River, it is unclear how changes in high flow events and sediment supply caused by dam operations and land use changes have affected sedimentation rates in former channels.

To assess potential changes in the sedimentation rates in secondary channels of the middle Sacramento River (Red Bluff to Colusa), we will compare sedimentation rates of secondary channels that cutoff prior to and after the closure of Shasta Dam. Estimating sedimentation rates in former channels provides an indication of probable longevity and future evolution of such channels.

To estimate the rate of sedimentation in former channels, we will collect sediment cores to determine the depth of fine sediment that has accumulated in them since the time of cutoff and compare sediment depth with the estimated age of each sampled channel. The age of each sampled unit will be estimated by examining historical aerial photos and discharge records.¹ Cores will be collected using a hand auger with a screw bit that is capable of penetrating fine-grained sediment quickly, but which encounters resistance when it hits gravel, which we will initially presume to be the former channel bed at the time of cutoff.²

¹ A separate, but parallel, research effort conducted by Dunne and Constantine of UC Santa Barbara will use radiometric dating of sediments cored from secondary channels of the middle Sacramento River. Radiometric dating will support a more detailed assessment of sedimentation rates that will build on the results of this study.

² Former channels with acute angles to the mainstem may partially fill with gravels after the site has been cut off from the mainstem channel, especially near their upstream ends. We will take this into account in interpreting our results.

We will sample at least 15 former channels in the Sacramento River corridor, sampling virtually all former channels for which we can obtain permits and landowner access (Table 1). We will take at least three samples at each location—at an upstream, midpoint, and downstream location along the axis of each secondary channel. Coring depths will be limited to a maximum of 20 feet because of equipment limitations. Depths may be less when groundwater or coarse gravels are encountered.

Former channels that are inundated year-round will be cored by boat when flow magnitudes in the Sacramento River are sufficient to facilitate navigation. Former channels that are dry at low river stage will be cored when water stages have receded, allowing access by foot.

Key personnel: Matt Kondolf (PI), Julien Levrat, Jose Constantine, Hervé Piégay

Table 1. Sacramento River Cut-off Channels: Potential Study Sites, Ownership, and Access

No.	River Mile	Bank	Name	Ownership
1	147.4	L	Colusa Unit North	CDFG
2	161.2	L	Boggs Bend	Private, soon to be CDFG (~Sept.)
3	167.2	R	Packer Lake	USFWS
4	168.4	R	Old Packer Lake	USFWS
5	168.8	R	Razor Slough	USFWS
6	170.0	R	Beehive Bend	DFG
7	178.0	R	N/A	Rec Board?
8	179.2	R	N/A	private - Llano Seco Rancho
9	180.8	L	Dodge Opening	private - Llano Seco Rancho
10	182.5	L	The Lagoon	private - Llano Seco Rancho
11	186.0	L	Deadman's Reach	USFWS
12	189.0	R	N/A	Rec Board/Private?/state lands
13	190.0	R	Sam's Slough	USFWS
14	190.0	L	Golden State	private
15	192.0	R	N/A	USFWS/state Lands
16	193.5	R	Capay	USFWS
17	194.5	R	Pine Creek West	DFG
18	195.0	L	Indian Fisheries	State Parks/DFG
19	196.0	L	(Pine Ck Backwater)	DFG/DWR/USFWS
20	203-205	L	Wilson's Landing	DFG
21	206.3	L	GCID	private
22	212.7	L	Merrills Landing	DFG
23	218.4	R	Kopta Slough Main	State Parks
24	221.6	R	Kopta Slough North	TNC
25	234.0	L	Ohm	USFWS
26	234.8	R	Ohm	USFWS
27	236.8	R	La Barranca	BLM/USFWS

Note: Highlighted sites indicate locations for which permits have been obtained (blue) or provisional access has been granted (green).

3.2 Hydrologic Connectivity of Off-Channel Habitats

The manner in which a former channel habitat is connected to the mainstem channel (e.g., whether the channel is connected at the upstream end, at the downstream end, or at both ends) can affect sediment dynamics in the off-channel water body and the rate of sedimentation. Similarly, the magnitude of flow required to inundate an off-channel water body, and the seasonal timing of inundation, can determine its ecological value for different species.

To provide an initial assessment of the hydrologic connectivity of secondary channel habitats, we will observe changes in river stage and flow direction in side channels during the recession limb of a flood, and survey the water surface elevations and establish benchmarks to which the stage can be associated. These benchmarks will then be surveyed by the Department of Water Resources with survey-grade GPS to an accuracy of 2-3 mm. We will work with Constantine at UC Santa Barbara to apply their hydraulic model with a digital elevation model of the river to determine the frequency of overbank flow at upstream and downstream entrances to the former channels, using our field-observed flood-recession-limb flow directions, flow velocities, and stage. We estimate the accuracy of the modeling to be about 1 foot.

Key personnel: Matt Kondolf (PI), Julien Levrat, Jose Constantine, Hervé Piégay

3.3 Macrophyte surveys and water quality sampling

The vegetative cover in an off-channel habitat can affect the habitat value for different species. For example, dense areas of water primrose (*Ludwigia*) may benefit the ambush tactics of non-native bass species that prey on juvenile salmonids (Moyle 2002), while areas of open water may provide better habitat for juvenile salmon (M. Limm, personal communication, May 1, 2005). Similarly, secondary channels with heavy loads of decaying vegetation can cause dissolved oxygen sags, which can favor some species over others. We will survey aquatic macrophytes in up to 15 secondary channels of the Sacramento River to better understand the composition and density of aquatic vegetation in these habitats. The surveys will identify the spatially dominant species of aquatic vegetation with an estimate of the percentage cover for each species.

Previous research on aquatic macrophytes in off-channel habitats of the Rhone River indicates that plant diversity is a function not only of hydrologic connectivity with the mainstem channel, but also of water quality. Water quality can also affect the quality of secondary channel habitats in the Sacramento River for aquatic species like juvenile salmonids. Conditions in secondary channels can range from heterotrophic to eutrophic. Members of the research team will use the Hydrolab Minisonde owned by the TNC Chico office to monitor pH, water temperature, electrical conductivity, and dissolved oxygen in 17 off-channel habitats of the Sacramento River. The secondary channels surveyed for water quality will overlap with those for which sediment cores will be collected and macrophyte surveys will be conducted (Table 1), provided that the sites are inundated during the period of water quality sampling.

Surveys of aquatic macrophytes will be conducted in the fall, 2005, and water quality sampling will be conducted in the fall, 2005 and spring, 2006.

Key personnel: Gudrun Bornette, Ingrid Morken, Sara Puijalon, Julien Levrat, Hervé Piégay

3.4 Scour Channels on Point Bars

Shallow-water habitat provides important rearing habitat for juvenile salmonids, especially salmon fry (Bjornn and Reiser 1991, Lister and Genoe 1970). In a large river system like the Sacramento River, shallow-water habitat usually occurs within the channel along channel margins and point bars. Shallow-water habitat is also created outside of the channel as periodic high flows inundate floodplains that border the river.

Previous research in the Sacramento River suggests that seasonally inundated habitats that fall within the bankfull channel provide important rearing habitat for juvenile salmonids (Limm and Marchetti 2003). Many of these habitat types are associated with point bars where scour channels form on the inner edge of the bar (Figure 2), creating a surface that becomes inundated during periods of elevated flow. When discharge magnitudes drop, these scour channels can become hydraulically disconnected from the mainstem channel, stranding juvenile salmonids (Limm and Marchetti 2003). Subsequent flow pulses that re-connect these seasonally inundated habitats permit stranded juvenile salmonids to re-enter the mainstem channel and continue their downstream migration. Estimating the discharge magnitudes that inundate these seasonal, shallow-water areas can provide flow targets designed to enhance growth opportunities for juvenile salmonids during periods of fry dispersal. Estimating the discharge magnitudes that connect these seasonal habitats with the mainstem channel can also inform the design of spring flow pulses that prevent or reduce stranding of juvenile salmonids. This study component focuses on the reach below Red Bluff Diversion Dam (RBDD) (RM 243.5) because it is the alluvial reach of the Sacramento River where point bar dynamics are still active, and because little is known about salmonid rearing habitat between RBDD and Knight's Landing (RM 89).

Using recent aerial photos (NAIP 2005), we will identify seasonally inundated habitats that occur within the bankfull channel of the middle Sacramento River to develop a pool of candidate study sites. We will conduct a field reconnaissance of the candidate study sites to select at least ten representative sites to sample. For each selected study site, we will use a high resolution GPS to survey a water surface elevation in inundated sites, which we will correlate with the nearest flow gauge to develop a stage-discharge relationship.



Figure 2. Example of a scour channel that forms on the downstream end of a point bar. (Photo Source: CDWR 1999)

Field crews will also plant miniature water temperature recorders within each study site to record areas and periods of inundation. The temperature recorders will sample temperatures at 15-minute intervals. When the temperature recorders are exposed to the open air, the diurnal fluctuations are typically more pronounced than when the recorders are inundated (Figure 3).

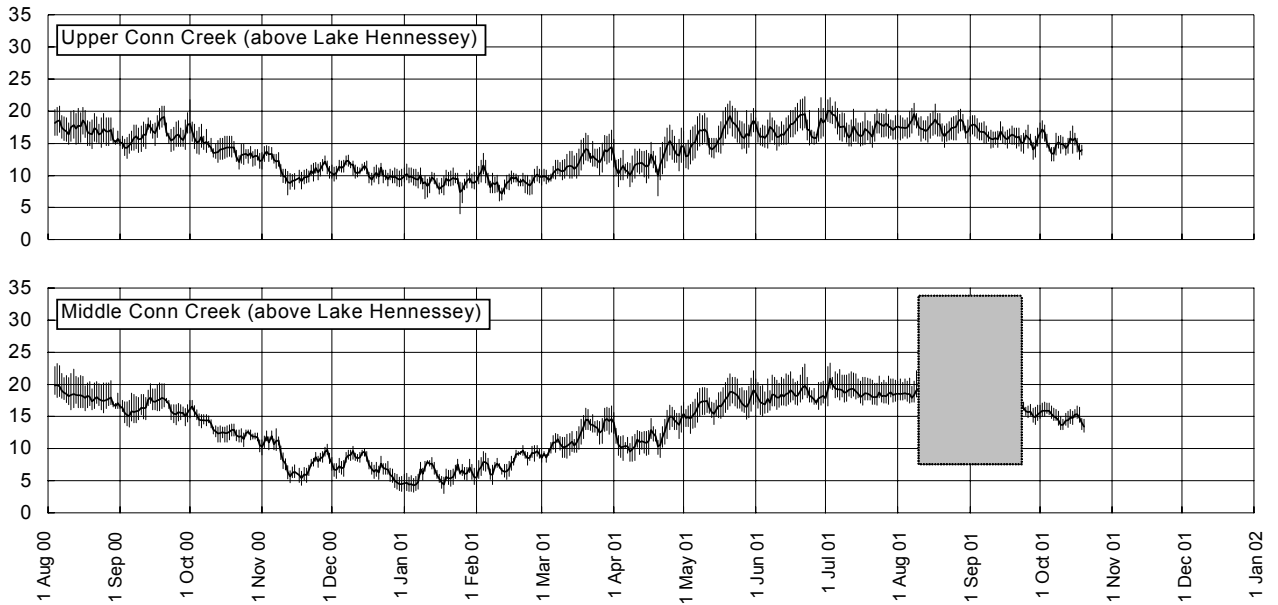


Figure 3. Miniature water temperature recorders can be used to identify periods of inundation and desiccation. Diurnal temperature fluctuations are generally muted during periods of inundation, and more pronounced when they are exposed to the open air (gray box).

By planting temperature recorders throughout the study sites (Figure 4), the time series can be correlated with discharge data from nearby gauges to estimate a stage-discharge relationship. The temperature recorders will also be placed so that estimates of the inundated surface area can be developed at several of the study sites. The elevation of each temperature recorder will be surveyed relative to a temporary benchmark, and the elevation of each temporary benchmark will be surveyed using a differential GPS unit. By comparing the resultant dataset with data from nearby flow gauges, we will develop estimates of the discharge required to inundate the study sites and to characterize inundation characteristics (e.g., depth and area).

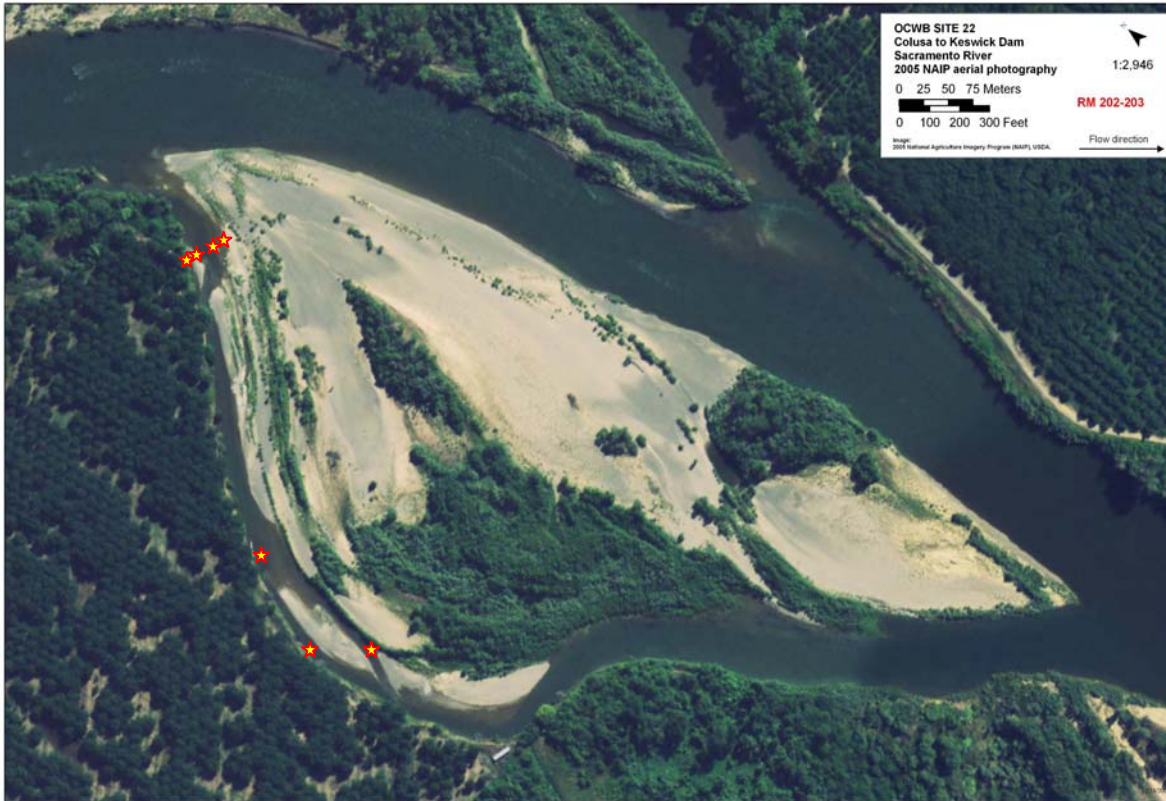


Figure 4. Temperature recorders can be planted throughout a sample site to identify when different elevations are inundated and desiccated. By correlating periods of inundation and desiccation at each temperature recorder with discharge data from nearby flow gauges, it is possible to estimate a stage-discharge relationship for each site. It is also possible to characterize inundation characteristics (e.g., depth, area) for different discharges by correlating the temperature and flow data. The stars in the figure represent the hypothetical location of temperature recorders to facilitate the development of local stage-discharge relationships and inundation characteristics.

For each seasonally inundated habitat unit identified by the inventory, field crews will also estimate the area of inundated habitat by measuring the axial length and width of the inundated surface. For those habitat units that are not inundated during the time of the survey, field crews will measure the axial length and width of the graded surface. We will also characterize sampled habitats in terms of inundated area, water depth, water temperature, and other habitat metrics (e.g., vegetative cover, substrate composition, etc.).

The field survey will be conducted in the winter of 2006-2007 to capture habitat conditions during a period of elevated flow when the target habitats are inundated.

Although the field crew will not directly sample juvenile salmonids, they will record any observations of salmon fry, including the number observed and estimated fork lengths.

Key Personnel: Frank Ligon, Russ Liebig, Michael Fainter, John Wooster

4.0 Modeling

4.1 Chute Cutoff Modeling

Oxbow lakes are a type of off-channel habitat, and they form when meanderbends eventually cut off as flow occupies a new, straighter main channel alignment. Oxbow lakes can form from neck or chute cutoffs. Neck cutoffs occur when the radius of curvature of a meanderbend becomes so extreme that bank erosion eventually scours the narrow “neck” of floodplain that separates the upstream and downstream end of a meanderloop. Therefore, neck cutoffs are primarily a function of bank erosion.

In comparison, chute cutoffs form during high flow events when overbank flows scour a pilot channel on the floodplain and eventually capture the discharge, as illustrated in Figure 5.

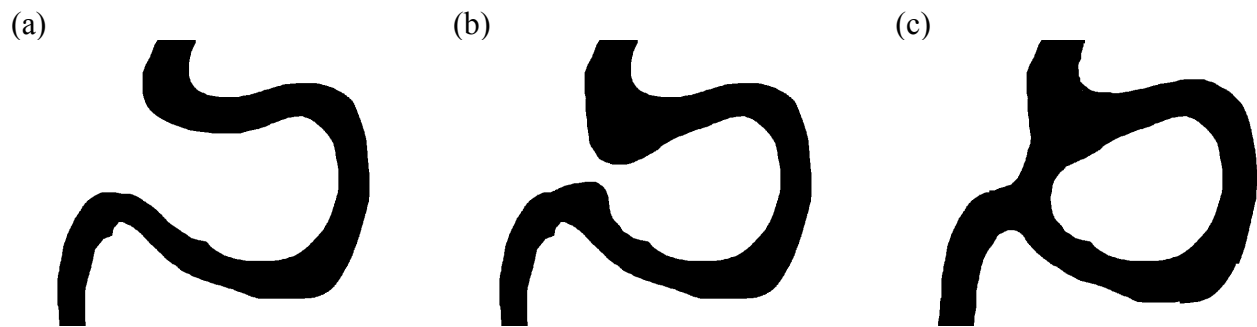


Figure 5. Evolution of a chute cutoff.

During low flow events, flows pass through the existing channel (Figure 5a). With an increase in discharge, water will inundate the lower area near the bend where previous high flow events may have carved the topography lower (Figure 5b). Once the discharge increase is high enough, flow will pass through both the existing channel and the area where the cutoff is to occur (Figure 5c). Although the water in the cutoff area is shallow, its gradient is significantly higher than the existing main channel, which will result in scouring and the promotion of channel cutoff.

Thus, the physical processes that initiate a chute cutoff are different than those that create neck cutoffs. It is possible to identify the potential for neck cutoffs by applying a meander migration model like the one developed by UC Davis, because the model simulates the effects of bank erosion. There is currently no model to simulate how flows initiate chute cutoffs.

We will develop a mechanistically-based, one-dimensional, numerical model to simulate the initiation and evolution of chute-cutoff in low-gradient alluvial rivers. The model can be used to examine what potential flow event is needed to initiate a chute cutoff at a specific site by running different hydrographs through the model. The model will require the following input parameters for an identified cutoff route: (1) topographic data; (2) discharge record; (3) critical shear stress for erosion; (4) other erosional characteristics. Because the model is one-dimensional, the potential cutoff route has to be identified outside of the model and incorporated as an input parameter. The model can be used to evaluate the potential for cutoff for any identified cutoff route on any bend in the river.

The chute cutoff model will be developed using a potential chute cutoff at RM 172 to predict the

flow events required to initiate chute cutoff at that site.

Conceptual model and coding for the chute cutoff model will be conducted between March and July, 2005. A field tour of potential chute cutoff sites will be conducted in July, 2005. De-bugging of the chute cutoff model, using site-specific information from the cutoff at RM 212-215, will be conducted between November, 2005 and June, 2007. Application of the chute cutoff model to a potential chute cutoff at RM 172 will be conducted between October, 2006 and July, 2007.

Key Personnel: Yantao Cui, Lisa Micheli, Bill Dietrich

5.0 References

- Bjornn T.C. and D.W. Reiser. 1991. Habitat requirements of salmonids in streams. American Fisheries Society Special Publication 19:83-138.
- CDFG (California Department of Fish and Game). 1983. Sacramento River and tributaries bank protection and erosion control investigation--evaluation of impacts on fisheries. Final Report. CDFG, Bay-Delta Fishery Project.
- CDWR (California Department of Water Resources). 1994. Sacramento River bank erosion investigation memorandum progress report. Internal memorandum to R. Scott and L. Brown from K. Buer, Chief, Geology Section, California Department of Water Resources, Northern District, Red Bluff.
- Limm, M. P., and M. P. Marchetti. 2003. Contrasting patterns of juvenile Chinook salmon (*Oncorhynchus tshawytscha*) growth, diet, and prey densities in off-channel and main stem habitats on the Sacramento River. Prepared for The Nature Conservancy, Chico, California.
- Lister, D. B., and H. S. Genoe. 1970. Stream habitat utilization of cohabiting underyearlings of Chinook (*Oncorhynchus tshawytscha*) and coho (*O. kisutch*) salmon in the Big Qualicum River, British Columbia. *Journal of the Fisheries Research Board of Canada* 27: 1215-1224.
- Moyle, P. B. 2002. *Inland fishes of California*. Revised edition. University of California Press, Berkeley.
- Sommer, T., B. Harrell, M. Nobriga, R. Brown, P. Moyle, W. Kimmerer, and L. Schemel. 2001. California's Yolo Bypass: evidence that flood control can be compatible with fisheries, wetlands, wildlife, and agriculture. *Fisheries* 26: 6-16.